Imperial College London

Department of Earth Science and Engineering

DECISION MAKING AND UNCERTAINTY QUANTIFICATION FOR SURFACTANT-POLYMER FLOODING

A dissertation submitted to the Department of Earth Science and Engineering of

Imperial College London in partial fulfilment of the requirements for the degree of

Doctor of Philosophy

Ali Alkhatib

November 2013

Supervised by Prof. Peter R. King

Declaration

I hereby declare that this thesis titled '**DECISION MAKING AND UNCERTAINTY QUANTIFICATION FOR SURFACTANT-POLYMER FLOODING**' is entirely my own work and all else is appropriately referenced. This work has not been previously submitted in its entirety or in part to any other academic institute for a degree or qualification.

Ali Alkhatib

Department of Earth Science and Engineering

Imperial College London

© 2013 Ali M. Alkhatib

The copyright of this thesis rests with the author and is made available under a Creative Commons Attribution Non-Commercial No Derivatives licence. Researchers are free to copy, distribute or transmit the thesis on the condition that they attribute it, that they do not use it for commercial purposes and that they do not alter, transform or build upon it. For any reuse or redistribution, researchers must make clear to others the licence terms of this work.

Abstract

The aim of this thesis is to develop a robust parametric uncertainty quantification method and a decision making method for a chemical EOR process. The main motivation is that uncertainty is detrimental to the wide scale implementation of chemical EOR. Poor scale-up performance is not in line with the success in laboratory applications. Furthermore, economic uncertainty is also an important factor as low oil prices can deter EOR investment. As an example of chemical EOR we used Surfactant-polymer flooding due to its high potential and complexity.

The approach was based on using Value of Flexibility evaluation in order to optimize the surfactant-polymer flooding in the presence of economic and technical uncertainty. This method was inspired by real options theory which provides a framework to value flexibility and captures the effect of uncertainty as the process evolves through time. By doing so, it provides the means to capitalize on the upside opportunities that these uncertainties present or to help mitigate worsening circumstances. In addition, it fulfils a secondary objective to develop a decision making process that combines both technical and economic uncertainty.

The Least Squares Monte Carlo (LSM) method was chosen to value flexibility in surfactant-polymer flooding. The algorithm depends on two main components; the stochastic simulation of the input state variables and the dynamic programming approach that produce the optimal policy. The produced optimal policy represents the influence of uncertainty in the time series of the relevant input parameters. Different chemical related parameters were modelled stochastically such as surfactant and polymer adsorption rates and residual oil saturation. Static uncertainty in heterogeneity was incorporated using Gaussian and multiple-point statistics generated grids and dynamic uncertainty in heterogeneity was modelled using upscaling techniques. Economic uncertainties such as the oil price and surfactant and polymer cost were incorporated into the model as well.

The results obtained for the initial case studies showed that the method produced higher value compared with static policy scenarios. It showed that by designing flexibility into the implementation of the surfactant-polymer flood, it is possible to create value in the presence of uncertainty.

An attempt to enhance the performance of the LSM algorithm was introduced by using the probabilistic collocation method (PCM) to sample the distributions of the technical state input parameters more efficiently, requiring significantly less computational time compared to Monte Carlo sampling. The combined approach was then applied to more complex decisions to demonstrate its scalability.

It was found that the LSM algorithm could value flexibility for surfactant-polymer flooding and that it introduces a new approach to highly uncertain problems. However, there are some limitations to the extendibility of the algorithm to more complex higher dimensional problems. The main limitation was observed when using a finer discretization of the decision space because it requires a significant increase in the number of stochastic realization for the results to converge, thus increasing the computational requirement significantly.

The contributions of this thesis can be summarized into the following: an attempt to use real options theory to value flexibility in SP flooding processes, the development of an approximate dynamic programming approach to produce optimal policies, the robust quantification of parametric uncertainty for SP flooding using PCM and an attempt to improve the efficiency of the LSM method by coupling it with the PCM code in order to extend its applicability to more complex problems.

List of Publications

The following publications are a result of this work:

Alkhatib, A. and King, P. 2011. Applying Real Options Theory in Determining Optimal Policies for a Surfactant Flood. Paper SPE 144869-MS presented at the SPE Enhanced Oil Recovery Conference, Kuala Lumpur, Malaysia, 19-21 July.

Alkhatib, A., Babaei, M. and King, P. 2012. Decision Making under Uncertainty in EOR: Applying the Least Squares MonteCarlo (LSM) Method in Chemical EOR Implementation. Paper SPE 154467-MS presented at the SPE Europec/EAGE Annual Conference, Copenhagen, Denmark, 4-7 June.

Alkhatib, A. and King, P. 2013. Uncertainty Quantification of a Chemically Enhanced Oil Recovery Process: Applying the Probabilistic Collocation Method to a Surfactant-Polymer Flood. Paper SPE 164244-MS presented at the 18th Middle East Oil & Gas Show and Conference (MEOS), Manama, Bahrain, 10-13 March.

Alkhatib, A., Babaei, M. and King, P. 2013. Decision Making Under Uncertainty: Applying the Least-Squares Monte Carlo Method in Surfactant-Flooding Implementation. *SPE J.* (in press: published online 9 April 2013, SPE154467-PA).

Alkhatib, A. and King, P. 2013. Applying the Probabilistic Collocation Method to Surfactant-Polymer Flooding. Paper EAGE 15560 presented at the 17th European Symposium on Improved Oil Recovery, St. Petersburg, Russia, 16-18 April.

Alkhatib, A. and King, P. 2013. The Use of the Least Squares Probabilistic Collocation Method in Decision Making in the Presence of Uncertainty for Surfactant-Polymer Flooding. Paper SPE 164860-MS presented at the 75th EAGE Conference & Exhibition incorporating SPE EUROPEC 2013, London, UK, 10-13 June.

Alkhatib, A. and King, P. 2013. Robust Quantification of Parametric Uncertainty for Surfactant-Polymer Flooding. Submitted to *Computational Geosciences*.

Alkhatib, A. and King, P. 2013. An Approximate Dynamic Programming Approach to Decision Making in the Presence of Uncertainty for Surfactant-Polymer Flooding. Submitted to *Computational Geosciences*.

Table of Contents

Abstract 3

List of Publications 4

Table of Contents 5

List of Figures 9

List of Tables 13

1 Introduction 14

2 Enhanced Oil Recovery: Surfactant-Polymer Flooding 17

2.1 Surfactants Chemistry and Structure 18

2.2 IFT Reduction 18

2.3 Phase Behaviour 20

2.3.1 Effect of Salinity 20

2.3.2 IFT and Phase Behavior 22

2.3.3 Variables that Affect IFT and Phase Behavior 22

2.4 Retention 23

2.4.1 Adsorption 23

2.4.2 Ionic Exchange 24

2.4.3 Precipitation 24

2.4.4 Phase Entrapment 24

2.5 Mobility Control 25

2.5.1 Polymer 25

2.5.2 Retention 25

2.5.3 Viscosity 26

2.5.4 Mobility Control Design 26

2.5.5 Surfactant-Polymer Interaction and Compatibility 27

2.6 Design Considerations 28

2.6.1 Laboratory Results 29

2.6.2 Field Implementation 30

2.6.3 Improvements and Variations 31

2.7 Performance Forecasting-Simulation 32

2.7.1 Commonly Used Simulators 32

2.7.2 Reservoir Simulator used for this Study: ECLIPSE 100 33

2.7.3 Recent Developments and Other approaches 37

2.8 Sources of Uncertainty 38

2.9 Concluding Remarks 39

3 Decision Making in E&P 40

3.1 Decisions and Decision Analysis 40
3.1.1 Definitions 40
3.1.2 Decisions in the Presence of Uncertainty 41

3.2 Decision analysis in Exploration and Production 41
3.2.1 Review of Decision Analysis Methods used in E&P 41
3.2.2 Review of Decision Analysis Methods for Chemical EOR Processes 43

3.3 Real Options Theory 46
3.3.1 Definition 46
3.3.2 Valuation Methods 48
3.3.3 Examples in E&P 51

3.4 Concluding Remarks 58

4 Theory and Methodology 60

4.1 **LSM Theory and Implementation 60**
4.1.1 The Least-Squares Monte Carlo Algorithm 62
4.1.2 Implementation 64
4.2 Uncertainty in Heterogeneity 68

4.4 **PCM Background and Theory 69**
4.4.1 Polynomial Chaos Expansion 70
4.4.2 Probabilistic Collocation 71
4.4.2.1 Gaussian Quadrature 71
4.4.2.2 Linear Regression 72
4.4.3 Selection of Collocation Nodes 73
4.4.4 Computation of Statistical Moments 75
4.4.5 Implementation 76

4.5 **The LSPCM Algorithm 76**
4.5.1 Coupling of LSM with PCM Algorithm 77
4.5.2 Implementation of the LSPCM Algorithm 78

5 The Least Squares Monte Carlo Method: Case Studies 79

5.1 **Application: Case Study 1 79**
5.1.1 Problem Definition 79
5.1.2 Monte Carlo Simulation 82
5.1.3 Code Validation 89
5.1.4 Results for Case Study 1 89
5.1.5 VoF Sensitivity Analysis 91
5.1.5.1 Varying the Static Policy Scenario 91
5.1.5.2 Convergence as a Function of the Number of Realizations 92
5.1.5.3 Decision Space Discretization 93
5.1.5.4 Mobility Control 105

5.2 **Basis Function Design and Regression 106**
5.2.1 Simple Polynomials 106
5.2.2 Orthogonal Polynomials 107
5.2.3 Clustered Linear Regression 110

5.3 **Application: Case Study 2 113**
5.3.1 Mobility Control 116
5.3.2 Well Placement 117

5.3.3 Permeability Field 118
5.3.4 Summary 120

5.4 **Uncertainty in Heterogeneity 121**
5.4.1 Moving Average Method 121
5.4.2 Multiple-Point Statistics 124
5.4.3 Summary 128

5.5 **Concluding Remarks 128**

6 The Probabilistic Collocation Method: Case Studies 130

6.1 **Case Studies 130**
6.1.1 Example 1: Homogeneous three-dimensional reservoir model 132
6.1.2 Example 2: Heterogeneous two-dimensional reservoir model 136
6.1.3 Example 3: PUNQ-S3 three-dimensional reservoir model 141
6.1.4 Example 4: Modified SPE10 three-dimensional reservoir model 144

6.2 **Discussion 145**

6.3 **Concluding Remarks 148**

7 The Least Squares Probabilistic Collocation Method: Case Studies 149

7.1 LSPCM Case Studies 149
7.1.1 Initial Application 149
7.1.2 Incorporating Uncertainty in the Time Series 155

7.2 **Possible Extensions 157**
7.2.1 Mutually Exclusive Decisions 157
7.2.2 Application to Alkaline-Surfactant-Polymer Flooding 160

7.3 **Concluding Remarks 163**

8 Conclusions and Recommendations 165

8.1 **Conclusions 165**

8.2 **Recommendations for Future Work 166**

References 169

Appendices 186

Appendix A: Reservoir and Surfactant Properties for Homogeneous and SPE10 Layers 1, 5, 10, 15 and 20 Reservoir Models 186

Appendix B: Basis Function Orthogonal Polynomials 188

Appendix C: Reservoir and Fluid Data for Moving Average and FILTERSIM Reservoir Models 189

Appendix D: Orthogonal Polynomials Used for PCM 190

Appendix E: Golub-Welsch Algorithm for Gaussian Quadrature 191

Appendix F: Inverse Cumulative Distribution Function and Inverse Rosenblatt Transform 192

Appendix G: Surfactant-Polymer Properties and Simulation Constraints 193

Appendix H: Alkaline Model in ECLIPSE 194

Appendix I: Alkaline Properties 196

List of Figures

Fig. 2.1— The effect of salinity on IFT and solubiliztion of surfactant. C_{23}/ C_{33} refers to solubilization parameter between the mircoemulsion-oleic phases (for type II(-) and III phase behavior) and C_{13}/C_{33} refers to solubilization parameter between the microemulsion-aqueous phases (for type II(+) and III phase behavior). This figure is reproduced from Lake (1989). 19
Fig. 2.2— The effect of the log of capillary number on final residual oil saturation. This is based on the correlation by Healy and Reed (1977). σ_{mo} *is the microemulsion-oil interfacial tension and* σ_{mw} *is the microemulsion-water interfacial tension. Reproduced from Green and Willhite (1998).* 20
Fig. 2.3— The effect of salinity on a generalized phase diagrams. Reproduced from Green and Willhite (1998). 21
Fig. 2.4— Surfactant adsorption as a function of surfactant concentration. This is based on stylized data. 24
Fig. 2.5— Effect of adding polymer to a surfactant flood on oil recovery. This is based on adding a 500ppm polymer slug to surfactant core flood using a Bentheim core (Reproduced from Taugbol et al. 1995). 26
Fig. 2.6— Field performance plot of the ratio of actual to predicted SP flooding recovery vs. incremental oil recovery (plot data from Hammershaimb et al. 1983). 31
Figure 3.1— Discrepancy between DCF (Discounted Cash Flow) and ROV(Real Options Valuation) Approaches. Reproduced from Jafarizadeh and Bratvold (2009). 47
Fig. 3.2— Compound option diagram. This diagram shows decision contingent on previous decisions over a two year period. Once a decision is made after the first time step (1 year), a new decision becomes available contingent on the previous decision. 48
Fig. 3.3— Binomial model lattice. (p) and (1-p) are the probabilities of the up (u) and down (d) moves. 49
Fig. 4.1— The LSM method framework 61
Fig 4.2— Algorithm flow chart illustrating the steps followed in the MATLAB code. 66
Fig 4.3— Algorithm flow chart illustrating decision rule in the MATLAB code. 67
Fig. 4.4— Flow chart illustrating the steps in generating the stochastic realizations for the technical and economic parameters and heterogeneity fields which are used to obtain the production profiles and determine the objective function for each scenario. 68
Fig. 4.5— Two-dimensional quadrature grid, where moving from left plot to the right, are the second, third and fourth order PCM nodes. 73
Fig. 4.6— Two-dimensional mapped Fejer grid, where moving from left plot to the right, are the second, third and fourth order PCM nodes. 74
Fig. 4.7— Two-dimensional boxed Fejer grid, where moving from left plot to the right, are the second, third and fourth order PCM nodes. 74
Fig. 4.8 —Number of nodes for a four-dimensional random input scenario, as a function of approximation order. 75
Fig. 4.9— PCM flowchart illustrating the implementation steps. 76
Fig. 4.9— LSPCM code flowchart illustrating the implementation steps. 78
Fig. 5.1—Decision (flexibility) flow chart. 80
Fig. 5.2—Decision state space representation where X(ω) represents the state variables per ω realization. 81
Fig. 5.3— Surface plot for recovery factor and NPV as a function of D_s and S_{orc}. Each surface color is illustrates a different policy (surfactant flooding initiation). 82
Fig. 5.4— Serial test plots for six iterations for the pseudo-random number generator used in MATLAB. Each iteration consists of 1000 samples of a uniformly distributed variable with unit interval. 83
Fig. 5.5— Residual oil saturation to chemical flooding and surfactant adsorption variation with time for case study 1. 85
Fig. 5.6— Production profiles for case study 1. 85
Fig 5.7— Ornstein-Uhlenbeck price model, showing the mean of 1000 paths and the corresponding standard deviation. 87
Fig 5.8— Normalized NPV for the case study 1. 88
Fig 5.9— Value of flexibility probability density function (PDF) plot and policy histogram for case study 1. 90
Fig 5.10— VoF PDF plot and policy histogram for case study 1 using different static scenarios. 91
Fig 5.11— Histogram of optimal policy (adjusted to a basis of 10^3 realizations in order to compare with the original run) and plot of convergence of the averaged normalized option value for the homogeneous reservoir model with increasing number of realizations. The averaged normalized option value is taken as the difference between the averaged (over all realizations) normalized option and the averaged normalized static scenarios, the normalization is with respect to the corresponding

waterflood scenario NPV (averaged over all realizations). A value > 0 is considered to be favouring flexibility while a value <0 favours the static scenario. 93
Fig 5.12— VoF PDF plot for case study 1 for different decision space discretizations. 94
Fig 5.13— Policy histograms for case study 1 for different decision space discretization's. 94
Fig 5.14— VoF PDF for one-dimensional homogeneous reservoir model assuming S_{orc} as the technical uncertainty for different decision space discretization's. 95
Fig 5.15— Policy histograms for one-dimensional homogeneous reservoir model assuming S_{orc} as the only technical uncertainty for different decision space discretization's. 96
Fig 5.16— VoF PDF for three-dimensional homogeneous reservoir model assuming S_{orc} as the technical uncertainty for different decision space discretization's. 96
Fig 5.17— Policy histograms for three-dimensional homogeneous reservoir model assuming S_{orc} as the only technical uncertainty for different decision space discretization's. 97
Fig 5.18— VoF PDF for one-dimensional homogeneous reservoir model assuming S_{orc} and D_s as the technical uncertainties for different decision space discretization's. 97
Fig 5.19— Policy histograms for one-dimensional homogeneous reservoir model assuming S_{orc} and D_s as the technical uncertainties for different decision space discretization's. 98
Fig 5.20— VoF PDF for three-dimensional homogeneous reservoir model assuming S_{orc} and D_s as the technical uncertainties for different decision space discretization's. 98
Fig 5.21— Policy histograms for three-dimensional homogeneous reservoir model assuming S_{orc} and D_s as the technical uncertainties for different decision space discretization's. 99
Fig 5.22— Plot of mean NPV and RF (recovery factor) over 1000 realizations as a function of injection policy. The legend in the upper right corner refer to the right axis (RF) and the legend in the upper left corner refers to the left axis (NPV). The plot on the left was determined for the base case three dimensional homogeneous reservoir model and the plot on the right was obtained using a one dimensional homogeneous reservoir model. 100
Fig 5.23— Figure showing the VoF PDF and the optimal policy histogram obtained for each decision space discretization case where the results for each water cost multiplier is plotted. These were obtained for the three-dimensional homogeneous reservoir model. 101
Fig 5.24— Plot of relative mean VoF as a function of the water cost multiplier. The mean VoF is normalized using the low water cost multiplier case (0.01) as the base case. These results were obtained using the three-dimensional homogeneous reservoir model base case. 102
Fig 5.27— VoF PDF plot for case study 1 using mobility control. 105
Fig 5.28— VoF PDF and optimal policy histogram using 1st order polynomial. 106
Fig 5.29— VoF PDF and optimal policy histogram using 3rd order polynomial. 106
Fig 5.30— VoF PDF and optimal policy histogram using 2nd order polynomial with cross-products. 107
Fig 5.31— VoF PDF and optimal policy histogram using 3rd order polynomial with cross-products. 107
Fig 5.32— VoF PDF and optimal policy histogram using 3rd order Legendre polynomials. 108
Fig 5.33— VoF PDF and optimal policy histogram using 3rd order Weighted Laguerre polynomials. 109
Fig 5.34— VoF PDF and optimal policy histogram using 3rd order Laguerre polynomials. 109
Fig 5.35— VoF PDF and optimal policy histogram using 3rd order Hermite polynomials. 109
Fig 5.36— VoF PDF and optimal policy histogram using 3rd order Chebyshev polynomials. 110
Fig 5.37— Cross-plot of NPV for surfactant injection for different policies as a function of adsorption. The data is separated into four different clusters. 111
Fig 5.38— VoF PDF and optimal policy histogram for results determined by using dynamic clustered regression based on adsorption. 111
Fig 5.39— Cross-plot of NPV for surfactant injection for different policies as a function of residual oil saturation to chemical flooding. The data is separated into four different clusters. 112
Fig 5.40— VoF PDF and optimal policy histogram for results determined by using dynamic clustered regression based on residual saturation. 112
Fig. 5.41— Heterogeneity variation with time, with the far left showing the coarsest realization and the far right showing the finest realization of the permeability field. 114
Fig. 5.42— Production profiles for case study 2. 114

Fig 5.43— Normalized NPV for the case study 2. 115
Fig 5.44— VoF PDF plot and optimal policy histogram for case study 2. 115
Fig 5.45— VoF PDF plot and optimal policy histogram for case study 2 with mobility control. 116
Fig 5.46— Well placements for case study 2. 117
Fig 5.47— VoF PDF plot and optimal policy histogram for case study 2 using different well placements. 118
Fig 5.49— VoF PDF plot and optimal policy histogram for case study 2 using different permeability fields. 119
Fig 5.50— Uncorrelated and correlated permeability grid obtained using the moving average method. The scale for the correlated grid is logarithmic. 122
Fig. 5.51— Heterogeneity variation with time, with the far left showing the coarsest realization and the far right showing the finest realization of the permeability field. The scale is logarithmic. 123
Fig. 5.52— Inverted five-spot pattern that is used for reservoir models obtained via the moving average method. 124
Fig. 5.53— VoF PDF and policy histogram for the moving average permeability realizations with renormalization with time. The results for fixed heterogeneity with time (fine scale constant through time) were also added for comparison. 124
Fig. 5.54— Original channelized training image. 125
Fig. 5.55— Sample realizations generated from the training image using FILTERSIM algorithm. 126
Fig. 5.56— Sample upscaled realizations generated from the training image using FILTERSIM algorithm. 126
Fig. 5.57— VoF PDF and policy histogram for the FILTERSIM generated permeability realizations with renormalization with time. The results for fixed heterogeneity with time (fine scale constant through time) were also added for comparison. 127
Fig. 6.1— Example reservoir models used showing well placement and permeability field. The legend for each model is shown in the upper left corner for the permeability values 131
Fig. 6.2—Probability density function plots for example 1 for PCM by Gaussian quadrature. The number of collocation nodes used is shown in the legend in parenthesis for each approximation order 132
Fig. 6.3—Probability density function plots for example 1 for PCM by linear regression using boxed Fejer sampling. The number of collocation nodes used is shown in the legend in parenthesis for each approximation order. 133
Fig. 6.4—Probability density function plots for example 1 for PCM by linear regression with quadrature sampling. The number of collocation nodes used is shown in the legend in parenthesis for each approximation order. 134
Fig. 6.5—Probability density function plots for example 1 for PCM by linear regression with mapped Fejer sampling. The number of collocation nodes used is shown in the legend in parenthesis for each approximation order. 135
Fig. 6.6— Plots of the first two moments as a function of approximation order for example 1 for multivariate PCM by Gaussian quadrature and linear regression using quadrature (LS+quadrature), Fejer mapped and boxed collocation nodes. (LS: linear regression, HD: high dimensional random input) 136
Fig. 6.7—Probability density function plots for example 1 for PCM by Gaussian quadrature. The number of collocation nodes used is shown in the legend in parenthesis for each approximation order. 137
Fig. 6.8—Probability density function plots for example 1 for PCM by linear regression using quadrature. The number of collocation nodes used is shown in the legend in parenthesis for each approximation order. 138
Fig. 6.9—Probability density function plots for example 1 for PCM by linear regression with boxed Fejer sampling. The number of collocation nodes used is shown in the legend in parenthesis for each approximation order. 139
Fig. 6.10—Probability density function plots for example 1 for PCM by linear regression with mapped Fejer sampling. The number of collocation nodes used is shown in the legend in parenthesis for each approximation order. 140
Fig. 6.11— Plots of the first two moments as a function of approximation order for example 2 for PCM by Gaussian quadrature and linear regression, using quadrature (LS+quadrature), Fejer mapped and boxed collocation nodes. 141
Fig. 6.12— Probability density function plots for example 3 for multivariate PCM by Gaussian quadrature and linear regression using quadrature, Fejer mapping and boxing collocation nodes. The number of collocation nodes used is shown in the legend in parenthesis for each approximation order. 142
Fig. 6.13— Plots of the first two moments as a function of approximation order for example 3 for PCM by Gaussian quadrature and linear regression using quadrature, Fejer mapped and boxed collocation nodes. 143
Fig. 6.14— PDF plots for the modified SPE10 reservoir model for multivariate PCM by Gaussian quadrature and linear regression using quadrature, Fejer Mapped and Boxed collocation nodes. The number of collocation nodes used is shown in the legend in parenthesis for each approximation order. 144
Fig. 6.15— Plots of the first two moments as a function of approximation order for example 4 for PCM by Gaussian quadrature and linear regression using quadrature, Fejer mapped and boxed collocation nodes. 145

Fig. 6.16— Plot of computational time reduction achieved by PCM as a function of PCM order. The Y-axis shows the ratio of the computational time required to run MCS for 1000 realizations as the benchmark to the computational time required to run PCM. [Uni: Univariate, Bi: Bivariate and HD: High Dimensional] _____ *147*
Fig. 7.1— PDF for the option value (i.e. VoF) determined by the LSPCM method using second, third and fourth order collocation nodes compared with that determined by MCS (the original LSM). The number of realizations used is shown in parentheses for each sampling method in the first row. Each row is specific to a reservoir model while each column is specific to the sampling method mentioned at the top of the column. _____ *150*
Fig. 7.2— Histograms of the optimal policy produced by the LSPCM method using second, third and fourth order collocation nodes and compared with that produced by the LSM method. Each row is specific to a reservoir model while each column is specific to the sampling method mentioned at the top of the column. The frequency obtained for the LSPCM generated policy is scaled to the frequency of the LSM (using MCS) generated policy. _____ *152*
Fig. 7.3— RMSE plots as a function of PCM order for the different reservoir models. _____ *153*
Fig. 7.4— Results comparing the performance of the LSPCM algorithm with the LSM algorithm for the homogeneous, PUNQ-S3 and SPE10M reservoir models without incorporating uncertainty in the time series. _____ *154*
Fig. 7.5— VoF PDF plots and optimal policy histograms for the LSPCM generated results for the PUNQ-S3 reservoir model incorporating uncertainty in the time series. Histogram frequency values are scaled to 10^3 realizations. _____ *155*
Fig. 7.6— RMSRE plots as a function of PCM order for the PUNQ-S3 reservoir model incorporating uncertainty in the time series. _____ *156*
Fig. 7.7— Results comparing the performance of the LSPCM algorithm with the LSM algorithm for the PUNQ-S3 reservoir model incorporating uncertainty in the time series. The LSPCM results were obtained using 2^{nd} order mapped Fejer nodes. Realizations are scaled to 10^3 realizations. _____ *157*
Fig. 7.8— Results for embedded decision scenario. The first row shows the PDFs of the option values. The second row shows the optimal policy histograms of the initiation decision and the third row shows the histograms of the optimal embedded policy which is the surfactant slug properties (CS: surfactant concentration). _____ *159*
Fig. 7.9— VoF PDF and policy histograms for the ASP flooding decision evaluation for the PUNQ-S3 reservoir model. The first row shows the PDFs of the VoF. The second row shows the optimal policy histograms of the initiation decision and the third row shows the histograms of the optimal alkaline policy, the frequency is scaled to 10^3 realizations in order to be compared with the LSM generated results. _____ *161*
Fig. 7.10— RMSRE plots as a function of PCM order for the PUNQ-S3 reservoir model for the ASP flooding decision. _____ *162*
Fig. 7.11 —Results comparing the performance of the LSPCM algorithm with the LSM algorithm for the PUNQ-S3 reservoir model for the ASP flooding decision. The LSPCM results were obtained using 3^{rd} order mapped Fejer nodes. _____ *162*

List of Tables

Table 5.1: Range Adjustment Values for S_{orc} and D_s Stochastic Models 84
Table 5.2: Ornstein-Uhlenbeck Process Parameters 87
Table 5.3: Capital Expenditure Data 88
Table 5.4— VoF mean for different static scenarios. 92
Table 5.5— VoF mean for different decision space discretization's. 95
Table 5.6— VoF mean for using mobility control. 105
Table 5.7— VoF mean obtained for the original and clustered regressions. 113
Table 5.8— VoF mean for case study 2 using mobility control. 117
Table 5.9— VoF mean for case study 2 using different well placements. 118
Table 5.10— VoF mean for case study 2 using different permeability fields. 120
Table 5.11— VoF mean for moving average generated permeability. 124
Table 5.12— VoF mean for FILTERSIM generated permeability. 127
Table 6.1 Random input parameters and their distributions 131
Table 7.1 Random input parameters and their distributions 160
Table A1: Homogeneous and SPE Layers (1,5,10,15 and 20) Reservoir Simulation Model Properties 186
Table A2: Immiscible Relative Permeability Data 186
Table A3 Surfactant Viscosity and Surfactant/Oil Surface Tension 187
Table A4: Capillary De-Saturation Curve 187
Table A5: Reservoir Simulation Constraints 187
Table A6 Polymer Properties 187
Table C2: Immiscible Relative Permeability Data 189
Table C2 Simulation Constraints the Case Studies 189
Table G1 Simulation Constraints the Case Studies 193
Table I1 Surfactant/Polymer Adsorption Multipliers as a function of Alkaline Concentration 196
Table I2 Water/Oil Surface Tension Multipliers as a Function of Alkaline Concentration 196

1 Introduction

Increasing oil recovery from existing oil reservoirs around the world has become a priority because of the scarcity of new giant oil field discoveries in recent times. Thus in order to meet the increasing world energy demand it is essential to maximize oil recovery from existing fields in an efficient manner. Oil recovery processes can be categorized into three sequential phases with respect to their recovery mechanism; primary recovery which depends on the existing energy potential of the reservoir (natural depletion), secondary recovery which usually is concerned with applying pressure maintenance techniques (e.g. waterflooding or gas cap) in order to account for the loss of energy and tertiary recovery processes (e.g. chemical or thermal flooding) which aim to recover the remaining oil in place that cannot be recovered using secondary processes. Most oil reservoirs around the world have been producing under secondary recovery processes for many years. With the maturing of the worlds giant oil fields and increasing energy demand, enhanced oil recovery (EOR) processes have received increasing attention recently.

EOR methods are mostly used as tertiary recovery processes. They are usually applied when secondary recovery processes, such as waterflooding, become uneconomical. However, EOR processes have also been used in the secondary recovery stage in conjunction with waterflooding. EOR targets a wide range of crudes with respect to their physical and chemical properties. No single EOR process can be used for all types of crude oil. Furthermore, the diversity of oil reservoirs types complicates EOR application. Given that EOR is usually applied in the secondary or tertiary phase of recovery, the oil saturation profile, distribution and physical state as a result of past production must be considered in designing EOR processes (**Willhite and Green 1998**). Previously, EOR processes were not applied widely due to their relatively high cost and complexity.

Of these processes, surfactant-polymer flooding is considered to have the highest potential in tertiary oil recovery yet it is also the most complex process to implement (**Lake 1989**). This complexity results from the numerous sources of uncertainty that are encountered in surfactant-polymer flooding. One of the main reasons is the resulting poor scale up from laboratory to field implementation (**Gogarty 1976; Lowry et al. 1986; Adams and Schievelbein 1987; Green and Willhite 1998; Stoll et al. 2011**).

Since uncertainty is detrimental to the success of SP flooding, it is essential to take it into consideration in field implementation. Uncertainty can be categorized into technical and economic uncertainty. Technical uncertainty refers to uncertainty in the realization of reservoir parametric or spatial properties and economic uncertainty refers to uncertainty in the oil price and chemical costs.

There were different attempts to model these issues and produce optimal policies for SP or surfactant flooding processes. For instance, decision trees and optimization algorithms were coupled with Monte Carlo sampling to produce decisions given uncertainty (**Barua 1986; Sanz and Miller 1994**). These methods were based on using analytical SP or surfactant flooding models which do not take into consider the transport of the chemical slug through porous media and thus produced simplistic forecasts. Decision trees can also become very complicated very quickly due to the curse of dimensionality and it cannot deal efficiently with a large number of uncertain parameters. Optimization techniques used for decision making can be difficult to implement because they might need access to the numerical simulator code which might not always be possible.

One of the main limitations of these approaches is that they did not consider the effect of uncertainty in the time series of economic and technical state variables. As the realization of these uncertainties evolve through time, the set of decision or control variables need to be modified as information is revealed. This is similar to the time evolution of the realization of reservoir state variables in Ensemble Kalman Filter methods **(Evensen 2007; Aanonsen et al. 2009)**. Due to this behaviour,

it is necessary to incorporate flexibility into the decision making process in order to capitalize on how uncertainty resolves over time.

The main focus of this thesis was an attempt to develop an approach that can value flexibility in decisions as uncertainty varies. The value of flexibility (VoF) is defined as the value of splitting decisions into multiple decisions over time with the opportunity to learn between decisions and having the option to respond to that learning (**Bratvold and Begg 2010)**. Real options theory was considered to be an appropriate tool to meet this requirement because it is based on producing optimal policies conditional on the resolution of uncertainty and recognizes that uncertainty can create value as well as reduce it (**Smith and McCardle 1999; Copeland and Antikarov 2003; Jafarizadeh and Bratvold 2009; Sick and Gamba 2010**). To manage the effects of uncertainty, flexibility is incorporated into the field implementation process. By valuing this flexibility it was desired to produce an optimal policy in the presence of uncertainty.

The method developed incorporated technical and economic uncertainties in a decision making approach. This was inspired by real options theory by adapting the least-squares Monte Carlo (LSM) method to SP flooding. The LSM algorithm consists of a forward stochastic simulation that is coupled with a recursive dynamic programming process and was introduced in the financial mathematics literature. A MATLAB code was written to perform this algorithm by coupling it with a reservoir simulator (ECLIPSE). The code was applied to a variety of stylized reservoir models to test whether it produces meaningful optimal policies. Different sensitivities were also performed to test the different aspects of the algorithm.

Since the LSM algorithm is dependent on Monte Carlo stochastic sampling, this requires a large number of realizations to converge. This incurs significant computational cost due to the use of a reservoir simulator to predict the performance of SP flooding for each stochastic realization of the technical state variables. An attempt to enhance the efficiency of the sampling method in the LSM algorithm was made by incorporating the probabilistic collocation method (PCM) with the LSM algorithm. Using PCM significantly reduces computational requirement by reducing the number of simulation runs because it requires significantly fewer stochastic samples (i.e. significantly less computational time) to cover the distribution of the technical uncertain parameters. Robust quantification of uncertainty for SP flooding using the PCM was attempted. The coupling of the PCM with the LSM algorithm was introduced as the LSPCM algorithm. This was performed on examples and verified using the LSM method as a benchmark. It was then extended to more complex problems.

Chapter two introduces the main EOR processes and then focuses on SP flooding. The different physical phenomena that occur in the reservoir are discussed. The simulation of SP flooding is also discussed with respect to the numerical simulator used in this thesis. A review of SP flooding field implementation is also presented.

A review of decision making methods in E&P is presented in chapter three. A further discussion of decision making methods used previously for SP flooding is also presented. Real options theory is then introduced and its different valuation methods are reviewed. The chapter concludes with the description of the LSM algorithm.

Chapter four discusses the methodology and theoretical background of the LSM algorithm, the PCM approach and the coupling of both approaches. The chapter first introduces the theoretical background of each component and then discusses their implementation with respect to the MATLAB code.

Chapter five discusses initial examples of LSM application using a simple homogeneous reservoir model and a basic decision problem. This is followed by performing different sensitivity analyses to the implementation of the algorithm. The algorithm is then applied to heterogeneous reservoir models using more complex decisions. This chapter consists of some material that was published as a journal paper **(Alkhatib et al. 2013)**.

The PCM is discussed in detail in chapter six. The theoretical background is presented and is followed by example problems. Different sampling methods were used along with two approaches to solve for the coefficients of the output polynomial chaos expansion. The produced results were compared to statistical outputs of Monte Carlo simulation. Some of the results of this chapter have been submitted for peer review.

Chapter seven presents the results of coupling the LSM method with the PCM code. This chapter shows the enhancement of the computational efficiency of the algorithm due to the significant reduction of computational requirement that results from using fewer stochastic samples. The accuracy of the LSPCM algorithm is determined by using the results of the LSM algorithm as a benchmark. The LSPCM algorithm is then applied to more complex decision problems. Some of the results of this chapter have been submitted for peer review.

Chapter eight discusses the main conclusions of this thesis and the recommendations for future work.

2 Enhanced Oil Recovery: Surfactant-Polymer Flooding

Enhanced oil recovery (EOR) methods are mostly used as tertiary recovery processes. They are usually applied when secondary recovery processes, such as waterflooding, become uneconomical. However, EOR processes have also been used in the secondary recovery stage in conjunction with waterflooding. EOR targets a wide range of crudes with respect to their physical and chemical properties. No single EOR process can be used for all types of crude oil. Furthermore, the diversity of oil reservoirs types complicates EOR application. Given that EOR is usually applied in the secondary or tertiary phase of recovery, the oil saturation profile, distribution and physical state as a result of past production must be considered in designing EOR processes (**Willhite and Green 1998**).

There are three main categories of EOR: thermal, chemical and solvent methods (**Lake 1989**). The main oil recovery mechanisms for solvent methods are extraction, vaporization, dissolution, solubilization and condensation. These processes could also lead to secondary oil recovery mechanisms such as oil swelling, solution gas drive and reduction of viscosity. CO_2 flooding is an example of a solvent EOR method. Thermal EOR methods are considered to be the most commercially successful. The main recovery mechanism is the reduction of oil viscosity as temperature is increased. Steam drive process is an example of thermal EOR methods. Chemical methods generally cover a number of recovery mechanisms: mobility ratio adjustment through polymer flooding, interfacial tension reduction through injecting surface-active agents (i.e. surfactants), and wettability reversal through alkaline or surfactant flooding. A combination of these processes could also be used such as surfactant-polymer flooding or alkaline-surfactant-polymer flooding (**Lake 1989**).

Some EOR methods have been commercially applied for some time such as thermal recovery. Other methods, such as surfactant-polymer (SP) flooding have not been as successful although, theoretically and experimentally it can achieve a significant increase in oil recovery. A main reason for this is that there are many sources of uncertainty when the process is scaled from lab to field application (**Gogarty 1976; Lowry et al. 1986; Adams and Schievelbein 1987; Green and Willhite 1998; Stoll et al. 2011)**.

SP flooding is implemented by injecting a surfactant slug that is followed by a polymer bank to maintain sweep efficiency. Its main recovery mechanism is via interfacial tension (IFT) reduction between the oil and water phases in the reservoir which results in a miscible phase that can theoretically achieve 100% displacement of residual oil (**Carcona 1992).** This occurs because reducing the IFT reduces the capillary forces that trap the oil in the reservoir (**Lake 1989**). There are many factors that control the efficiency of this process. These are discussed below.

In this chapter, SP flooding is introduced and the recovery mechanism of SP flooding is discussed. The different elements and factors that affect the oil recovery of SP flooding are reviewed as well. Numerical simulation methods that are used to produce predictive forecasts for SP flooding are also discussed briefly with a focus on the description of ECLIPSE(**Schlumberger 2010**) which was used for this thesis. The sources of uncertainty in SP flooding are then introduced and reviewed.

2.1 Surfactants Chemistry and Structure

There are four main types of surfactants: anionic, cationic, nonionic and amphoteric. This categorization is based on the polarity of the surfactant. The anionic surfactants, such as sulfonates, are the most commonly used surfactants in EOR due to their good performance and relative stability (**Lake 1989**). Surfactants usually consist of a polar and a non-polar portion. The polar or hydrophile portion interacts strongly with water molecules thus undergoing solvation, whereas the non-polar or hydrophobic portion interacts weakly with water molecules. (**Green and Willhite 1998).**

The structure of the suflonates that are used for EOR applications is conditional on the feedstock chemical composition, the number of sulfonate groups that are attached to each molecule and the degree of sulfonation. Feedstock molecular weights are usually in the range from 350 to 450. (**Green and Willhite 1998)**.

As the concentration of the surfactant in the solvent increases, the dissolved surfactant molecules (monomers) tend to aggregate. Once the concentration reaches a critical threshold known as the critical micelle concentration (CMC), any further increase in surfactants in the solvent leads to formation of micelles while the concentration of the monomers remains constant. At the CMC, some of the solution properties vary abruptly as a function of surfactant concentration. The main properties that change are the surface tension, electrical conductivity and osmotic pressure. A microemulsion is a micellar solution of the solvent and an immiscible phase. This is a liquid phase that consists of oil, water and surfactant. The microemulsions can be either water-external or hydrocarbon-external, where the external phase is known as the continuous phase (**Green and Willhite 1998**).

Harwell et al. (1984) argue that for wide variations in molecular weight and surfactant type, having large-PV slugs exhibits the greatest chromatographic stability. They suggested the use of the lowest concentration-highest PV slug given it achieves the ultralow IFT.

2.2 IFT Reduction

IFT is a function of salinity, temperature, surfactant type, surfactant concentration, surfactant purity and the nature of the hydrocarbon phase. A detailed discussion of the IFT reduction mechanism by surfactants is present in **Green and Willhite (1998).** The interfacial tension also depends on interfacial charge, viscosity and wettability. The desired ultra-low interfacial tension is obtained at specific surfactant concentration. This depends on many factors including oil chain length, salt concentration, surfactant molecular structure and average molecular weight (**Donaldson et al. 1989). Fig. 2.1** depicts IFT and the solubility parameters as a function of salinity.

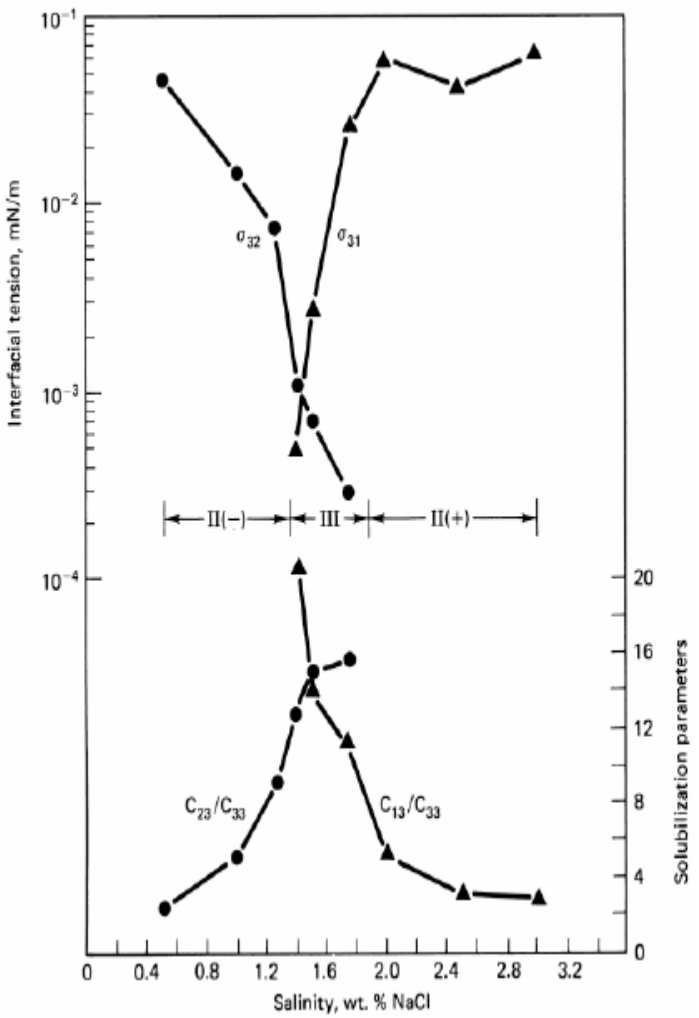


Fig. 2.1— The effect of salinity on IFT and solubiliztion of surfactant. C_{23}/ C_{33} refers to solubilization parameter between the mircoemulsion-oleic phases (for type II(-) and III phase behavior) and C_{13}/C_{33} refers to solubilization parameter between the microemulsion-aqueous phases (for type II(+) and III phase behavior). This figure is reproduced from Lake (1989).

Usually, there is a sharp reduction in the IFT as the concentration of the surfactant increases until it reaches the CMC. After the CMC, there is little change in the IFT because the excess surfactant contributes only to micelle formation and not to the concentration at the water/hydrocarbon interface. The behavior is different for petroleum sulfonates (which are mixtures) compared with single component surfactant systems. For petroleum sulfonates, the IFT decreases significantly at concentrations higher than the CMC (**Green and Willhite 1998)**.

The capillary number which is a function of IFT controls the amount of residual oil that remains in the reservoir. This entity illustrates the effect of reduced IFT on oil recovery. The capillary number, which is a dimensionless entity, is defined as:

$$N_c = \frac{\mu v}{\sigma} \qquad \text{(Eq. 2.1)}$$

, where μ is the viscosity, σ is the IFT and v is the interstitial velocity. Thus, as the IFT is reduced, N_c increases and leads to a reduction in the residual oil saturation. See **Fig. 2.2** which illustrates the residual oil saturation as a function of N_c.

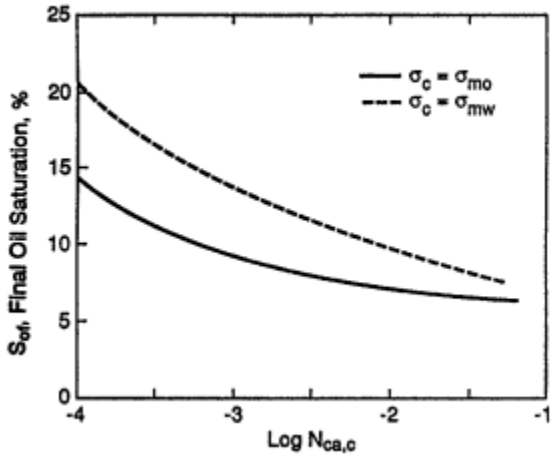


Fig. 2.2– The effect of the log of capillary number on final residual oil saturation. This is based on the correlation by Healy and Reed (1977). σ_{mo} is the microemulsion-oil interfacial tension and σ_{mw} is the microemulsion-water interfacial tension. Reproduced from Green and Willhite (1998).

2.3 Phase Behaviour

Microemulsion phase behavior is complex and is a function of numerous parameters such as the concentrations and types of surfactants, cosurfactants, hydrocarbons, and brine pressure and temperature. The phase behavior is measured experimentally as there are no universal equations of state for microemulsions. The results are usually depicted in graphical form. Typical microemulsions consist of at least five main components: hydrocarbon, surfactant, cosurfactant, water and NaCl (salt). The effect of each component has to be determined for a range of compositions in order to rigorously study phase behavior. Due to time and economic constraints, the number of components is usually reduced via psuedocomponents which combine one or more component. The brine pseudocomponent combines water and NaCl. In this case the microemulsion will consist of four components and a quaternary diagram is used to represent the phase behavior. By introducing another psuedocomponent, combining the surfactant and cosurfactant, it is possible to use a psuedoternary diagram to represent the phase behavior **(Green and Willhite 1998).**

2.3.1 Effect of Salinity

The effect of brine salinity is significant on phase behavior. This is due to the reduction in surfactant solubility as the salinity of an aqueous phase is increased. (**Green and Willhite 1998**).

At low brine salinity, surfactant exhibits good aqueous phase solubility and poor oil-phase solubility. Two phases will exist, a pure oil phase and a water-external microemulsion phases. The tie lines in the corresponding ternary diagram are negative, this is known as a type II(-) system. An extraction mechanism in oil recovery is possible due to the induced solubility of oil in the brine rich phase. However, this is relatively small compared with IFT reduction. At high brine salinity, the surfactants solubility is drastically reduced in the aqueous phase due to electrostatic forces. The two phases that exist in this system are an excess brine phase and an oil-external microemulsion phase. This is known as an upper-phase microemulsion, type II(+) system (since the tie lines have a positive slope). At intermediate salinity, the solubility of the surfactant in the oil and brine rich phases is never equal. A third surfactant rich phase is formed over a range of salinities. An excess oil (II(-)), excess brine (II(+)) and a microemulsion phase exist. This is defined as a type III system or a middle phase microemulsion. There are two

IFTs in this region, an IFT between the oil and microemulsion and one between with water and microemulsion. During the shift from type II(-) to type II(+), the surfactant concentration in the microemulsion phase reaches a minimum where the brine-oil ration at the invariant point is 1. The invariant point is where the microemulson exists on the ternary diagram. This migration of the invariant point means that the solubility of brine and oil in a single phase is unlimited. It is important to note that the salinity at which the phases invert is not necessarily the optimal salinity. Also, there are other variables that can cause the phase environment shifts other than brine salinity. Any condition change which enhances the surfactants oil solubility shifts the system from type II(-) to II(+) (**Lake 1989).** The effect of salinity on phase behavior is illustrated in **Fig. 2.3**. A model developed by **Knickerbocker et al. (1982)** describes the evolution of the three phase region as a function of one principal variable (e.g. salinity).

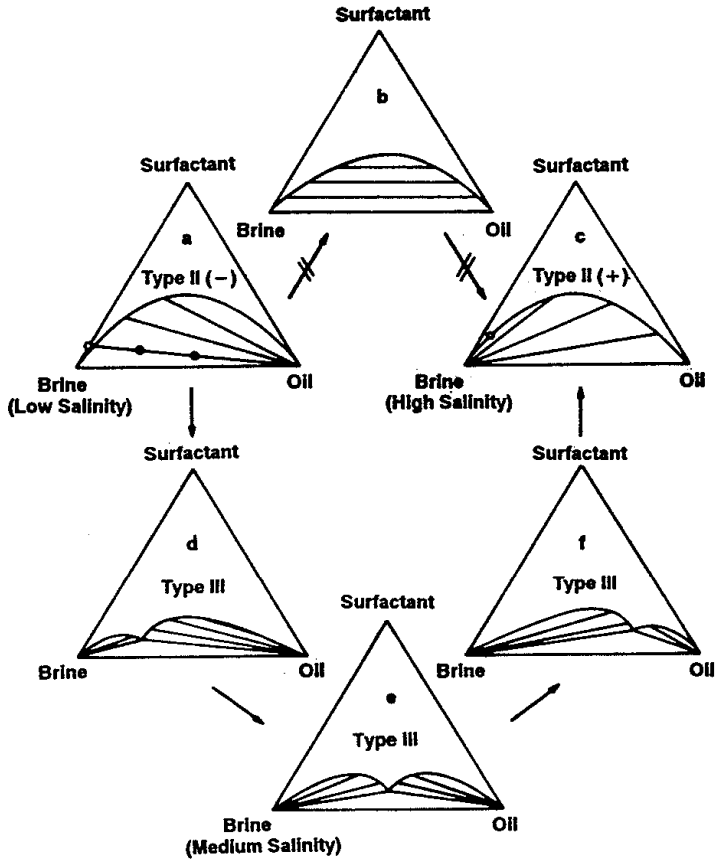


Fig. 2.3– The effect of salinity on a generalized phase diagrams. Reproduced from Green and Willhite (1998).

The previous description of phase behavior is based on ideal behavior. In reality, the micellar systems do deviate from this ideal behavior. Usually, the multiphase region will contain several middle phase compositions. Pseudocomponents such as brine might partition into different phases in different ratios. Furthermore, other phases can exist under some conditions such as gel-like phases when polymer is present in the micellar solution **(Green and Willhite 1998).** These other phases usually occur at high surfactant concentrations, at low temperatures or in the presence of pure surfactants. These can be described as condensed form phases such as high viscosity liquid crystals which exhibit large viscosity. This could be detrimental to the oil recovery as it can cause viscous instabilities during displacement or it could result in decreased injectivity (**Lake 1989).**

2.3.2 IFT and Phase Behavior

The IFT between the equilibrium phases is strongly correlated with the phase behavior of microemulsion systems. Thus the IFT is a function of salinity (**Green and Willhite 1998)**. When salinity increases, the phase behavior progresses from a lower to middle to an upper phase system which results in a reduction of IFT between the microemulsion phase and the excess oil phase. This is due to an increase in the solubilization of oil. IFT between the microemulsion phase and the excess brine phase increases with this progression as water is expelled from the microemulsion phase which is due to decreased water solubilization in the microemulsion phase. When IFT between the microemulsion phase and the excess oil phase equals the IFT between the microemulsion phase and the excess brine phase, this is known as the optimal IFT salinity. This usually coincides with the phase behavior optimal salinity (**Green and Willhite 1998).** This is useful because measuring IFTs is quite difficult whereas solubilization measurements are relatively easy. **Healy et al. (1976), Nelson (1982) and Huh (1979)** proposed different equations that describe the correlation of IFT and solubilization parameters. These have been verified experimentally by **Glinsmann** (1979) and **Graciaa et al.** (1982). The optimal phase behavior salinity is the same as the maximum oil recovery salinity. However, the optimal salinity does not correspond to the minimum surfactant retention salinity (**Lake 1989)**.

Due to dilution effect, the maximum oil recovery occurs when the electrolyte, surfactant and cosurfactant concentrations achieve the maximum solubilization parameters. Therefore there are optimal conditions and not only optimal salinity (which is an intrinsic property of the oil-brine-surfactant combination), even though the latter has been emphasized greatly in the literature **(Lake 1989)**.

2.3.3 Variables that Affect IFT and Phase Behavior

Surfactant structure does have an effect on IFT. It was found that the lowest IFT's were obtained for petroleum sulfonates with equivalent weights between 400 to 450 (**Green and Willhite 1998).** Oil solubility can be increased by increasing the nonpolar end of the surfactant. This can be done by reducing the tail branching, increasing the nonpolar molecular weight, reducing the number of polar portions of the surfactant and reducing the polar strength. The competition between the lipophile and hydropohile portions of the surfactant indicate oil solubility by two common measures: surfactant charge density (which is the number of dissociated ions/molecule divided by the molecular size) and the hydrophilie-lipophile balance (HLB) number. The surfactant brine solubility increases as the charge density increases. Both measures are difficult to use for petroleum sulfonates due to the many species that they contain (**Lake 1989**).

Hydrocarbon composition does have an effect on phase behavior and correspondingly IFT. Different approaches were suggested to correlate the hydrocarbon composition with phase behavior such as the equivalent alkane carbon number and a three-parameter correlation of **Puerto and Reed (1983)**. In general, as oil polarity increases, this makes it a better solvent for surfactant. Low surfactant solubility occurs when using high specific gravity oils that are usually rich in organic acids and also when using low specific volume crudes (**Lake 1989**).

The type and concentration of cosurfactants do affect the phase behavior, IFT and the viscosity of the micellar system. Adding alcohol can decrease solubilization of oil and water in the microemulsions which increases the minimum IFT that is obtained with surfactants. The addition of alcohols as cosolvents can be avoided if surfactants with branched hydrocarbon chains are used, by adding ethylene oxide to the surfactant or by using surfactant mixtures of different hydrocarbon-chain lengths or structures. These are possible for temperatures below 60^{o}C. These measures resist the tendency to form condensed surfactant films by the long, straight hydrocarbon chains (usually of nearly equal length). As for higher temperatures, a more-

flexible surfactant film is promoted due to increased thermal motion. This also supports the disruption of ordered structures, although the elimination of the viscous phases and emulsion does not always occur. Using branched hydrocarbon chains that minimize (or eliminate) the alcohol requirements is also a possible strategy. Surfactant stability for temperatures below 60^{o}C can be maintained for the long-term given that calcium concentrations are not too high and that the pH is at slightly alkaline levels. This limits the hydrolysis of the sulfate surfactants. For higher temperature reservoirs, sulfonates or carboxylates are needed **(Hirasaki et al. 2011)**. Most recent research focused on EOR in sandstone reservoirs due to the high-divalent-ion environment of carbonate reservoirs, which can cause high retention of petroleum or synthetic sulfonates. Recent studies on carbonate reservoirs show that by adding ethoxy groups, it is possible to increase the tolerance to divalent ions **(Hirasaki et al. 2011).**

If the temperature increases, the solubilization parameters decrease. This increases the IFT and increases the optimal salinity. The phase behavior shifts from an upper to middle to lower phase system (**Green and Willhite 1998)**. Since the micellar systems are all-liquid processes, pressure has negligible effect (Lake 1989; **Green and Willhite 1998)**. Mobility control of the micellar slug is achieved by adding polymer to the micellar slug. The phase behavior and IFT can be affected by the polymer due to dispersion which causes mixing at the micellar/polymer slug interface. More details can be found in **Pope et al. (1982).**

Phase behavior is an important aspect of SP flooding that needs to be considered when designing SP processes. The purpose here was to explain phase behavior and illustrate how it can affect IFT reduction. However, phase behavior is not modeled directly by ECLIPSE. A discussion of how ECLIPSE works is presented in section 2.7.

2.4 Retention

Surfactant loss or retention in porous media is detrimental to the success of the EOR process because it reduces the amount of surfactant flowing through the reservoir and thus reduces the amount of residual oil that can be recovered (**Glover et al. 1979; Friedmann 1986**; **Lake 1989; Green and Willhite 1998; Al-Sulaimani et al. 2012;)**. Surfactant retention also varies between the lab and field tests (**Green and Willhite 1998**). Therefore, retention is an important design aspect of SP flooding. Usually the total surfactant loss is used without specifying which loss mechanism occurred. The main surfactant loss mechanisms can be summarized as the following:

2.4.1 Adsorption

Adsorption is a function of surfactant concentration, equivalent weight and type, rock minerals, clay content, temperature, flow rate and redox conditions. For surfactant mixtures of different equivalent weight compounds, the different surfactant species will separate due differential adsorption where higher-equivalent weight species will adsorb more readily. Usually adsorption increases with surfactant concentration until it reaches a maximum after which it becomes negligible as surfactant concentration continues to increase (**Green and Willhite 1998)**. Langmuir-type isotherms are used to reproduce the main features of surfactant adsorption isotherms (**Sheng 2011**). See **Fig. 2.4** for an illustration of adsorption as a function of concentration.

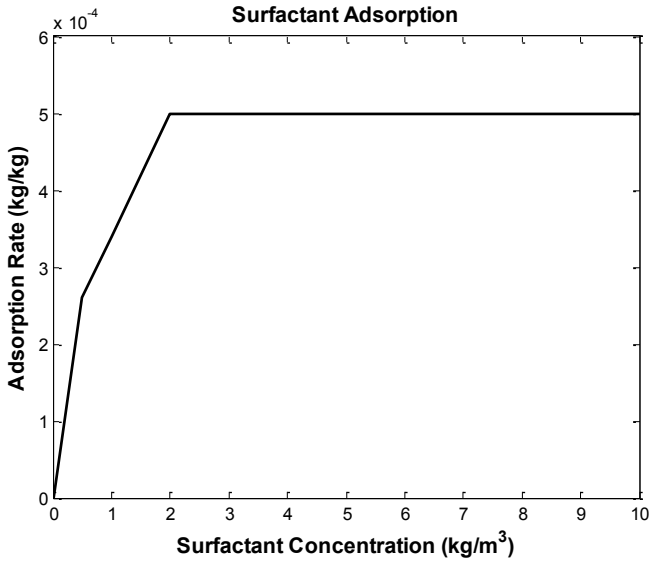


Fig. 2.4– Surfactant adsorption as a function of surfactant concentration. This is based on stylized data.

2.4.2 Ionic Exchange

Due to the ionic nature of the clays in the reservoir rock, the ionic components (e.g. anionic surfactant) in the micellar slug can be exchanged. This can significantly affect the composition of the micellar slug. As an example, if Ca ions are exchanged with the surfactant slug, this results in a shift from a lower phase that has effective oil displacement to an upper phase microemulsion which can be trapped by the mobility buffer (**Green and Willhite 1998)**. The effect of divalent cations is more pronounced than monovalent cations. Usually low-salinity prefulshes are implemented in order to unload the divalent cations from the clays (**Lake 1989**). An early treatment of ion exchange effect on surfactant flooding is presented by **Hirasaki (1982).**

2.4.3 Precipitation

Precipitation is the result of phase separation of surfactant and cosurfactants and of chromatographic separation of different surfactant species. This occurs due to the presence of multivalent ions. Notably, surfactant-divalent complexes form which have low solubility in brine and thus precipitate (**Lake** 1989). Precipitation is a complex process and it is difficult to predict (**Green and Willhite 1998)**.

2.4.4 Phase Entrapment

This mechanism is based on the partitioning of surfactant into all liquid phases present in the system. If the oil is present in a type II(+) system, the surfactant partitions to the oleic phase which is relatively slow in a displacement. As a result the surfactant is removed from the displacement front due to this phase trapping which results in poor efficiency. Other sources of phase trapping occur due to shifts in phase boundaries which are caused by ion exchange. This is usually of the same order of magnitude as adsorption (**Green and Willhite 1998).** This form of surfactant loss is related to multiphase flow **(Sheng 2011**).

2.5 Mobility Control

Mobility control is considered to be one of the most important concepts in any EOR process because it improves the volumetric sweep efficiency of the displacement process and maintains the integrity of the chemical slug flowing through the reservoir (**Sheng 2011**). It is desired to reduce the mobility ratio to less than or equal to one. This is done by adding chemicals (polymer) to the injected fluid which increase the apparent viscosity of the fluid and can reduce the effective permeability of the reservoir to the injected fluid (**Green and Willhite 1998)**. **Sheng (2011)** suggests that for mobility control, the displacing fluid mobility should only be related to the mobility of the displaced oil phase rather than the total mobility of the displaced phases or fluids.

Mobility control for surfactant flooding is essential. The surfactant slug requires mobility control in order to prevent fingering of the surfactant into the oil/water bank which can result in dissipation of the surfactant slug due to dispersive mixing. Furthermore, dissipation of the surfactant slug via mixing with the mobility buffer (polymer bank) is minimized by mobility control. Finally, the drive water is prevented by mobility control from fingering through the polymer bank reaching the surfactant slug (**Green and Willhite 1998)**.

2.5.1 Polymer

There are two main polymer types that have been used for EOR application: polyacrylamides and polysaccharides (biopolymers). Polyacrylamides used in polymer flooding are partially hydrolysed. This causes the anion carboxyl groups to be located along the backbone chain. Thus the hydrolyzed polyacrylamides are negatively charged and the degree of hydrolysis is usually between 30% and 35%. The degree of hydrolysis is chosen in order to optimize water solubility, retention and viscosity. For instance, if the hydrolysis is too large, it will be more sensitive to hardness and salinity (**Shupe 1981)**, if it is too small then the polymer will not solubilize in water. Viscosity is increased by the large molecular weight of polyacrylamdies. This is more pronounced by the anionic repulsion that occurs between the polymer molecules and between other segments on the same molecule. This leads to elongation of molecules in the solution which ultimately entangle with other elongated molecules. This accentuates the mobility reduction as concentration increases. However, this repulsion effect is reduced if brine salinity or hardness is high. Polysaccharides are formed by the polymerization of saccharide molecules via a bacterial fermentation process. This polymer type is susceptible to bacterial attack which cause degradation of the polymer viscosity effect. However, its main advantage is that it is insensitive to brine salinity and hardness because it is relatively nonionic (**Lake 1989)**. Polymer stability at reservoir conditions is necessary for EOR application. Polymer degradation can occur due to oxidation, thermal instability, reservoir brine salinity and hardness and bacterial attack (**Green and Willhite 1998)**.

2.5.2 Retention

Adsorption and mechanical entrapment are the primary causes of retention of polymer molecules in porous media. Usually, polymer retention is considered instantaneous and irreversible. Retention is measured experimentally and can be correlated using Langmuir-type isotherms. One consequence of retention is permeability reduction. This is a function of polymer type, amount retained, pore-size distribution and the average size of polymer molecules relative to reservoir pores (**Green and Willhite 1998)**.

2.5.3 Viscosity

Polymer solutions often exhibit non-Newtonian rheological behavior. Usually, in EOR applications, the polymer solution viscosity decreases with increasing shear rate. This is known as shear thinning behavior. Because the polymer molecules reduce internal friction by aligning with the shear field, the apparent viscosity is reduced. Due to the structure of polyacyrlamides, salinity and divalent-ion content can influence the rheological behavior of the polymer solution, whereas viscosities of biopolymers are less affected by salinity and divalent ion content. Shear thinning polymer mobility can be obtained by using correlations of experimental data (**Green and Willhite 1998)**. When frontal-advance rates are high, polyacrylamides become more viscous with increasing flow rate; this is defined as shear thickening. This is a function of temperature, salinity, permeability, molecular weight and polymer concentration. Shear degradation occurs when flexible polymer molecules (e.g. polyacrylamides) are subjected to high shear rates. This leads to a rupture of the polymer chain which affects viscosity (**Lake 1989; Green and Willhite 1998**).

2.5.4 Mobility Control Design

The mobility-control design is based on selecting the properties of the injected fluids that produce a mobility ratio of unity. Based on **Gogarty et al. (1970)** it is suggested that the design mobility of the oil/water bank should be chosen as the minimum total relative mobility which is encountered over the saturation range of the oil/water bank. After determining the design mobility for the oil/water bank, it is possible to determine the mobility requirements for the mobility buffer and the surfactant slug. In order to have mobility control at the surfactant/oil-bank interface, the relative mobility of the surfactant slug must be designed to be less than or equal to the design mobility. The surfactant slug mobility is controlled by adjusting its viscosity which can be done by adding polymer. As for the mobility buffer (the polymer bank), it must be immiscible with the chemical slug in order to avoid trapping the surfactant slug as a residual saturation. Mobility control is achieved when the polymer concentration is increased so that unit mobility exists between the surfactant slug and the leading edge of the mobility buffer. The mobility of the polymer bank is controlled by adjusting the polymer concentration (**Green and Willhite 1998)**. **Fig. 2.5** shows the effect of adding polymer to a surfactant core flood on oil recovery.

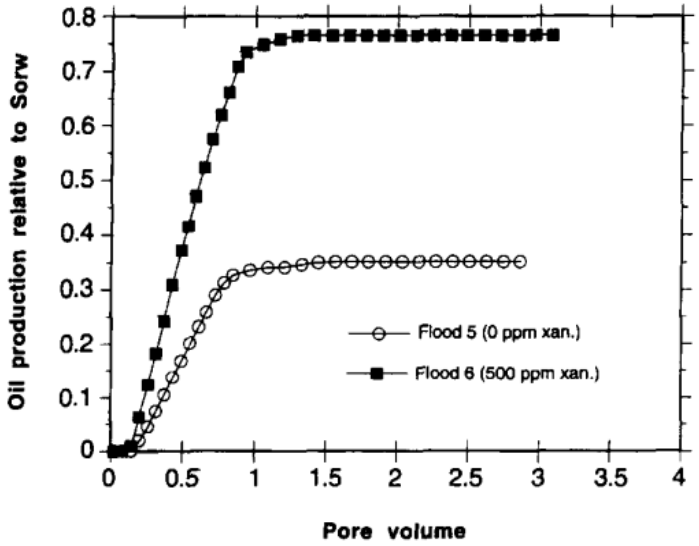


Fig. 2.5– Effect of adding polymer to a surfactant flood on oil recovery. This is based on adding a 500ppm polymer slug to surfactant core flood using a Bentheim core (Reproduced from Taugbol et al. 1995).

2.5.5 Surfactant-Polymer Interaction and Compatibility

There are compatibility issues when surfactant and polymer are injected in the same slug. Polymer is sometimes injected prior to surfactant for conformance improvement or as a sacrificial agent for adsorption. Polymer can be injected behind surfactant in order to avoid fingering in the surfactant slug by the chase water. Even when polymer is not injected in the same slug with surfactant, mixing will occur at their interface due to dispersion and diffusion (**Sheng et al. 2011**). The inaccessible pore volume of polymers can make the polymer mix with the surfactant when it is injected behind the surfactant. This behavior is known as surfactant-polymer interaction or incompatibility (**Trushenskie et al. (1974, 1977) and Szabo (1979)**). What follows is a summary of the some of the main observations of the surfactant-polymer interaction.

Surfactant can exist in oleic, aqueous or middle microemulsion phase. Almost all the polymer in surfactant-polymer solution exists in the most aqueous phase (**Szabo 1979; Nelson 1981**). The effect of IFT values slightly vary, if at all, with or without polymer. The optimum salinity decreases slightly in the presence of polymer (**Healy et al. 1976; Pope et al. 1982**). In the absence of oil, the IFT between the surfactant-rich phase and the polymer-rich phase can be very low **(Szabo 1979**). This indicates the trapping of sulfonates occurs due to the difference in mobilities of the separated phases rather than the capillary force (**Trushenski 1977**).

The oil-free surfactant rich phase exhibits high viscosity. This is usually higher than the polymer rich phase. This occurs even though there is no polymer (**Szabo 1979; Pope et al. 1982**). The polymer is expelled by the surfactant rich phase to the polymer rich phase (**Szabo 1979**). For systems with oil, the effect of polymer increases the viscosity of only the water rich phase. It has little effect on the microemulsion phase except when it is the water rich phase (**Pope et al. 1982**).

There are two polymer related critical concentrations when polymer is mixed with a surfactant system: the CMC_2 and CAC. The CMC_2 is concentration of surfactant at which micelles form in the presence of polymer, this is higher than CMC (**Li et al. 2002**). The CAC is the critical adsorption concentration when the surfactant begins to adsorb on polymer chains, this is lower than CMC. CMC_2 and CAC are on the order of magnitude of CMC. Polymer viscosity is influenced by surfactants in two ways: surfactant brings cations (e.g. NA+) to reduce polymer viscosity and aggregates are formed when surfactant is added which increases polymer viscosity. Hydrophobic associating polymers are very sensitive to surfactant concentration (**Sheng 2011)**.

Polymer preflush was found to improve vertical conformance of surfactant solution which increases recovery (**Gogarty 1983a, 1983b**). Polymer preflush improves SP flooding recovery when a high concentration surfactant solution is used (**Murtada and Marx 1982**). Injection of polymer slug prior to surfactant slug can lead to higher experimental recovery than mixing surfactant and polymer slug because the surfactant-polymer interaction problems seem to be mitigated (**Chen and Pu 2006**).

There are many factors that affect the surfactant-polymer interaction. The most important are the electrolyte concentration, the addition of cosovlents, the oil type, competitive adsorption and polymer IPV, and phase trapping.

The effect of electrolyte concentration

Lowering salinity of the polymer slug behind the surfactant slug is favorable to phase stability (**Trushenski 1977**). Oil displacement efficiency decreases when polymer water salinity increases (**Trushenski 1977; Szabo 1979**). The two phase

region that exists in the equal salinity surfactant-polymer system is much larger than if the polymer salinity was lower. By adding cosolvent to the polymer slug it is possible to eliminate phase separation (**Sheng 2011**).

In order to maintain a favorable mobility ratio, it is essential to include polymer in the surfactant slug because surfactant results in an increase of water relative permeability. Thus it is desired to counter this increase by reducing the aqueous mobility with polymer (**Hirasaki and Pope 1974**). In the absence of polymer in the surfactant slug, the surfactant will finger into the oil bank which results in poor reservoir sweep. Another advantage of using polymer in the slug and drive is that it can help mitigate the effects of permeability variation and improve overall sweep efficiency. Acceptable core flood results without polymer can be misleading in regards to field performance because homogeneous cores only show some of the benefits of adding polymer, not all (**Hirasaki et al. 2006**).

The Effect of Adding Cosolvent

Surfactant solubility can be increased by using low-carbon alcohols. Thus surfactant-polymer interaction can be mitigated by adding cosolvents. The effect of alcohols on the compatibility of surfactant-polymer systems is complex. Compatibility cannot be improved by all alcohols (**Sheng 2011**).

The Effect of Oil Type

By adding oil to the surfactant and polymer solution, this results in an oil-in-water microemulsion (nearly spherical drops). Within a certain range, the amount of oil needed to formulate the single phases with polymer that support mobility control is reduced as the molecular weight of oil is increased (**Hirasaki et al. 2008)**.

The Effect of Polymer IPV and Competitive Adsorption

Surfactant-polymer interaction occurs when surfactant and polymer are injected in the same slug and when surfactant is injected prior to the polymer slug. If surfactant is injected ahead of polymer then adsorption sites are occupied by surfactant. This reduces polymer adsorption. This effect is known as competitive adsorption (**Sheng 2011**). Usually, inaccessible pore volume is greater than adsorption loss of polymers (**Trushenski et al. 1974**). Polymer may penetrate the surfactant slug that is ahead of it due to competitive adsorption and IPV.

The Effect of Phase Trapping

Trushenski (1977) showed that for surfactant-polymer processes, polymer presence in the surfactant slug can cause an increase in surfactant loss. This was due to polymer bypassing the surfactant, which is known as phase trapping.

2.6 Design Considerations

In order to perform an efficient SP flood, the following criteria should be met: low IFT between the oil bank and the primary chemical slug and between the mobility buffer and the primary chemical slug, favorable mobility ratio between the oil bank and the chemical slug and between the mobility buffer and primary chemical slug, and the maintenance of the chemical slug integrity (**Green and Willhite 1998**).

Initially, the flood is designed to have the lowest retention possible by minimizing chemical and physical adsorption and eliminating phase trapping (propagation of slug in low-salinity environment). Using sacrificial agents and cosurfactant in preflush is also appropriate. The other limiting factors are surfactant concentration and slug size. Concentration is required to

be sufficient enough to produce a type III region under optimal salinity and minimized to a level where it can be easily handled and transported by being in a single phase and moderate viscosity. It is important to note that very small slugs might be sensitive to dispersive mixing in the reservoir. Slug size must be large enough to be more than retention. This is dependent on economics and reservoir characteristics (**Lake 1989)**. The slug must be less mobile than the oil bank in order to prevent fingering. Also the buffer mobility needs to be designed in tandem with the slug mobility. Total relative mobility curves can be used to find initial mobility control values (**Lake 1989)**. **Hirasaki et al. (2011)** suggest that injecting alcohol as a cosurfactant is not always necessary.

Sheng (2011) argues that it is best to start the SP flooding process as early as possible, however this is usually inapplicable due to the long preparation time that is required for designing chemical floods, the higher technical requirement needs, and because reservoir characterization usually requires early waterflood history.

The literature is rich with laboratory and field applications. A brief review of some of these applications over the past few decades is presented below.

2.6.1 Laboratory Results

Designing a micellar process usually requires significant laboratory work (**Green and Willhite 1998**). This is the only way to obtain the optimal conditions to perform the EOR process. Once the surfactant selection, phase behavior and IFT measurements are performed, coreflood experiments are conducted using the most promising systems. With regards to optimal salinity design, three main approaches can be followed:

- Adjusting the optimal salinity of the chemical slug to be equal to the resident brine salinity of the reservoir. If this salinity is high, then it is recommended to use salinity tolerant synthetic surfactants (**Lake 1989**).
- Adjusting the reservoir salinity by applying a preflush prior to the chemical slug. However this usually requires a large volume and it does not always prevent the mixing of the chemical slug with the original reservoir brine (**Lake 1989**).
- Applying a salinity gradient design **(Hirasaki et al. 1983)** to optimize recovery. This is achieved by having an overoptimal resident brine and an underoptimal mobility buffer salinity. This minimizes retention, supports the polymer in the mobility buffer, makes it insensitive to surfactant dilution effect and resilient to design and process uncertainties (**Lake 1989)**.

Chemical slug concentration and pore volume are also important design parameters where two strategies exist: large pore volume with low chemical concentration and small pore volume with high chemical concentration slugs (**Green and Willhite 1998)**. **Michels et al. (1996)** support the use of low concentration slugs instead of the high concentration approach because this would lead to high surfactant concentrations in the microemulsions which delays the propagation of the surfactant. This also leads to an increase in viscosity which can cause displacement stability problems. **Wellington and Richardson (1997)** also present experimental results for low surfactant concentration slugs.

In a review of results of more than 40 core floods for surfactant-polymer flooding, it was found that there exists an optimal surfactant IFT and polymer viscosity for the process, although these were not the absolute minimum or maximum values respectively (**Wang et al. 2010)**. This optimized surfactant-polymer system improves oil recovery more than systems that have the lowest IFT, due to improved sweep efficiency. Emulsification and emulsion trapping might be one reason for the

optimized surfactant-polymer system critical values. **Wang et al. (2010)** suggests that for heterogeneous reservoirs, it is best to balance sweep efficiency and displacement efficiency in order to achieve maximum recovery.

Most laboratory and field applications were performed on sandstone reservoirs. The application of surfactant flooding in mixed/oil-wet fractured carbonate reservoir is desired because the waterflooding recovery is usually poor. Recent experimental efforts were performed by **Seethepalli et al. (2004)**. The need for experimental study of time-dependent (i.e. dynamic) IFT behavior at reservoir conditions such as high temperatures and pressures is also suggested (**Xu et al. 2008)**. **Tabary et al. (2012)** discuss the design of a surfactant-polymer flood for a reservoir with hard brine. Because of the high content of divalent ions (especially calcium), this makes the use of alkalis irrelevant. Conventional strategies such as salinity gradient (usually applied to soft brine situations) fail for hard brine scenario due to the high adsorption of chemicals. This was demonstrated via corefloods. An alternative strategy was proposed, this was based on using specific adsorption inhibitors. Design of surfactants that can tolerate high salinities and high temperature systems is another approach to mitigate harsh conditions (**Puerto et al. 2012).**

2.6.2 Field Implementation

The application of surfactant-polymer flooding was limited due to the complexity and high cost of the process. A field-scale commercial application by Marathon Oil Co. known as the M-1 project (**Howell and Thomas 1980**) achieved significantly lower recoveries compared with those predicted by laboratory studies. This was attributed to salinity or hardness effects and poor volumetric sweep. Another commercial scale application was performed by Conoco at the Big Muddy Field (**Ferrell et al. 1988)**. This also achieved significantly lower recoveries than those predicted. This was attributed to the migration of displacing fluids from the project area due to poor completion and natural fractures. The Loudon field tests (**Bragg et al. 1982)** by Exxon also produced significantly lower oil recovery compared with the predicted values. This was due to the polymer drive bank failure to propagate through the reservoir as intended (**Green and Willhite 1998)**. These tests were conducted on sandstone reservoirs. **Howell et al. (1979), Taggart and Russell (1981) , Holm (1982) and Widmyer et al. (1988)** describe different field applications of surfactant-polymer flooding which achieved relatively good results. **Adams and Schievelbein (1987)** discuss one of the earliest applications of surfactant flooding in carbonate reservoirs. Two-well configurations were used for a dolomite reservoir in west Texas. The tests measured the tertiary oil potential of the reservoir. The results achieved significant oil recovery and shows that it is possible to implement surfactant flooding in low permeability carbonate reservoirs.

Hammershaimb et al. (1983) summarize the results from a number of surfactant floods. Initial recovery expectations were high and actual recovery from large scale field tests were found to be lower and more delayed than expected. See **Fig. 2.6** which plots the ratio of actual to predicted recovery versus the actual incremental recovery. For most tests, actual recovery was less than 50% the initial prediction, with some tests achieving only about 10% of initially predicted recovery. This is a significant discrepancy that can be detrimental to the success of SP flooding in field applications. This implies poor scale up from lab to field application where parameter values estimated in the lab might vary from the actual values in the reservoir. Also, some factors may not have been accounted for effectively during lab trials such as the extent of heterogeneity. An early offshore surfactant flooding test for a North Sea reservoir was discussed by **Cooper et al. (1985)**. A follow-up test of the North Burbank surfactant-polymer pilot found that the pilot test was affected by the degradation of the chemical slug and by heterogeneity. Flow diversion was also assumed to be a significant factor in the overall recovery (**Lorenz et al. 1986)**.

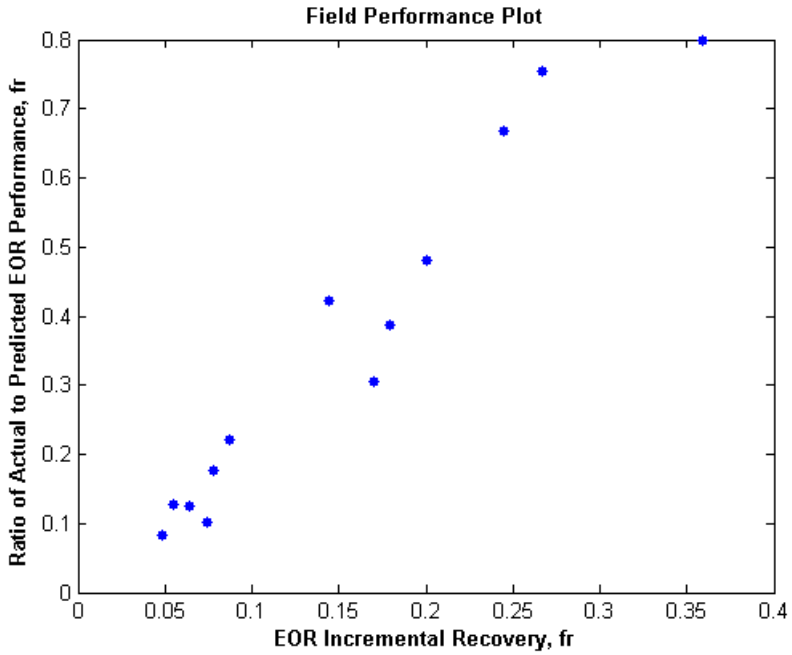


Fig. 2.6– Field performance plot of the ratio of actual to predicted SP flooding recovery vs. incremental oil recovery (plot data from Hammershaimb et al. 1983).

Loss of mobility control due to polymer slug degradation also significantly affects recovery in field tests (**Taggart and Russell 1981). Holland and Porter (1983)** discuss the evaluation program for surfactant-polymer design. Field test achieved 70% recovery compared to coreflood value of 81% for Berea sandstone. The performance of the Long Beach micellar/polymer pilot found that the recovery efficiency achieved was two-thirds of the recovery from coreflood and simulation studies, this was due to the uncertainties in the quantitative description of the reservoir and of the micellar/polymer process (**Fanchl and Caroll 1988)**.

For most field applications, SP flooding was not efficient compared to initial estimates. This highlights the importance of understanding the uncertainty in obtaining accurate predictions of the process on the field scale which is necessary to ensure its commercial success.

2.6.3 Improvements and Variations

Alkaline addition to SP systems can contribute to oil recovery through wettability alteration and reduction of surfactant adsorption. Alkalis also generate soap in situ from the naphthenic acid present in the crude oil. The wettability alteration due to the combined effect of alkali and surfactant can enhance recovery from fractured oil-wet reservoirs (**Hirasaki et al. 2011)**. More detailed discussions on the effects of adding alkaline to surfactant systems on oil recovery and the effects of salinity, dispersion and permeability can be found in **Krumrine et al. (a and b, 1982), Shen et al. (2009)** and **Liu et al. (2010)**. Significant uncertainties do exist for alkaline-surfactant-polymer flooding, similar to SP flooding (**Stoll et al. 2011**).

Recently, **Al-Sulaimani et al. (2012**) suggested the use of biosurfactant as a possible surface tension agent. Its performance is enhanced via mixing with other surfactants. This is actually a form of microbial EOR. Recycling produced chemicals can increase recovery efficiency by reducing costs (**Wang and Gu 2005).** The development of surfactant systems that can tolerate high salinity and high temperature reservoir conditions can increase the applicability of SP flooding (**Puerto et al. 2012)**.

In order to better understand the reservoir that is a candidate for SP flooding, interwell tracer tests can be used **(Cheng et al. 2012)**. This method tests surfactant field implementation using inexpensive tracers and within confined spacing prior to a surfactant field test. For the case study in the reference, it was found that the tracer test did not recover a significant amount of the injected tracer. This was due to low sweep efficiency and for some of the tracer tests being unconfined. These tests improved the understanding of the reservoir while using inexpensive tracers which can help optimize the surfactant field test.

2.7 Performance Forecasting-Simulation

Initial simple estimates of oil recovery by chemical flood can be found using material balance calculations. More complex analytical estimates were found using the frontal-advance (fractional flow) theory (**Pope 1980**). Currently, the performance of the process is predicted using numerical simulation where a system of equations that define the transport of each chemical species through the porous media are solved. This is usually performed using finite difference techniques (**Green and Willhite 1998)**.

There are a number of commercial solvers that simulate SP flooding. There are also research solvers that are developed and used by academic institutions and energy companies. What follows is a brief discussion of the most commonly used simulators.

2.7.1 Commonly Used Simulators

UTCHEM (**UTCHEM 2000)** is a three-dimensional, multicomponent, multiphase, compositional finite difference simulator. It is capable of modeling three-phase relative permeabilities, capillary pressures, diffusion, dispersion, adsorption, chemical reactions, and non-equilibrium mass transfer between phases. Second and third order approximations are used by the finite difference method for all the time and space derivatives. The surfactant phase behavior is modeled using the Hand representation of the ternary phase diagram, where a pseudophase theory is used to reduce the surfactant, co-surfactant, oil and water fluid mixtures into a pseudoternary compositional space. The simulator models the following major physical phenomena: viscosity, density, velocity-dependent dispersion, adsorption, molecular diffusion, interfacial tension, capillary pressure, relative permeability, capillary trapping, cation exchange and the gel and polymer properties (e.g. inaccessible pore volume, permeability reduction and non-Newtonian rheology). Phase mobilization is modeled via an entrapped phase saturation and the relative permeability dependence on trapping number. Aqueous electrolyte chemistry, ion exchange reactions with the matrix, precipitation/dissolution of minerals, reactions of acidic components of oil with the aqueous solution bases and the polymer reactions with crosslinking agents that form gel are the reaction chemistry included in the model. The system of flow equations is solved using a block-centered finite-difference scheme which is implicit in pressure and explicit in concentration, similar to IMPES (**UTCHEM 2000)**.

ECLIPSE 100 (**Schlumberger 2010)** is a three phase and three dimensional general purpose black oil simulator that is fully-implicit. In the surfactant model of ECLIPSE, the detailed chemistry of a surfactant process is not modeled. Rather the important features of surfactant floods on a full field basis are modeled.

ECLIPSE assumes the surfactant only exists in the aqueous phase (Type II(-)). UTCHEM, GPAS**(Najafabadi et al. 2012)**, REVEAL **(Petroleum Experts 2012)**, STARS(**Computer Modelling Group 2012**) support a full treatment of the microemulsion phase. UTCHEM cannot represent the EACN variations that result from mass transfer between oil and gas. This is because it is based on a dead oil or dry gas hydrocarbon description. The GPAS simulator is limited to reservoirs that

have no free gas when chemical flooding is initiated. Limitations of UTCHEM for large field studies is that it only supports single processor computations and that it is IMPEC, where only the pressure is considered implicitly. Thus it is subject to CFL stability restrictions (**Coats 2003)** that set a maximum for flow between two cells in a single time step. REVEAL also faces similar limitations when microemulsion is present. STARS is fully implicit although it replaces the gas phase with the microemulsion. GPAS was intended to have a fully implicit code in order to handle longer time-steps (**Patacchini et al. 2012)**.

2.7.2 Reservoir Simulator used for this Study: ECLIPSE 100

The simulator used for this research was ECLIPSE 100 due to its stability in contrast to UTCHEM which uses an implicit pressure explicit concentration scheme to solve the system of flow equations. This could lead to instability when using larger time steps. ECLIPSE was deemed sufficient because it uses a fully implicit scheme and it does model the main features of surfactant polymer flooding on full field basis. Furthermore, the objective of this thesis was not to design a specific SP flooding process. The focus was on developing and applying a decision making algorithm that requires stable and reliable SP flooding performance forecasts which can be provided by ECLIPSE. The treatment of SP flooding by the simulator is discussed briefly. The following discussion is adapted from the technical description manual **(Schlumberger 2011).**

A conservation equation for surfactant in the aqueous phase is solved to model the distribution of injected surfactant. The concentration of the surfactant is updated the end of each time step after the computation of the oil, water and gas flows using a fully implicit scheme. The surfactant is assumed to exist in the aqueous phase only (i.e. resulting in a Type II(-) microemulsion). As for the transport of polymer solution through porous media, ECLIPSE assumes that this does not have an effect on hydrocarbon flow in the model **(Schlumberger 2011)**.

The capillary number is calculated as follows:

$$N_c = \frac{|K.\mathrm{grad}P|}{ST}.C_{unit} \qquad \text{Eq. 2.2}$$

ST : is the interfacial tension provided using the SURFST keyword.

P: is the potential.

C_{unit}: is the units conversion factor.

K: is the permeability.

And $|K.\mathrm{grad}P|$ is calculated as

$$|K.\mathrm{grad}P| = \sqrt{(K_x.\mathrm{grad}P_x)^2 + (K_y.\mathrm{grad}P_y)^2 + (K_z.\mathrm{grad}P_z)^2} \qquad \text{Eq. 2.3}$$

$$\text{For cell i; } K_x.\mathrm{grad}P_x = 0.5\left[\left(\frac{K_x}{D_x}\right)_{i-1,i}.(P_i - P_{i-1}) + \left(\frac{K_x}{D_x}\right)_{i,i+1}.(P_{i+1} - P_i)\right] \qquad \text{Eq. 2.4}$$

This is done also for the y and z directions

Here the K/D value is determined in an analogous manner to transmissibility and depends on the geometry. The surface tension is input in table form and is assumed to be a function of surfactant concentration.

As for polymer flow, this can be described as follows:

$$\frac{d}{dt}\left(\frac{V^{*}S_{w}C_{p}}{B_{r}B_{w}}\right)+\frac{d}{dt}\left(V\rho_{r}C_{P}^{a}\frac{1-\varphi}{\varphi}\right)=\sum\left[\frac{Tk_{rw}}{B_{w}\mu_{p\,eff}R_{k}}(\delta P_{w}-\rho_{w}gD_{z})\right]C_{p}+Q_{w}C_{p} \qquad \text{Eq. 2.5}$$

The standard aqueous equation is then modified to account for polymer flow:

$$\frac{d}{dt}\left(\frac{VS_{w}}{B_{r}B_{w}}\right)=\sum\left[\frac{Tk_{rw}}{B_{w}\mu_{w\,eff}R_{k}}(\delta P_{w}-\rho_{w}gD_{z})\right]+Q_{w} \qquad \text{Eq. 2.6}$$

, where $V^{*}=V(1-S_{dpv})$ Eq. 2.7

S_{dpv}: is the dead pore space within each grid cell.

C_{P}^{a}: is the polymer adsorption concentration.

ρ_{r}: is the mass density of the rock formation.

φ: is the porosity.

ρ_{w}: is the water density.

R_{k}: is the reduction factor of the relative permeability of the aqueous phase due to polymer retention.

C_{p}: is the polymer concentration.

$\mu_{p\,eff}$: is the effective viscosity of water ($a=w$) or polymer ($a=p$).

D_{z}: is the cell center depth.

B_{r}: is the rock formation volume.

B_{w}: is the water formation volume.

T: is the transmissibility.

k_{rw}: is the water relative permeability.

S_{w}: is the water saturation.

V: is the block pore volume.

Q_{w}: is the water production rate.

P_{w}: is the water pressure.

g: is the gravity acceleration.

Assumptions of the polymer model were (**Schlumberger 2011**):

- formation volume factor and Density of water (aqueous phase) are independent of polymer concentration.
- Polymer solution and injected water are represented as miscible components in the aqueous phase.

- Degree of mixing of the miscible components is defined by the viscosity terms in the conservation equations.
- Fluid viscosities are dependent on the local concentration of polymer.
- Pore blocking and adsorption effects are incorporated by the term R_k.

A fully implicit time discretization is used to avoid numerical stability problems that might occur due to significant variations in the properties of the aqueous phase during a time step **(Schlumberger 2011)**. This is an advantage of using ECLIPSE.

As for determining relative permeability, the model used is a based on transitioning from the immiscible relative permeability curves at a low capillary number to the miscible relative permeability curves at a high capillary number. This data is supplied as a table which describes this transition as a function of the log10 of the capillary number **(Schlumberger 2011)**.

At a specific value of the miscibility function between the miscible and immiscible curves, the relative permeability values are obtained by interpolating the end points of the curves after which the miscible and immiscible curves are scaled to adhere to these interpolated points. Then the relative permeability values are identified on both curves and by interpolating between these two values, the final relative permeability is obtained. The water relative permeability is treated in a similar manner to the oil relative permeability **(Schlumberger 2011)**.

As surfactant concentration increases, the water oil capillary pressure will decrease. The oil water capillary pressure is determined by the following equation;

$$P_{cow} = P_{cow}(S_w)\frac{ST(C_s)}{ST(C_s=0)} \qquad \text{Eq. 2.8}$$

$P_{cow}(S_w)$: The capillary pressure obtained from the immiscible curves that were initially scaled to the interpolated end-points calculated in the relative permeability model.

$ST(C_s)$: The surface tension at the present surfactant concentration.

$ST(C_s = 0)$: The surface tension at zero surfactant concentration.

A reduction in reservoir permeability can occur due to polymer adsorption. This is directly correlated with the adsorbed polymer saturation. The residual resistance factor (RRF) must be defined for each rock type in order to determine the permeability reduction. The actual resistance factor is calculated by:

$$R_k = 1.0 + (RRF - 1.0)\frac{C_p^a}{C_p^{a\,max}} \qquad \text{Eq. 2.9}$$

, where $C_p^{a\,max}$: is the maximum adsorbed concentration. This is defined using the PLYROCK keyword.

The inaccessible pore volume to polymer solution (i.e. the dead pore volume) is also input using the PLYROCK keyword. Because of this, the polymer solution travels at a greater velocity in contrast to the inactive tracers that are embedded in the aqueous phase. This leads to chromatographic separation which is modeled by assuming the dead pore space to be constant for each rock type and independent of the water saturation **(Schlumberger 2011)**.

The water-surfactant solution viscosity is determined after inputting the surfactant viscosity as a function of surfactant concentration using the SURFVISC keyword. This is determined by;

$$\mu_{ws}(C_s, P) = \mu_w(P)\frac{\mu_S(C_s)}{\mu_w(P_{ref})} \qquad \text{Eq. 2.10}$$

In the presence of polymer in the solution, the effects of fingering at the rear edge of the solution and the physical dispersion effects at the leading edge are incorporated by allocating effective viscosity values for the fluid components. These are calculated using the Todd-Longstaff technique (**Todd and Longstaff 1972**). The effective polymer viscosity is determined to be:

$$\mu_{p,eff} = \mu_m(C_p)^{\omega} . \mu_p^{1-\omega} \quad \text{Eq. 2.11}$$

, where $\mu_m(C_p)$: is the viscosity of a fully mixed polymer solution as a function of polymer concentration in solution.

μ_p: is the viscosity of the solution at the maximum injected polymer concentration in solution.

ω: is the Todd-Longstaff mixing parameter. This is input using the TLMIXPAR keyword.

The mixing parameter is used to model the degree of segregation between the injected polymer solution and water. Full mixing in each block is assumed when $\omega = 1$. Complete segregation is assumed when $\omega = 0$. Using the pure water viscosity and the fully mixed polymer viscosity, the partially mixed water viscosity is calculated as:

$$\mu_{w,e} = \mu_m(C_p)^{\omega} . \mu_w^{1-\omega} \quad \text{Eq. 2.12}$$

, where μ_w: is the pure water viscosity.

$\mu_{w,eff}$ is then found using the total water equation as the sum of contributions from pure water and polymer solution:

$$\frac{1}{\mu_{w,eff}} = \frac{1-\bar{C}}{\mu_{w,e}} + \frac{\bar{C}}{\mu_{p,eff}} \quad \text{Eq. 2.13}$$

$$\text{, where } \bar{C} = \frac{C_p}{C_{p,max}} \quad \text{Eq. 2.14}$$

$\bar{C}$: is the effective saturation of injected polymer solution as a fraction of the total aqueous phase in the cell.

There are two models that can be used to incorporate the effects of non-Newtonian rheology of polymer solutions. The first model focuses on the shear thinning effect of polymers by reducing the polymer viscosity at higher flow rates. The shear rate is assumed to be proportional to the flow viscosity. However, this is not, in general, a valid assumption due to the discrepancy in pore throat sizes of varying permeability layers. It is assumed to be a reasonable assumption when dealing with a single reservoir. The second model is based on the Herschel-Bulkley equation (**Herschel and Bulkley 1926**) which is used to model both shear thinning and thickening and yield stress as functions of polymer concentration **(Schlumberger 2011)**.

Whether non-Newtonian rheology model is used or not, this should have minimal effect on the performance of the algorithm developed in this thesis as it will only influence the physical accuracy of modeling the EOR process and not the algorithm progression. No shear effects were assumed for the polymer viscosity used for the applications in this thesis.

Adsorption of surfactant is assumed to be instantaneous and the amount of adsorbed surfactant is defined as a function of the surrounding surfactant concentration. An adsorption isotherm as a function of surfactant concentration is defined using the SURFADS keyword. Alternatively, an analytical adsorption isotherm, which takes into account the effects of rock permeability and effective brine salinity, can be specified using the ADSORP keyword. The amount of surfactant adsorbed is given by;

$$\text{Mass of adsorbed surfactant} = \text{PORV}.\frac{1-\varphi}{\varphi}.\text{MD}.\text{CA}(C_s) \quad \text{Eq. 2.15}$$

PORV is the cell pore volume.

MD is the rock mass density and is input using the keyword SURFROCK.

$\text{CA}(C_s)$ is the adsorption isotherm as a function of local surfactant solution concentration.

ECLIPSE has two adsorption models; a reversible adsorption model where the adsorption isotherm is retraced in each grid block as the concentration of the surfactant decreases in the cell, and an irreversible adsorption model which assumes no decrease with time of the adsorbed surfactant concentration on the rock which implies that de-adsorption is not allowed. Polymer adsorption is handled in a similar manner can be defined using the PLYADS keyword or by a generic analytical adsorption model via the ADSORP keyword **(Schlumberger 2011)**. For the applications in this thesis, the tabulated form of adsorption input was used.

Finally, the simulator can allow for wettability alteration as the surfactant accumulates on the rock surface by using the SURFACTW keyword. If either oil-wet or water-wet immiscible saturation functions were defined initially, it is possible to define additional immiscible saturation functions which are used to define the opposite wetting situation. To determine the immiscible relative permeabilities and capillary pressure, the oil-wet and water-wet endpoints are interpolated and the curves are scaled to adhere to these points. **(Schlumberger 2011)**. To calculate the new immiscible relative permeability, the following equation is required;

$$k_r = Fk_r^{ow} + (1-F)k_r^{ww} \quad \text{Eq. 2.16}$$

F: is the wettability weighting fraction and is a function of adsorbed surfactant concentration. It is defined using the SURFADDW keyword.

k_r^{ow}: the scaled oil-wet k_r that is previously provided using the SATNUM keyword.

k_r^{ww} : the scaled water-wet k_r that is previously provided using the SURWNUM keyword.

The new immiscible saturation function is defined by this equation which is then used in the relative permeability and capillary pressure models that are used in the simulator.

As mentioned earlier, SP flooding is sensitive to reservoir brine salinity. ECLIPSE does allow for the treatment of salinity and its effects on SP flooding, however, this is optional. Regarding the case studies in this thesis, the explicit effect of salinity was neglected. It is important to note that the IMPES approach is not feasible when the Polymer option is activated **(Schlumberger 2011)**.

2.7.3 Recent Developments and Other approaches

A fully implicit, parallel, compositional reservoir simulator was recently developed incorporating a cubic equation of state model for handling the hydrocarbon phase behavior and Hand's rule for handling the surfactant/oil/brine phase behavior (**Han et al. 2005)**. The surfactant, polymer and salt components were included as aqueous species in the chemical model. Interfacial tension, viscosity, adsorption, surfactant/oil/brine phase behavior and relative permeability as a function of trapping number were included in the physical property models. The model considered a surfactant/oil/brine Type II(-) phase

behavior similar to ECLIPSE. Adsorption is modeled using a Langmuir-type isotherm as a function of salinity and concentration. The phase behavior model is based on **Winsor (1954), Nelson and Pope (1978), Reed and Healy (1977), Prouvost et al. (1985) and Camilleri et al. (1987)**. Interfacial tension is modeled using the modified Chun-Huh (**Huh 1979**) equation (incorporating Hirasaki's **(Hirasaki 1981**) correction factor). Oleic phase viscosity is modeled using Lohrenz's **(Lohrenz 1964)** correlation. The performance of the simulator was found to be in agreement with UTCHEM.

To model the chemical processes that lead to wettability alteration that occurs in naturally fractured reservoirs an existing numerical reservoir simulator was adapted (**Delshad et al. 2009)**. The wettability alteration is performed using surfactant flooding. To model the wettability alteration, multiple relative permeability and capillary pressure curves that correspond to different states of wetting. The impact of uncertainty in fractures and matrix properties, matrix diffusion, reservoir heterogeneity, initial water saturation, buoyancy-driven flow and formation wettability are investigated via simulation. The wettability alteration model was validated experimentally. It was found that modeling and dynamic laboratory experiments are needed in order to evaluate chemical floods for naturally fractured reservoirs. A disadvantage of the imbibition cell experiments is that they are not representative of field operations and that the lack the viscous forces that are essential to field design and scale up studies.

The effect of pressure and solution gas on the microemulsion phase behavior and how it affects oil recovery were investigated using UTCHEM (**Roshanfekr et al. 2012)**. Furthermore, simulating SP flooding in the presence of gas was investigated by developing a fully implicit simulator (**Patacchini et al. 2012)**. A gas-oil-water-microemulsion equilibrium model was coupled with an in-house research reservoir simulator. The equilibrium is divided into two stages: the hydrocarbons and aqueous components are equilibrated first, then the resulting Gas, Water and oil phases are lumped into pseudo-phases that are equilibrated using a microemulsion model (this is based on Hand's representation). This is a conceptual splitting approach where at each converged time-step the four phases are in equilibrium with each other when they are simultaneously present.

In order to consider the chemical reactions that occur during SP flooding, an effort by **Farajzadeh et al. (2012)** present an approach to model chemical EOR in a more detailed manner with respect to the geochemical reactions and phase behavior by coupling a multipurpose reservoir simulator to a chemical simulator.

2.8 Sources of Uncertainty

As mentioned earlier, SP flooding varies between laboratory and field tests (**Gogarty 1976; Lowry et al. 1986; Adams and Schievelbein 1987; Green and Willhite 1998; Stoll et al. 2011**). This is mostly due to uncertainty in the scale up process from lab to field applications. Since actual SP flooding oil recovery can achieve as low as 10% of the predicted recovery, uncertainty can be detrimental to the wide-scale commercial success of SP flooding **(Pope et al. 1979; Hammershaimb et al. 1983; Brown and Smith 1984; Barua et al. 1986; Lake 1989; Jakobsen and Hovland 1994; Michels et al. 1996; Thomas 2006**). The existence of these uncertainties could imply an inability to predict variable behaviour in the reservoir (**Lowry et al. 1986)**.

To design and implement a successful SP flooding process in the field requires the optimization of large number of decision variables (**Lake 1989**). As discussed in the previous sections, there are many aspects that need to be investigated in order to implement this EOR process. There are numerous sources of uncertainty in SP flooding such as heterogeneity, brine salinity, surfactant and polymer adsorption and residual oil saturation to chemical flooding. The effect of reservoir heterogeneity on chemical flooding is recognized as a dominant factor which influences volumetric sweep efficiency (**Kossack and Bilhartz**

1976; Brown and Smith 1984; Hankins and Harwell 1996; Cheng et al. 2012). Residual oil saturation to chemical flooding is considered to be the most significant factor in oil recovery, whereas surfactant adsorption is also considered to have a significant adverse effect as well **(Brown and Smith 1984; Dang et al. 2011; Solairaj et al. 2012)**. Salinity effects were studied extensively and found to influence oil recovery significantly since the IFT and phase behaviour are functions of salinity and surfactant/ polymer adsorption is a function of multivalent ion content which is dependent on salinity **(Gerbacia 1978; Pope et al. 1979; Hirasaki et al. 2011; Puerto et al. 2012; Lohne and Fjelde 2012)**. Polymer viscosity is essential for the effectiveness of the mobility buffer that follows surfactant injection; therefore uncertainty in the behaviour of polymer viscosity in the reservoir is important to the success of the mobility buffer (**Weiss and Baldwin 1985**).

As mentioned earlier, to implement SP flooding successfully, all of these factors need to be considered in the design process. The high-dimensionality of the design aspects increases the complexity of implementing SP flooding in the field. Furthermore, economic factors such as oil price and chemical costs are also essential to the applicability of SP flooding given that they vary with time. Thus, there are many parameters that need to be considered simultaneously for successful implementation. Due to subsurface uncertainty, the design process is complicated even further. Therefore, economic and technical uncertainty is an important and detrimental design aspect.

2.9 Concluding Remarks

SP flooding is considered to be the most complicated EOR process in terms of the required decision variables (**Lake 1989)**. The design of SP flooding is time consuming and requires extensive laboratory assessment to determine the optimal SP system under reservoir conditions. This is then scaled up to be applied on pilot field tests in order to determine if the SP system achieves sufficient recovery to justify its application on a full field scale. There is significant uncertainty when scaling up from laboratory application to field implementation. These issues have been introduced and discussed in this chapter.

Most field tests produced mixed results when some detrimental factors were not predicted accurately. Some field tests in the U.S.A during the 1980s did recover good amounts of oil and were deemed successful; however, these tests depended on tax credits provided by the Department of Energy (**DOE 2008**). Recent interest in SP flooding has increased due to the maturing of many hydrocarbon reservoirs around the world and to the high energy demand from emerging economies.

Although it is essential to simulate the complete phase behavior during the propagation of the SP system through the reservoir when designing a SP flooding, ECLIPSE 100 was deemed sufficient for the purpose of the study. This is due to the stability of ECLIPSE compared with other simulators such as UTCHEM because it uses a fully implicit scheme. Furthermore, the purpose here was not to design a specific SP flooding process, rather the purpose is to demonstrate the applicability of the method developed in this thesis. However, the decision making method could be applicable with any commercial or in house simulator.

After reviewing the different components of SP flooding, the next chapter discusses briefly the origin and purpose of decision making and then proceeds to review the different approaches presently used.

3 Decision Making in E&P

The previous chapter shows that the process of implementing SP flooding in the field is complex and requires many decisions over a long term horizon which must be made in the presence of technical and economic uncertainties. This is also true for most of the important field recovery decisions as petroleum exploration and production are still very complex (**Suslick and Schiozer 2004)**. Investment decisions in the oil and gas industry are usually very crucial because they are capital intensive (**Deore 2012**). To make the necessary decision, numerous decision analyses methods have been used. Decision analysis methods spurred interest for evaluating decisions in the oil and gas industry since the early 1960s (**Grayson 1962**).

There is a rich literature of the various decision analysis methods in a wide range of disciplines. This chapter will first provide the necessary definitions of the terms that are usually employed with decision analysis. This is then followed by a brief review of the most common methods used for analyzing decisions. Examples of decision making methods used for SP or chemical EOR problems are then presented and discussed. Then a discussion of the type of decisions that this study aims to address is shown. The approach suggested for evaluating these types of decision in this study is inspired by real options theory. A review of the different valuation methods in real options theory is presented.

3.1 Decisions and Decision Analysis

3.1.1 Definitions

A decision is defined as an irrevocable allocation of resources (**Howard 1966)**. Decision Analysis is defined as a systematic procedure that transforms opaque decision problems into transparent decision problems using a sequence of transparent steps (**Howard 1966; Howard 1988)**. **Newendorp and Schuyler (2000)** state the main advantages of decision analysis are: to explicitly recognize possible outcomes, to highlight key parameters or factors, to communicate clearly the judgements about risk to compare projects that have different risk characteristics and to handle complex investment decisions. It is not a procedure to determine the output probability density function based on using probability density functions for the inputs. The purpose of decision analysis is to generate insight and clarity rather than control (**Howard and Matheson 1968; McNamee and Celona 1990).** It is important to note that a good decision is a logical decision (**Howard, 1966; Begg and Bratvold 2002)** and that good decisions do not always produce good outcomes **(Bickel and Bratvold 2007**).

Field management decisions are usually complex because of the number and type of decisions involved, the resources required to obtain performance prediction and the dependency of production strategy which is affected by different types of uncertainty on the method of risk quantification (**Suslick and Schiozer 2004)**. In this thesis, decision analysis and decision making are used interchangeably.

An option is considered to be one of the vey essential concepts in practicing decision analysis (**Howard 1996)**. This is not restricted to financial or real options only. It is defined as an alternative that results in a new decision situation after new

information is revealed. It is found that the inability to recognize options and incorporating them as sequential decisions is detrimental to decision analysis (**Howard 2007)**.

3.1.2 Decisions in the Presence of Uncertainty

Uncertainty can occur due to error, lack of knowledge and incomplete analyses (**Begg et al. 2002**). Decision making is not synonymous with uncertainty quantification. "Uncertainty quantification creates value only to the extent that it holds the possibility of changing a decision that would otherwise be made differently" (**Bickel and Bratvold 2007**). Modelling uncertainty does not lead to reduced uncertainty. The model is an explicit representation of uncertainty which is implicit in the decision. Uncertainty reduction is achieved by our choices. A decision model is finalized if it cannot be refined further. This is in contrast to study based methods which are more linear. Significant detail is incorporated into the model from the beginning rather than adding detail in important areas when required. The produced results are then used in the next phase and so on. These methods do not accommodate learning or refinement (**Bickel and Bratvold 2007**). Because most models involved in decision making are non-linear, it is essential to consider uncertainty by modelling the entire range of possible outcomes not by using expected (average) values of uncertain quantities (**Begg et al. 2004**). Thus obtaining the P10, P50 and P90 (for example) of the model from the respective random input values is not accurate. The best estimate of reservoir performance are generated from taking the average performance of many models using realizations over the full range of the random inputs, and not by using best-estimates of the random inputs (**Begg et al. 2004**).

3.2 Decision analysis in Exploration and Production

Decision making or analysis approaches have been widely used and justified for E&P problems **(Stripe et al. 1993; Thakur 1995; Evans 2000; Cunha 2007; Saputelli et al. 2009; Begg and Bratvold 2010)**. Whether these approaches are based on optimization or decision trees, their objective is to produce an optimal policy given certain conditions. The literature is quite rich in optimization and decision making approaches for E&P problems under uncertainty. A review is presented below.

3.2.1 Review of Decision Analysis Methods used in E&P

Zolotukhin (1992) introduced a decision making approach for reservoir engineering problems. This was based on systems analysis and optimization under incomplete and fuzzy information. The study argues that due to the physical uncertainty encountered in the reservoir, it is possible to assume that the technical parameters to be modelled as fuzzy information. The study presented conceptual examples. It did not consider uncertainty in the time series of these parameters.

Suslick et al. (2001) provide an interesting example of incorporating the effect of technology improvement on the objective function of deep sea E&P projects. They use a utility function to simulate the improvement of technology. **Yeten et al. (2004)** developed a method to determine the optimal performance of smart wells. A gradient-based optimization technique is used along with a reservoir simulator (ECLIPSE). The optimization incorporates geological uncertainty and the risk failure

of inflow control devices (ICD's). The decision analysed is whether to deploy the ICD in the presence of these uncertainties. This study also uses decision making techniques to evaluate smart wells. The decision analysis is based on using a utility function. In order to make tradeoffs among the different objectives, the study used the multi-attribute utility theory (**Keeney and Raiffa 1976**). This is based on the construction of individual utility functions per each criteria (these functions quantify the preference amongst the alternatives under uncertainty) and then these utility functions are aggregated into one function. The geological uncertainty is modeled as five unconditional realizations of the reservoir description. This was done using the Fluvsim software (**Deutsch and Tran 2002).** Permeability was generated within each facies independently and unconditionally using sequential Gaussian simulation. The other uncertain parameter was the reliability of the ICD. The decision analysis used a decision tree to calculate the objective function. It found that geologic uncertainty was more dominant than that of engineering uncertainty for the cases studied. Using utility functions for decision analysis however is not always the best approach (**Aven and Korte 2002**).

A method that minimizes the subjectivity in decision and risk analysis which can be updated with time was developed by **Hultzsch et al. (2007)**. It uses MCS to simulate the economic outcomes. Uncertainty is updated using Bayes theorem. The study recognizes that single value methods (NPV, DCF) fail to account for uncertainty. A Tank model was used to simulate reservoir behaviour. Uncertainty in the time series was assumed for the skin factor, reservoir thickness and other reservoir properties. The homogeneous properties were replaced with the new found values (e.g. from well tests) while the heterogeneous properties were updated with Bayes theorem. MCS was used to estimate expected mean value and the risk level. This method provides a more robust approach with regards to uncertainty as it assumes the state parameters vary with time. However it does not consider uncertainty in the time series of economic parameters. Furthermore, reservoir predictions are obtained using a simplistic analytical model.

An integrated asset model for offshore field development in the presence of uncertainty was presented by **Ogunyomi et al. (2011)**. The model is based on simple analytical models for the different elements of the model. The technical uncertainties considered were reservoir thickness and transmissibility. The model did not consider economic uncertainty. This approach also simplifies reservoir predictions by using an analytical model.

Closed loop reservoir management (CLRM) schemes have been widely applied recently. These schemes allow for incorporating geological uncertainty to produce optimal control variables. The geological uncertainty is based on dynamically assimilating production data in real-time (**Wang et al. 2009**). The assimilation process is based on assuming there is noise in the production data. The method developed by **Wang et al. (2009)** updates the reservoir model using the ensemble Kalman filter (EnKf) method (**Burgers et al. 1998; Evensen 2003)**. This is coupled with an optimization scheme. It was assumed that only the bottom hole pressure as the control variable to be optimized within a lower and upper bound constraints. It does not assume uncertainty in any other state variables other than geology.

Chen et al. (2009) used an approach that follows two steps: updating the geological model and optimizing production. Ensemble based methods acquire the gradient information using correlations that are provided by the ensemble. This leads to optimal controls that are independent of the number of the control variables, the reservoir simulator and the simulation solver. The study introduces an ensemble-based closed-loop optimization method which combines EnOpt (ensemble-based optimization scheme) with the EnKf. EnKf is found to be more suitable for sequential data assimilation in large-scale nonlinear dynamics. The method introduced by this study is robust and completely adjoint-free. The case examples presented assume that permeability is the only uncertain geological property. **Foss and Jensen (2011)** provide a good review on the

performance of CLRM with respect to control settings. They emphasize that one of the limitations of CLRM is the time delay effect which is the time needed to complete the workflow and implement a new strategy. Also the control sampling time is important. This is because time delays can have a detrimental effect on obtainable CLRM results. In general CLRM methods focus on the evolution of spatial uncertainty such as permeability. Other parametric uncertainties are not incorporated (**Foss and Jensen 2011)**.

With the advent of intelligent fields, decision making has become very crucial due to the availability of significant amounts of real time data that need to be analysed to produce optimal policies (**Fernandez et al. 2012**). Furthermore, decision making becomes complicated when assimilating data under uncertainty (**Ciaurri et al. 2012**).

Financial decision making methods have been also combined with decision analysis for E&P problems. These approaches apply modern portfolio management techniques (**Omarna and Duggan 1999; Walls 2004)**. Portfolio optimization allows for the valuation of individual projects on the basis of the total project portfolio. This enables examination of how capital allocation influences value creation and risk. This can be performed in one stage or in several. For single-stage approaches, the reward and risk of individual projects are estimated. An efficient frontier is then obtained based on these estimates using linear programming. For multi-stage approaches, efficient frontiers are first obtained at the district level. Then an efficient frontier is obtained for the corporation using the district return functions. Portfolio analysis will not produce meaningful results if there are poor uncertainty estimates. However, it is recognized that portfolio optimization can improve decision quality (**Davidson 2001)**.

A summary of decision making in the industry can be found in **Dinnie et al. (2002), Suslick and Schiozer (2004) and Deore (2012)**. **Mackie et al. (2006)** discuss the development of a theoretical E&P decision making taxonomy. **Karakaya (2012)** provide a comprehensive literature review of decision analysis methods in the industry and also presents the results of a recent industry-wide survey about the perceived value and popularity of these methods.

3.2.2 Review of Decision Analysis Methods for Chemical EOR Processes

There have been several attempts to evaluate decisions for chemical EOR methods. A review of these studies follows. Methods applied to other forms of chemical EOR were reviewed as well since they are easily extendable to SP flooding. The different components of these methods are presented and some aspects are elaborated on in more detail, specifically how these methods handle uncertainty.

Anderson (1979) provides an early application of risk analysis to surfactant flooding pilot tests in the presence of uncertainty. Although it does not address decision making explicitly, this study does provide an approach to quantify risk which can be integrated with decision making methods. This study used Monte Carlo simulation to obtain the objective function and uses economic criteria to test the pilot's success. After the pilot tests, the model assumes that uncertainty does not reduce to zero. Thus another phase of sampling for the economically successful pilots is performed, this time using triangular distribution. It uses the discounted cash flow rate of return as the objective function. This study recognized that uncertainty varies with time which is the framework used in this thesis. It considered the reserves to be the only technical state variable and the remaining state variables were the oil price, chemical cost and fixed capital expenditure. Another limitation is that it uses a simple linear model to forecast reservoir production.

A decision making methodology was introduced by **Barua et al. (1986)** to aid in making prudent business and technical decisions for surfactant flooding. The method uses the CFPM (Chemical Flood Predictive Model) (**Paul et al. 1982)** and aims to optimize the surfactant slug size without considering varying the concentration. The optimization process is based on Newton-Greenstadt method which is based on spectral decomposition. The method considers the following parameters: polymer buffer size, number of infill wells, Dykstra-Parsons coefficient, IFT, surfactant slug size and the NPV. This method optimizes the operational decisions of a surfactant flood project and produces the economic assessment of the project. This method also quantifies the effect of uncertainty and the financial risk. The method consists of three main parts; a mathematical model for surfactant flooding, an economic model and optimal engineering decisions algorithms that account for uncertainty. This study used the CFPM to model the surfactant flood because it is well documented and has produced reliable predictions in several field studies. It accounts for surfactant adsorption, reservoir wettability, reservoir heterogeneity and other parameters. The main outputs of this model are the tertiary oil production start time, peak oil production time, end of tertiary oil production time and peak oil rate. A triangular function is defined by these four parameters, which describe the variation of oil rate with time. The main disadvantage of this model is that it does not take into account the complex details of surfactant movement through porous media such as phase changes. The aim of the optimization is to determine the decision variable values that maximize the objective function such as the NPV or some other parameter. Non-linear optimization is required since the models used for surfactant flooding are non-linear. The non-linear optimization is based on Newton's method. Because some modifications were needed, the Newton-Greenstadt method was used. NPV was chosen as the economic criteria. For an EOR process, the decision made must be optimal. The optimization method was combined with MCS to incorporate uncertainty. The disadvantages of this method is that the. surfactant-polymer flooding process was estimated using a simple analytical method, thus it did not consider the transport through porous media of the chemical slug. Furthermore, uncertainty in the time series was not incorporated.

Decision analysis was applied to the design of a chemical flood by **Sanz & Miller (1994)** using as a base case the pilot test. A deterministic simulation of surfactant flooding/cash flow analysis was performed through the MCPALK model (**DOE 1986**), while variations in design (e.g. injection rate, slug surfactant concentration, and pattern area) were analyzed through decision trees and MCS. In the deterministic design, unique values were assigned to input variables and it was assumed that no uncertainty exists. As for the predictive model, the US Department of Energy version of MCPALK incorporates uncertainty in economic design parameters (operational expenses, oil price, etc) by using the basic parameters method. However uncertainties in other variables (e.g. reservoir parameters) were not treated. To mitigate this, and to incorporate MCS, the original treatment of uncertainty was overlooked through setting an equal value for the minimum, most likely and maximum input values which forces the predictive model to produce a deterministic design. Discounted cash flow analysis was used to produce economic evaluation. This is a procedure that evaluates profit by considering the time value of money. The objective functions used to screen decision and stochastic variables were; RPI (profit to investment ratio) for deterministic sensitivity and NPV (net present value) for stochastic analysis. The deterministic sensitivity analysis was performed mainly to specify which variables had the most impact on the objective function. The decision variables specified in this study were surfactant concentration, polymer slug size, injection rate, pattern area and surfactant slug size. The stochastic variables that were considered not to be well known were the microscopic displacement efficiency, porosity , permeability, residual oil saturation to waterflood, Dykstra-Parson's coefficient, crossflow factor, formation clay content, injectivity factor, oil price and surfactant adsorption. In the deterministic analysis, three values were specified for each of these variables: minimum, maximum and most likely. These values were obtained from literature. After the sensitivity analysis was performed and the most sensitive parameters to the outcomes from the decision variables (Surfactant concentration, injection rate, slug size and pattern area) and the stochastic variables (surfactant adsorption, porosity, net pay

thickness, residual oil saturation, microscopic displacement efficiency, formation clay content, cross flow factor, injectivity factor, oil prices and permeability) were identified. The beta function was the probability density function used. The Von Neumann (**von Neumann and Morgenstern 1947**) distribution sampling method was used for sampling from the frequency distributions. The outputs of MCS were then further processed for stochastic analysis. This entails obtaining a probability distribution of output values (histogram of RPI or NPV). Stochastic dominance was used in the stochastic sensitive analysis. It was found that, a complete decision analysis cycle would require a feedback process where assumptions can be corrected if need be and the problem formulation is refined. Thus the need to refine the probabilities, probability ranges, frequency distributions and expected outcomes. The limitations of this approach are the simplistic forecasting of the EOR process, the neglect of the effect of uncertainty in the time series and the assumption of constant control variables.

Fuzzy expert systems were also developed for decision analysis in EOR. **Chung and Caroll (1995)** used a fuzzy expert system to assess EOR projects. This is based on incorporating a database of the past EOR project costs and oil prices into the system. The method follows three stages: preliminary screening of EOR processes, the estimation of field performance and economic analysis. This study argues that it is possible to avoid the use of numerous laboratory and field data because the system is based on EOR past data and experts input. The displacement and sweep efficiencies were assumed to be fuzzy variables. The objective technical function is the recovery factor. Then the economic analysis is performed using the estimated recovery factor, the oil price, operating costs and the residual oil in place. The sensitivity of the profit of EOR projects to the oil price was emphasized in this study and that data and information are usually incomplete and are highly uncertain. This approach requires the availability of databases of laboratory experiments and field trials which is not easily available to most decision makers.

An optimization method that is coupled with an economic model and an expert system was developed by **Gharbi (2005)**. The purpose of this approach was to optimize the NPV of field development using EOR processes. The EOR expert system followed three steps: selecting an appropriate EOR process based on reservoir characteristics, preparing appropriate input data sets that will be used in EOR design using simulation, and applying DCF methods to optimize selected EOR process. The economic model used is a function of estimated recovery, oil price, residual oil in place, and operating costs. The study acknowledges the complexity and uncertainty of EOR process performance. Sensitivity analysis was used to evaluate the economic uncertainty. The uncertainties of the technical parameters were not considered explicitly whereas only the sensitivity towards control variables is assessed in this approach.

Costa et al. (2008) introduced a method to quantify the impact of chemical uncertainties related to ASP flooding, in order to improve the sweep and displacement efficiency in a Brazilian onshore field. This study focused on using representative models in decision making for an ASP flood. This approach was based on finding the parameters with the highest impact on performance through sensitivity analysis and then obtaining a risk curve which is similar to a probability distribution. Then three representative models were chosen to represent the P10, P50 and P90 cases. Economic uncertainty was then integrated with the representative models to improve decision making. Performance prediction was numerically simulated using (STARS/CMG) to evaluate field performance. The study focused on selecting and using representative model to provide probabilistic scenarios that can represent the chemical and dynamic uncertainties to be able to integrate them with economic uncertainties in order to improve decision making. However the study did not take into account uncertainty in heterogeneity. It also does not consider uncertainty in the time series. It considered adsorption, viscosity and residual oil saturation as the technical uncertain parameters.

Recent efforts include that of **Gao et al. (2010)** who provided guidelines for evaluating feasibility of SP flooding and optimizing profitability. Approach is based on screening, lab measurements, simulation, economic analysis, pilot tests and field implementation. The optimization of chemical systems, well patterns, slug and injection design are also presented. Applying the smart fields concept to EOR processes was suggested recently (**Regtien 2010**) with an emphasis on using cost effective surveillance methods to monitor the propagation of the flood front and sweep efficiency.

These various decision making methods were applied to SP flooding or other EOR processes. Each method was unique in its approach and in how it incorporated uncertainty, if considered, whether economic or technical. One of the main limitations of these approaches is that they did not consider the effect of uncertainty in the time series of economic and technical state variables. As these uncertainties evolve through time, the set of decision or control variables need to be modified as information is revealed. The main focus of this thesis is to apply an approach that can value flexibility in decisions as uncertainty varies. The value of flexibility (VoF) is defined as the value of splitting decisions into multiple decisions over time with the opportunity to learn between decisions and having the option to respond to that learning (**Bratvold and Begg 2010)**. Real options approach was considered to be an appropriate tool to meet this requirement because it is based on producing optimal policies conditional on the resolution of uncertainty and recognizes that uncertainty can create value as well as reduce it (**Copeland and Antikarov 2003; Jafarizadeh and Bratvold 2009**).

3.3 Real Options Theory

VoF can create value under four general conditions: when it is not possible to acquire information to reduce uncertainty, when it creates value (objective is to exploit uncertainty), if is used to manage the residual uncertainty after acquisition of information and when it is found to be cheaper than information acquisition. For the remaining three conditions the objective is to mitigate the negative impacts of uncertainty (**Begg et al. 2002**). To gain value from flexibility it is essential to think creatively about splitting single decisions into multiple decisions where it is possible to learn between decisions and given the option to react according to this learning. VoF is a way of thinking about how uncertainty is dealt with just as it is a value calculation technique (**Begg et al. 2002; Bratvold and Begg 2010**). Flexibility implies that decisions are made contingent on information that arrives regarding the state variables. Flexibility allows for capturing the upside potential and mitigating downside risk (**Sick and Gamba 2010**). Modeling flexibilities improves the accuracy of decision valuations. Another important benefit is that by attempting to describe project flexibilities, new options and strategies can be defined. The final benefit is that optimal policies are then generated from the analysis which can then be implemented (**Smith and McCardle 1999)**. Value of flexibility tools have as yet to achieve wide acceptance and use for E&P problems (**Karakaya 2012**). Real options theory does provide the framework for evaluating VoF. The main advantage of real options approach is that it incorporates uncertainty in the time series of the state variables in decision making. Real options is appealing for exploration and production projects because they usually involve several decision stages and each stage has an investment schedule (**Suslick and Schiozer 2004**).

3.3.1 Definition

Real options theory is a paradigm in investment analysis that associates the creation of value with the upside aspect of uncertainty. This mind-set entails a conscious effort to appreciate the impact of uncertainty on investments and produce value from favourable outcomes (**Jafarizadeh and Bratvold 2009**). In the past, based on traditional discounted cash flow (DCF) methods, the relationship between value and uncertainty was that more uncertain assets have relatively less economic value

in the future. Because conditions are constantly changing, a dynamic model of analysis that addresses these changing circumstances is required for good decision making. Uncertainty in DCF is a synonym for risk. The more uncertain the investment the more it is penalized with higher discount rates. Thus riskier investments are less attractive. Under real options valuation, uncertainty has a valuable impact on investments if managerial flexibilities are correctly exercised (**Jafarizadeh and Bratvold 2009**). See **Fig. 3.1** for comparison of DCF and real options valuation methods. Real options valuation emphasizes the managerial flexibility in making optimal decisions under uncertainty. Real options analysis maximizes NPV subject to economic and technical uncertainties and relevant options or decisions such as option to defer investment or option to expand production (**Dias 2004)**.

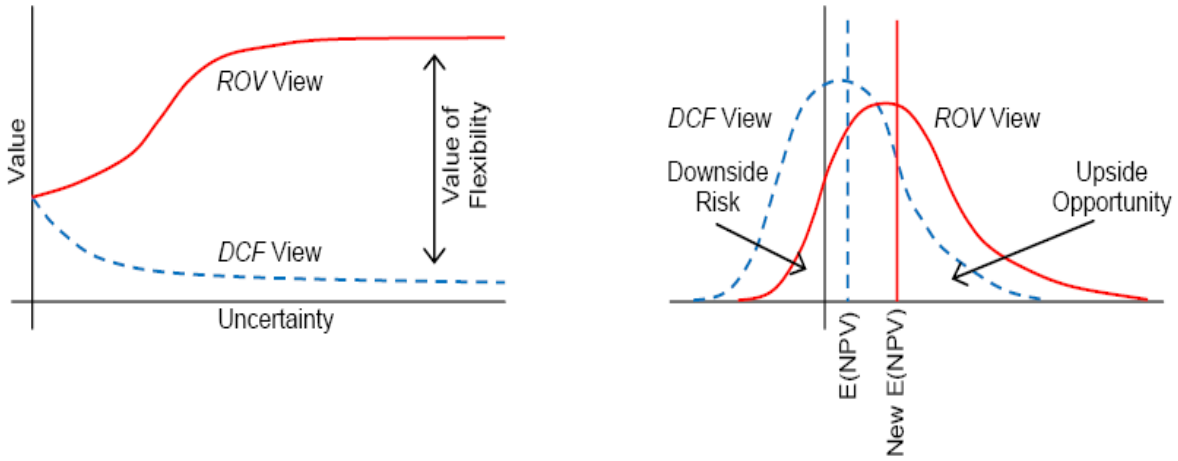


Figure 3.1— Discrepancy between DCF (Discounted Cash Flow) and ROV(Real Options Valuation) Approaches. Reproduced from Jafarizadeh and Bratvold (2009).

It is necessary to introduce some of the main real options terminology before continuing the discussion. Call options are the right to buy an underlying asset by paying the exercise price. The profit on the option is the difference between the value of the underlying asset and the exercise price. The opposite of a call option is the put option which is the right to sell the underlying asset to receive the exercise price. American option is an option that can be exercised at any time during the life of the option while European options can only be exercised on their maturity date. There are different types of real options in regards to the flexibility they offer; deferral option: this is an American option that gives one the right to delay the start of a project. The exercise price mimics the investment needed in starting the project. The abandonment option is an American put option. Other options include; the option to contract (scale back), the option to expand and the option to extend. More complicated options exist such as options on options which are defined as compound options (see **Fig. 3.2**). Here each option is contingent on the earlier exercise of other options. Rainbow options are options that are driven by multiple sources of uncertainty. Most real world applications, such as exploration and production problems, are modelled as compound rainbow options **(Copeland and Antikarov 2003).**

This shows us that real options provide a framework to model most investment decisions. Once the problem is defined the next step is to quantitatively evaluate the flexibility given by the options that are designed for the problem. The valuation methods used in the literature have been inspired by methods used for financial options evaluation. Although these methods have proven applicability to financial options, not all are well suited for real world applications. Furthermore, modifications are required to extend some of these methods to value real options. In the next section, a brief review of the common valuation methods is presented for real options valuation.

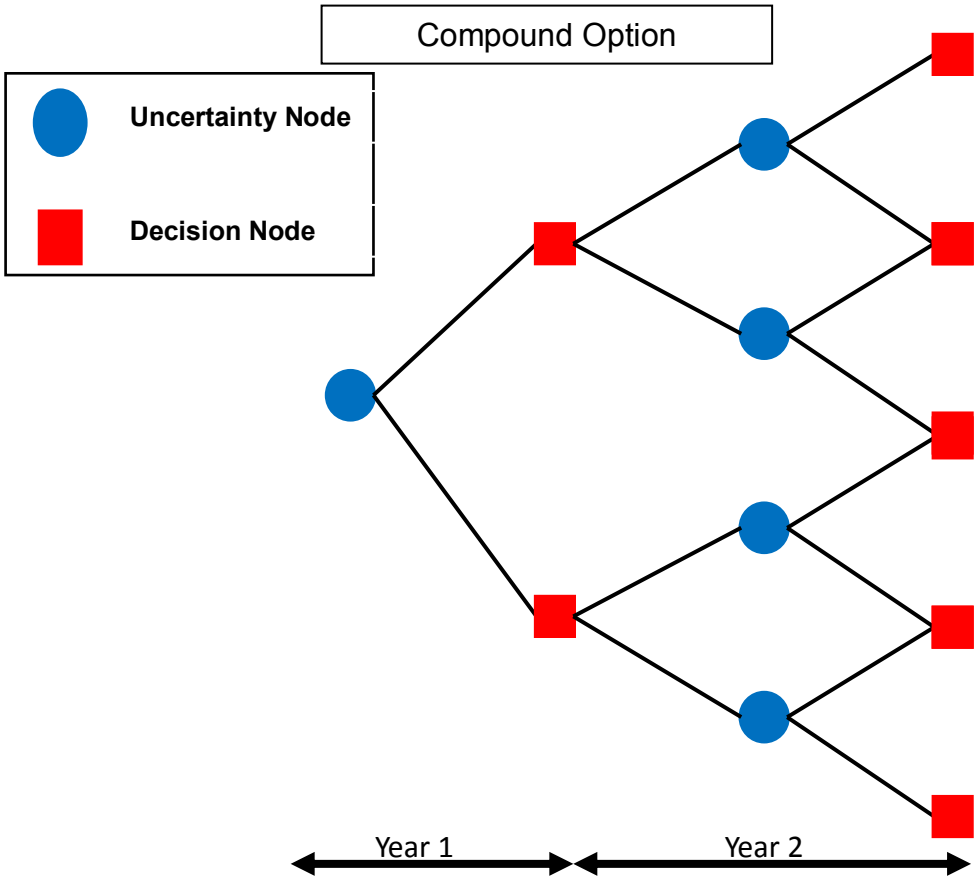


Fig. 3.2– Compound option diagram. This diagram shows decision contingent on previous decisions over a two year period. Once a decision is made after the first time step (1 year), a new decision becomes available contingent on the previous decision.

3.3.2 Valuation Methods

Four basic computational methods are used for assessing real options value. These methods are compatible with each other and can be used separately. It is best to use the simplest method the produces useful results. (**Sick and Gamba 2010**).

Decision Trees or Lattices

Decision trees are a sequence of alternating decisions by the decision maker and nature. These are solved in a recursive manner. The decision is then made by choosing the most highly valued decision at the node. Decision trees can be complex and time consuming to build and analyze. Another disadvantage is that it combines information about risk out comes and decisions, where decision makers would prefer to leave the risk analysis to other more specialized practitioners (**Sick and**

Gamba 2010). These are useful and easy methods which are efficient for American and European options. However, they increase in complexity when there are multiple risk factors (state variables). For multi-dimensional lattice models, their complexity is similar to that of numerical solution of partial differential equations. The solution to decision trees is obtained via a recursive approach which is based on the Bellman equation of dynamic programming. Decision trees can become intractable with increasing number of flexibilities or options (**Smith and McCardle 1999)**. One form of lattice models is the binomial model (**Cox et al. 1979**) which assumes that the objective function can only move in one of two possible directions: up or down. This is a discrete-time model. See **Fig. 3.3** for a depiction of a binomial model. Decision tree analysis also offers the same advantage over traditional DCF methods although in contrast to option pricing theory, the probability of the occurrence of a specific event needs to be estimated. This is done implicitly when using option pricing theory through calculating a so-called pseudo probability (**Zettl 2000**).

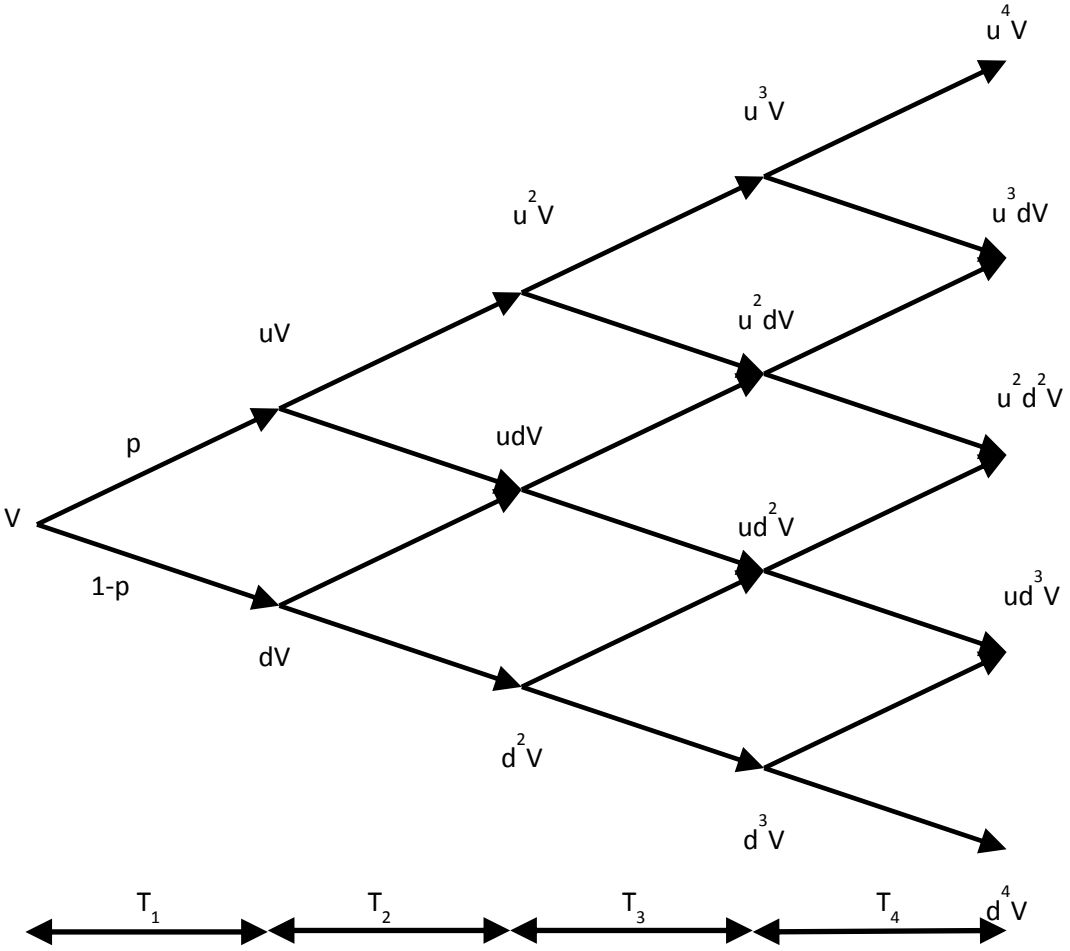


Fig. 3.3– Binomial model lattice. (p) and (1-p) are the probabilities of the up (u) and down (d) moves.

From **Fig. 3.3**, the value, V, at the end of the first node (T_1) is given by:

$$V = e^{-r\Delta t}(puV + (1-p)dV) \qquad \text{Eq. 3.1}$$

, where r is the discount rate, assuming continuous discounting.

When considering technical uncertainty, it is possible to separate this from the economic uncertainties. This might be required because technical uncertainties resolve discontinuously in time. As an elaboration on binomial lattices, it is possible to use quadranomial approach when having two separate uncertainties. This approach is defined as a two-variable binomial

tree where the decision tree has four branches at each node (**Copeland and Antikarov 2003**). However, this approach is not easily scalable to incorporate a large number of uncertainties.

Closed form Analytic Solutions

These are considered to be the best methods to use when possible. They include Black-Scholes formulas (**Black and Scholes 1973**) for European call and put options, perpetual American call and put options that are based on normally or lognormally distributed assets. It is important to note that most real options do not meet the requirements for this method (**Smith and McCardle 1999; Davidson 2001; Copeland and Antikarov 2003;Damodaram 2005**). Also, real options use more types of stochastic processes than are used for financial options. There are some limiting cases for which these methods can be used (**Sick and Gamba 2010**). The Black-Scholes model is a limiting case of the binomial model. This model assumes that the state variables are continuous and that there are no jumps in their values (**Damodaran 2005**). The Black-Scholes model for a European style option is defined as follows:

$$V = S\,N(d_1) - Ke^{-rt}N(d_2) \qquad \text{Eq. 3.2}$$

Where: $d_1 = \frac{\ln\left(\frac{S}{K}\right)+\left(r+\frac{\sigma^2}{2}\right)t}{\sigma\sqrt{t}}$ and $d_2 = d_1 - \sigma\sqrt{t}$

S= Current value of the underlying asset

K=Strike price of the option

T=life to expiration of the option

R=riskless interest rate corresponding to the life of the option

σ^2=Variance in the ln(value) of the underlying asset

N( )= cumulative normal distribution functions.

Numerical Solutions to PDEs

These are used mostly in academic real option problems because they require a custom PDE solution for every real option problem it is considered to be impractical for industry use (**Sick and Gamba 2010**).

Simulation Models

Simulation was used for European options but it was considered to be not useful for American options because simulation is a forward approach while the Bellman equation is solved using a recursive approach. It is now known that simulation can be used to estimate conditional expected payoffs and the continuation values used in a lattice approach. The advantage of simulation is that it can incorporate multiple risk factors (state variables) and complex processes (**Sick and Gamba 2010**).

Dynamic Programs

Since dynamic programming was mentioned earlier and will be an essential part of the valuation method enveloped in this thesis, a quick overview of this approach is presented. Using dynamic programming techniques, it is possible to construct an infinite horizon dynamic programming model. The main issue to be considered when constructing a dynamic programming model is to identify a reasonably small set of state and decision variables which are essential to describe the value of the project over time. Dynamic programming approaches usually face computational restrictions. Problems could also be modeled using finite-horizon dynamic programs. Simulation can be used to solve dynamic programming approaches. The main disadvantage of using simulation is that it is difficult to obtain optimal policies for downstream decisions. Because the number of policies can grow very quickly when simulation is used to calculate the expected values for all possible policies from which the optimal policy is chosen (**Smith and McCardle 1999)**. When using dynamic programming approaches, the whole sequence of decisions is broken up into two components: the immediate decision and the value function which captures the consequences of all the subsequent decisions. An advantage of using dynamic programming approaches to contingent claims approaches (e.g. replicating portfolios or Black-Scholes model), is that when risk cannot be traded in the markets, the objective function simply reflects the subjective valuation of risk of the decision maker (**Dixit and Pindyck 1994**).

3.3.3 Examples in E&P

Attempts of applying real option valuation in the petroleum industry has proliferated in the past decade and has provided various methodologies and approaches. Until now, no unique general methodology has been proven to be applicable to most projects. Therefore, a review of these methodologies is necessary in order to investigate which method can be used as the initial real options approach in an SP flooding project.

One of the earliest considerations of the applicability of real options valuation to the petroleum industry was by **Markland (1992)**. The study discussed option theory as possible basis for developing methods to estimate the market value of a wide variety of investments under uncertainty. It also presented a review of the current state of project evaluation using the DCF method. The conventional method of economic evaluation analysis is based upon a discrete time simulation of the projected cash flows associated with the project, which take into account taxation and inflation and uses time periods that are appropriate for the fiscal regime and rates of change. Thus the resulting cash flows are discounted using a rate of return that is set at a uniform level. Or as an alternative, an internal rate of return is derived using the general discounting mechanism to compare with the required rate of return. The choice of discount rate is used to reflect the level of risk. The key to implementing projects is the management of risk. Risk in any project either presents downside or upside opportunities. Risk has many potential sources such as: geological, regulatory, technical, environmental, commercial, financial, and fiscal. The study used oil price as an example of a time dependent risk. It then discusses the practical treatment of risk in DCF analyses: scenario analyses, sensitivity analyses, distribution of outcomes, expected monetary values and simulation (stochastic). In each of these methods the discount factor is required in order to be able to estimate the NPVs and thus higher discount rates are required for riskier projects. Although the DCF approach is not incorrect it does present practical difficulties in determining the correct discount rate. This is where the modelling of operating options can be used. It was suggested in this study that inaccuracies can be reduced if projects are modelled by option pricing models. Thus these models should produce

more realistic valuations of the business opportunities which in turn are a considerable improvement over the application of DCF methods. For option pricing models to be successful the following constraints must be adhered to (**Markland 1992**):

- The ability to incorporate the essence of the time dependent risks in a project into the descriptions of a small number of state variables.
- The ability to model adequately the management response to any variation in the state variables.
- To have a mathematically tractable problem.

If these restraints are not adhered to then it is better to use the conventional DCF method. The main contribution of option pricing models is to improve the project evaluations where the discount rate choice is particularly difficult and where stochastic calculus can be used to cope with man decision points. Yet the success of option pricing will depend on practical results. Another important contribution of option pricing is that it provides a useful paradigm for different business situations such as marginal field developments and acquiring operational flexibility (**Markland 1992)**.

Chorn et al. (1998) also argued similarly that DCF as an example of traditional financial tools routinely underestimate the impact of incremental reservoir knowledge on uncertainty investments in relation to management intuition. Traditional tools do not adequately value the flexibility in investments by management and the use of new knowledge. With new knowledge management can be flexible with project scope, rate of investment, production rates and other factors to accommodate price, market and cost uncertainties. The value of Incremental knowledge can be assessed through its impact on improving investment outcomes. Through examples, The study found that due to the failure of DCF method to value long-term, uncertain investments, real-options is recommended because it is capable of valuing embedded opportunities, it is able to value knowledge as it becomes available, and it overcomes the invest now or never time frame of the DCF method. In general, the study found that real options mimic actual investment processes more accurately.

When real option valuation is compared to other evaluation methods, such as decision trees or Monte Carlo Simulation (MCS), **Galli et al. (1999)** found that these three approaches attempt to determine the expected value of the project but have different assumptions regarding the underlying distributions, variation with time of input variables and the correlations between the input variables. Also they differ in the method they use to handle the time value of money. Decision trees and MCS use the traditional discount rate while option pricing uses the financial concept of risk neutral probabilities. MCS ignore managerial flexibility and focus on modelling uncertainty in parameter values. Decision trees focuses on analysis of different managerial strategies and choosing the maximum NPV value strategy, yet due to time constraints, only a few strategies can be studied. Options pricing similarly studies possible management choices but it is limited to certain well-known models (e.g. Black-Scholes, mean reverting) in order to make the computations tractable, however as mentioned earlier, these models are not well suited for real life problems. The study suggested that for real option to be realistic, they must incorporate more technical information (e.g. advances in reservoir characterization) and must be able to measure the value of information in a meaningful way (**Galli et al. 1999**).

Smith and McCradle (1999) illustrated the options approach by applying it on real oil and gas investment examples. Interest in using options pricing theory models was expressed because these models do not require the use of a risk-adjusted discount rate. However, there were concerns that models described in real options literature greatly simplify problems. The study found that option pricing and decision analysis approaches are similarly and equally capable of modelling flexibility. Both approaches should be considered as complementary modelling approaches that can be nicely integrated. It is important to note that applying off-the-shelf option pricing models to real projects (e.g. Black-Scholes formula to value an undeveloped field) is not advised due to their restrictive assumptions. Yet the option pricing approach presents a simple technique for

incorporating market information into project values that are easily incorporated into decision-analytic or dynamic programming models. Thus option pricing methods are viewed as a refinement on decision analytic and dynamic programming methods.

When discussing the existing applications of option pricing, **Zettl (2000)** considered the two main types of option pricing application: continuous models that are based on the Black-Scholes equation and the discrete models that are based on the Cox-Ross-Rubinstein binomial model (**Cox et al. 1979**). The main difference between these models arises from the different assumption of the price process of the underlying asset. Black-Scholes uses a time continuous price process (prices change continuously), usually done by using geometric Brownian motion with mean-reverting process. Then Partial differential equations are derived to define the option value. For the discrete models, the assumption is that price changes occur only at discrete points in time through using a multiplicative binomial process (prices rise or fall by a constant factor). Continuous models are mathematically advanced thus discrete models are more user friendly. The study also found that option pricing should be used in the development phase rather than in the exploration and appraisal phases because at those phases the geological risk is paramount to the economic risk (which is the focus of option pricing). It also recommends the use of traditional methods along with option pricing to obtain the optimal information required for the decision making process.

Saito et al. (2001) present an analysis of managerial flexibility that is embedded in exploration and production. The economic impact of implementing different production techniques on the valuation of oil reserves was demonstrated. DCF and real options are both used. It was found that an increase in oil recovery value is possible by combining different production techniques using real options and achieves higher value compared with the DCF value. It is suggested that real options are a better approach because of the many managerial choices in oil recovery. This study uses the approach of **Paddock et al. (1998)** for real options evaluation. The main objective of the study is to price oil reserves' using real options and DCF analysis. The PSS model(**Paddock et al. 1998**) demonstrates how to integrate explicit market equilibrium model using option valuation to assess the value of the option. It uses a modified Black-Scholes equation. This is a weakness of the model given the assumptions required by Black-Scholes. It produces a real options analysis for developing an oil reservoir by incorporating managerial flexibility in control variables (e.g. water injection or well location) in evaluating reservoirs. This paper presents an early approach to determine value of flexibility. However, it does not include uncertainty in the time series for the state variables and its evaluation model is based on a modified Black-Scholes equation which is not very suitable for determining the value of oil reserves.

Real options have also been used for deepwater field development. **Dezen et al. (2002)** used real options valuation as an extension of the traditional DCF techniques for evaluating the alternatives for an offshore oilfield. Real option valuation estimates the project worth with managerial flexibility which results in the expanded NPV. The model was based on the Black-Scholes equation. It was found from the example that the value of flexibility can be substantially greater than the static NPV, which can be greatly beneficial to the development if there is sufficient volatility and time to expiration. The study argues that real option valuation can be considered as a decision tool that can assist the process of selecting the optimal field development plan through providing an insight into the value of managerial flexibility.

When applying real option valuation to a production enhancement project, a binomial lattice was used to solve the valuation by **Bailey et al. (2002)**. It was found that real option valuation is best suited for situations when there are future uncertainties,

response flexibility is available and when DCF techniques indicate marginal project viability. In contrast, real option valuation does not meet all valuation needs nor does it provide much insight when a project is highly lucrative or highly uneconomical, that is when there is minimal uncertainty. Also, applying real options does not imply the blind application of a Black-Scholes type model, because it is bound by a number of assumptions and caveats that are not compatible with real life projects. **Bailey et al. (2004)** provide a discussion of the use of real options in the industry.

An attempt to incorporate technical uncertainties into option evaluation models was presented by **Armstrong et al. (2004)**. The example was that of evaluating the option to acquire more information in the future. A form of Bayesian updating that was based on copulas was used. The study argued that new information can radically change state parameter distributions. The evaluation method used a Black-Scholes model to quantify the impact of new information. Although the study presented an interesting approach to incorporate the technical uncertainties and update the state parameters as more information is obtained, the application of this method is limited due to the restrictive assumptions of using the Black-Scholes model for real options.

Investigating the Black-Sholes equation further**, Rasmussen et al. (2005)** presented a functional analysis of the Black-Sholes equation. The study also developed analytical solutions under various conditions through derivation using Laplace transforms. The applicability of the Black-Sholes formula is very limited because it is a special closed-form solution of the general Black-Sholes partial differential equation with boundary conditions representing the European options. Thus the Black-Sholes partial differential equations response and its analytical solutions under commonly applied conditions were analyzed. The modified Black-Sholes equation was analytically solved as well. It was found that the analysis of the modified Black-Sholes equation under various boundary conditions reinforced the fact that solutions of the equations will vary by the initial and boundary conditions imposed on it. Therefore, the frequently used analytic solution provided by **Black and Scholes (1973)** is only one of the specific solutions available, which may have limited applicability.

Bratvold et al. (2005) discussed the following approaches to real option valuation:

- Complete decision tree approach that uses the market-based valuation and the DCF evaluation.
- Marketed asset disclaimer approach that uses the DCF to value the underlying asset without flexibility.
- Marketed asset disclaimer approach using market-based valuation without flexibility.
- Financial option analogy approach that uses both the market-based valuation and DCF to value the asset without flexibility.

These different methods were applied to an option of drilling one production well now or in the next four years in a deepwater offshore oilfield. These different methods suggested different patterns of value. This pattern of difference can be attributed to the different limitations of these methods. The best method, from a technical point of view, was found to be the complete market-based valuation decision tree approach (**Bratvold et al. 2005**).

Another comparison by **Yao et al. (2006)** considered four other approaches using a case study of a company considering whether to develop a liquefied petroleum gas (LPG) distribution project with two strategies available: to invest immediately (no flexibility) or to begin a trial investment that is followed by an expansion decision. This case study had the following main uncertainties: oil price, liquid gas production costs, sales price and volume. The real options valuation methodologies compared were;

- The Luehrman Approach (**Luehrman 1997; Luehrman 1998a; Luehrman 1998b)**: this approach is advocated for the evaluation of phased projects where initial investments do not have a cash flow, but provide the right to make further investment decisions after resolving uncertainty. The valuation problem is divided into two parts: a traditional NPV that is based on cash flow discounting for the initial investment and the valuation of the subsequent optional investment to expand. The Black-Scholes pricing formula is used in this method to value the expansion opportunity where volatility is either an: educated guess, implied volatility calculated from market data or the standard deviation of returns calculated from a MCS of the project cash flows.
- Marketed Asset Disclaimer Approach (**Copeland and Antikarov 2005**): this approach uses the NPV of the base project (without any flexibility) as the underlying asset. This is known as the best unbiased estimate of the price that it would attract if it were a marketed asset. A main advantage of this approach is that it is built upon the traditional NPV valuation.
- Smith et al. (**Smith and Nau 1995; Smith and McCardle 1999**) Approach: this approach recognizes and treats two different types of uncertainty based risk; private (e.g. OOIP) and public risk (oil price). This approach then solves the valuation by integrating decision tree analysis (subjective probability assessments used to value private risks) and option pricing (used to value market risk).
- The Luenberger Approach (**Luenberger 1998**): this approach proposes a variation on the Smith et al. approach in assuming that investors should first purchase the project and then carry it on as an option. Subjective probabilities and a certainty equivalent are used in private uncertainty while market information and risk neutral probability are applied for market uncertainty.

The study found that the approaches differ from each other in the assumptions they make or the modeling method they use. To select an appropriate approach, a full understanding of the nature of the options being considered is required (nature of uncertainties, nature of flexibilities). The Smith et al. approach was found to be the most robust and widely applicable approach to real options valuation (**Yao et al. 2006)**.

A valuation model that integrates DCF, real option valuation and preference theory was presented by **Lima et al. (2005)**. Results of the model tended to diverge from the traditional valuation models as uncertainty increases. An operational definition of real option pricing was suggested by **Wilkinson et al. (2005)** and introduced a criterion for deciding if a given method generates an outcome that is consistent with this definition. Two real option techniques: consolidated (combines all uncertainties into a single effective volatility) and multi-lattice (retains the fundamental degrees of freedom in the problem) were also considered. It was found that the consolidated approach is not favoured because of the difficulty of estimating the consolidated volatility and that the method is subject to the ambiguities of implementation (e.g. Geometric Brownian Motion assumption). In contrast, the multi-lattice approach is easier to motivate because market uncertainties can be simply incorporated using risk-neutral probabilities and it deals exclusively in observable variables. The method is also considered to be straight forward.

Using decision analysis to evaluate real options, **Hahn et al. (2007)** showed that the traditional decision analysis methods are able to provide an intuitive generalized approach to valuing real options. The approach presented here is based on a binomial decision tree with risk-neutral probabilities rather than on a binomial lattice framework with replicating portfolios (usually implemented in the discrete-time approach in financial literature). This presented an equivalent yet more intuitive framework for approximating the uncertainty associated with changes in project value over time.

Real option valuation was also suggested to complement the structured framework of stage and gate management processes with value of information evaluation resulting in a tool that can improve financial discipline and preserves the advantages of stage and gate management processes (**Azzarone and Bruni 2008**). Implementing the real options pricing technique within the stage and gate management processes framework by introducing a new process at the "screen and evaluate" phase was suggested which resulted in a more financially disciplined stage and gate management process. This approach also used the Black-Scholes equation and the binomial lattice approach to obtain the value of the option.

It is important to be cautious when adapting financial option valuation methods directly to the real world. **Glavis and Villarreal (2008)** discussed using an example, the limitations of the binomial tree approach for real options valuations when directly extended from financial options valuation. This was due to the fact that the strong assumptions that support the theory cannot always apply to real investments. They suggested an extension of the binomial approach that complies with the conditions that are imposed on for real options valuations. The extended binomial tree allows for sign changes to occur inside the underlying assets tree in contrast to the traditional binomial approach. It also prevents the skewing of the distribution of the rate of return from occurring. They note that valuation tools are applied to the representation of a project by mathematical models, not to the project itself, thus the need for these models to be adjusted to reality as much as they can. Using extended binomial trees for real option valuation was found to be a reliable tool that is consistent with reality that produces accurate results without disregarding binomial model assumptions.

Real option valuation was also suggested in handling uncertainties of a portfolio of oil projects (**Costa Lima et al. 2008**). This was done using an integrated methodology of real options, portfolio theory, and Monte Carlo Simulation. The valuation of the option was based on the expectation and standard deviation of NPV by using MCS. Numerical results indicated the importance of considering the value of real options or managerial flexibilities in analyzing the portfolio of projects because it greatly increases the efficiency of the planning process. This is done by focusing on the effect of managerial flexibility on the total business performance and on the interactions between projects (**Costa Lima et al. 2008**).

A methodology to model real option valuation of an investment opportunity concerning an exploratory project that has high uncertainty regarding the future production rates was introduced by **De Abrue and Cavalcante (2009)**. The decision was whether to develop the reservoir or not. Stochastic processes are used to model the uncertain variables. The main aim of the model was to define a decision making rule that incorporates the value of flexibility due to the possibility of delaying the investment due to the availability of better geological information. The option value was determined by a continuous time real option model and the results were compared with estimates that were obtained from traditional DCF methodologies. The methodology presented is seen as an additional economic analysis decision-making tool that can help in decision making in an uncertain environment; however it is not suggested to be a replacement of the traditional evaluation methodology. The study suggested that more information can be incorporated with the model when using a complete uncertainty analysis that is numerically simulated. It was also found that the decision rule is very sensitive to production uncertainty: the greater the uncertainty of the quantity of produced barrels the greater the trigger value to invest in the oil project (**De Abrue and Cavalcante 2009)**.

A risk-neutral binomial valuation model was suggested by **Xu et al. (2012)** to evaluate the option of having flexibility in the switching time from primary recovery to waterflood. The production profiles were obtained using numerical simulation (UTCHEM). The main state variable considered was the oil price which was modelled using GBM and mean reverting processes. The technical uncertainty was considered by having a normally distributed permeability, porosity and initial water saturation field of the model. However, it does not consider the uncertainty in the time series of these technical parameters.

Because most projects in the industry consist of numerous uncertainties (such as reservoir heterogeneity, decline rate, oil price, etc), a valuation model that can handle multiple uncertainties is required. **Jafarizadeh and Bratvold (2009)** recommend the use of the Least Square Monte Carlo Simulation (LSM) technique as a potential real options valuation technique. Its main advantage is that it is suited for investment decisions that have multiple uncertain factors and that have compounded options that can be exercised at any time. The LSM method was originally developed to value American options in the financial markets (**Longstaff and Schwartz 2001**). This method has been applied mostly initially in financial literature (**Cortazar et al. 2008;**) and has been extended to real life problems (**Chiara et al. 2007; Boogert and de Jong 2008; Willigers and Hansen 2008;Willigers et al. 2010;Denault et al. 2011)**. Real options in the petroleum industry are much more complex than financial options. These real options usually involve multiple sources of uncertainty, complex cash-flow streams and long time spans. Therefore careful analysis is required in order to extend the financial option methodologies to real options. Real options valuation must be able to model flexibilities and incorporate a realistic number of uncertainties and to derive simple valuation methods that can be applied effectively. LSM algorithm is able to provide a simple enough valuation method. This is done by simulating thousands of realizations, and then it uses a regression function (calculated from simulation data) to estimate the optimal policy at each exercise date. The LSM was implemented using a linear regression function. The efficiency of the LSM algorithm is not affected by the number of basis functions used and the complexity of the regression equation. The complexity of the LSM algorithm increases with number of decisions and alternatives. Although most petroleum industry decisions are high dimensional and have multiple sources of uncertainty with complex cash-flow structures, the LSM method is a powerful evaluation method if the number of decisions can be kept low (usual for these investments) without losing much realism. Risk-neutral approach is recommended to be applied to project evaluations in the petroleum industry. The LSM algorithm is recommended to be suitable for many petroleum projects, specifically those with multiple uncertainties or complex cash flows. The main disadvantage of this approach is its dimensionality when the number of decisions or alternatives increases. Thus to successfully implement LSM, a good understanding of the problem structure is required, and also a good choice of basis functions (**Jafarizadeh and Bratvold 2009**).

Willigers and Bratvold (2009) demonstrated how LSM simulation can handle more realistic valuation situations with more realistic price models and multiple uncertain variables. The objective was to value a gas field where there exists a decision to either trade the gas on the spot market or to sell the gas based on a long-term supply contract. The traditional DCF methodologies are based on the unrealistic assumption that when the initial investment is made the course of the project will run without intervention neglecting the possibilities of abandonment or expansion, while real options valuation allows for systematic assessment of the available choices, exposure to risk and the expected outcome of an option. It is not limited to an initial stop/go decision; rather real options valuation entails a sequence of choices as more information becomes available. **Willigers and Bratvold (2009)** argued that the main failings of the real options valuation methodology are the limitations in the techniques used for valuation that make it unable to model real world problems and the complexity level of valuation that has limited its understanding and accessibility to a limited subset of the decision making community. Yet, recently there have been new advances that have made real options valuation more accessible and applicable (e.g. powerful and flexible real options valuation techniques such as the LSM developed by **Longstaff and Schwartz (2001)**). The economic model used in this paper showed the versatility of the LSM real option technique and its capability to handle complex economic problems (multiple uncertainties and commercial constraints). The real options valuation methodology enhances the accuracy of economic assessment and provides critical insights into management strategies. It was found that LSM can be readily generalized to more-complex problems. It is relatively insensitive to the number of uncertainties. Its only limitation is that it becomes more complex as the number of options and decisions increases.

It is apparent that applying real option valuation methods can capture the value of flexibility for highly uncertain E&P projects. Most of the literature on applying real option valuation methods to E&P problems focused on economic uncertainty, usually the oil price, and emphasized the importance of the discount factor approach used whether it is risk-adjusted or risk-neutral. Although these are important elements in any economic assessment of reservoir recovery processes, technical state variables are either neglected or treated in a simplistic manner. The review also shows that there are a variety of valuation methods have been applied to E&P problems

3.4 Concluding Remarks

Decision analysis methods have been used in the industry for some time now. Their application has varied widely depending on the nature of the problem and on the increase in computational capability. The justification for using these methods is the need to make good decisions even if this does not always guarantee good outcomes. Uncertainty is imperative to the decision making process. Otherwise in the absence of uncertainty, decisions would be much easier to make. There are a variety of approaches for decision making in the presence of uncertainty that have been used in the industry.

Decision analysis methods used in decision making for SP flooding or other chemical EOR process were reviewed. The methods varied in their objective and how they handled uncertainty. Uncertainty in the time series was not considered. Some studies considered only technical uncertainty while others considered both technical and economic uncertainty. All studies recognized that uncertainty was detrimental to the success of chemical EOR processes. None considered the up side potential that this uncertainty can create.

Thus there is a need for an approach that can incorporate both technical and economic uncertainty, consider uncertainty in the time series and produce meaningful results conditional on how this uncertainty resolves. Real options theory provided the inspiration for developing such an approach. By valuing flexibility, real options provides a means to produce optimal policies in the presence of uncertainty and can capture the upside potential of this uncertainty in addition to mitigating its negative consequences. A review of real options and their application to E&P problems was presented. Most valuation methods are direct extensions from financial option valuations. Some of these methods such as the Black-Scholes equation cannot be applied in most cases to real options because of its restrictive assumptions. Caution is required when considering applying valuation methods originating from financial literature directly to value flexibility for reservoir recovery processes (**Smith and McCradle (1999)** ;**Bailey et al (2002);Glavis and Villarreal (2008); Sick and Gamba 2010)**. Most of the E&P focused literature emphasized only economic uncertainty such as uncertainty in oil prices. Technical uncertainty was either neglected or treated in a simplistic manner where production profiles were obtained analytically.

An important distinction should be made between real options thinking and real options valuation. Thinking refers to assessing the value of options of information acquisition to reduce uncertainty and VoF to exploit or mitigate the effects of uncertainties as they resolve. This can be considered as an extension of traditional decision analyses methods. Valuation, on the other hand, refers to determining the value of risky cash flows from an external investor perspective (**Begg et al. 2002**). The focus of this thesis is to apply real options thinking in the first place to surfactant-polymer flooding and then investigate whether any of the real options valuation methods can be extended to incorporate the technical uncertainties with the economic state variables within one model.

The LSM method can capture the value of flexibility and is easily scalable to handle multiple sources of uncertainty. This method was applied recently to E&P problems (**Jafarizadeh and Bratvold 2009; Willigers and Bratvold 2009**). However, the focus was mostly on economic uncertainty. In the next chapter, the application of this method to value flexibility for SP flooding is discussed.

4 Theory and Methodology

4.1 LSM Theory and Implementation

After reviewing real options and its applications in the E&P context, the LSM method was found to be the most suitable approach to value flexibility for SP flooding due to is easy scalability to incorporate an increasing number of uncertainties, its consideration of uncertainty in the times series and its relatively straight forward implementation.

The LSM method is based on a forward looking stochastic simulation, a Monte Carlo simulation, coupled with a backward recursive dynamic programming technique that evaluates the option or decision using least-squares regression (**Gamba 2003**). A good understanding of the decisions or problems is needed to implement LSM successfully (**Jafarizadeh and Bratvold 2009**).

The main steps of the LSM method can be summarized as follows (see **Fig. 4.1**) (**Gamba 2003**):

I. Generating a large number of possible realizations of the state variables and obtaining the objective function from the Monte Carlo simulation model.
II. Starting recursively from the last decision node, the expected future value of holding the option is compared with the immediate value of exercising the option. The expected future value is conditional on the resolution of the uncertainties until that time. This expected future value is equivalent to the value of continuation.
III. Estimating the continuation value by regressing (using least-squares regression) the simulated future outcomes onto basis functions of the state variables at the time of the decision. This relates the continuation value to the state variables at a specific time.
IV. Determining the optimal policy by choosing the option that achieves the highest value given the known information.

At each time step or decision node, the problem is divided into two components from the dynamic programming point of view, the value of exercising the option or strategy at the current time step and the value of continuation where no action is undertaken at the current time step. These decisions (or options) are valued conditional on the full or partial resolution of the relevant uncertainties with time. The detailed discussion of the algorithm is presented in the next section.

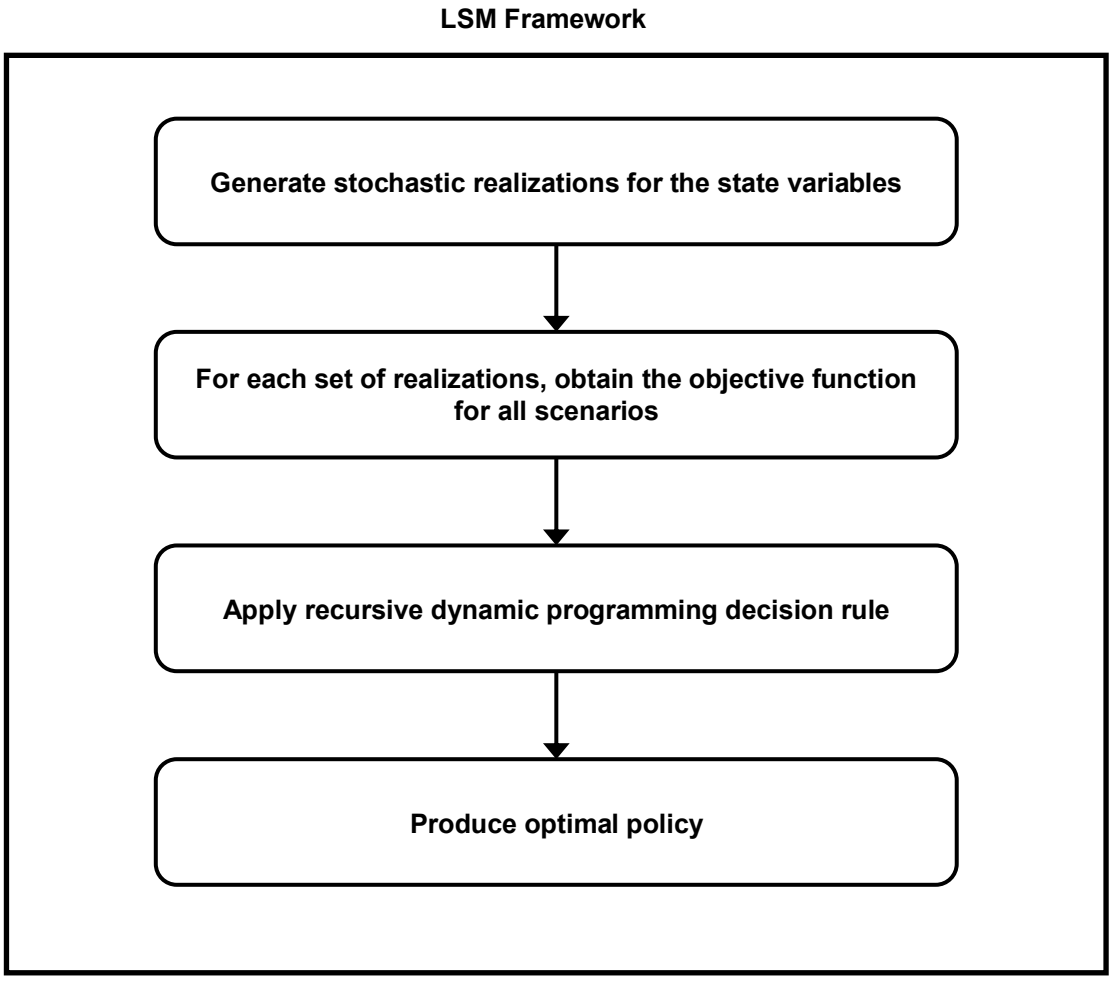


Fig. 4.1– The LSM method framework

4.1.1 The Least-Squares Monte Carlo Algorithm

The LSM algorithm is introduced in the context of flexibility in surfactant injection where the objective is to determine whether having flexibility in the timing of a surfactant flooding process is beneficial compared to a static injection policy.

A variable τ is defined as the optimal time to initiate the surfactant flood, i.e. exercise the option, and $\tau(x)$ is the optimal exercise time for a certain realization path. (x) is defined as one realization path of the evolution of the state variables over a time horizon of, for example, 10 years and that $x \in X$. X is the total number of stochastic simulations. The state variables used in the algorithm are the economic uncertainties: the oil price (P_o) and the surfactant price (P_s) which are summarized by the variable, $\mathbb{P}_i = \{P_o, P_s\}$. The technical uncertainties are separate from the economic uncertainties and their influence is manifested in the production profile of the reservoir model. They are summarized by the variable $\mathbb{T}_{i,y_n} = \left\{T_{S_{orc},y_n}, T_{D_s,y_n},\right\}$. The other economic parameters are correlated with P_o and they are incorporated in the NPV calculation. There will be a distinct realization of the state variables for each path, (x). Since we assume that our knowledge or information set evolves through time, the state variables are assumed to evolve through time. Hence, $\mathbb{P}_{i,y_n}(x)$ is the set of economic state variables at the decision node time y_n along the x-th simulated path, which will illustrate the time dependencies of the state variables. Here y_n is the decision time which is an element of the set of decision space, $Y = [y_1, \dots, y_n]$ and consequently the optimal exercise time, $\tau(x) \in Y$. Assume we have the payoff function $V(y_n, \mathbb{P}_{i,y_n}(x), \mathbb{T}_{i,y_n}(x))$ which is the net present value of the process (NPV at the end of the 10 year simulation interval) when we exercise the option to initiate the surfactant flood, dependent on the realization of the state variables, at time y_n. This function will be defined as the immediate option exercise value.

OV is defined as the optimal value function, which is the value of the optimal NPV at the end of the simulated field life dependent on the exercise of the optimal surfactant initiation policy. Then:

$$\tau(x) = y_n \text{ , if } OV(y, \mathbb{P}_{i,y}(x), \mathbb{T}_{i,y_n}(x)) = V(y_n, \mathbb{P}_{i,y_n}(x), \mathbb{T}_{i,y_n}(x)) \quad \text{Eq. 4.1}$$

Since τ (x) is the optimal surfactant initiation policy per path (x), it is assumed to follow this condition that defines its optimality over all paths:

$$\tau = \inf\{y \mid OV(y, \mathbb{P}_{i,y}, \mathbb{T}_{i,y}) = V(y_n, \mathbb{P}_{i,y_n}, \mathbb{T}_{i,y_n})\} \quad \text{Eq. 4.2}$$

, which is the first time (i.e. decision node) where the option value equals the value achieved from exercising the option.

At this step, $OV(y, \mathbb{P}_{i,y}, \mathbb{T}_{i,y})$ is not available. However, it can be determined using Bellman's (**Bellman 1957**) formula:

$$OV(y, \mathbb{P}_{i,y}(x), \mathbb{T}_{i,y}(x)) = \max\{V(y_n, \mathbb{P}_{i,y_n}, \mathbb{T}_{i,y_n}), e^{-r(y_{n+1}-y_n)}\, E^*_{y_n}[OV(y_{n+1}, \mathbb{P}_{i,y_{n+1}}(x), \mathbb{T}_{i,y_{n+1}}(x))]\} \quad \text{Eq. 4.3}$$

, where r is the discount factor and $E^*_{y_n}$ is the expectation function. The continuation function is defined as:

$$\Phi(y_n, \mathbb{P}_{i,y_n}(x), \mathbb{T}_{i,y_n}(x)) = e^{-r(y_{n+1}-y_n)} \quad E_{y_n}{}^*[OV(y_{n+1}, \mathbb{P}_{i,y_{n+1}}(x), \mathbb{T}_{i,y_{n+1}}(x)) \mid \vartheta_{y_n}] \quad \text{Eq. 4.4}$$

, where ϑ_{y_n} is the information set $\mathbb{P}_i, \mathbb{T}_i$ at time y_n. Thus the decision rule at time y_n along the x-th path is:

$$\text{if } \Phi(y_n, \mathbb{P}_{i,y_n}(x), \mathbb{T}_{i,y_n}(x)) \le V(y_n, \mathbb{P}_{i,y_n}(x), \mathbb{T}_{i,y_n}(x)) \text{ then } \tau(x) = y_n \quad \text{Eq. 4.5}$$

To determine the optimal policy, the decision rule is applied recursively from $y_n = y_N$ back to $y_n = y_1$. When the algorithm reaches $y_n = y_1$ and all the optimal policies have been determined along all paths, the mean value of the option (optimal

policy) is determined by calculating the average of the optimal values of the objective function (simulated NPV in this case) for all paths:

$$\overline{OV}(y_1, \mathbb{P}_i, \mathbb{T}_i) = \frac{1}{X}\sum_{x=1}^{X} e^{-r\tau(x)} V(\tau(x), \mathbb{P}_{i,\tau(x)}(x), \mathbb{T}_{i,,\tau(x)}(x)) \quad \text{Eq. 4.6}$$

The use of averaging is justified because the value of an American option[6] (the timing decision considered in this study is analogous to an American option) can be represented by the Snell envelope (**Bensoussan 1984; Karatzas 1988**). This implies that the value of an American option equals the maximized value of the discounted cash flows from the option. The maximum is taken over all stopping times. The main objective of the LSM algorithm is to provide a path-wise approximation to the optimal stopping rule which maximises the value of the American option (in this case the analogous SP flooding timing decision).

The VoF is then defined as the difference between the averaged optimal scenarios and the averaged static scenarios:

$$\text{VoF} = \overline{OV}(y_1, \mathbb{P}_i, \mathbb{T}_i) - \overline{SV}(\mathbb{P}_i, \mathbb{T}_i) \quad \text{Eq. 4.7}$$

, where $\overline{SV}(\mathbb{P}_i, \mathbb{T}_i)$ is the average NPV of the static scenarios over all realizations. Thus if VoF is positive this implies that by incorporating flexibility into the decision, value is added. On the other hand, if VoF is negative, then flexibility does not add value.

To apply the decision rule, the continuation function, Φ, needs to be determined at $(y, \mathbb{P}_{i,\tau(x)}(x), \mathbb{T}_{i,\tau(x)}(x))$. The algorithm assumes that the continuation value is the expectation, dependent on the available information at the time of the decision, of the future optimal values. This is described by the following expression: if $V(y, \omega, \tau, x)$ is the optimal NPV achieved by exercising the optimal policy at time ω with respect to $\tau(x)$ for realization x, conditional on ϑ_y, assuming the optimal poicy has not been implemented yet then:

$$V(y, \omega, \tau, x) = \begin{cases} V\left(\omega, \mathbb{P}_\omega(x), \mathbb{T}_\omega(x)\right) & \text{if} \quad \tau(x) = \omega \\ 0 & \text{if} \quad \tau(x) \neq \omega \end{cases} \quad \text{Eq. 4.8}$$

Thus the continuation value is the present value of the future expected payoffs:

$$\Phi\left(y_n, \mathbb{P}_{i,y_n}(x), \mathbb{T}_{i,y_n}(x)\right) = E^*_{y_n}\left[\sum_{i=n+1}^{N} e^{-r(y_i - y_n)} V(y_n, \mathbb{P}_{i,y_n}(x), \mathbb{T}_{i,y_n}(x))\right] \quad \text{Eq. 4.9}$$

The continuation value can be represented as follows since Φ is an element of a linear vector space, belonging to the Hilbert space:

$$\Phi\left(y, \mathbb{P}_{i,y}, \mathbb{T}_{i,y}\right) = \sum_{j=1}^{\infty} \emptyset_j(y) L_j(y, \mathbb{P}_{i,y}, \mathbb{T}_{i,y}) \quad \text{Eq. 4.10}$$

L_j is the *j*-th element in the orthonormal basis and $y \in Y$. $L_j(y, \mathbb{P}_{i,y}, \mathbb{T}_{i,y})$ can be powers of the state variables, Laguerre or Hermite polynomials (**Longstaff and Schwartz 2001**). Here, for simplicity, it is assumed to be a simple polynomial of the second order without cross products (**Stentoft 2004**).

[6] An American option is an option that can be exercised during any time until it expires.

If $J < \infty$ elements in the basis are used to determine Φ then we obtain an approximation of the continuation value

$$\Phi^{J}\left(y, \mathbb{P}_{i,y}, \mathbb{T}_{i,y}\right) = \sum_{j=1}^{J} \emptyset_j(y) L_j(y, \mathbb{P}_{i,y}, \mathbb{T}_{i,y}) \quad \text{Eq. 4.11}$$

It is assumed that the unknown functional form of the continuation equation can be represented as a linear combination of a countable set of the information set (state variables) measurable basis functions. The continuation function is approximated[7] using the first $\mathbf{J} < \infty$ basis functions **(Longstaff and Schwartz 2001)** $\emptyset_j(y)$ can be represented by a linear least squares regression (hence the name Least-Squares Monte Carlo Method) of $\Phi^{J}\left(y, \mathbb{P}_{i,y}, \mathbb{T}_{i,y}\right)$ onto the basis $\left\{L_j(y, \mathbb{P}_{i,y}, \mathbb{T}_{i,y})\right\}$:

$$\{\hat{\theta}_j(y_n)\}_{j=1}^{J} = \arg\min_{\{\emptyset_j\}_{j=1}^{J}} \left\| \sum_{j=1}^{J} \emptyset_j(y_n) L_j\left(y_n, \mathbb{P}_{i,y_n}, \mathbb{T}_{i,y_n}\right) - \sum_{i=n+1}^{N} e^{-r(y_i - y_n)} V(y, \mathbb{P}_{i,y}, \mathbb{T}_{i,y}) \right\|^2 \quad \text{Eq. 4.12}$$

Since the values of the basis functions are independently and identically distributed across paths, weak assumptions about the existence of moments enable the use of Theorem 3.5 of **White (1984)** to demonstrate that the resultant fitted value of the regression converges in mean square and in probability to the approximation function as the number of paths tends to infinity. Theorem 1.2.1 (**Amemiya 1985**) implies that the fitted values of the regression are the best linear unbiased estimator of the approximation function based on a mean-squared metric (**Longstaff and Schwartz 2001**). The main assertion of the LSM method is that if at a certain time the option is still available then the continuation value is the expectation (conditional on the information available at that time) of the future optimal payoffs from the option (**Gamba 2002**). The regression provides a fitted value that is a direct estimate of the conditional expectation function **(Longstaff and Schwartz 2001**). The LSM method is a form of approximate dynamic programming (**Powell 2011**).

Therefore, the estimated continuation value estimate is

$$\widehat{\Phi}^{J}\left(y_n, \mathbb{P}_{i,y_n}, \mathbb{T}_{i,y_n}\right) = \sum_{j=1}^{J} \hat{\theta}_j(y_n) L_j(y, \mathbb{P}_{i,y_n}, \mathbb{T}_{i,y_n}) \quad \text{Eq. 4.13}$$

Accuracy of the estimated values of the option can be enhanced by increasing the number of time steps, number of simulated paths and number of basis functions (**Gamba 2003**). For some cases, it might be more efficient to use other regression techniques such as weighted least squares, generalized least squares, and generalized method of moments in estimating the conditional expectation function (**Longstaff and Schwartz 2001**). The algorithm can be easily extended to incorporate a larger number of technical and economic state variables, this results in a redefinition of the basis functions used to determine the continuation value.

4.1.2 Implementation

The first component of the method is to perform a Monte Carlo simulation of the surfactant flood for all options considered. That requires running the reservoir simulator and obtaining the NPV for surfactant initiation at the specified decision intervals encompassing the option scenario. The realizations of the technical state variables were obtained using the pseudo-random number generator in MATLAB. This is based on the algorithm known as the multiplicative congruential method (Feres 2012).

Then ECLIPSE simulation is run per each stochastic realization of the technical uncertain parameters for each scenario (i.e. different injection policies). ECLIPSE is called from the MATLAB code and the results are then read from the same code.

[7] The continuation value approximation is truncated to $J = 4$ for the examples in this thesis.

After obtaining the production profiles for the different injection policies, the economic objective function is determined. First the economic state variables are generated via a stochastic process with the total of the number of realizations used for the stochastically generated technical state variables. The oil price is stochastically modeled using a mean reverting process and the chemical costs are simulated using the pseudo-random number generator in MATLAB. The objective function is then determined per each stochastic realization per each injection policy. This is performed by the LSM MATLAB code written for this thesis.

Once the objective function is determined for all realizations and for all injection policies the second component of the LSM algorithm is performed: the dynamic programming decision rule.

The dynamic programming decision rule is applied recursively to produce the optimal policy over all realizations. This is done by starting at the last decision node and moving backwards one time-step at a time. At each time-step (i.e. decision node) two values are compared: the value of implementing the decision (i.e. initiating the surfactant flood) at the current time-step and the value of waiting and continuing to the next available time-step. To perform this comparison, the continuation value is assumed to be the expectation of the future optimal value. This expectation is approximated by linear least-squares regression of the value of exercising the decision at the next time-step onto a set of basis functions of the realization of the state variables at the current time-step. After moving recursively back to the first time-step, the optimal policy is obtained for each stochastic path. The individual VoF is determined by taking the difference between the NPV of the optimal policy and the NPV of the static policy for each stochastic path. VoF is then obtained as the mean of the individual VoF's for each realization path. **Fig. 4.2** illustrates the main steps in implementing the method in the MATLAB code and **Fig. 4.3** illustrates how the decision rule is performed. This component is also written in the MATLAB code.

The LSM algorithm is applied to stylized case studies in chapter five. This chapter also includes sensitivity analyses with regards to the different aspects of the algorithm and of the decision problem. Chapter five also presents results for incorporating uncertainty in heterogeneity. This is discussed in the next section.

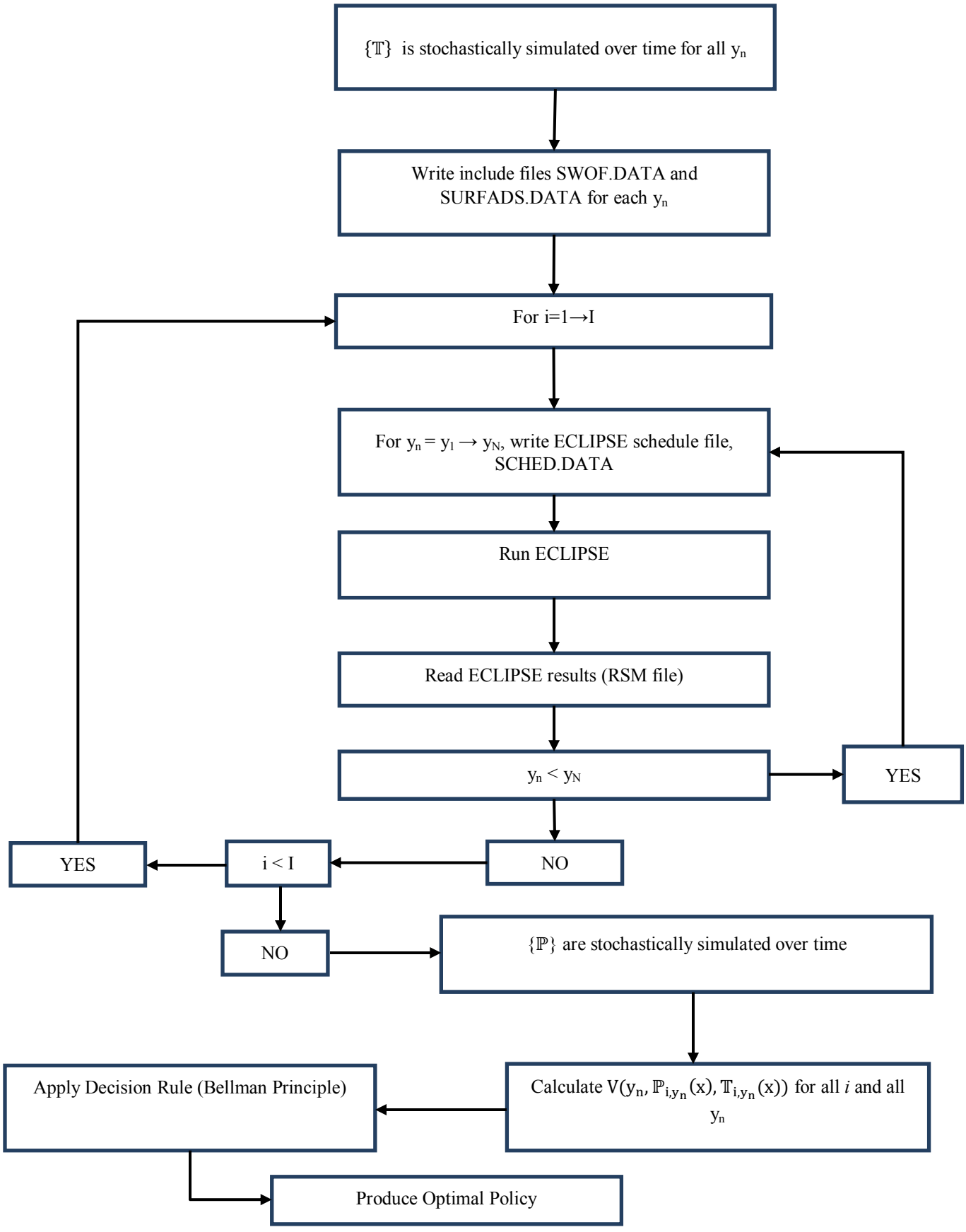


Fig 4.2– Algorithm flow chart illustrating the steps followed in the MATLAB code.

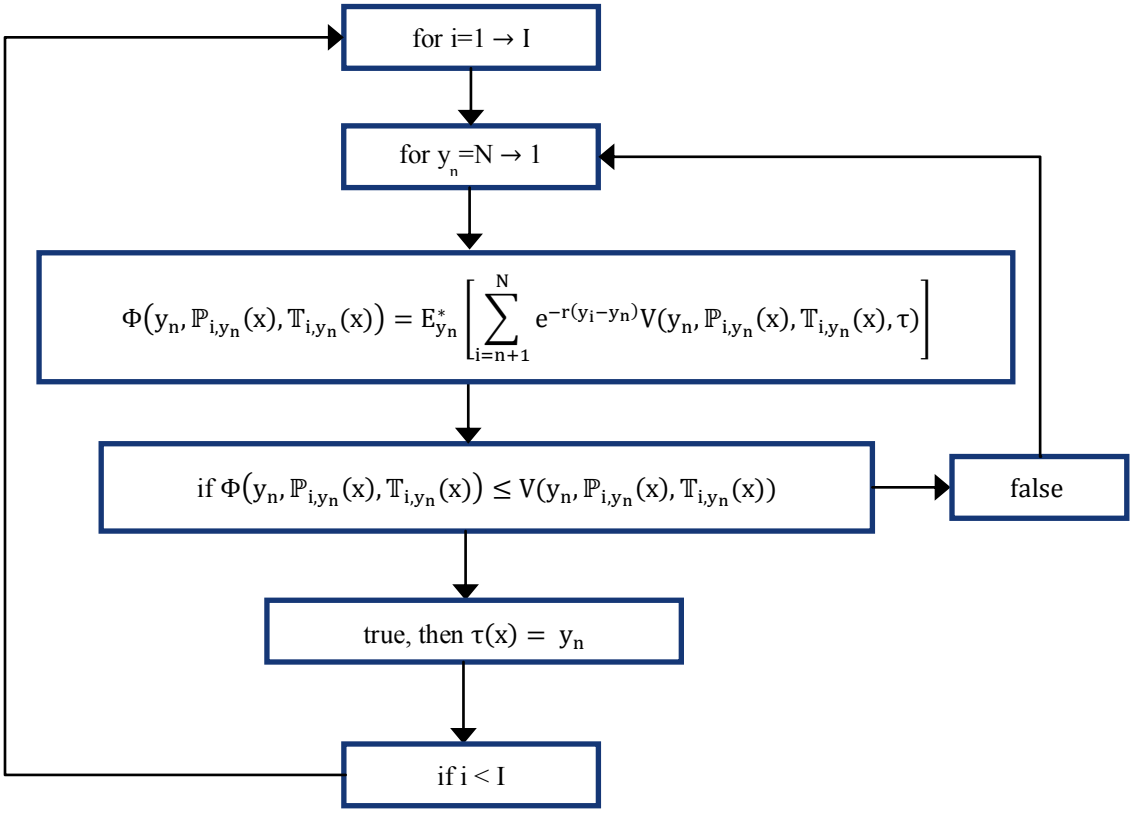


Fig 4.3– Algorithm flow chart illustrating decision rule in the MATLAB code.

4.2 Uncertainty in Heterogeneity

For Case Study 2 in chapter five (see section 5.3), uncertainty in heterogeneity, specifically the permeability field, was assumed to vary with time however the original permeability field is assumed to be constant for all realizations in the LSM method. In section 5.4, the treatment of uncertainty in heterogeneity is extended to stochastically generated permeability fields that are realization-unique. Two further case studies are presented and discussed. The first assumes that the permeability field is Gaussian and uses the moving average **(Dean 1995**) method to generate realizations. The latter generates permeability realizations using multiple point statistics algorithm **(Schneiderman and Kanade 2004**). **Fig. 4.4** illustrates the work flow for this section.

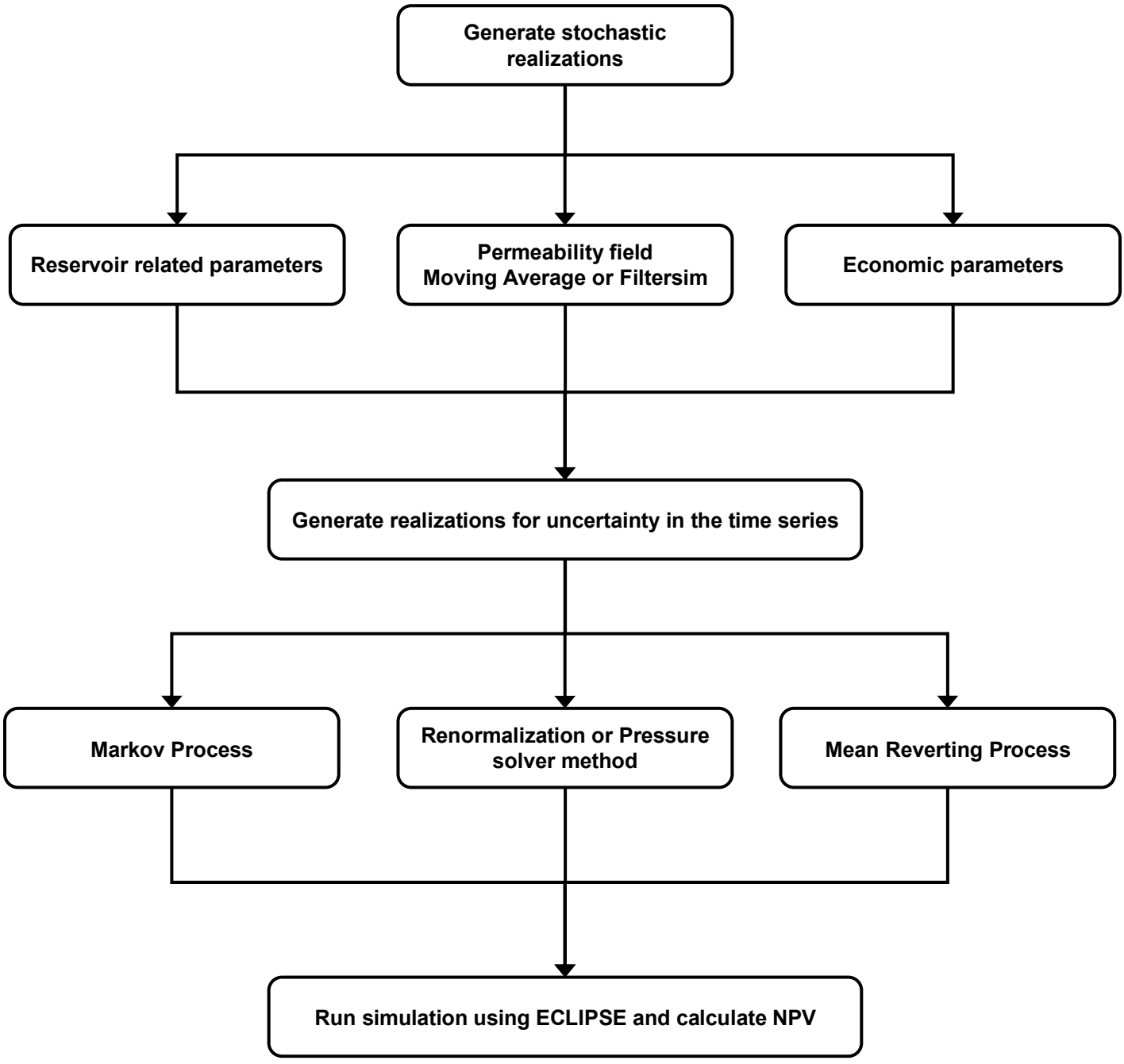


Fig. 4.4– Flow chart illustrating the steps in generating the stochastic realizations for the technical and economic parameters and heterogeneity fields which are used to obtain the production profiles and determine the objective function for each scenario.

4.3 LSM Enhancement

To produce the stochastic behavior in the LSM method, MCS is performed to generate a large number of realizations over which the different alternatives are evaluated and then the VoF is determined by taking the difference between the mean of the maximum (optimal) values obtained from the decision scenario and the mean of the value for the static (inflexible) scenario. Since it uses MCS, a large number of realizations are required to produce a convergent result. Generating realizations for the economic state parameters requires a negligible computational effort because it only requires the evaluation of discretized stochastic differential equations over a range of time. The production profiles that are based on the technical uncertainties need a relatively significant computational effort because they require solving the partial differential equations of a reservoir model simulator for each set of realizations of the state input parameters.

The efficiency of the technical stochastic process depends on the complexity of the reservoir model. The case studies in the chapter 5 used simplistic reservoir models, to the order of 10^3 to 10^4 grid cells. These models were solvable within a manageable time frame. However, in order to apply the LSM method to more sophisticated reservoir models, a more efficient approach is required.. One possible enhancement of this algorithm for more complex reservoir models is to design surrogate reservoir models such as artificial neural networks (**Karambeigi et al. 2011**) or model approximations obtained from experimental designs (**Cheong and Gupta 2005**). However, one weakness of experimental design is that it does not incorporate the full probability distributions of the random input parameters in a consistent manner when creating the response surface. Furthermore it assumes inherently that the distributions of the parameters are uniform because all samples are equally weighted (**Li et al. 2011**). Perturbation methods are also commonly used; however they are restricted to systems with relatively small random inputs and outputs, which is a difficult condition to satisfy for nonlinear problems where small random inputs may result in large random outputs (**Xiu and Hesthaven, 2005).** Another method to reduce computational requirement is to use reduced order modeling (**Cardoso and Durlofsky 2009**). However, this is an intrusive approach requiring access to the numerical simulation algorithm which is not always feasible, especially on commercial simulators. Optimizing the performance of the LSM algorithm using parallelization is also a potential improvement (**Choudhury et al. 2008**).

The efficiency of sampling techniques could be enhanced in order to sample the high probability regions of the distributions of the input technical state variables using methods such as polynomial chaos theory **(Ghanem and Spanos 1991**) or probabilistic collocation (**Tatang et al. 1997**). This could reduce computational requirements as reservoir simulation is the most demanding computational element in the LSM process. The main advantage of probabilistic collocation method (PCM) is that it is non-intrusive.

There are many directions from which the LSM method could be enhanced to be applied to more realistic scenarios. The main aspect considered in choosing which direction was to increase the efficiency of the LSM method by reducing the computational requirement. From the various methods mentioned above, enhancing the sampling efficiency of the technical variables was deemed to be a priority. This was done by using the probabilistic collocation method. This is discussed in detail in the next section.

4.4 PCM Background and Theory

Chapter six introduces the use of PCM in parametric uncertainty quantification for surfactant-polymer flooding using four stylized reservoir models. A maximum of four sources of uncertainty were considered: the chemical flood residual oil

saturation, surfactant and polymer adsorption and the polymer viscosity multiplier. The output parameter approximated was the recovery factor. The output metric is the probability density function and this will be compared with the probability density obtained from Monte Carlo simulation over a large number of realizations. Chapter six will compare using Gaussian quadrature and linear regression to solve for the output polynomial chaos coefficients. The following section will introduce the theory behind the probabilistic collocation method which will focus on the polynomial chaos theory that is used to produce the orthogonal polynomials which approximate the input state variables and will also be used to approximate the output. The collocation methods used to obtain the coefficients for the orthogonal polynomials are then introduced. This section will discuss the Gaussian quadrature approach and the regression approach.

4.4.1 Polynomial Chaos Expansion

Polynomial chaos expansion (PCE) is a spectral expansion of random variables that expresses stochastic quantities as orthogonal polynomials; it is a spectral representation in random space that exhibits fast convergence when the expanded function depends smoothly on the random parameters. When applied to differential equations with random inputs, the expansion coefficients of the PCE are solved for (**Xiu and Hesthaven 2005**).

This approach was introduced by **Ghanem and Spanos (1991)**. PCE is based on the homogeneous chaos theory introduced by **Wiener (1938)**. PCE for a specific response y is defined as:

$$y = \alpha_0\Gamma_0 + \sum_{i_1=1}^{\infty}\alpha_{i_1}\Gamma_1(x_{i_1}) + \sum_{i_1=1}^{\infty}\sum_{i_2=1}^{i_1}\alpha_{i_1 i_2}\Gamma_2(x_{i_1},x_{i_2}) + \sum_{i_1=1}^{\infty}\sum_{i_2=1}^{i_1}\sum_{i_3=1}^{i_2}\alpha_{i_1 i_2 i_3}\Gamma_3(x_{i_1},x_{i_2},x_{i_3}) + \cdots \quad \text{Eq.4.14}$$

, where α are the coefficients to be solved for. Γ are the orthogonal polynomials that approximate the random input variables x.

This expression can then be simplified and truncated using term-based indexing and truncated up to the d-th order as:

$$\mathrm{y} = \sum_{\mathrm{k}\leq\mathrm{d}}\alpha_{\mathrm{k}}\Gamma_{\mathrm{k}}(\mathrm{x}) \quad \text{Eq.4.15}$$

, where d is the highest order of the expansion, α_{k} is the deterministic coefficient and $\Gamma_k(x)$ is the kth order multidimensional polynomial of the random variables, $\mathrm{x} = (\mathrm{x}_1, \mathrm{x}_2, \ldots, \mathrm{x}_{\mathrm{N}})^{\mathrm{T}}$.

When representing the random input variables, the input distribution determines the types of the orthogonal polynomials to be used. **Xiu and Karniadakis (2002)** developed a generalized chaos expansion based on the different polynomials in the Askey scheme for different types of input random variables. This scheme is used for the application of the PCM in this chapter. The reason for using this scheme is that for a given input distribution, the chosen PCE converges at a better rate than other expansions (**Li et al. 2011**). See **Appendix D** for further details. For arbitrary distributions the associated orthogonal polynomial expansions need to be constructed numerically using the suite of algorithms introduced by **Gautshci (1994)**.

One of the main advantages of PCE's is that they guarantee the convergence of the approximation distribution to the true distribution of the parameter with increasing PCE order (**Field and Mircea 2007**). Thus PCE's do not suffer from the problem of over-fitting which affects many other proxies. However, this requires the correct estimation of the coefficients. Galerkin projection is commonly used to obtain these coefficients, however this results in a coupled system of deterministic equations which in turn makes it an intrusive method (**Loeven et al. 2007**). The probabilistic collocation method, however, is a non-intrusive approach to solving for the coefficients.

4.4.2 Probabilistic Collocation

Following the notation in (**Tatang et al. 1997**), if a numerical model is defined:

$$y = f(x) \qquad \text{Eq. 4.16}$$

, where y can be approximated by a set of specified functions such as orthogonal polynomials, $\{g_i(x)\}$:

$$\hat{y} = \sum_{i=0}^{N} \alpha_i \, g_i(x) \qquad \text{Eq. 4.17}$$

, where N is the order of the approximation. Since the approximation does not reproduce the actual model, a residual is defined as:

$$R(\{\alpha_i\}, x) = \hat{y}(x) - y(x) \qquad \text{Eq. 4.18}$$

By requiring each member of $\{g_i(x)\}$ and the residual to be orthogonal it is possible to obtain the set of coefficients in the approximation $\{\alpha_i\}$:

$$\int_x R(\{\alpha_i\}, x) g_i(x) dx = 0, \; i = 0, \dots, N \qquad \text{Eq. 4.19}$$

In this chapter, two approaches of solving equation (4.19) are discussed. The first is Gaussian quadrature which uses the Golub-Welsch algorithm (**Golub and Welsch 1969**) to obtain the weights and nodes of the quadrature. See **Appendix E**. This method is based on full tensor product rule. The second method is linear regression which uses different sampling methods to obtain the collocation nodes and then performs a regression of the model response at these nodes onto a basis of the PCE's.

4.4.2.1 Gaussian Quadrature

Equation (5.6) can be solved by Gaussian quadrature approximation:

$$\int_x R(\{\alpha_i\}, x) g_i(x) dx \cong \sum_{j=1}^{N} v_j R\big(\{\alpha_i\}, x_j\big) g_i\big(x_j\big) \qquad \text{Eq. 4.20}$$

, where $i = 0, \dots, N$ and v_j and x_j are the weights and abscissas respectively.

When $v_j g_i\big(x_j\big)$ has the same sign and does not equate to zero for all i and j then equation (4.19) is approximated by

$$R(\{\alpha_i\}, x_j) = 0,\ j = 0, \dots, N \quad \text{Eq. 4.21}$$

This demonstrates the use of collocation points $\{x_j\}$ in calculating the set of coefficients $\{\alpha_i\}$. This implies that the collocation method does not require the complete definition of the residual function. The ability to calculate the value of the residual at several given values of inputs in order to obtain the coefficients is all that is required (**Tatang et al. 1997**).

Stochastic models are used to define input and output variables as random variables. In order to attain an approximation of the model, the collocation method can be extended to incorporate the stochastic nature of the variables. Equation (4.19) is thus transformed to the probabilistic space by incorporating the joint density function of the inputs $f_{x(\omega)}(x(\omega))$:

$$\int_{x(\omega)} f_{x(\omega)}(x(\omega)) R(\{\alpha_i\}, x(\omega)) g_i(x(\omega)) dx(\omega) = 0 \quad \text{Eq. 4.22}$$

, where $i = 0, \dots, N$. Equation (4.21) is then transformed to

$$f_{x(\omega)}(x_j) R(\{\alpha_i\}, x_j) = 0 \quad \text{Eq. 4.23}$$

, where $j = 0, \dots, N$. When x_j is chosen such that $f_{x(\omega)}(x_j)$ is positive for all j, equation $R(\{\alpha_i\}, x_j) = 0,\ j = 0, \dots, N$, can still be applied to cases where x is a stochastic variable.

Because $\{g_i(x)\}$ are chosen as the orthogonal polynomials for which the weighting function is the PDF of x, $f_{x(\omega)}(x(\omega))$, the collocation points $\{x_j\}$ are defined simply as the roots of the $(N+1)$th order orthogonal polynomials of the uncertain parameter. The collocation nodes and weights are found using the Golub-Welsch algorithm, while the coefficients of the output polynomial chaos are solved for using the Gaussian quadrature rule.

4.4.2.2 Linear Regression

This approach is based on a single linear least-squares solution:

$$\mathbf{g\alpha = y} \quad \text{Eq. 4.24}$$

, in order to solve for the complete set of PCE coefficients α which best match the set of response values **y**. These response values are found by performing a design of experiments within the density function of x where each row of matrix **g** contains N multivariate polynomial terms $\mathbf{g_i}$ evaluated at a specific *x* sample. Traditionally, in this method, oversampling is typically advised resulting in a least-squares solution for the over determined system. A probabilistic collocation approach can be used by choosing a subset of the *N* Gaussian quadrature points (the points with the highest tensor-product weighting) rather than using random over-sampling. This provides better collocation locations and preserves the interpolation properties (**Eldred 2009**). For the examples in this chapter, the Fejer sampling methods (**Fejer 1933)** in addition to the Gaussian quadrature generated nodes are used for generating collocation nodes in the linear regression approach. This is discussed in more detail in the following subsection.

4.4.3 Selection of Collocation Nodes

The choice of collocation nodes sampling strongly affects the efficiency of the PCM (**Lin and Tartakovsky 2009**). The collocation nodes used in Gaussian quadrature are found by using the roots of the next-higher order PCE of the random input variables with respect to the desired approximation order, see **Fig. 4.5**.

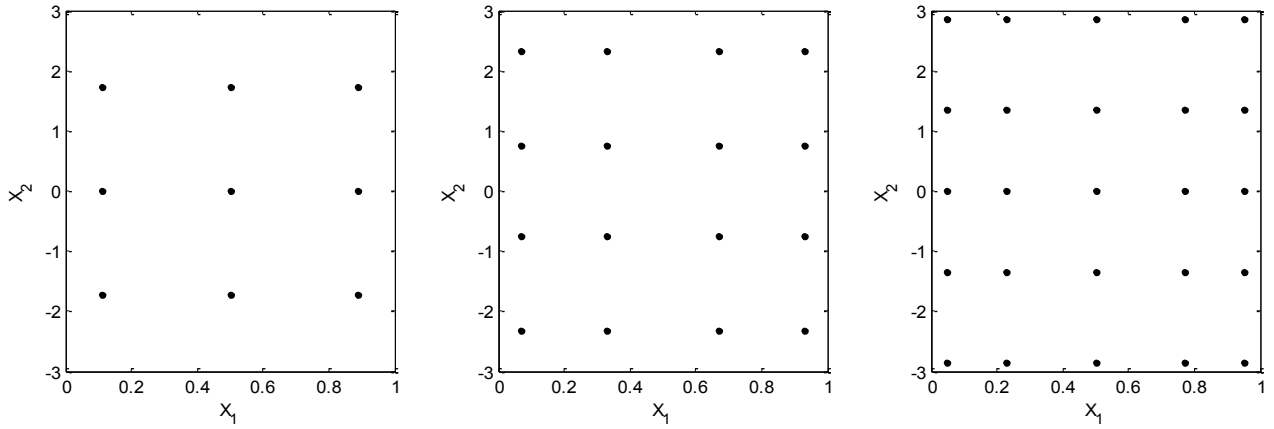


Fig. 4.5– Two-dimensional quadrature grid, where moving from left plot to the right, are the second, third and fourth order PCM nodes.

For solving the PCM using the linear regression approach, the Fejer nodes are used via two variants: mapping and boxing methods. The first variant refers to mapping points from the unit hypercube to the desired domain using the inverse of the cumulative distribution function while the second variant, boxing, refers to scaling the nodes to the bounds of the distributions of the input parameters. The boxing method is used to scale the nodes which are generated for the interval (0, 1) to the distribution bounds. The Fejer nodes are defined as the Chebyshev extrema of the second type over interval (0,1):

$$x_i = \frac{1}{2} + \frac{1}{2}\cos\frac{i\pi}{\mathrm{N}+2}\text{, for } i = 1, \dots, \mathrm{N}+2 \qquad \text{Eq. 4.25}$$

, where N is the order of the PCE.

Fejer nodes were used because for infinitely bound distributions (e.g. normal) Clenshaw-Curtis sampling would not work well, whereas Fejer nodes, since they use only the interior Chebyshev extrema and neglect the boundary values, are better suited.

The mapping method is used to sample uniformly around the high probability region. The mapping method is based on inverse transform sampling. Once the Fejer nodes are obtained in the interval (0,1), the inverse cumulative distribution function (for random univariate cases) or inverse Rosenblatt transform (**Rosenblatt 1952**)(for multivariate cases) of the random input parameters are applied to find the value of the collocation nodes. See **Appendix F** for more details on these approaches.

An additional step is then added in order to reduce the number of total nodes by including only the order-unique nodes of the originally generated Fejer grid. See **Fig. 4.6** and **4.7** for illustrations of the mapped and boxed Fejer nodes.

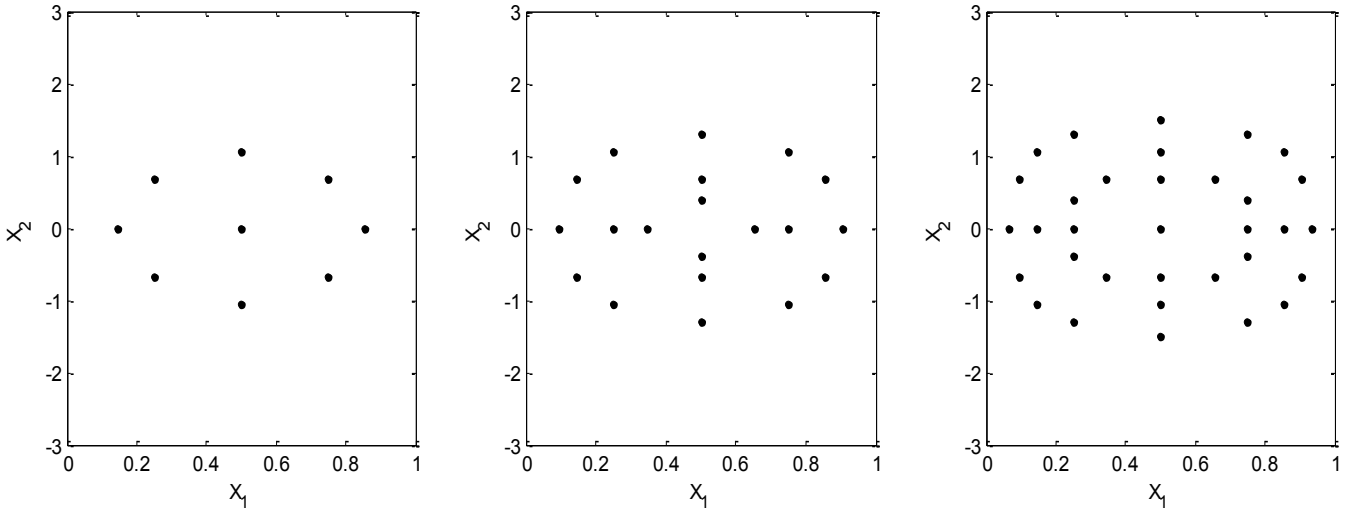


Fig. 4.6– Two-dimensional mapped Fejer grid, where moving from left plot to the right, are the second, third and fourth order PCM nodes.

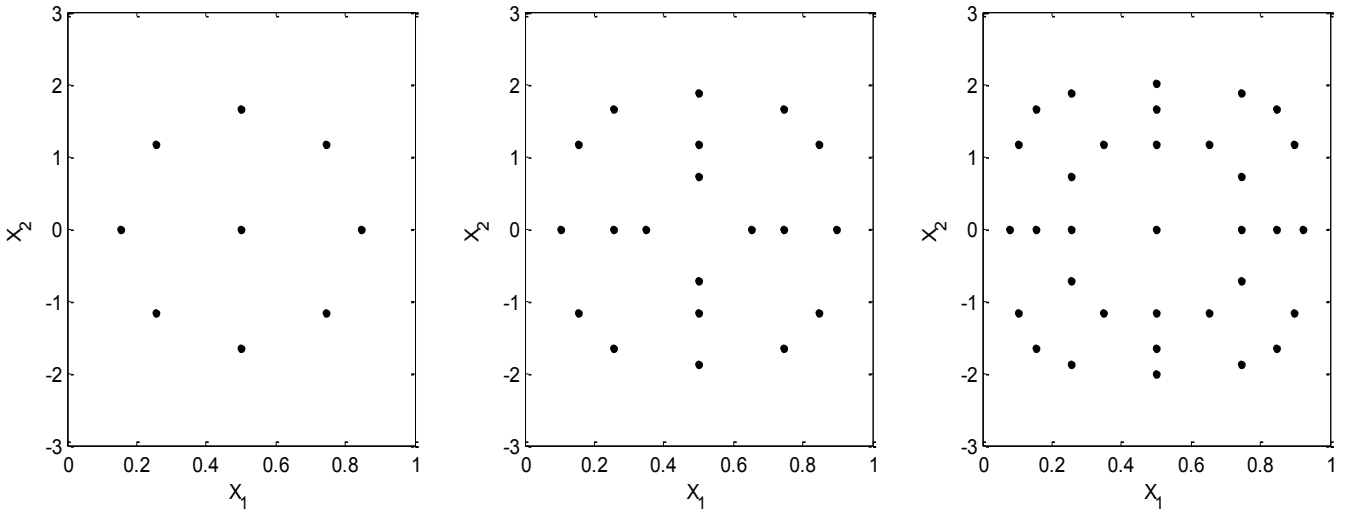


Fig. 4.7– Two-dimensional boxed Fejer grid, where moving from left plot to the right, are the second, third and fourth order PCM nodes.

Fig. 4.8 shows how the number of collocation nodes increases with varying approximation order for a four-dimensional random input scenario. Clenshaw-Curtis nodes are displayed as well for comparison. It can be seen that the Fejer nodes increase significantly slower than Clenshaw-Curtis and Gaussian quadrature nodes.

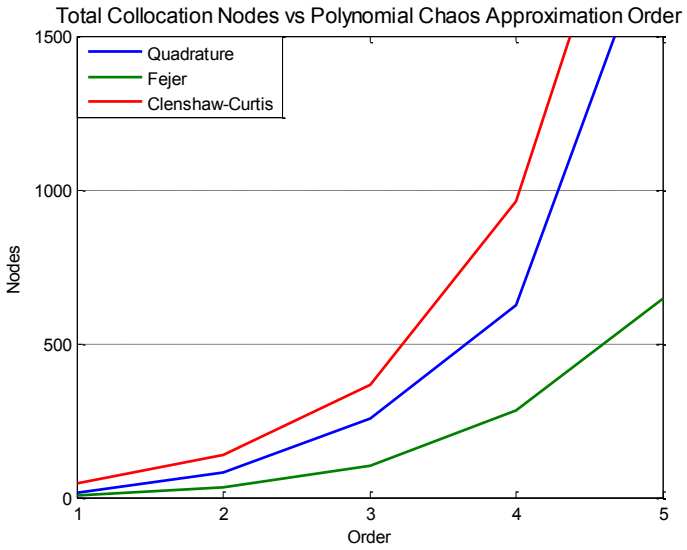


Fig. 4.8 —Number of nodes for a four-dimensional random input scenario, as a function of approximation order.

4.4.4 Computation of Statistical Moments

After obtaining the PCE for the output variable, it is possible to generate statistical properties using this polynomial proxy model by running Monte Carlo simulation or any other stochastic process for a large number of realizations. Since the proxy model is in polynomial form, this requires an insignificant amount of time to run. The probability density function can then be obtained and compared with the density function obtained from running a Monte Carlo simulation on the reservoir simulator (ECLIPSE). The first two-moments are also determined using the results of the Monte Carlo simulation of the proxy model.

4.4.5 Implementation

The PCM was implemented using a PYTHON module developed by **Feinberg (2012)**. A PYTHON code was written to couple ECLIPSE with the PCM PYTHON module. A MATLAB code was then written to run the coupling PYTHON code sequentially for different orders of approximation and to store the results and compute the statistical moments and PDF used as the output metrics. See **Fig. 4.9**.

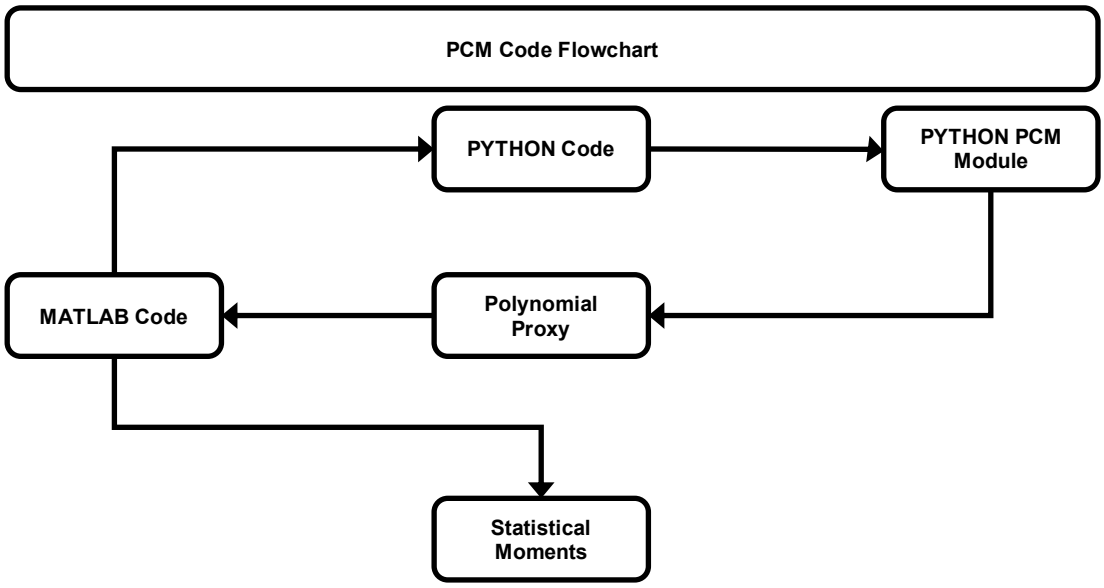


Fig. 4.9– PCM flowchart illustrating the implementation steps.

4.5 The LSPCM Algorithm

Chapter seven proposes the use of the efficient sampling approach of the PCM method to substitute the MCS of the recovery profiles and ultimately reduce the computational effort required to perform the LSM method. The PCM was shown to produce robust and efficient uncertainty quantification for flow in porous media (**Li and Zhang 2007; Li and Zhang 2009; Li et al. 2011**) and was applied by **Alkhatib and King (2013a**) to a chemical EOR process to quantify parametric uncertainty.

The Least Squares Probabilistic Collocation Method (LSPCM) is presented as a robust and efficient decision making method that can evaluate flexibility in the presence of uncertainty.

In this section the LSPCM is introduced with respect to the algorithm and its implementation. An initial application to stylized reservoir models is presented in chapter seven. These applications are based on the same decision problem of timing the SP flooding process. The results obtained by the LSM method are used as the benchmark for evaluating the robustness of the LSPCM. Additional extensions are then introduced and evaluated using the LSPCM. Here the complexity of the decision is enhanced to include other control variables such as chemical slug size and component concentration. Another more complex decision was considered based on whether adding alkaline to reduce surfactant adsorption adds value or not.

4.5.1 Coupling of LSM with PCM Algorithm

The elements of the vector $\mathbb{T}_i$ are generated by a Monte Carlo simulation. For each realization, the finite difference equations of the simulator are solved for per defined strategy. The forward simulation is thus the most computationally demanding component of the method. The objective here is to substitute the MCS with a procedure that would require fewer realizations while guaranteeing convergence.

The collocation nodes selection processes presented in the previous chapter are incorporated with the LSM method. This could significantly reduce the number of reservoir simulations required to cover the range of uncertainty of the random technical inputs. As mentioned in the previous chapter, the residual (Eq. 4.18) in the PCM is defined as the difference between the model and the approximation:

$$R(\{\alpha_i\}, q) = \hat{y}(q) - y(q) \qquad \text{Eq. 4.26}$$

, where $q \in Q$ is the set of collocation points. . Q is then used as the vector of random inputs in place of the MCS generated values. Different sampling methods can be used to generate the collocation points with varying efficiency. Based on the findings of the previous chapter and **Alkhatib and King (2013a)**, three methods are used: Gaussian quadrature nodes, mapped Fejer nodes and boxed Fejer nodes. The Bellman dynamic programming equation therefore becomes:

$$ONPV(y, \mathbb{P}_{i,y}(q), \mathbb{T}_i(q)) = \max\{NPV(y_n, \mathbb{P}_{i,y_n}, \mathbb{T}_i), e^{-r(y_{n+1}-y_n)}\, E^*_{y_n}[ONPV(y_{n+1}, \mathbb{P}_{i,y_{n+1}}(q), \mathbb{T}_i(q))]\} \qquad \text{Eq. 4.27}$$

, where $q \in Q$ and $Q \ll X$, where X is the total number of MCS realizations. The set of collocation nodes Q is obtained either by determining the Gaussian quadrature nodes using the Golub-Welsch algorithm or by using the Fejer sampling methods mentioned in the previous chapter. In reducing the number of realizations, the efficiency of the LSM method is enhanced. See **Fig. 4.8**.

4.5.2 Implementation of the LSPCM Algorithm

The algorithm is implemented by a MATLAB code which first runs a PYTHON written code that calls the PCM Python module (**Feinberg 2012)** and produces the requested collocation nodes to the order and sampling method specified in the MATLAB code. Then, the collocation nodes are written to a text file which is accessed by the MATLAB written code and runs the forward simulation (ECLIPSE) using these samples. The decision rule is then applied as shown in **Fig. 4.3** to produce the optimal policy and the VoF. See **Fig. 4.9**.

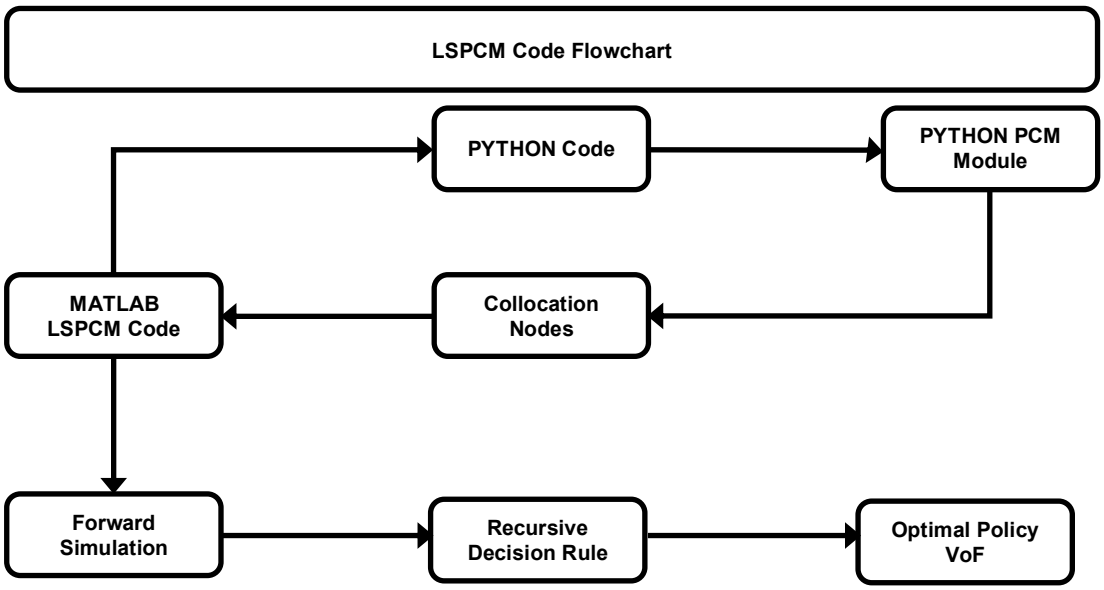


Fig. 4.9– LSPCM code flowchart illustrating the implementation steps.

5 The Least Squares Monte Carlo Method: Case Studies

5.1 Application: Case Study 1

To demonstrate the algorithm, a simple case study is presented. The reservoir model used for this application is a three-dimensional homogeneous model. The main objective of this case study is to introduce the method.

5.1.1 Problem Definition

The objective of this case study is to maximize the value of a surfactant flood by creating value from uncertainty and flexibility through capturing the effects of technical and economic state variables. The information set is assumed to vary with time because it is assumed that there is an uncertainty reducing process that is ongoing due to an external source of information such as core floods or alternative pilots. However, this is not always the case in reality. For this case study, surfactant flooding is initially considered without the presence of mobility control as the purpose was to adapt the LSM to an EOR framework. Mobility control is then added to the model in latter applications. The first case study was simple a three-dimensional homogeneous model. This was designed as a 10×10×10 grid and a quarter five-spot pattern with a total area of 2.02E4 m^2 (5 acres) and a reservoir thickness of 7.6 m. See **Appendix A** for fluid data and field constraints.

The timing of surfactant flooding initiation is the flexibility or option that is evaluated. Timing of these processes is usually detrimental to successful implementation (**Gao et al. 2010**). A field life of 10-years was assumed and the best time to start a surfactant flooding for this field was to be determined. The option here is whether to initiate a surfactant flood at the start of the 4^{th}, 5^{th}, 6^{th} or 7^{th} year of the field life. Therefore we assume a decision space $Y = [4,5,6,7]$ and a decision node $y_n \in Y$. These decision nodes were chosen because the water breakthrough time for the basic model in this case study occurred near the 5^{th} year and it is intended to investigate whether it was best to initiate a surfactant flood before, during or after water breakthrough. This defines our options or flexibility scenario. **Fig. 5.1** illustrates the decision problem with a flowchart. **Fig. 5.2** illustrates the state space representation.

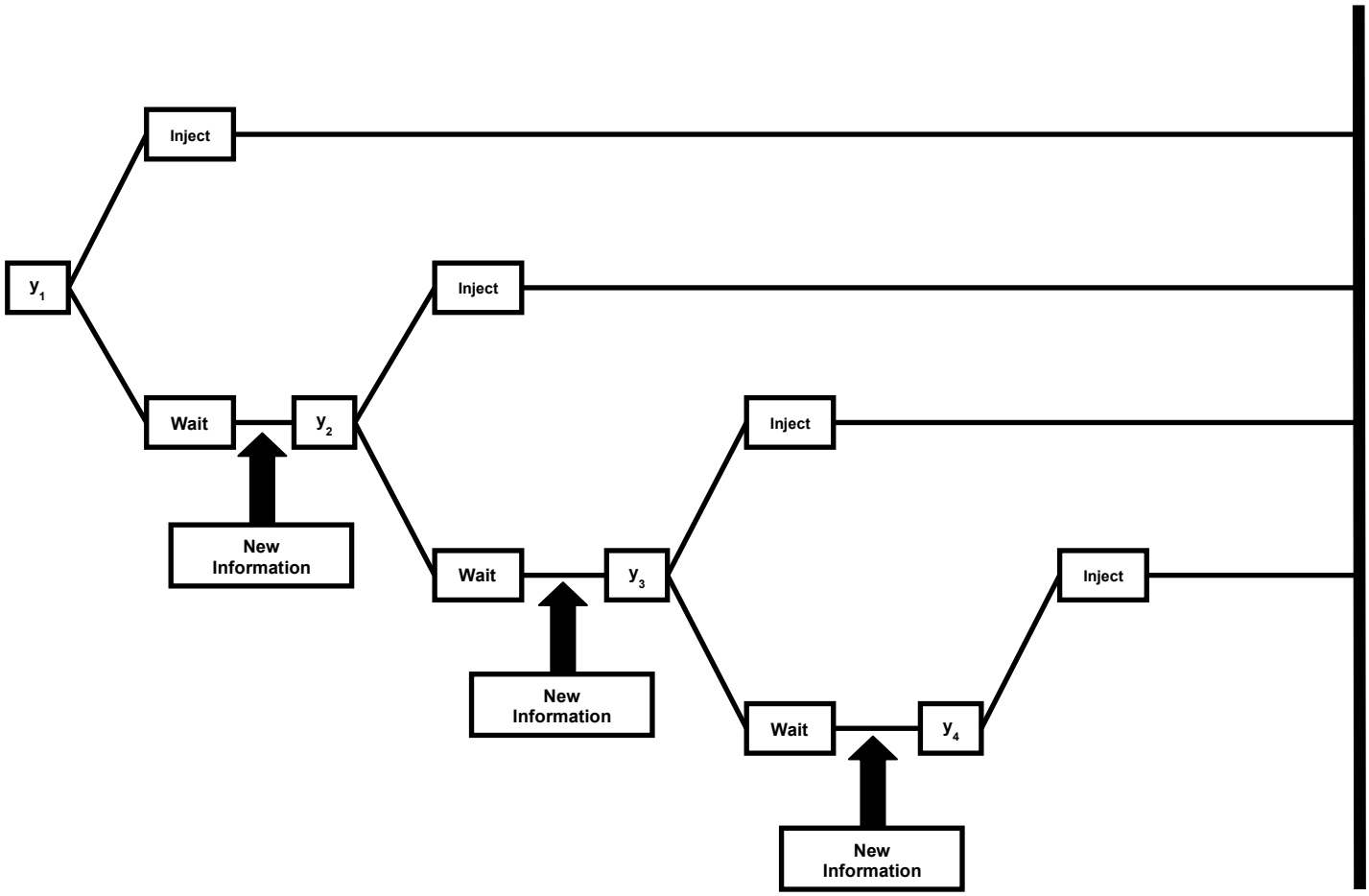


Fig. 5.1—Decision (flexibility) flow chart.

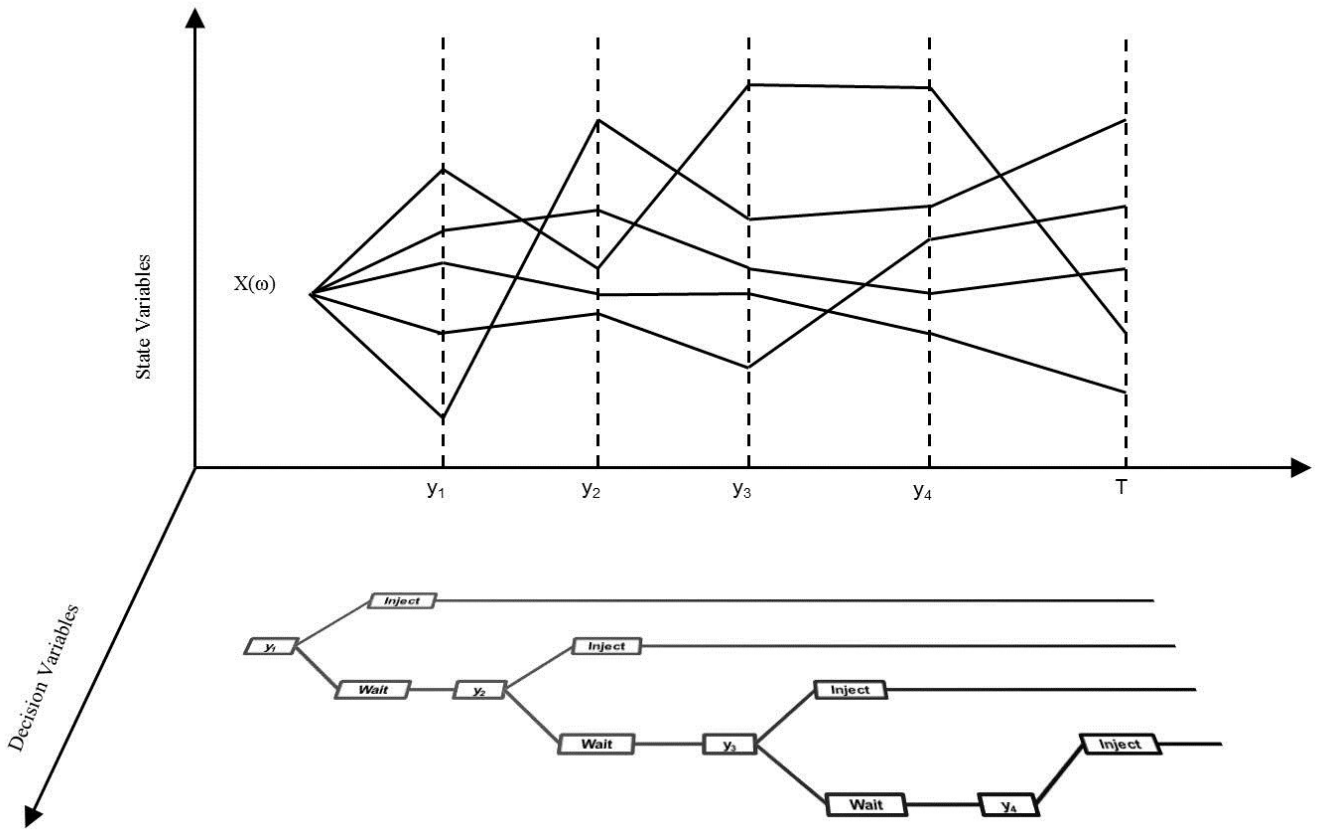


Fig. 5.2–Decision state space representation where X(ω) represents the state variables per ω realization.

A no-option or static (no flexibility) scenario is assumed to begin surfactant injection at the start of the field life. This was chosen through initial deterministic case simulations[8] and will form the basis of our analysis when evaluating flexibility. There will be a bias in the results depending on our choice of the static scenario. The reservoir state variables were assumed to be the residual oil saturation to surfactant flooding (S_{orc}) and the surfactant adsorption (D_s). The economic state variables were assumed to be the oil price (P_o), surfactant cost (P_s), water injection cost (P_{wi}) and water production cost (P_{wp}). **Fig 5.3**[9] illustrates the effect of uncertainty on the recovery factor and the NPV of initiating surfactant flooding at different decision nodes used for this case study. This figure was constructed from simulation runs over a discretized range of S_{orc} (0 to 0.20 with 0.025 increments) and D_s (10E-06 to 10E-03 with 10E0.5 increments) with a total of 252 runs using a simple homogenous reservoir model (see **Appendix A**). These simulations were performed while maintaining all control variables constant (constant injection rate and constant production pressure constraint) with the exception of the surfactant flooding initiation time. The purpose of this figure was to show how different realizations of D_s and S_{orc} favor different injection strategies with regards to recovery factor or NPV. It is clear from the NPV surface plot that different injection policies intermingle over a small region of D_s and S_{orc} values. Thus it is necessary to develop a method to obtain an optimal policy for such a problem in the presence of uncertainty due to this variety in response.

[8] These runs used a surfactant adsorption value of 10^{-4} g/g rock and 0% residual oil saturation to chemical flooding.
[9] The results for these surface plots were obtained using ECLIPSE and the economic model used for NPV is presented in section 4.2.2.b.

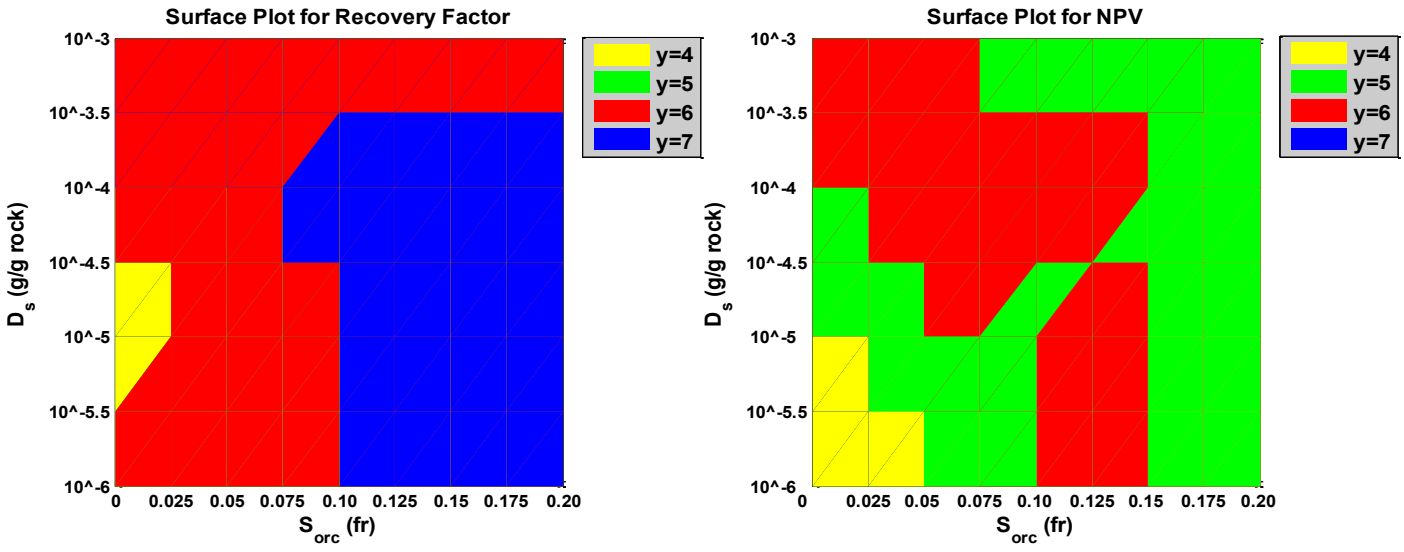


Fig. 5.3– Surface plot for recovery factor and NPV as a function of D_s and S_{orc}. Each surface color is illustrates a different policy (surfactant flooding initiation).

For this case study, a fixed set of control variables (slug size, surfactant concentration…etc) was assumed to simplify the decision process and demonstrate the method. In reality, practical considerations of the control strategies that take into account field or reservoir-specific peculiarities must be included in the decision process. This would include, for instance, varying the surfactant slug properties (volume or concentration) as the reservoir conditions evolve with time.

5.1.2 Monte Carlo Simulation

The first component of the method is to perform a Monte Carlo simulation of the surfactant flood for all options considered. That requires running the reservoir simulator and obtaining the NPV for surfactant initiation at $y_n = [4,5,6,7]$ encompassing the option scenario. A total of 10^3 paths were simulated to produce a statistical base. For each path, a unique realization of S_{orc} and D_s is obtained. These realizations were obtained using the pseudo-random number generator in MATLAB. This is based on the algorithm known as the multiplicative congruential method (**Feres 2012**). A serial test was applied to demonstrate that the algorithm produces sufficiently random sampling. This was performed for a variable sampled from a uniform distribution within the interval [0, 1]. Serial tests for six iterations of this sampler are illustrated in **Fig. 5.4.** It is clear that no trends are observed. The period used in the MATLAB generator is equal to 2^{31}-1 which significantly larger than what is required for the LSM (**Feres 2012**). Therefore the pseudo random number generator in MATLAB was deemed sufficient for the case studies in this thesis. The stochastic processes for each of these parameters are discussed below.

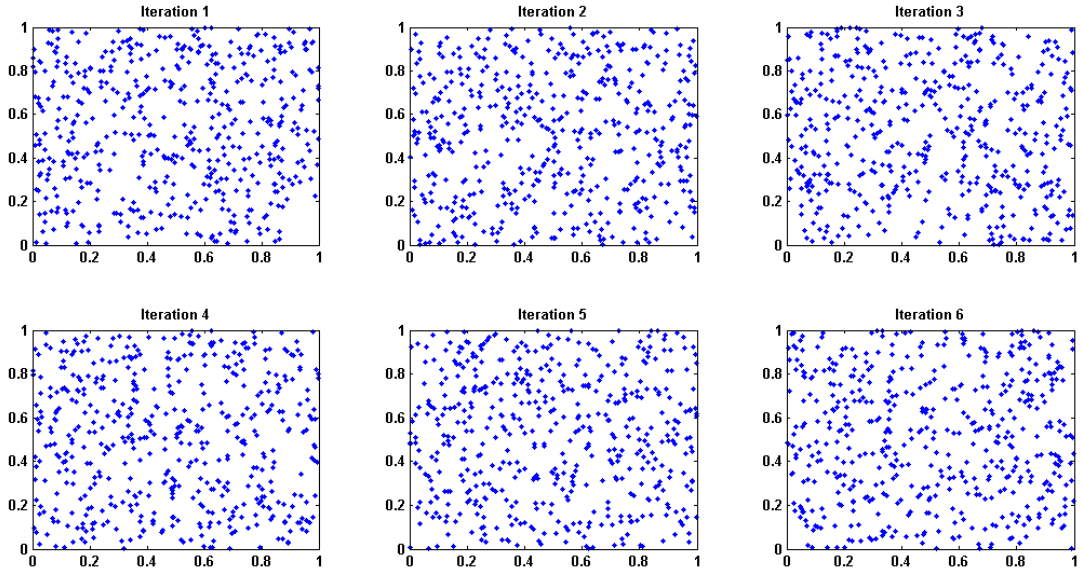


Fig. 5.4– Serial test plots for six iterations for the pseudo-random number generator used in MATLAB. Each iteration consists of 1000 samples of a uniformly distributed variable with unit interval.

a. Surfactant Flooding Modelling

For this case study, the residual oil saturation to chemical flooding, S_{orc}, and surfactant adsorption , D_s, were assumed to be the technical uncertainties and they are assumed to follow stochastic processes. No correlation was assumed between these two parameters.

A surfactant slug size of 0.1 PV and a concentration of 3% wt were assumed. The surfactant slug variables are assumed to be constant for all runs. It is important to state that since the aim of this application was not to solve a specific reservoir problem here, therefore standard distributions for the uncertain parameters were used to demonstrate the LSM method. The effect of the evolution of these parameters is then manifest in the production profiles that were obtained by simulation. See **Appendix A** for the reservoir and constraint data used for this reservoir model.

The reservoir state variables are S_{orc} (fraction) and D_s (g/g rock) which will initially follow a stochastic process of uniform $\sim U(0,0.20)$ and log-uniform $\sim \log U(-6,-3)$ distributions respectively. These distributions were chosen because they are simple standard distribution models that capture a specific range for each of the technical state variables. Other common distributions could also be applied such as normal or beta distributions. There will be a distinct realization of both for each path.

Since we assume that our knowledge or information set evolves through time, thus the state variables are assumed to evolve through time as well. However it is important to note that the actual value of these parameters is constant in time what is varying is our state of knowledge of what these values are. An attempt was made to reflect this. The purpose of this was to demonstrate that as fields are developed our understanding changes as we get new data and we build new models in response to the new data. A rather simple Markov process was used, in reality the updated values might be

obtained from ensemble based models or some other Bayesian updating models. This evolution of the state variables is akin to the time evolution of the reservoir state variables in ensemble methods (e.g. ensemble Kalman filter) **(Evensen 2007; Aanonsen et al. 2009).** The purpose of this approach was to demonstrate proof of concept that the algorithm used was able to cope with this variation.

This is assumed to follow a simple stochastic process defined as a discrete-time continuous-state random walk with jump process. It can be considered as a Markov process as the future value of the variable will only depend on its current value, not on the realized values in the past. Realizations are found at discrete points in time that coincide with the decision nodes (i.e. at y=4, 5, 6 and 7). The stochastic process for S_{orc} can be presented as follows:

$$S_{orc_t} = x_t = x_{t-1} + \rho\epsilon_t \quad \text{Eq. 5.1}$$

where x_t is the state variable (S_{orc}).

ρ is the jump direction, $\rho \in [-1,0,1], P(\rho = -1) = P(\rho = 1) = P(\rho = 0) = \frac{1}{3}$.

ϵ_t is a random variable with distribution: $\epsilon_t \sim U(\left(1 - q_t\right)x_{t-1}, \left(1 + q_t\right)x_{t-1})$ Eq. 5.2

q_t is the range adjustment, see **Table 5.1**.

The stochastic process for D_s follows a similar process:

$$D_{s_t} = 10^{x_t}, \text{ where } x_t = x_{t-1} + \rho\epsilon_t \text{ and } \epsilon_t \sim U(\left(1 - q_{Dt}\right)x_{t-1}, \left(1 + q_{Dt}\right)x_{t-1}) \quad \text{Eq. 5.3}$$

Table 5.1: Range Adjustment Values for S_{orc} and D_s Stochastic Models

t	1	2	3	4
q_t	0.4	0.3	0.2	0.1
q_{Dt}	0.2	0.1	0.05	0.01

The range adjustment values are stylized values used in order to demonstrate the method. The realization of the technical state variable is kept constant between decision nodes as the simulation proceeds. This process is intended to simulate our increasing state of knowledge of the value of these parameters with time. See **Fig. 5.5** for sample realizations of the first five paths used for this case study.

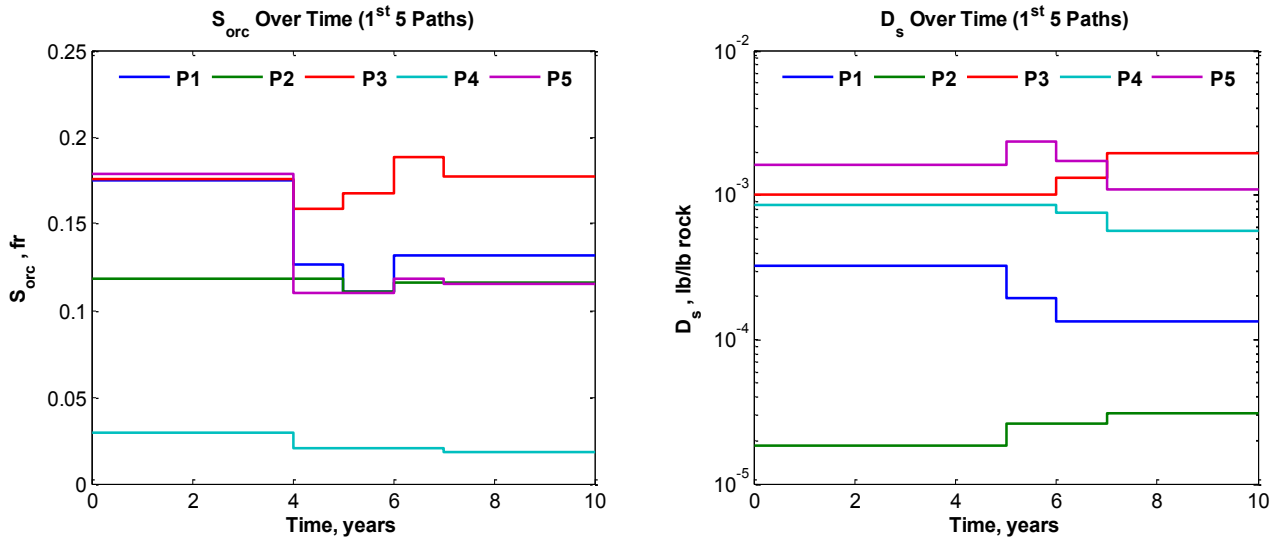


Fig. 5.5[10]– Residual oil saturation to chemical flooding and surfactant adsorption variation with time for case study 1.

Sample production profiles of the first five paths or realizations with surfactant flooding initiated at the start of the fourth year and of the first path for all injection scenarios are presented in **Fig. 5.6**. It is clear that different realizations of S_{orc} and D_s will affect the recovery factors achieved from the process. Also, it is clear that by initiating surfactant flooding at different times different recovery factors are achieved.

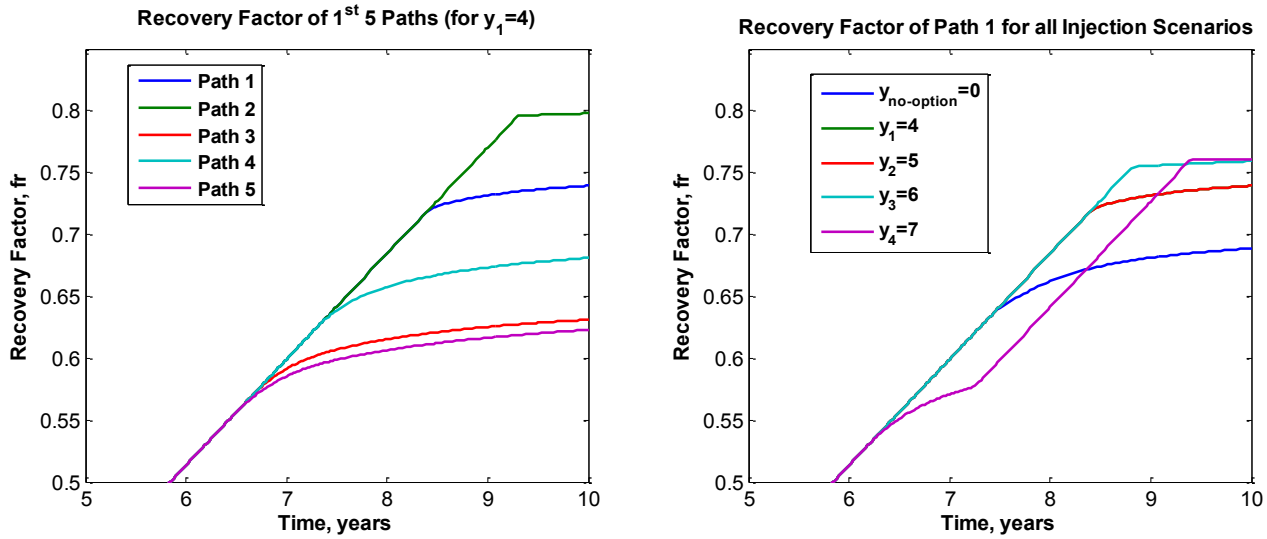


Fig. 5.6[11]– Production profiles for case study 1.

[10] Reproduced from **Alkhatib et al. (2013)**.
[11] Reproduced from **Alkhatib et al. (2013)**.

b. Economic Model

The objective function used was the Net Present Value (NPV). The economic model will be based on calculating net revenue as:

$$\text{Net Revenue} = \sum[\text{Oil Revenue} - (\text{Cost of Injected Water} + \text{Cost of Produced Water} + \text{Cost of Surfactant})] - \text{Capital Expenditure} \quad \text{Eq. 5.4}$$

Risk-neutral valuation approach is used where the oil price stochastic model is adjusted for risk using a risk premium of 3%[12]. This approach is considered to be more comprehensive in analyzing cash flows because it adjusts every component of the cash flow for risk and then discounts for time (at the risk-free rate) whereas traditionally a constant discount factor (including both time and risk) was used which could generate biased results due to the varying risk patterns of the component cash flows (**Jafarizadeh and Bratvold 2009**). Cash flows are then discounted using the risk-free rate, r, which is assumed to be constant over time and equal to 6%. Continuous discounting is assumed.

There are four economic state variables: the oil price (P_o), the surfactant cost (P_s), cost of water injection (P_{wi}) and the cost of produced water (P_{wp}). P_o (\$/stb) and P_s (\$/stb surfactant) are modeled independently while P_{wi}(\$/stb) and P_{wp} (\$/stb) are correlated[13] with P_o. P_o is modelled as a risk-neutral Ornstein-Uhlenbeck process (**Uhlenbeck and Ornstein 1930**) which is a mean reverting stochastic process :

$$dP_o = \lambda\left(\left[\mu - \frac{\delta}{\lambda}\right] - P_o\right)dt + \sigma dW_t \quad \text{Eq. 5.5}$$

Where:

W_t, is a Brownian-Motion, $dW_t \sim N\left(0, \sqrt{dt}\right)$.
λ is the measure of the speed of mean reversion.
μ is the long term mean that the process reverts to.
σ is the measure of the process volatility.
δ is the risk premium.

To simulate the oil price using the above equation it is necessary to discretize it with respect to time, the following expression provides an exact discrete-time expression as:

$$P_{o_t} = e^{-\lambda\Delta t}P_{o_{t-1}} + \left(1 - e^{-\lambda\Delta t}\right)\left(\mu - \frac{\delta}{\lambda}\right) + \sigma\sqrt{\frac{(1-e^{-2\lambda\Delta t})}{2\lambda}}dW_t \quad \text{Eq. 5.6}$$

[12] Risk premium value is obtained from the oil price model in Willigers and Bratvold (2009).
[13] This is following Jafarizadeh and Bratvold (2009).

Table 5.2: Ornstein-Uhlenbeck Process Parameters[14]

t, months	120
dt	1
λ	0.0012
μ, $/Bbl	66.67
σ	1.81
δ	0.03
P_{o_0}, $/Bbl	90

This discrete-time version of the process allows an exact discretization in that accuracy is not reduced when a larger time step is used (**Dias 2005**). A more detailed discussion of why the above discretization of a mean-reverting process is chosen can be found in **Dixit and Pindyck (1994)**. Mean reverting stochastic processes are well suited for modeling commodity prices because they reflect the economic paradigm that when prices are too high, supply will increase and demand will reduce. When prices become too low, the opposite effect occurs, pushing prices towards the long term mean (**Smith 2010**). The prices are generated using a MATLAB routine developed by **Smith (2010)**. **Fig. 5.7** shows the oil price model.

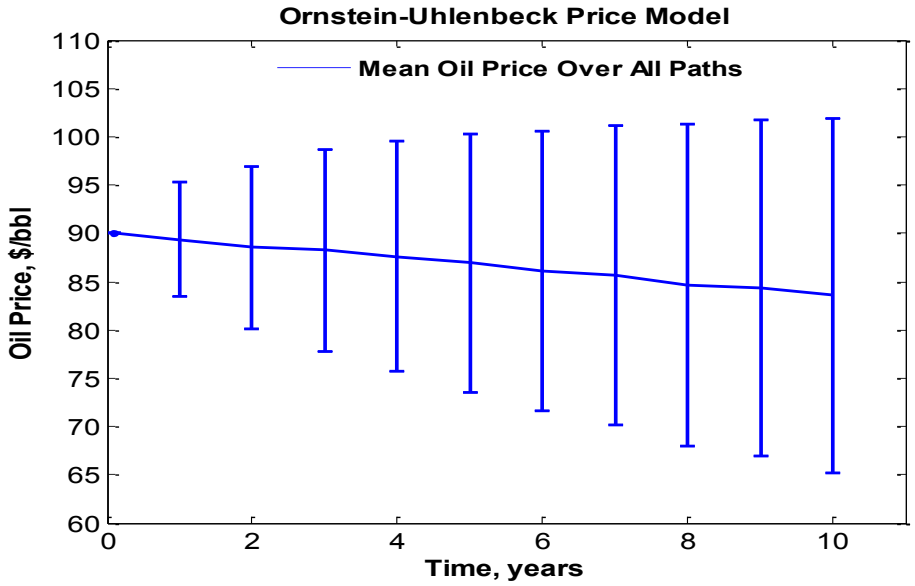


Fig 5.7[15]**– Ornstein-Uhlenbeck price model, showing the mean of 1000 paths and the corresponding standard deviation.**

The surfactant price[16] (P_s) is modeled using a uniform distribution, ~ U(1,3). Some types of surfactants such as alkyl polyglycosides are manufactured from renewable resources and are mostly uncorrelated with the price of oil (**Iglauer et al. 2004**). Therefore P_s was assumed to be independent of P_o. However, P_s and P_o could be correlated as other types of surfactants are synthesized from petroleum feedstock and thus are dependent on oil price. At each time step a unique realization is sampled from the distribution. For water injection cost (P_{wi}) and water production cost (P_{wp}) a cost multiplier factor of 0.10 was applied to the oil price (P_o). Capital expenditure parameters are shown in **Table 5.3**. The capital

[14] The λ, μ and σ parameters were obtained using the Least Squares method to estimate parameters of an observed Ornstein-Ulhenbeck Process (Smith, 2010). NYMEX futures prices from April 1983-July 2012 were used as the basis of the estimation (EIA, 2012). t and dt are based on a simulation period of 120 months (10 years) discretized into monthly timesteps.
[15] Reproduced from **Alkhatib et al. (2013)**.
[16] Surfactant price range was based on (**Anderson et al. 2006; Thomas 2006; Wyatt et al. 2008**).

expenditure is adjusted for each reservoir model by scaling to the maximum water injection rate encountered in the simulation.

Table 5.3: Capital Expenditure Data[17]

Facility Cost ($)	1,500,000
Laboratory and Engineering Design ($)	700,000
Incremental Operating Cost ($/Month)	10,000
Water Injection Rate Reference (Bbl/day)	5,000

Fig. 5.8 show sample normalized NPV charts for the same technical sample realizations presented in the previous section. This is done for all injection scenarios for the first path (realization) and for the first five paths under a constant injection scenario of y_1=4. These figures are normalized onto the basis of the NPVs calculated for regular waterflood using the same stochastic prices generated from the mean-reverting process discussed above for each path.

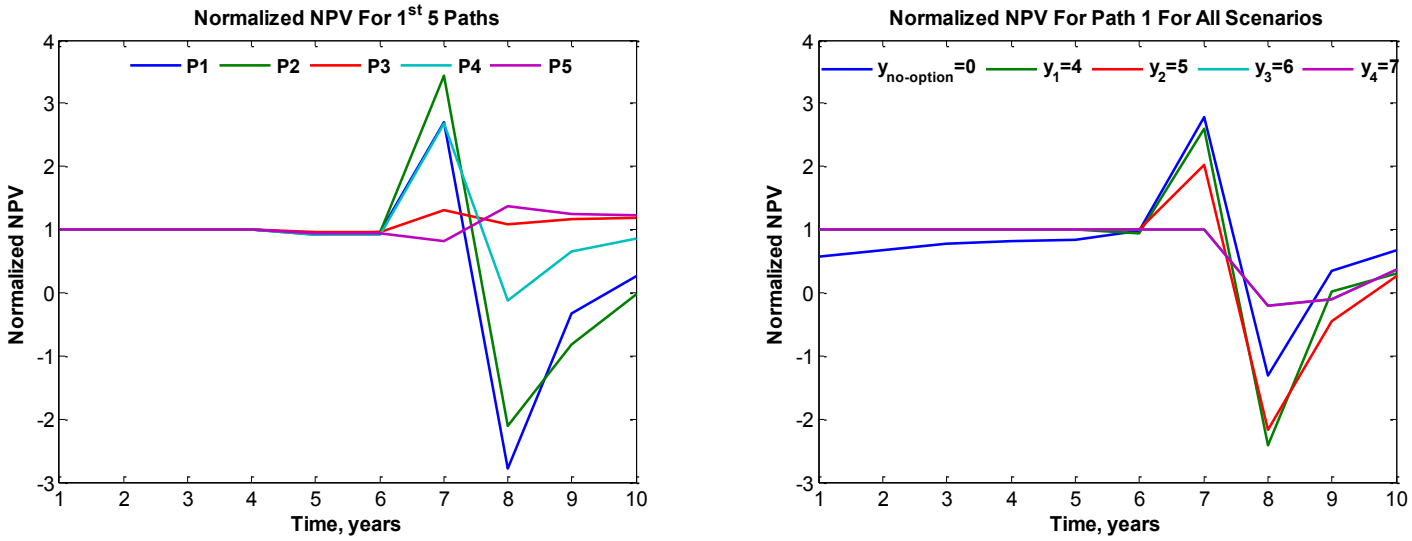


Fig 5.8[18]**— Normalized NPV for the case study 1.**

After obtianing the NPV for each path for every scenario, this completes the first component of the method (stochastic simulation). The next step is to apply the recursive decision rule or dynamic programming formula to the results of the stochastic simulation in order to produce the optimal policy and determine the VoF.

[17] The capital expenditure data was obtained from **Wyatt et al. (2008)**.
[18] Reproduced from **Alkhatib et al. (2013)**.

5.1.3 Code Validation

The algorithm was written as three separate modules. The first module samples the technical state variables, runs ECLIPSE and reads the output RSM files. The second module is concerned with calculating the objective function, NPV. This module performs the stochastic sampling of the economic state variables and then calculates the objective function based on the output from ECLIPSE and the realizations of the economic state variables. These two modules represent the forward stochastic simulation element of the LSM method. The third module performs the recursive dynamic programming component in order to produce the optimal policy. The main component of this module is to determine the value of the continuation function and compare it with the value of implementing the decision at the specified decision node. The continuation value is determined by linearly regressing the value of exercising the decision at the subsequent decision node onto a set of basis functions of the current realization of the state variables. The module performs this and then obtains the optimal policy for each path. It then determines the VoF by finding the averages of the NPV of the optimal policies over all paths and subtracting the average value of the static policy over the same set of paths.

The LSM algorithm was cross validated with basic examples performed with EXCEL. The first set of examples assumed the recovery factor as the objective function used in the LSM algorithm and the first of these examples assumed S_{orc} as the only uncertain parameter. The second example assumed both the S_{orc} and D_s as the sources of uncertainty. These examples are similar to the examples presented in **Alkhatib and King (2011)**. The second set of example consisted of a total of ten paths assuming S_{orc} and D_s as the technical state variables and assuming the oil price and surfactant cost as the economic state variables. Here the objective function was the NPV. In these examples the least-squares regression was performed in EXCEL. The third module (recursive least-squares regression) was additionally cross validated with example 1 provided by **Longstaff and Schwartz (2001)** in their paper.

5.1.4 Results for Case Study 1

The results show that for a most paths the VoF is positive; it is beneficial to have flexibility (see **Fig. 5.9**). The policy histogram shows that surfactant injection is optimal before (y=4) or after (y=7) breakthrough for most realizations. For this case study, by having the flexibility to inject surfactant at different decision nodes, it is possible not only to mitigate adverse circumstances but also increase value conditional on the resolution of uncertainty. The results for this initial application were obtained based on assuming the following:

- No mobility control present
- Simple powers were used for basis function design.
- The no-flexibility scenario was assumed to be surfactant injection at the start of field life.
- The VoF converges using 10^3 realizations.

It is important to check the sensitivity of the LSM method to these assumptions. This is discussed in the following subsections.

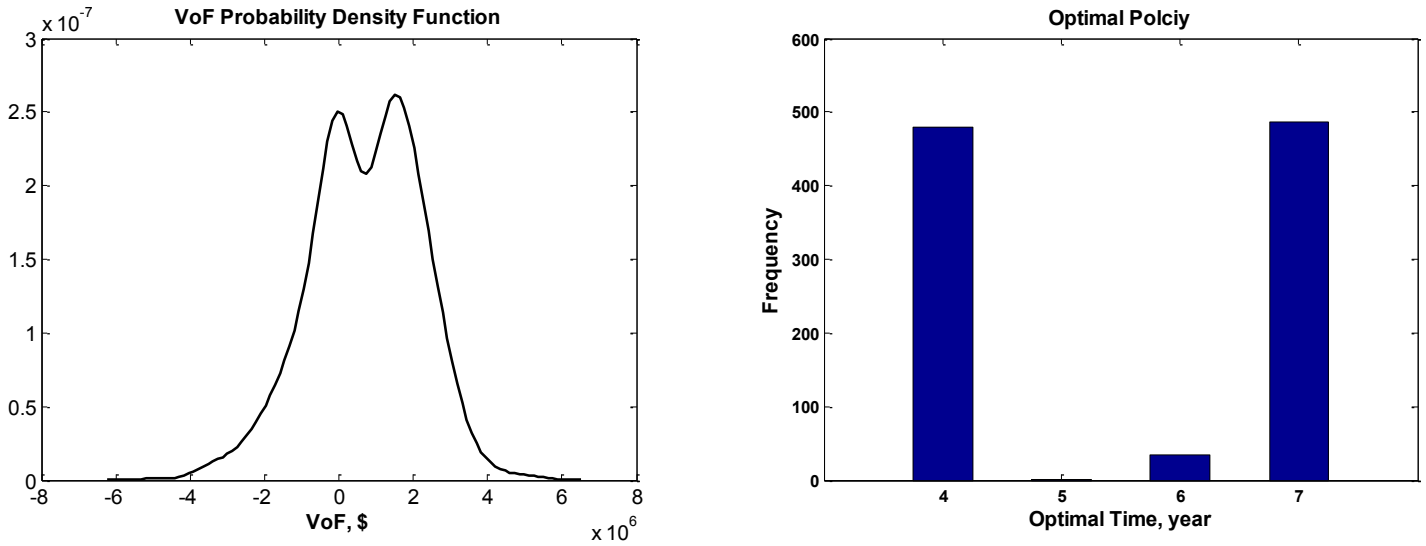


Fig 5.9– Value of flexibility probability density function (PDF) plot and policy histogram for case study 1.

5.1.5 VoF Sensitivity Analysis

The results in the previous subsection were based on the following assumptions:

- The static or no-flexibility scenario was assumed as surfactant injection at the start of field life.
- The VoF was assumed to have converged using 10^3 realizations.
- The decision space was discretized into yearly decision nodes, having a total of four elements.
- No mobility control was used.

In this subsection, the sensitivity of VoF towards these assumptions is tested in order to develop the best approach for applying the LSM to other reservoir models.

5.1.5.1 Varying the Static Policy Scenario

Fig. 5.10 shows the results for varying the static scenario over a range of yearly decision nodes beginning from the start of field life and ending at the start of the third year and **Table 5.4** shows the VoF as a function of the different static scenario. A significant variation is observed. However, for all other static scenarios, the VoF is increased and the policy histogram shows a significant shift towards favoring early surfactant injection. This is because of the unencumbered propagation of the surfactant bank in a homogenous media. When the surfactant bank is injected at the start of the field, it is in contact of most of the mobile oil due to the homogeneous permeability field. However, when the surfactant bank is injected at y=1,2 and 3, the mobile oil is less than when surfactant is injected at y=0. Thus the value of the no-flexibility scenario is reduced.

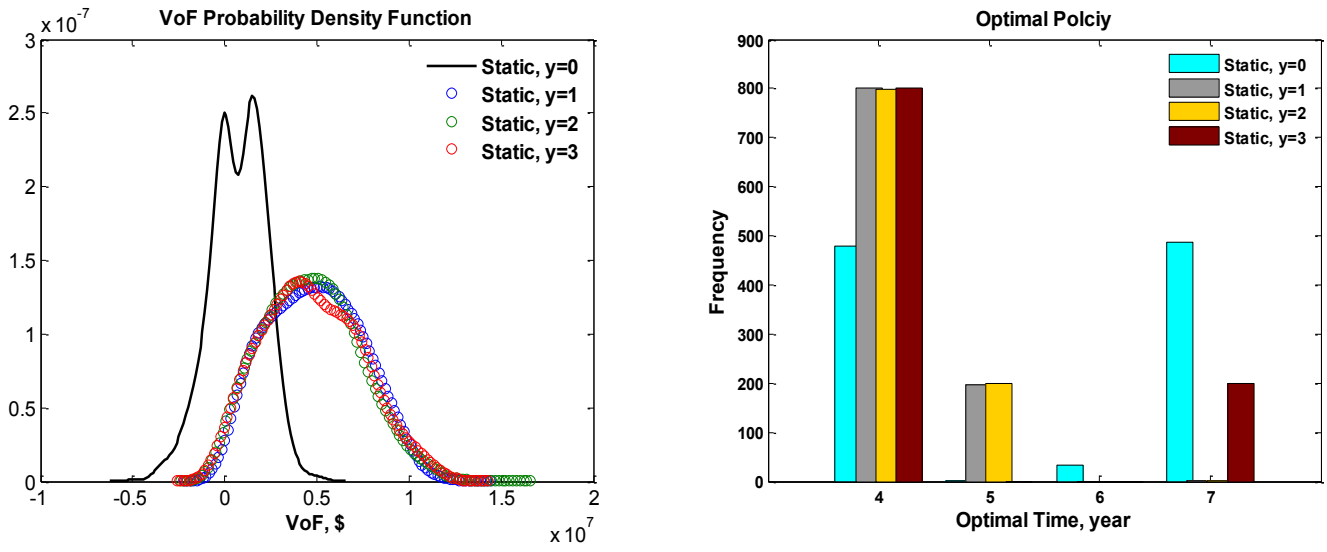


Fig 5.10— VoF PDF plot and policy histogram for case study 1 using different static scenarios.

Table 5.4– VoF mean for different static scenarios.

Static Scenario	Value of Flexibility (mean, $)
Static, y=0	7.15e+05
Static, y=1	4.88e+06
Static, y=2	4.70e+06
Static, y=3	4.76e+06

5.1.5.2 Convergence as a Function of the Number of Realizations

Fig. 5.11 shows the results for using an increasing number of realizations on the convergence of the VoF. This is important since the method uses Monte Carlo simulation which converges at a very slow rate. The policy histogram and the normalized option value (VoF) show that the results are relatively converged using 10^3 realizations. However, accuracy is increased with an increasing number of realizations. Here, it is important to balance computational requirement and the relative accuracy of the result. For subsequent case studies it was assumed that 10^3 realizations is sufficient for convergence.

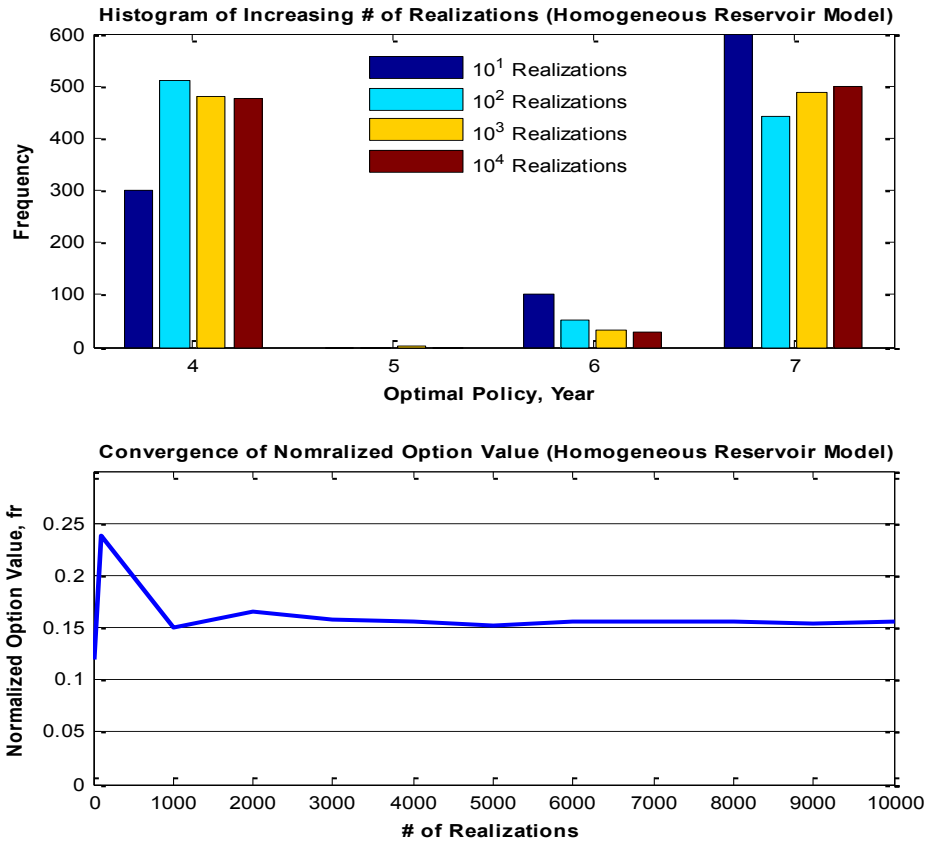


Fig 5.11[21]– Histogram of optimal policy (adjusted to a basis of 10^3 realizations in order to compare with the original run) and plot of convergence of the averaged normalized option value for the homogeneous reservoir model with increasing number of realizations. The averaged normalized option value is taken as the difference between the averaged (over all realizations) normalized option and the averaged normalized static scenarios, the normalization is with respect to the corresponding waterflood scenario NPV (averaged over all realizations). A value > 0 is considered to be favouring flexibility while a value <0 favours the static scenario.

5.1.5.3 Decision Space Discretization

Fig. 5.12 and 5.13 and Table 5.5 shows the results for varying the discretization of the decision space from yearly to twice-yearly and quarter-yearly decision nodes over the same bounds of the decision space. By increasing the discretization of the decision space, the accuracy of the results is expected to be enhanced. The policy histograms show that there is no significant discrepancy when adding more decision nodes with the decision space. The VoF PDF shows that relatively the same distribution is produced. The VoF for each case maintain the same trend that is they are positive although there is a relatively greater discrepancy in the VoF mean for quarter-yearly decision nodes when compared with the case of yearly decision nodes.

[21] This figure is reproduced from **Alkhatib et al. (2013).**

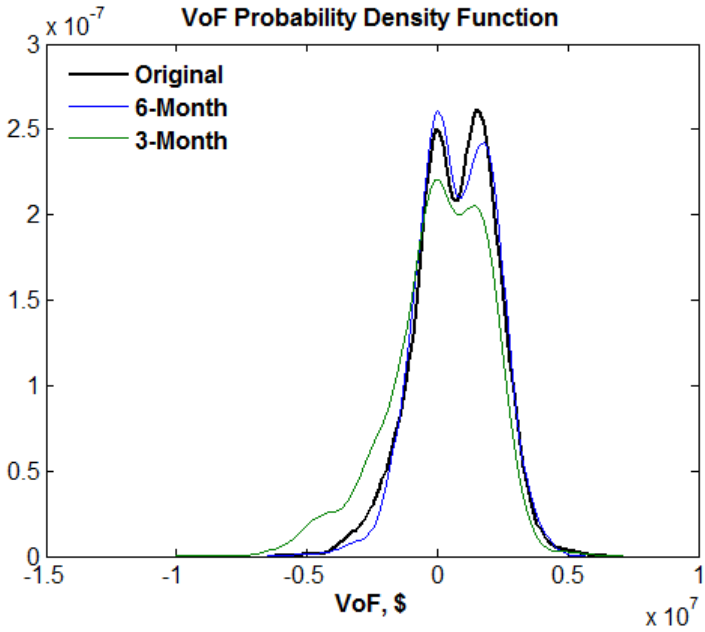


Fig 5.12– VoF PDF plot for case study 1 for different decision space discretizations.

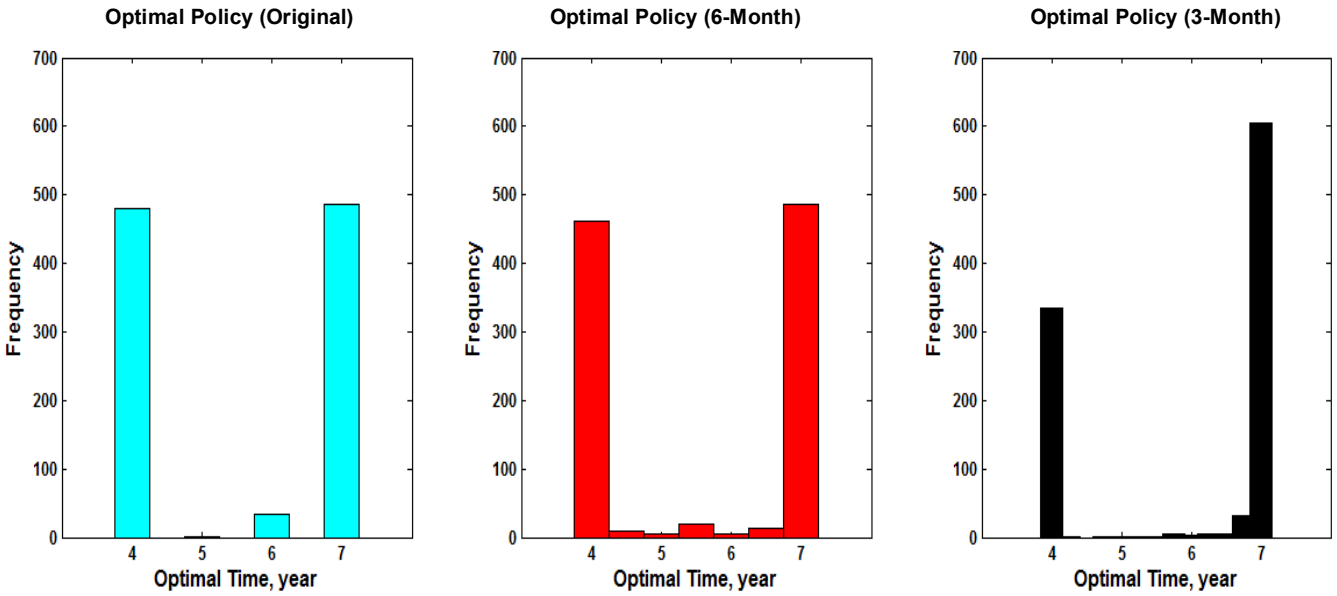


Fig 5.13– Policy histograms for case study 1 for different decision space discretization's.

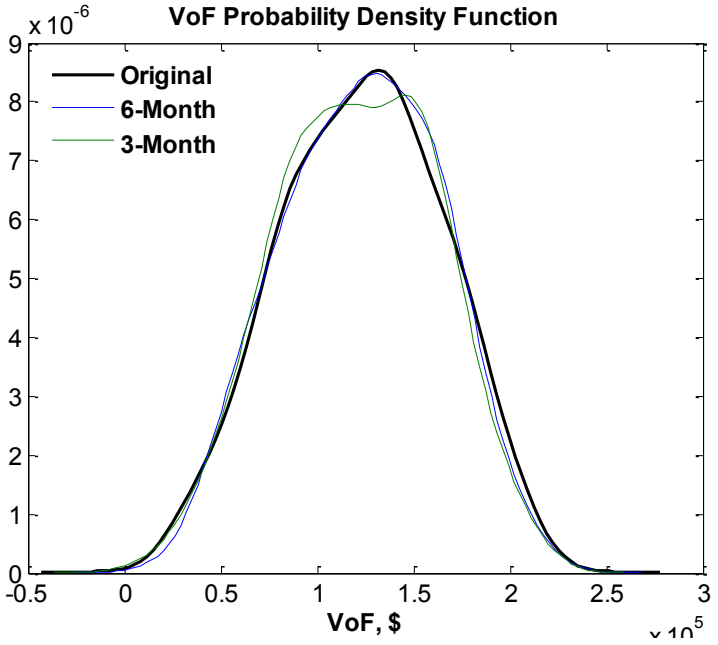
Table 5.5– VoF mean for different decision space discretization's.

Decision Space Discretization	Value of Flexibility (mean, $)
Yearly (Original)	7.15e+05
Bi-Annual	7.58e+05
Quarter-Annual	5.40e+05

This lack of discrepancy in the optimal policy did raise some suspicion on the performance of the algorithm. Therefore, a more in-depth investigation was warranted. This was attempted with respect to three aspects of the method: the validity of modelling SP flooding in ECLIPSE, the effect of the objective function calculation on the optimal policy produced and the accuracy of the algorithm itself in producing this optimal policy.

Surfactant-Polymer Flooding Modelling

To test the validity of the ECLIPSE simulations, the first step was to run the same decision space discretization cases using one dimensional homogenous reservoir models that are based on the same reservoir properties used for the three dimensional homogenous base case assuming S_{orc} is the only technical variable and that it is constant in time. **Fig. 5.14 and 5.15** shows the VoF PDF and policy histograms obtained for the one-dimensional reservoir model and **Fig. 5.16 and 5.16** for the three-dimensional reservoir model.



.

Fig 5.14– VoF PDF for one-dimensional homogeneous reservoir model assuming S_{orc} as the technical uncertainty for different decision space discretization's.

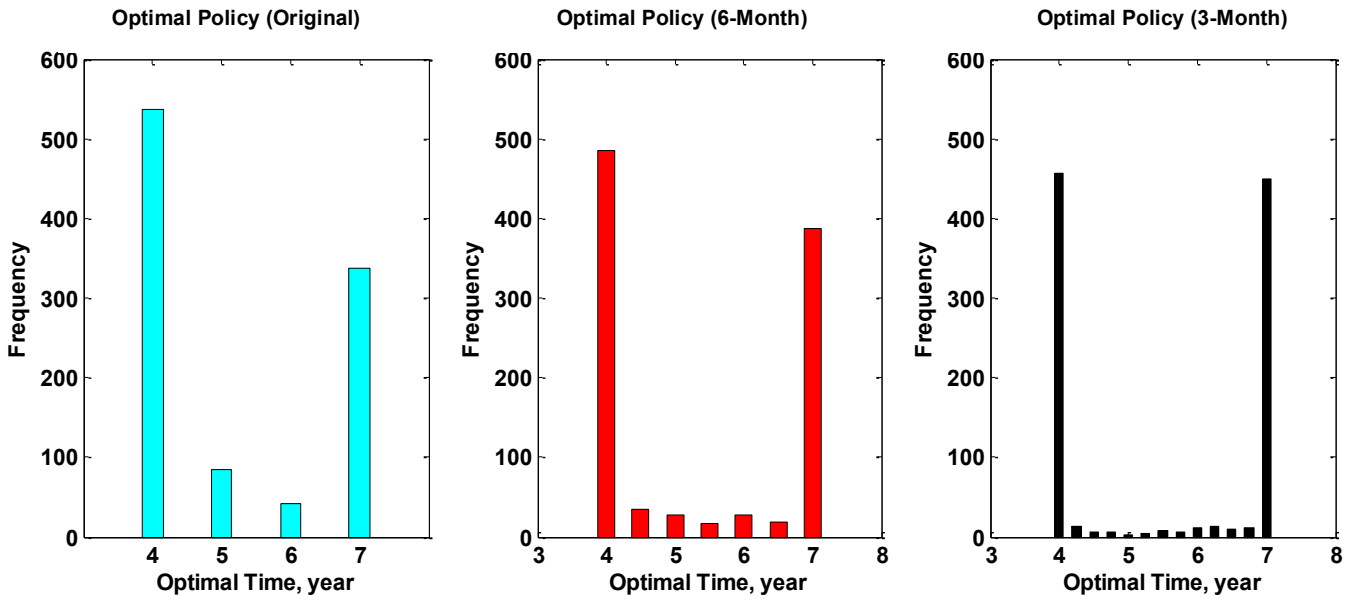


Fig 5.15– Policy histograms for one-dimensional homogeneous reservoir model assuming S_{orc} as the only technical uncertainty for different decision space discretization's.

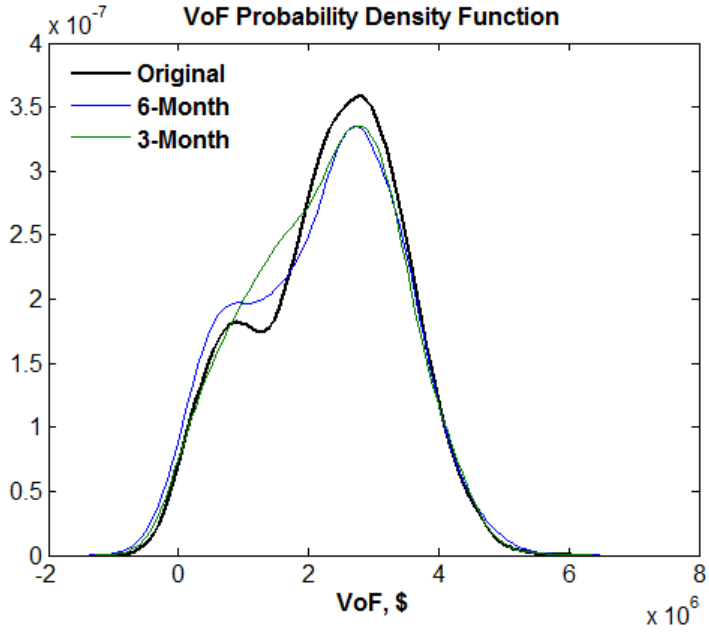


Fig 5.16– VoF PDF for three-dimensional homogeneous reservoir model assuming S_{orc} as the technical uncertainty for different decision space discretization's.

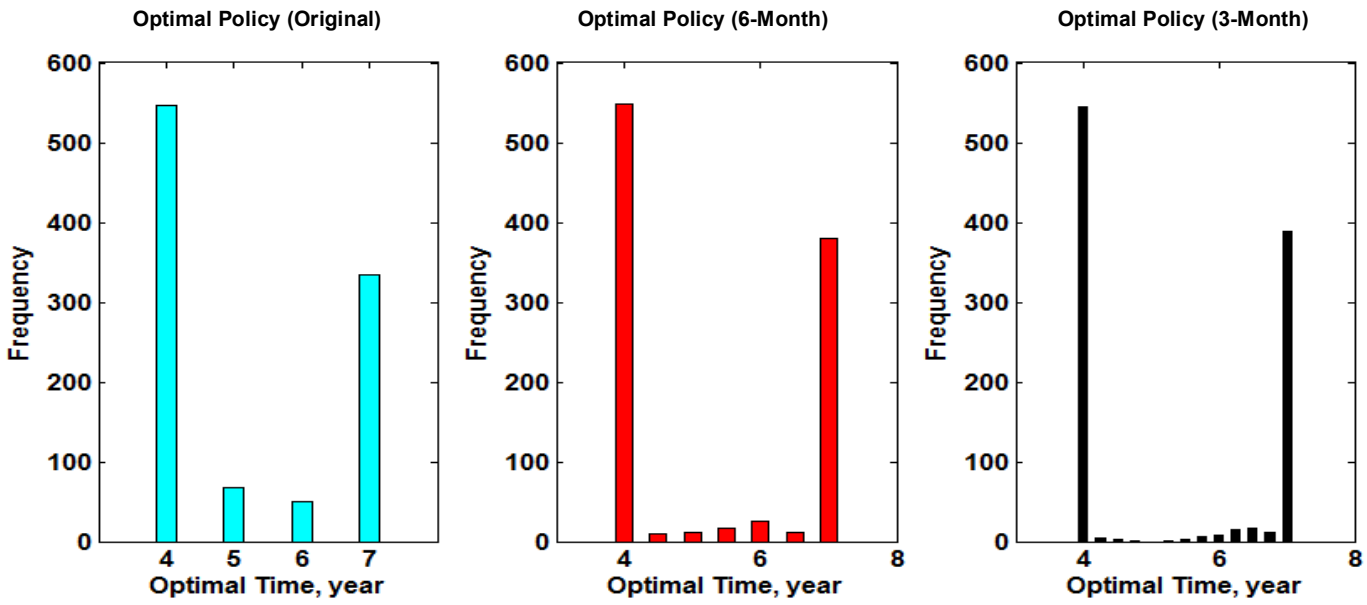


Fig 5.17– Policy histograms for three-dimensional homogeneous reservoir model assuming S_{orc} as the only technical uncertainty for different decision space discretization's.

For this case, the one-dimensional model (**Fig. 5.14 and 5.15**) produces similar policy trends compared with the three-dimensional model (**Fig. 5.16 and 5.17**). There is no significant variation in the trend of the histograms of the optimal policy. The only variation is apparent in the inner decision nodes, where they become more spread out as the decision space is discretized further. This was observed for both the one-dimensional and three-dimensional reservoir models.

Second step was to assume S_{orc} and D_s as the technical uncertainties constant in time and compare the results obtained from both the one-dimensional and three-dimensional reservoir models.

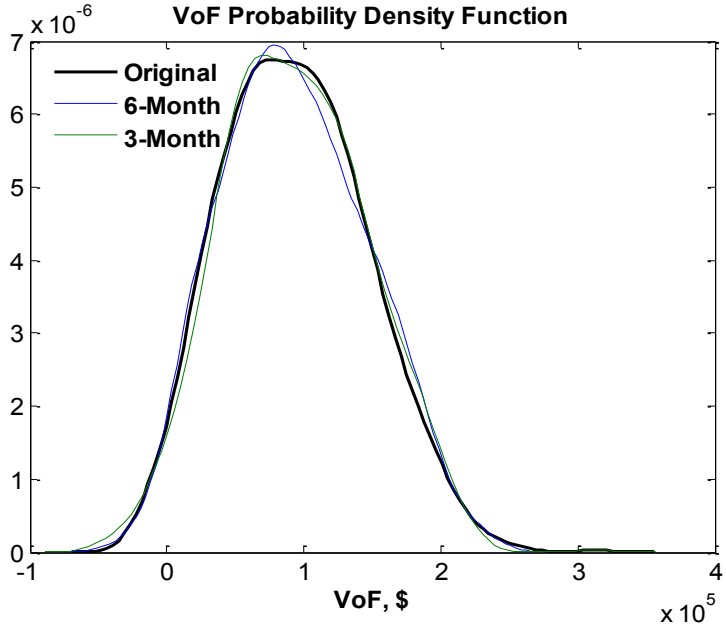


Fig 5.18– VoF PDF for one-dimensional homogeneous reservoir model assuming S_{orc} and D_s as the technical uncertainties for different decision space discretization's.

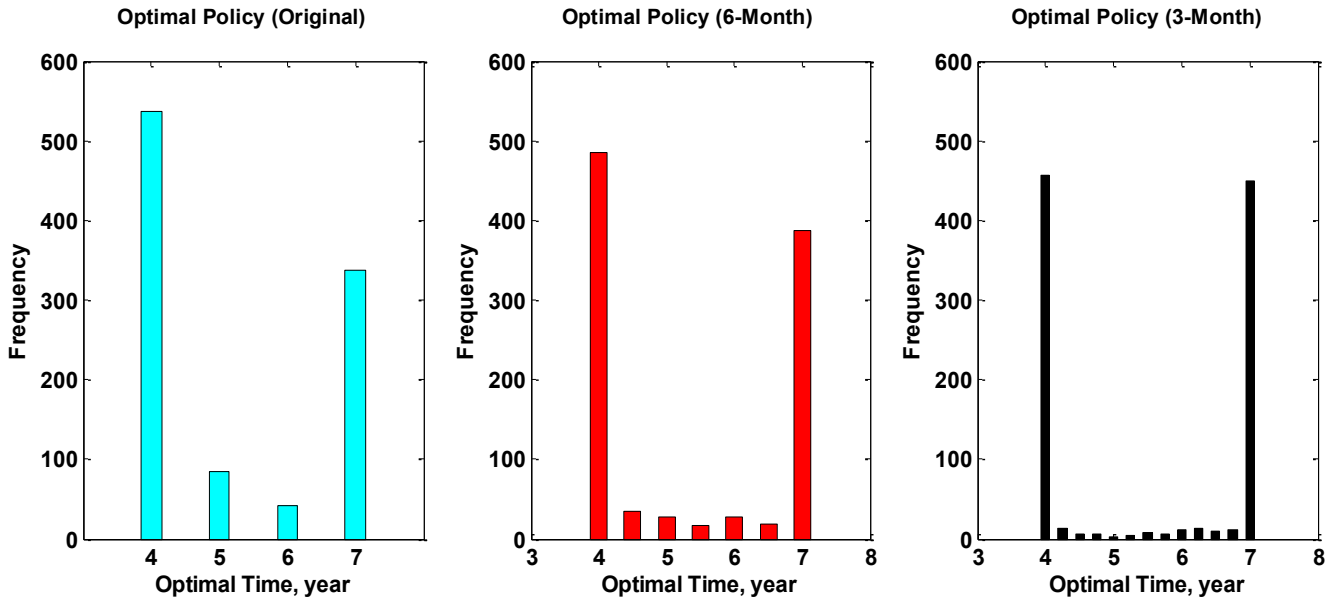


Fig 5.19– Policy histograms for one-dimensional homogeneous reservoir model assuming S_{orc} and D_s as the technical uncertainties for different decision space discretization's.

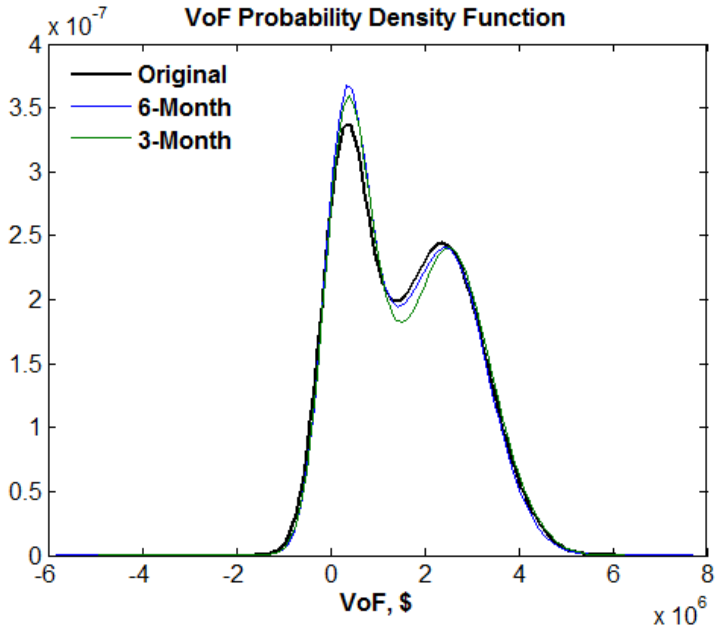


Fig 5.20– VoF PDF for three-dimensional homogeneous reservoir model assuming S_{orc} and D_s as the technical uncertainties for different decision space discretization's.

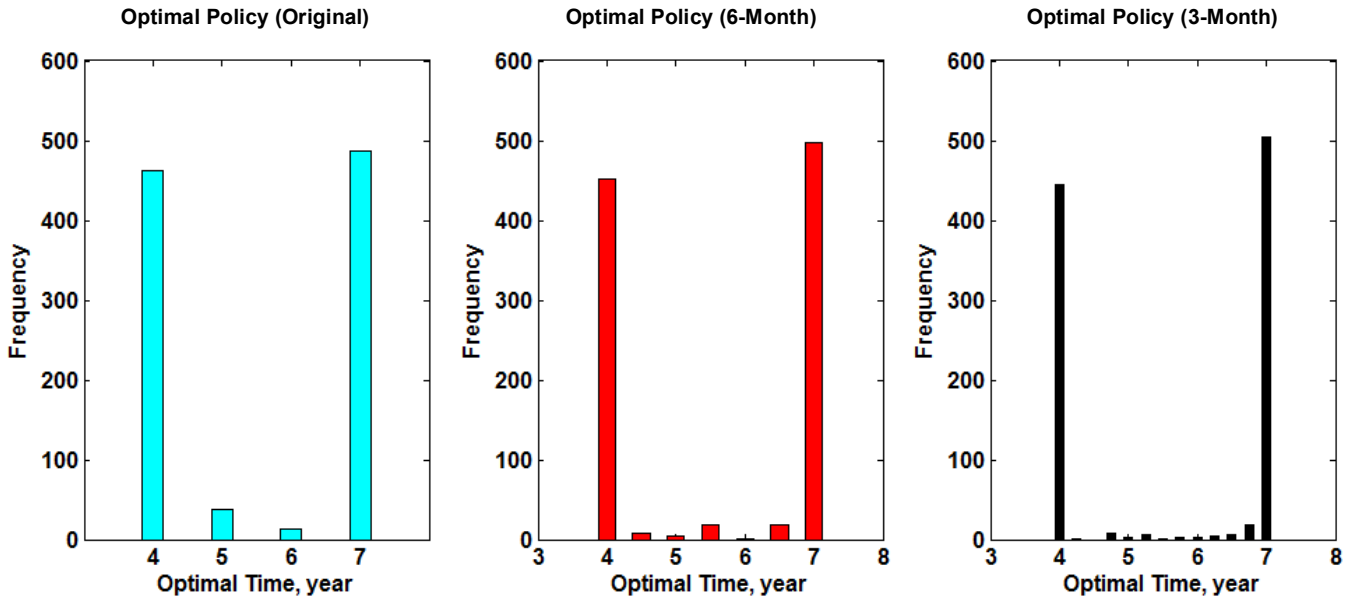


Fig 5.21– Policy histograms for three-dimensional homogeneous reservoir model assuming S_{orc} and D_s as the technical uncertainties for different decision space discretization's.

For this case, the one-dimensional model (**Fig. 5.18 and 5.19**) produces similar policy trends compared with the three-dimensional model (**Fig. 5.20 and 5.21**) in that the policy histogram does not spread out over the finer decision space discretization. Each reservoir model does produce unique results, this is attributed to the dimensionality of the reservoir model. In this case, the inner decision nodes become more spread out with increasing decision space discretization.

Objective Function

By calculating the objective function, a transformation in the optimal injection strategy is observed compared with the optimal injection time determined by considering the recover factor. This is due to the specific assumptions underlying the objective function calculation, especially, the assumptions regarding the price of water injection and production. Here it was assumed that water production and water injection costs are determined by applying a multiplier factor to the current oil price. A relatively high multiplier factor of 0.10 was used to penalise for increased water production and injection.

To illustrate this, **Fig. 5.22** plots the mean of the objective function (NPV) over 1000 samples of S_{orc} and D_s (assuming the same probabilistic distributions as the base case) as a function of injection time. This is performed for the yearly, bi-annual, and quarter annual cases. The mean of the recovery factor is also plotted on the same plot. This is obtained as the mean over the same 1000 samples. It is clear that the objective function and the recovery factor behave differently and are not in agreement. The peak mean of NPV is obtained by implementing different injection policies compared to the peak mean of RF. This is attributed to the transformation that is applied by the objective function calculation to the behaviour observed when considering the recovery factor. It does not reproduce the same behaviour.

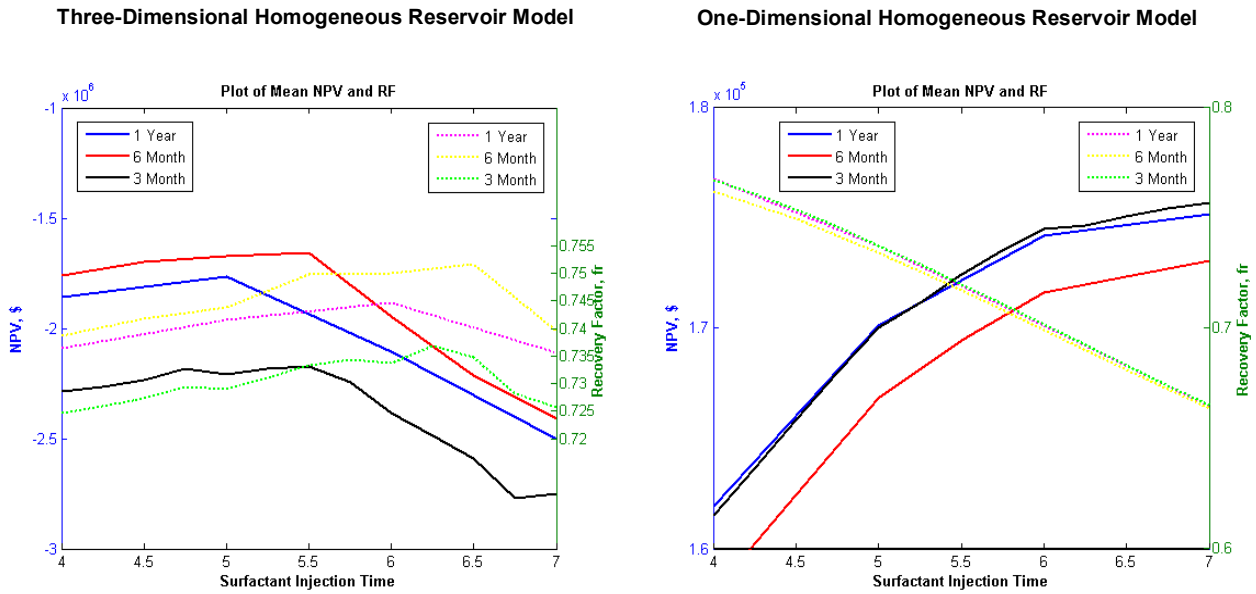


Fig 5.22– Plot of mean NPV and RF (recovery factor) over 1000 realizations as a function of injection policy. The legend in the upper right corner refer to the right axis (RF) and the legend in the upper left corner refers to the left axis (NPV). The plot on the left was determined for the base case three dimensional homogeneous reservoir model and the plot on the right was obtained using a one dimensional homogeneous reservoir model.

To test the effect of the cost multiplier on the results obtained from the algorithm, low (0.01) and high (0.30) values of the cost multiplier were applied to the results obtained when using the original cost multiplier (0.10). This was performed for the same decision space discretization cases. **Fig. 5.23** shows the VoF PDF's and policy histograms obtained for varying the cost multiplier value. With regards to the VoF PDF, the shape of the PDF behaves in a consistent manner over all decision space cases where the shape of the curve narrows as the value of the multiplier cost increases. This shows that for relatively high multiplier costs, the VoF is dominated by this assumption. This is apparent in **Fig. 5.24** where the relative mean VoF are plotted as a function of the cost multiplier value. Here it is clear that the highest VoF is obtained when using the highest cost multiplier (0.30). This can be attributed to the higher cost of the increasing water injection and production volumes required to maintain production over the life of the field simulation. Because the VoF is calculated based on a static policy scenario that assumes surfactant injection at the start of field life which results in an earlier production of the surfactant recovered oil thus an increased water injection and production requirement from a relatively earlier time compared with later surfactant injection scenarios. Therefore a high cost multiplier would result in a higher VoF.

The histograms in **Fig. 5.23** show that the policies vary with the cost multiplier value in a similar way for all decision space discretization cases. What is evident is that the value of the cost multiplier does influence the policy histogram although the behaviour is similar to that found in **Fig. 5.13**.

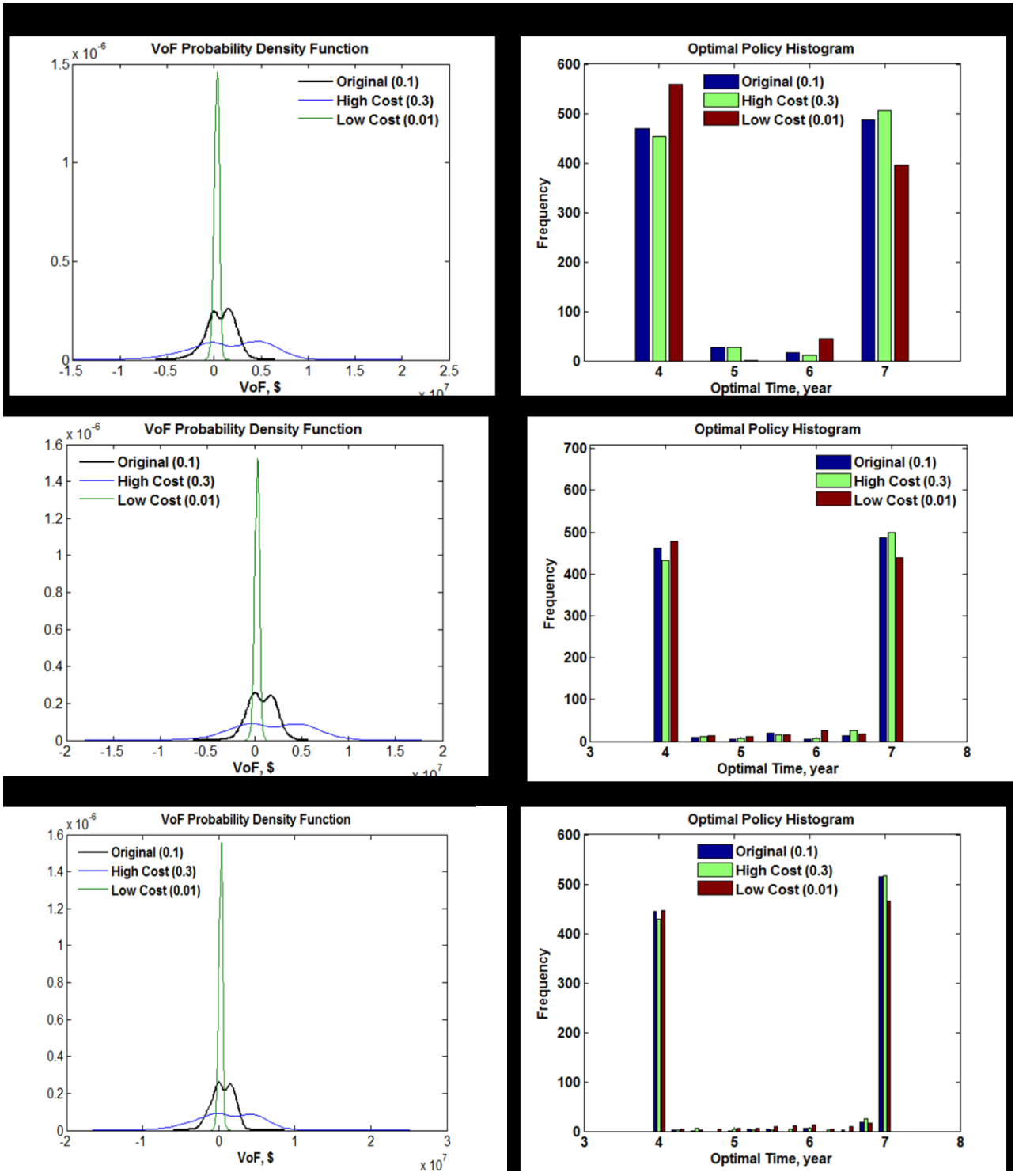


Fig 5.23– Figure showing the VoF PDF and the optimal policy histogram obtained for each decision space discretization case where the results for each water cost multiplier is plotted. These were obtained for the three-dimensional homogeneous reservoir model.

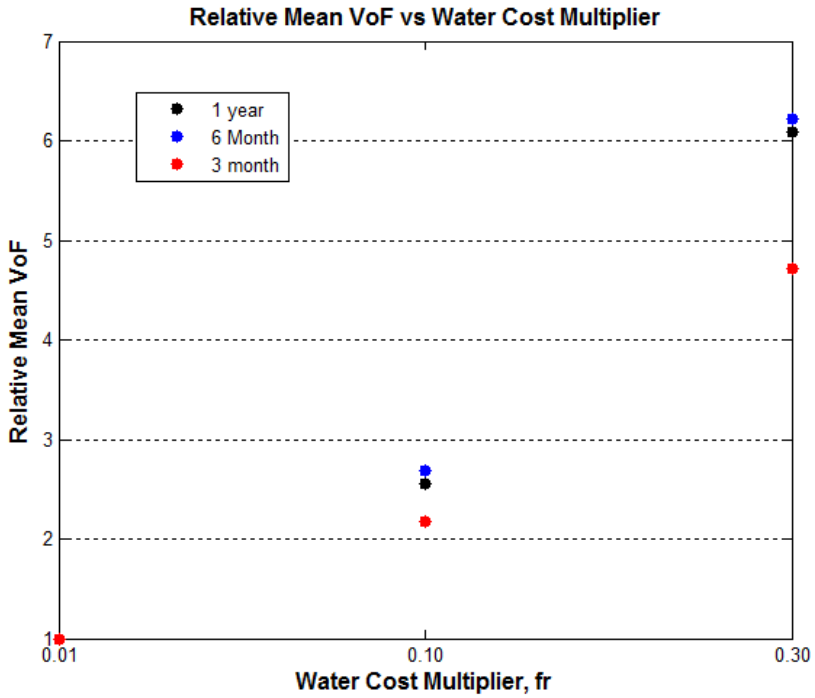


Fig 5.24– Plot of relative mean VoF as a function of the water cost multiplier. The mean VoF is normalized using the low water cost multiplier case (0.01) as the base case. These results were obtained using the three-dimensional homogeneous reservoir model base case.

In summary, the assumptions underlying the objective function do have a significant effect on the results obtained from running the LSM method. However, they do not explain why the policy histograms trends only vary slightly as a function of the discretization of the decision space.

Accuracy of Optimal Policy Produced by the Algorithm

As mentioned earlier, the policy produced by the LSM algorithm is near-optimal (i.e. sub-optimal) rather than the global optimum because the continuation function in the decision rule is approximated by linear regression. Furthermore, the accuracy of VoF and the near-optimal policy is a function of the number of realizations and the number of basis functions used for the least-squares linear regression. The accuracy increases as these tend to ∞.

With respect to increasing the discretization of the decision space (increasing the number of time steps), the LSM algorithm would require a better choice of basis functions along with an increase in the number of these basis functions (**Bender and Steiner 2010**). This leads to an increase in the number of realizations required. **Glasserman and Yu (2004)** show that the number of realizations required to produce convergent results increases exponentially with the number and the order of the basis functions used in the regression. Thus in order to produce accurate results for finer discretization of the decision space, a larger number of basis functions is required leading to an increase in the number of realizations. This leads to a significant increase in the computational cost of running the algorithm.

Fig. 5.25 illustrates this behaviour. This plot is based on data from **Bender and Steiner (2010)**. It plots the value of a financial option determined by the LSM algorithm as a function of the number of time steps (decision space discretization), basis functions and realizations. The plots show that finer time steps would require an increasing number of basis functions

which in turn will require an increasing number of realizations for the option value to converge. For this specific example, the solution begins to stabilise at approximately 30 time steps discretization which requires 45 basis functions. This corresponds to approximately 8000 realizations.

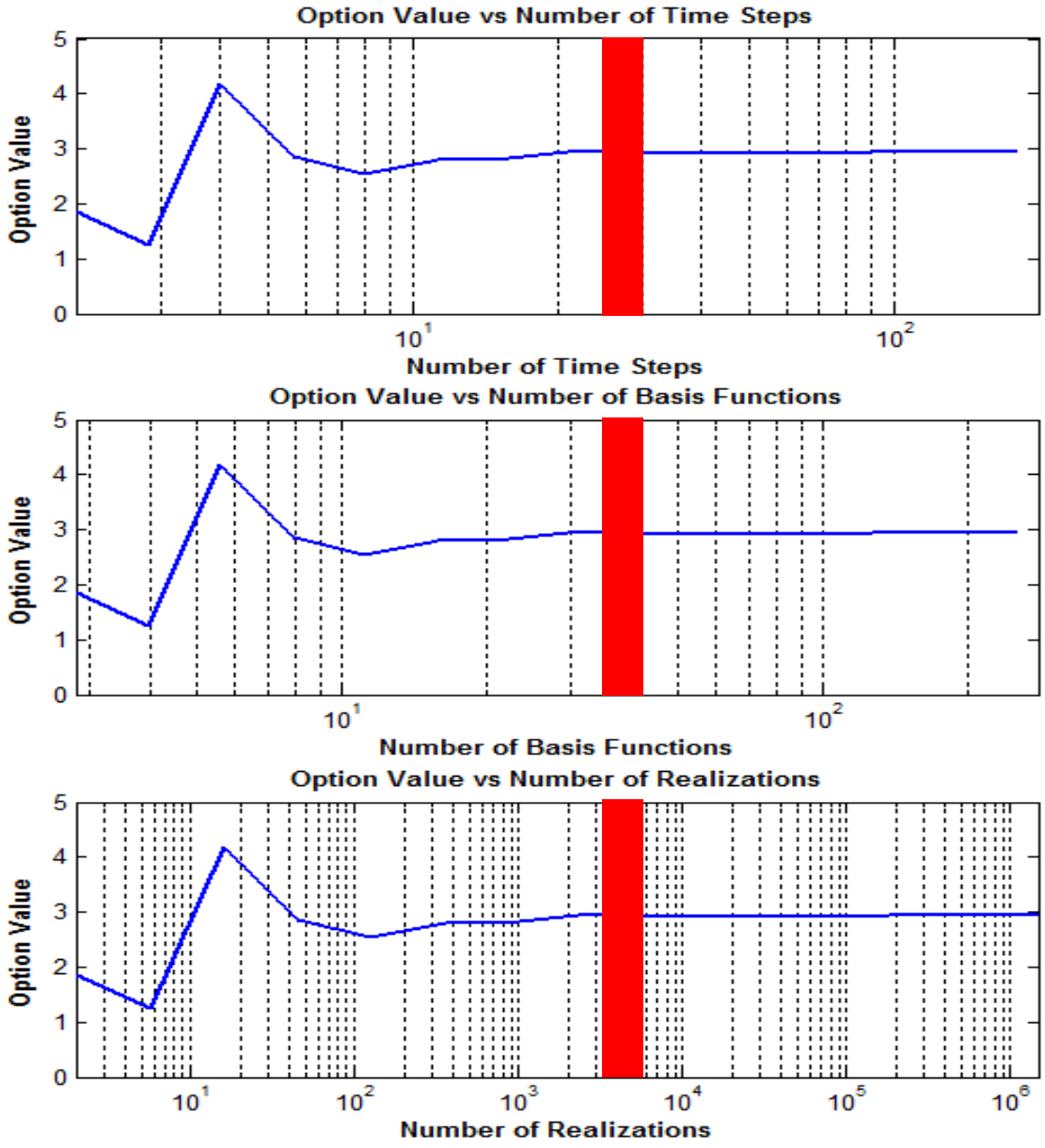


Fig 5.25– Plot of the option value from numerical case 1 in Bender and Steiner (2010) as a function of the number of time steps, basis functions and realizations. The red highlighted region shows where the option value begins to converge.

Fig. 5.26 shows the convergence of the mean squared error with respect to the vector of the estimated regression coefficients (obtained for the approximation of the continuation value) as a function of the number of realizations, N and the number of basis functions, K obtained from **Glasserman and Yu (2004)**. Assuming that 1000 realization is computationally possible for the case studies considered in this thesis, it is clear that the mean squared error of the estimated regression coefficients is relatively low upto a maximum of three basis functions. If the number of basis functions is increased to eight, a large error is

observed when using 1000 realizations. Thus a much higher number of realizations is required: the data indicate for this case the lowest number of realizations needed for convergence is 16000 which is computationally prohibitive for the decision cases considered and for application to complex reservoir models.

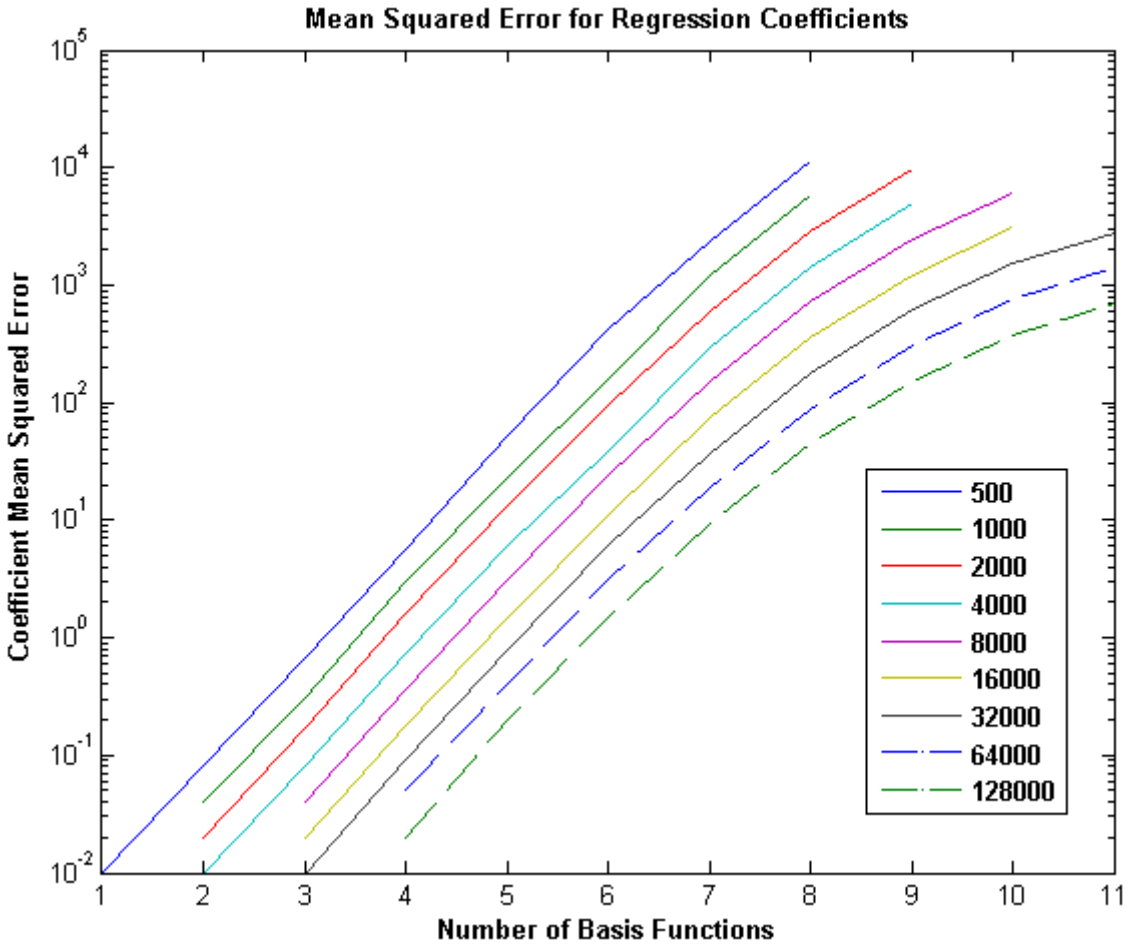


Fig 5.26– Plot of the mean squared error for the regression coefficients as a function of the number of basis functions and the number of realizations. The legend shows the number of realizations.

Conducting similar analysis on case study one would require intensive computational requirement and might not be feasible for large number of realizations (~10^5) and due to time limitations was not attempted. The results of **Bender and Steiner (2010)** and **Galsserman and Yu (2004)** were assumed to be valid because they were obtained for the LSM method. This seems to justify why the results obtained for the quarter and bi-annually decision scenarios did not vary from the benchmark yearly decision scenario because they did not converge and are not reliable. This example, illustrates a major limitation to the application of the algorithm to petroleum engineering decisions. The enhanced design of basis functions and the testing of the number of realizations that guarantee convergence are required as the discretization of the decision space (time steps) becomes finer.

Based on the findings here (from **Fig. 5.26,** using 1000 realizations produces convergent results for a total of three to four basis functions which is approximately the same as that used in the benchmark yearly case (J=4)) and on **Fig. 5.11** the results for the benchmark yearly decision scenario for the homogeneous reservoir model were assumed to be sufficiently converged. Section 5.2 further discusses basis function design for the coarse time-step case (yearly decisions).

Finer decision space discretization will not be attempted for the subsequent case studies due to the computationally prohibitive cost of running the algorithm for such cases in order to produce convergent and accurate results. This is an important aspect of the algorithm that will need further research and testing.

5.1.5.4 Mobility Control

By injecting a polymer slug post the surfactant slug, it is possible to enhance the mobility control and improve sweep efficiency. A polymer slug of size 1 PV and concentration of 3% wt. was injected after the surfactant slug. The price of polymer was assumed to follow a Uniform distribution with bounds [1,2] **(Anderson et al. 2006; Thomas 2006; Wyatt et al. 2008**). **Fig. 5.27 and Table 5.6** shows the results for including mobility control. The results show that the policy histogram exhibits a similar trend to surfactant only flooding. Although the VoF mean is positive it is less than the VoF of surfactant flooding. This is expected as there is little benefit of adding a mobility buffer in a homogeneous permeability field. The reduction in the VoF also implies the extra cost of polymer material.

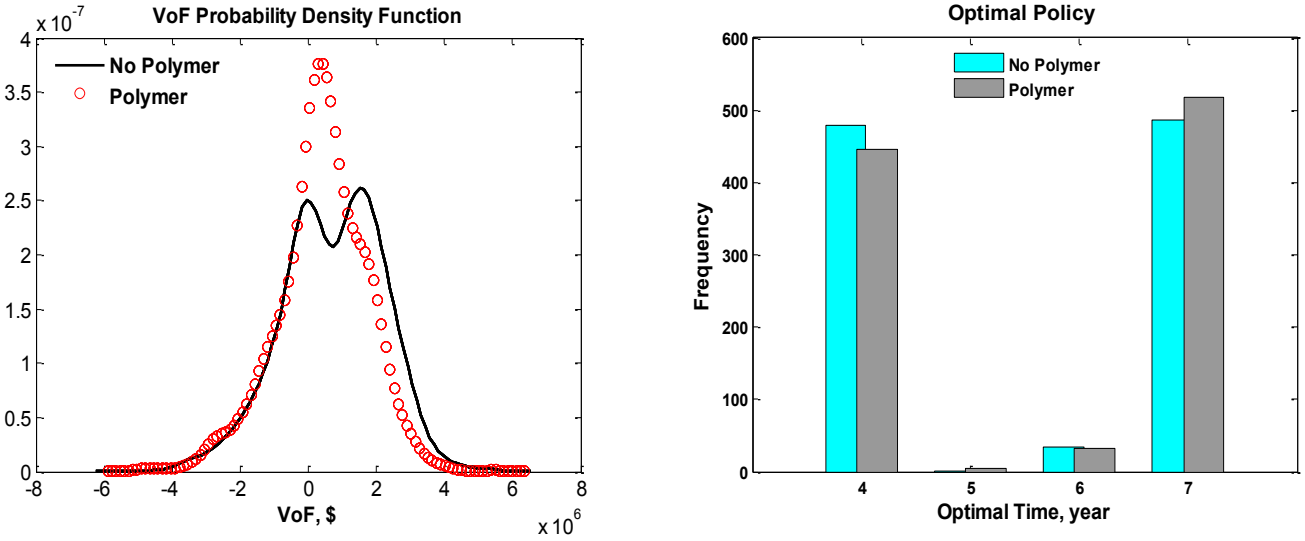


Fig 5.27– VoF PDF plot for case study 1 using mobility control.

Table 5.6– VoF mean for using mobility control.

Mobility Control	Value of Flexibility (mean, $)
No	7.15e+05
Yes	4.07e+05

5.2 Basis Function Design and Regression

For simple decision problems, the choice of basis functions can be straightforward and using different polynomials produce similar results, however, for more complex decision problems the type of basis functions can affect the results obtained (**Moreno and Navas, 2003**). Therefore it is important to perform a sensitivity analysis of the type of basis functions used in the algorithm. Also, a clustered regression approach is discussed that can correlate different types of state variables that contribute to the objective function in order to obtain the value of continuation in the LSM algorithm. This findings of this section is limited to the case of coarse decision space discretization (yearly decisions).

5.2.1 Simple Polynomials

Figures 5.28 and **5.29** show the results obtained for using first and third order polynomial of the state variables as the basis function compared with the results obtained using a second order polynomial. These polynomials did not include cross-products. **Figures 5.30 and 5.31** show results obtained using cross products. The main finding here is that there were no significant differences between these different approaches.

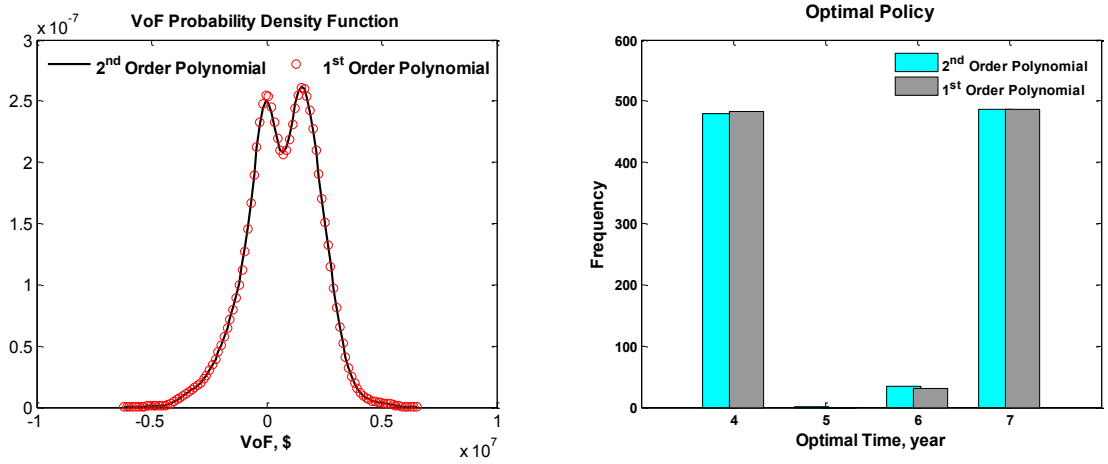


Fig 5.28– VoF PDF and optimal policy histogram using 1st order polynomial.

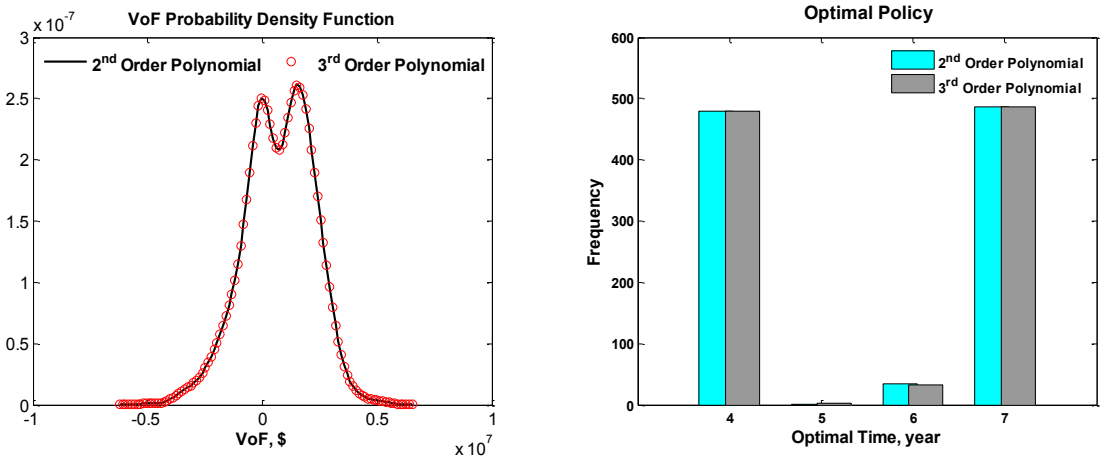


Fig 5.29– VoF PDF and optimal policy histogram using 3rd order polynomial.

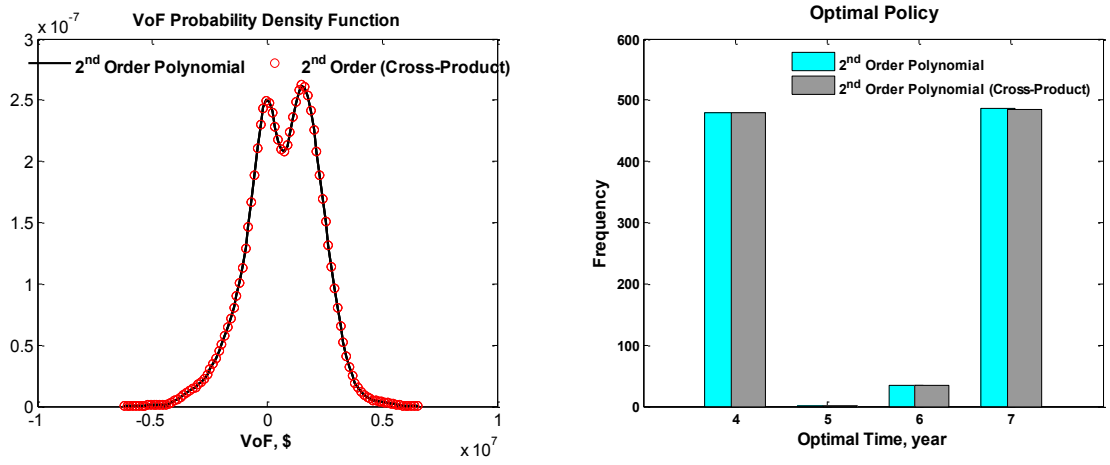


Fig 5.30– VoF PDF and optimal policy histogram using 2nd order polynomial with cross-products.

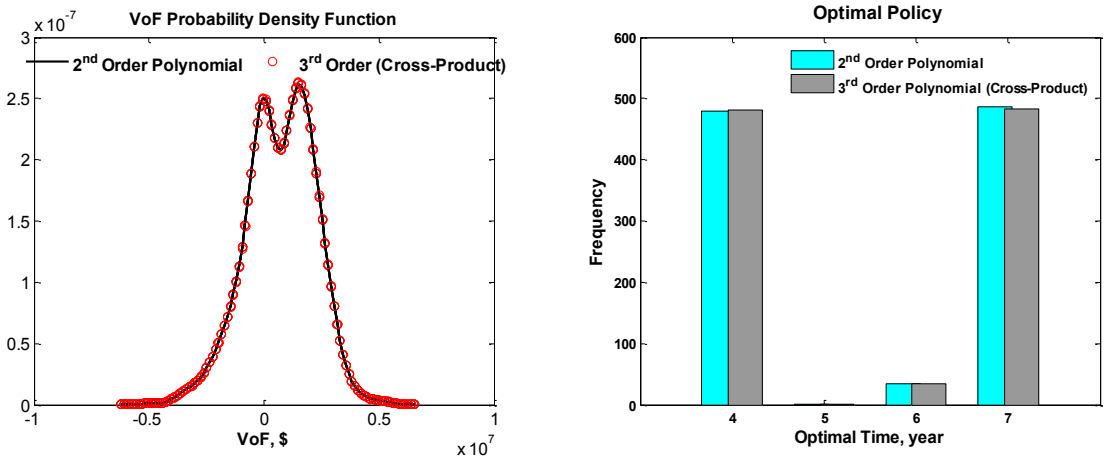


Fig 5.31– VoF PDF and optimal policy histogram using 3rd order polynomial with cross-products.

5.2.2 Orthogonal Polynomials

Another approach to designing basis functions of the state variables is to use orthogonal polynomials (**Longstaff and Schwartz 2001; Moreno and Navas 2003;Cortazar et al. 2008**). **Figures 5.32** through **5.36** show the results obtained using different orthogonal polynomials. Third order polynomials were used. For instance, the first four Laguere polynomials for both state variables are as follows:

$$L_0(y, P_{o,y}) = 1 \qquad L_0(y, P_{s,y}) = 1$$

$$L_1(y, P_{o,y}) = 1 - P_{o,y} \qquad L_1(y, P_{s,y}) = 1 - P_{s,y}$$

$$L_2(y, P_{o,y}) = \frac{1}{2}({P_{o,y}}^2 - 4P_{o,y} + 2) \qquad L_2(y, P_{s,y}) = \frac{1}{2}({P_{s,y}}^2 - 4P_{s,y} + 2)$$

$$L_3(y, P_{o,y}) = \frac{1}{6}(-{P_{o,y}}^3 + 9{P_{o,y}}^2 - 18P_{o,y} + 6) \qquad L_3(y, P_{s,y}) = \frac{1}{6}(-{P_{s,y}}^3 + 9{P_{s,y}}^2 - 18P_{s,y} + 6)$$

Combining these polynomials results in a total of ten basis functions:

$$L_0(y, P_{o,y})L_0(y, P_{s,y})$$

$$L_1(y, P_{o,y})L_0(y, P_{s,y})$$

$$L_0(y, P_{o,y})L_1(y, P_{s,y})$$

$$L_1(y, P_{o,y})L_1(y, P_{s,y})$$

$$L_2(y, P_{o,y})L_0(y, P_{s,y})$$

$$L_0(y, P_{o,y})L_2(y, P_{s,y})$$

$$L_2(y, P_{o,y})L_1(y, P_{s,y})$$

$$L_1(y, P_{o,y})L_2(y, P_{s,y})$$

$$L_3(y, P_{o,y})L_0(y, P_{s,y})$$

$$L_0(y, P_{o,y})L_3(y, P_{s,y})$$

The other orthogonal polynomials considered were weighted Laguerre, Hermite, Legendre and Chebyshev polynomials. See **Appendix B** for description of these polynomials. The results obtained using the different orthogonal polynomials produced the same results. This is because any polynomial can be expressed as a linear combination of others (**Moreno and Navas 2003**). See **Longstaff and Schwartz (2001) and Powell (2011)** for more discussion on basis function design.

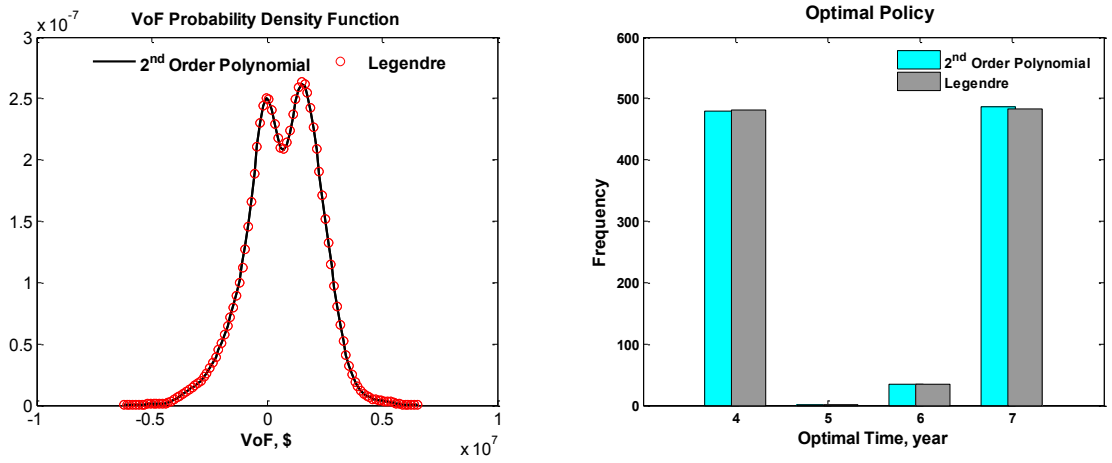


Fig 5.32– VoF PDF and optimal policy histogram using 3rd order Legendre polynomials.

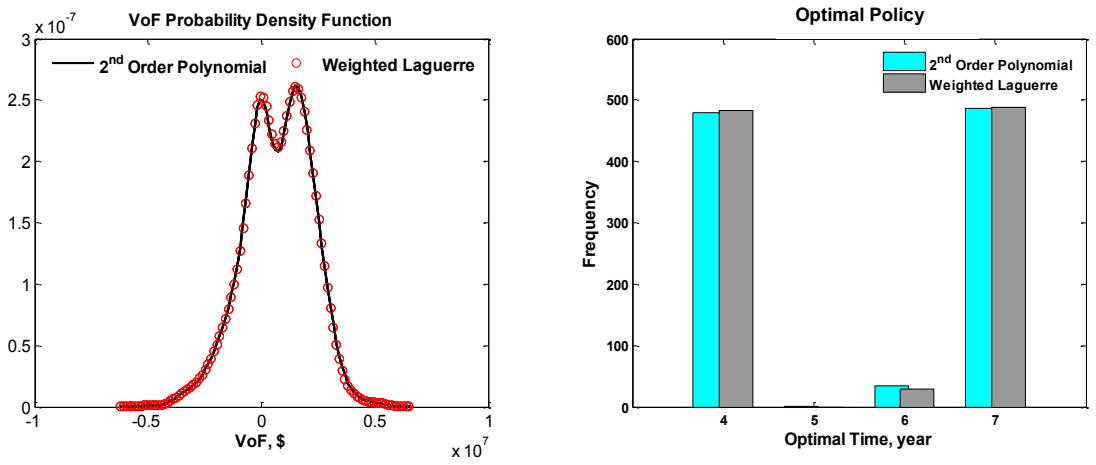


Fig 5.33– VoF PDF and optimal policy histogram using 3rd order Weighted Laguerre polynomials.

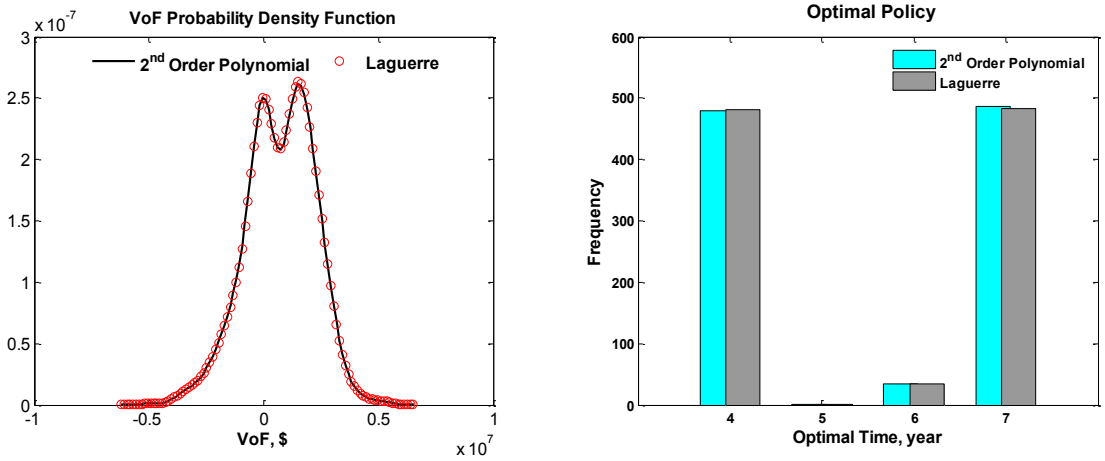


Fig 5.34– VoF PDF and optimal policy histogram using 3rd order Laguerre polynomials.

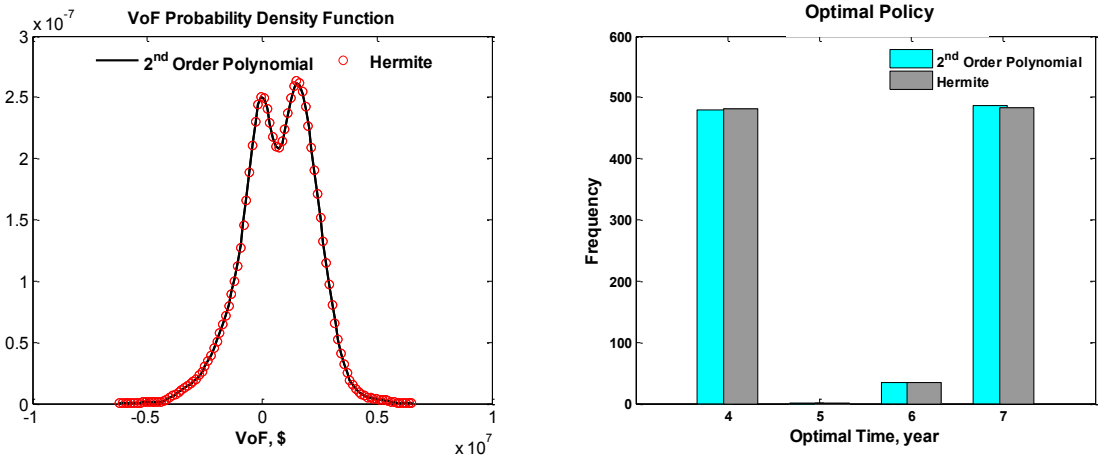


Fig 5.35– VoF PDF and optimal policy histogram using 3rd order Hermite polynomials.

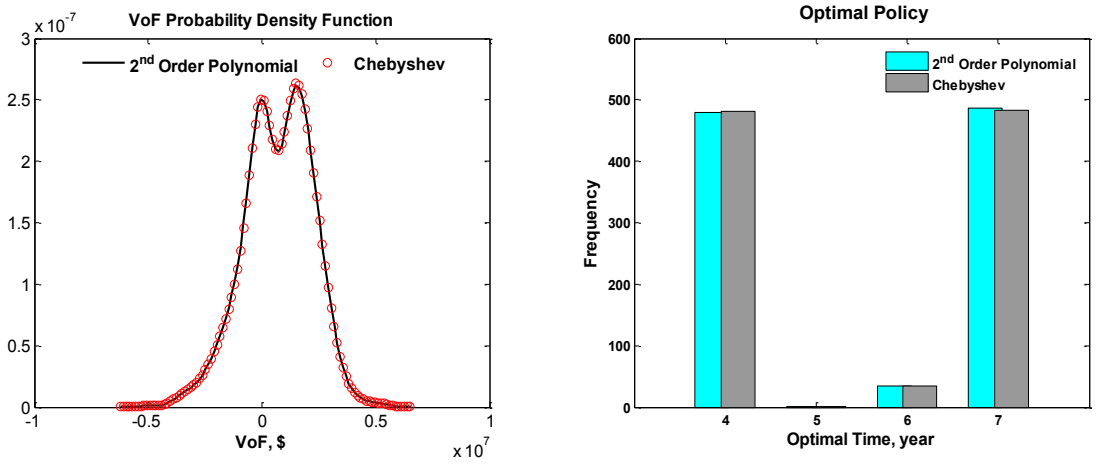


Fig 5.36– VoF PDF and optimal policy histogram using 3rd order Chebyshev polynomials.

5.2.3 Clustered Linear Regression

Since the technical and economic state variables are separate and the objective function is directly dependent on $\mathbb{P}_i$ and indirectly on $\mathbb{T}_i$, a clustering strategy **(Powell 2011)** is used to relate the objective function to $\mathbb{T}_i$ variables when approximating the continuation value via linear regression. It was found that the objective function is most sensitive to the surfactant adsorption rate, T_{D_s}, exhibiting a strongly nonlinear relationship which might not be captured effectively in the regression without clustering. Whereas the residual saturation, $T_{S_{orc}}$, exhibits a linear trend with the objective function, therefore clustering based on this variable might not be necessary for the regression process. See **Fig**. **5.37** for clustering based on surfactant adsorption and **Fig. 5.38** for clustering based on residual saturation. A set of clusters C^n based on n observations of states and values is obtained and a regression function $\nu(\vartheta_{y_n}|c)$ is fitted for each cluster $c \in C^n$. For example, a second order basis function (assuming J=4, which is used in this study) would take the following form:

$$\nu(\vartheta_{y_n}|c) = \alpha_0(c){P^2}_{o,y_n} + \alpha_1(c)P_{o,y_n} + \alpha_2(c){P^2}_{s,y_n} + \alpha_3(c)P_{s,y_n} + \alpha_4 \qquad \text{Eq. 5.7}$$

, where ϑ_{y_n} is the set of state variables at time y_n, $\vartheta_{y_n} = (\mathbb{P}_{i,y_n}, \mathbb{T}_i)$, $\{\alpha_i\}$ is the set of coefficients. C^n in this study was set to $\{c_1, c_2, c_3, c_4\}$, where $c_1$are the observations when $T_{D_s} < 10^{-5}$ g/g rock, $c_2$are the observations when $10^{-5} < T_{D_s} < 10^{-4}$ g/g rock and $c_3$are the observations when$10^{-4} < T_{D_s} < 10^{-3}$ and c_4 are the observations when $T_{D_s} > 10^{-3}$ g/g rock. From the results in **Fig. 5.38 (Fig. 5.39** shows the results obtained with clustering on residual saturation), a significant shift in the policy histogram is observed. This translates to a higher VoF. This indicates that by using clustering regression approach, it is possible to capture the technical and economic state variables that influence the objective function. See **Table 5.7** for the mean VoF of clustering on adsorption or residual saturation compared with the original regression approach.

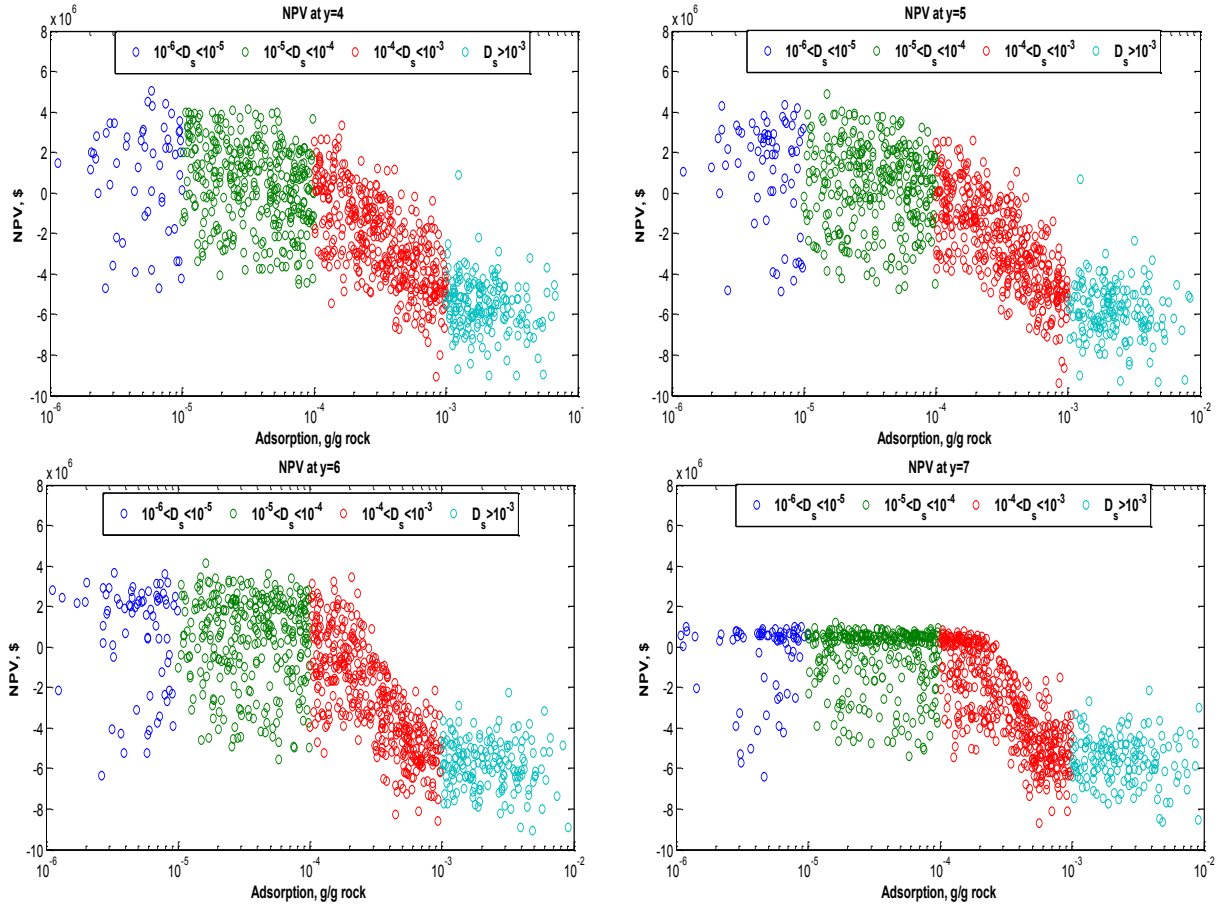


Fig 5.37— Cross-plot of NPV for surfactant injection for different policies as a function of adsorption. The data is separated into four different clusters.

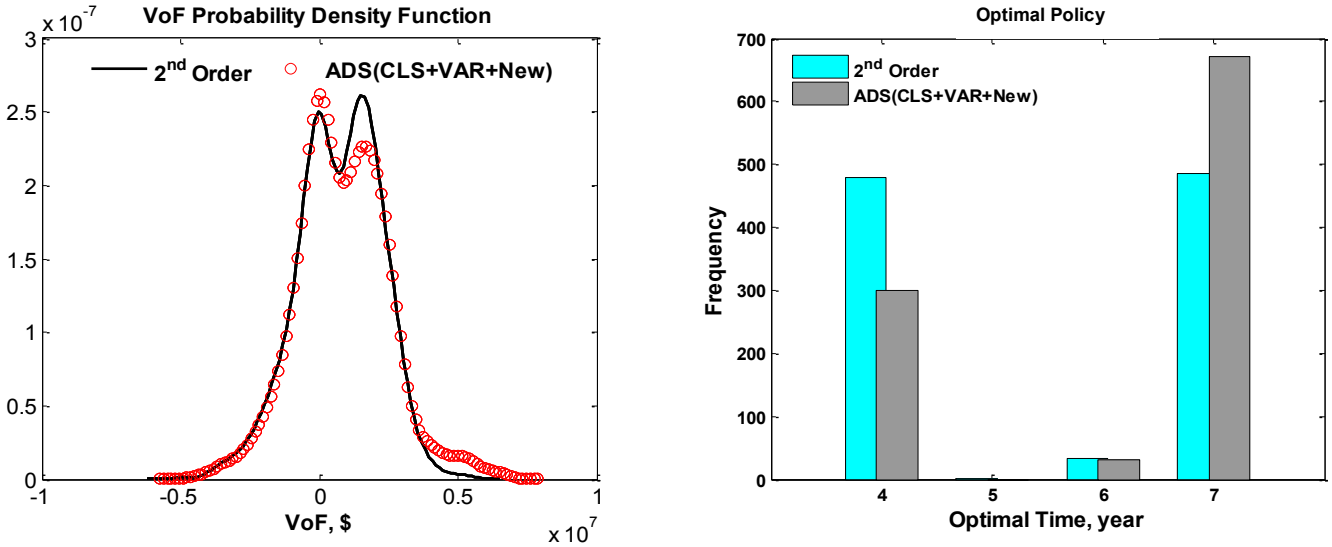


Fig 5.38— VoF PDF and optimal policy histogram for results determined by using dynamic clustered regression based on adsorption.

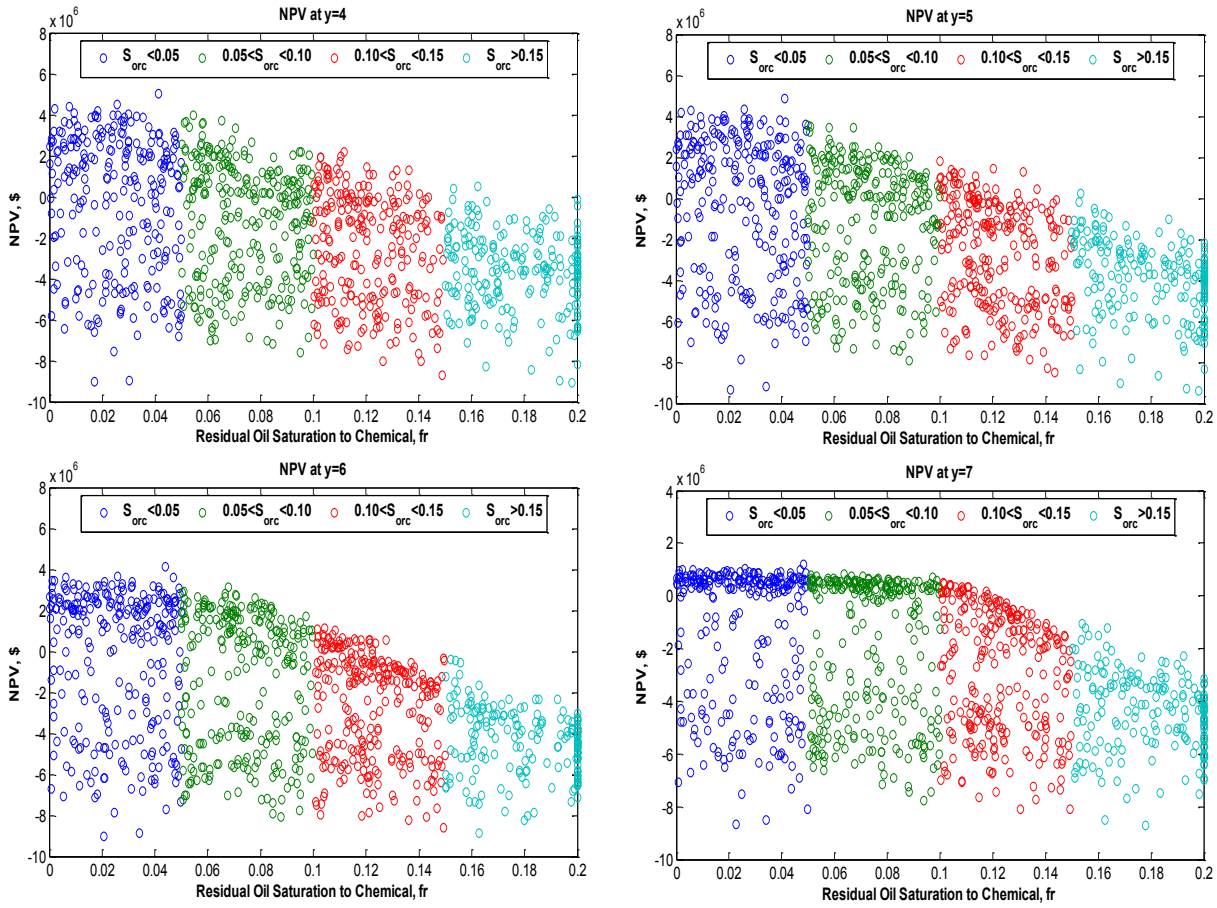


Fig 5.39– Cross-plot of NPV for surfactant injection for different policies as a function of residual oil saturation to chemical flooding. The data is separated into four different clusters.

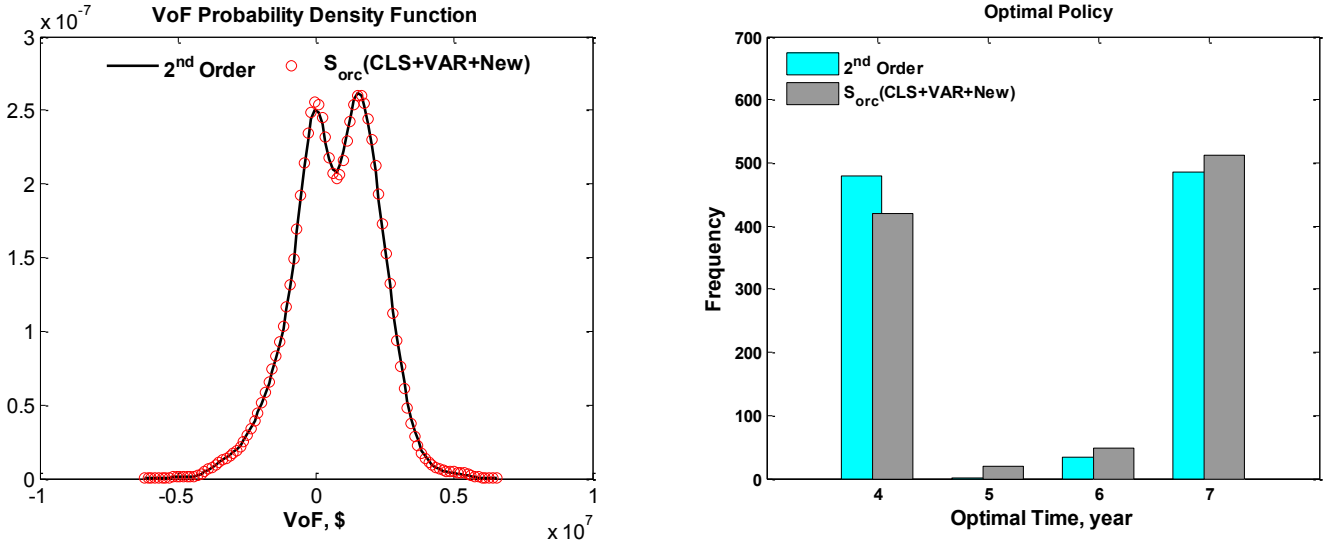


Fig 5.40– VoF PDF and optimal policy histogram for results determined by using dynamic clustered regression based on residual saturation.

Table 5.7– VoF mean obtained for the original and clustered regressions.

Basis Function type	Value of Flexibility (mean, $)
Original (no clustering)	7.15e+05
Clustering on D_s	8.51e+05
Clustering on S_{orc}	7.06e+05

5.3 **Application: Case Study 2**

This case study applies the LSM method to a two-dimensional reservoir models based on Layers 1of the SPE10 model (**Christie and Blunt 2001**) adapted to a 2.02E4 m^2 (5-acre) quarter five-spot pattern with a thickness of 7.62 m^2 (25ft). The fluid data used was that of the homogeneous model (see **Appendix A**). Heterogeneity is assumed to be an exogenous source of uncertainty and that it too evolves through time with our evolving state of information. It was assumed that the fine (60×220) model is realized at the last decision node (y=7) onwards. Going back in time, the model is upscaled at each decision node (y= 6, 5 and 4) until the first decision node at y=4 for which the realization is kept constant until the start of the field life.

Fig. 5.41 shows the evolution of heterogeneity with time in natural logarithm of permeability in millidarcy. The permeability fields evolve and take more details moving from left to right. In designing an artificial increase in detail, a reverse upscaling procedure is applied. The original geologically detailed model represents the most evolved state of permeability (at rightmost panel of **Fig. 5.41**). For the next step, an absolute upscaling permeability is performed on 60×220 grid layout to coarsen the model to 30×110 grid. A refining stage then maps the new layout back to 60×220 grid. This stage is performed simply by replacing each cell with four cells of similar values for permeability. This procedure was then continued to 15×55 and 6×22 grids. The upscaling procedure used here is the Pressure-Solver Method (**Warren and Price 1961; Begg et al. 1989**). A simple procedure is used to calculate the simulation gridblock equivalent permeabilities with only diagonal elements in the tensor. This is achieved by inverting a fine pressure solution that is calculated locally over the domain of each simulation coarse gridblock. For layer 1 of SPE10 model, the simulation results of upscaled model by a directional pressure solver method are of relatively good quality compared to the fine scale simulations. This is due to the smoothness of variation of permeability field for this layer. For such layers, the results of application of the most common upscaling methods (for example harmonic-arithmetic mean and renormalization method) are essentially identical to the Pressure-Solver Method and are equally satisfactory (**Alkhatib et al. 2013**).

From another perspective, as shown in a comparison study of several upscaling methods in **Babaei and King (2012)**, the upscaling errors of the directional Pressure-Solver Method for more heterogeneous layers can be significantly higher. In such circumstances, other advanced upscaling methods are required to prevent the upscaling error from undermining the reliability of the upscaled models. In other words, there will be additional scale related uncertainties in use of the models at different stages of upscaling or reverse upscaling. What is desired here is to have an accurate increase in detail in reservoir heterogeneity, or a fine scale model that matches with coarse scale. **Fig. 5.42** shows sample production profiles for the first five paths (realizations) for surfactant injection at the beginning of the 4th year and for path 1 for surfactant

injection under all scenarios. From both figures the difference in recovery factors is more pronounced, as is expected, when compared with the homogeneous model (**Alkhatib et al. 2013**).

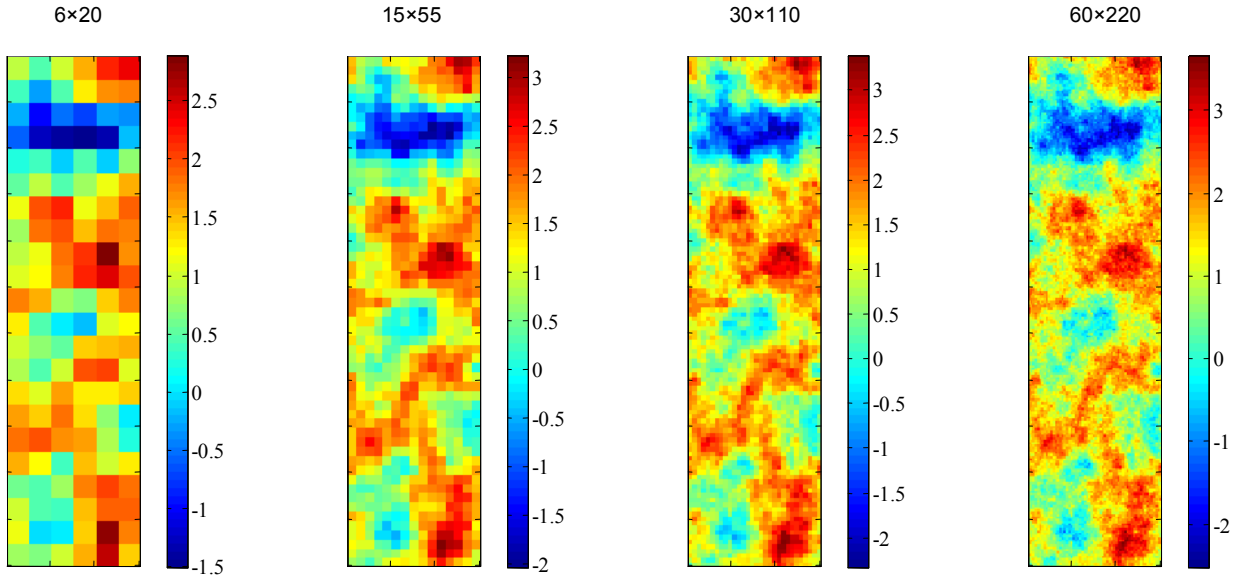


Fig. 5.41[22]— Heterogeneity variation with time, with the far left showing the coarsest realization and the far right showing the finest realization of the permeability field.

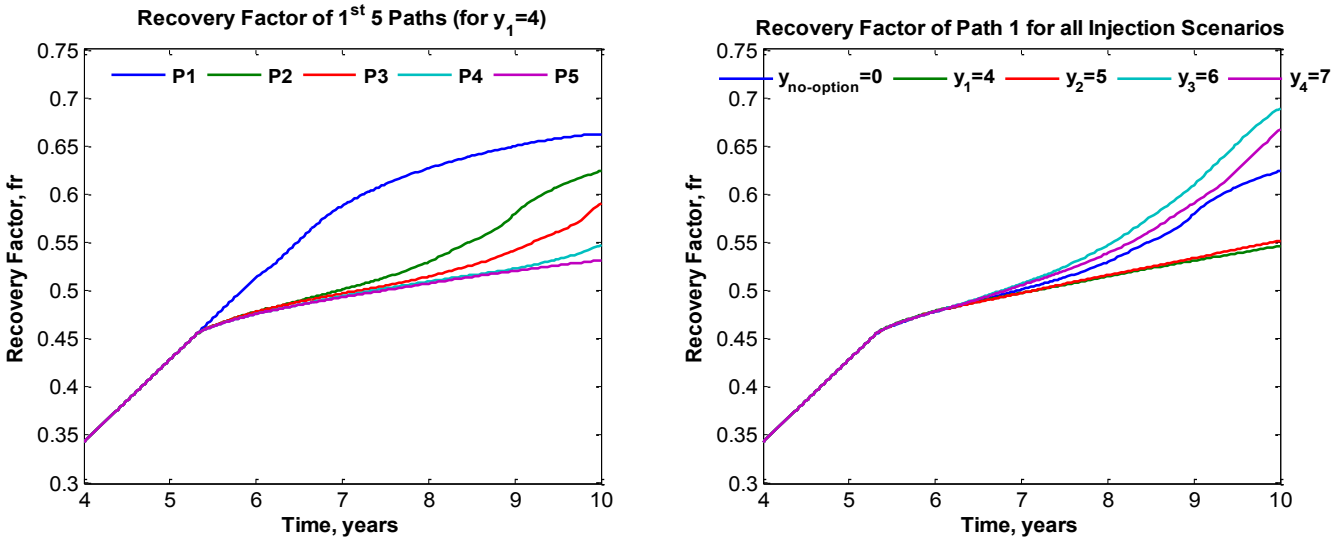


Fig. 5.42[23]— Production profiles for case study 2.

[22] Reproduced from **Alkhatib et al. (2013)**.
[23] Reproduced from **Alkhatib et al. (2013)**.

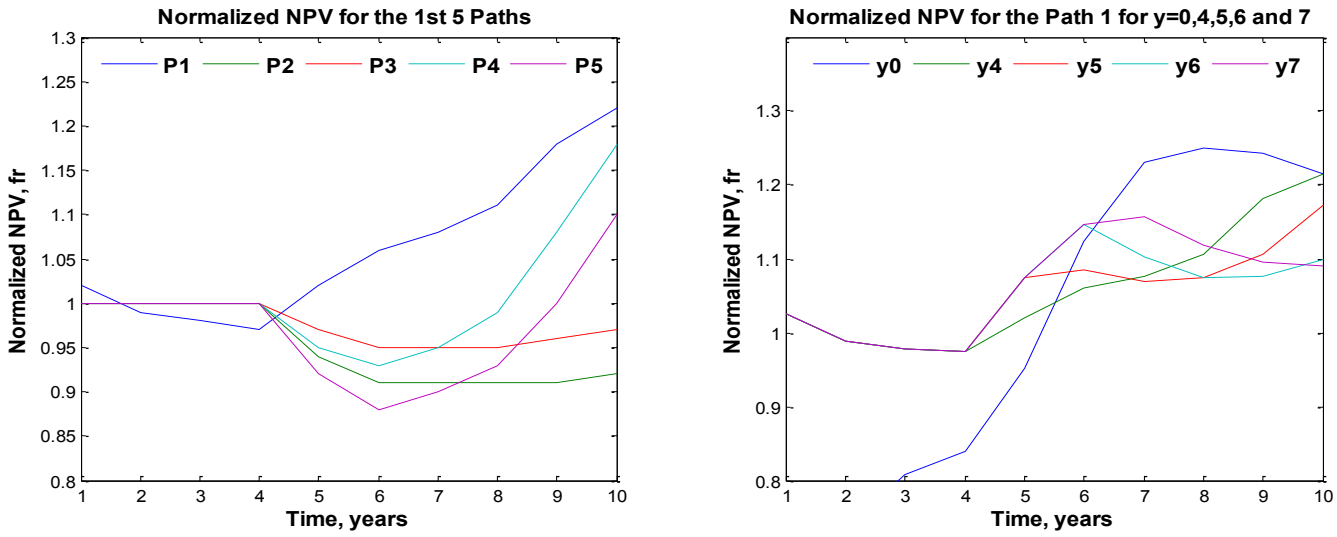


Fig 5.43[24]– Normalized NPV for the case study 2.

The results obtained for case study 2 are shown in **Fig. 5.44**. The optimal policy histogram shows that surfactant injection at y=4 is optimal for most realizations. Furthermore, the VoF PDF plot shows that it lies mostly in the negative region thus flexibility is not beneficial for most realizations. This suggests that the permeability field for this case study supports surfactant injection at the earliest possible time. The main reason for flexibility not being as beneficial in this reservoir model is the effect of channeling on the propagation of the surfactant bank through the reservoir. Consequently, we tend to get more channeling from the injector to the producer which translates into more unswept oil, or in other words poorer sweep efficiency. This allows the surfactant to travel through these high permeable channels and to not contact all the remaining oil.

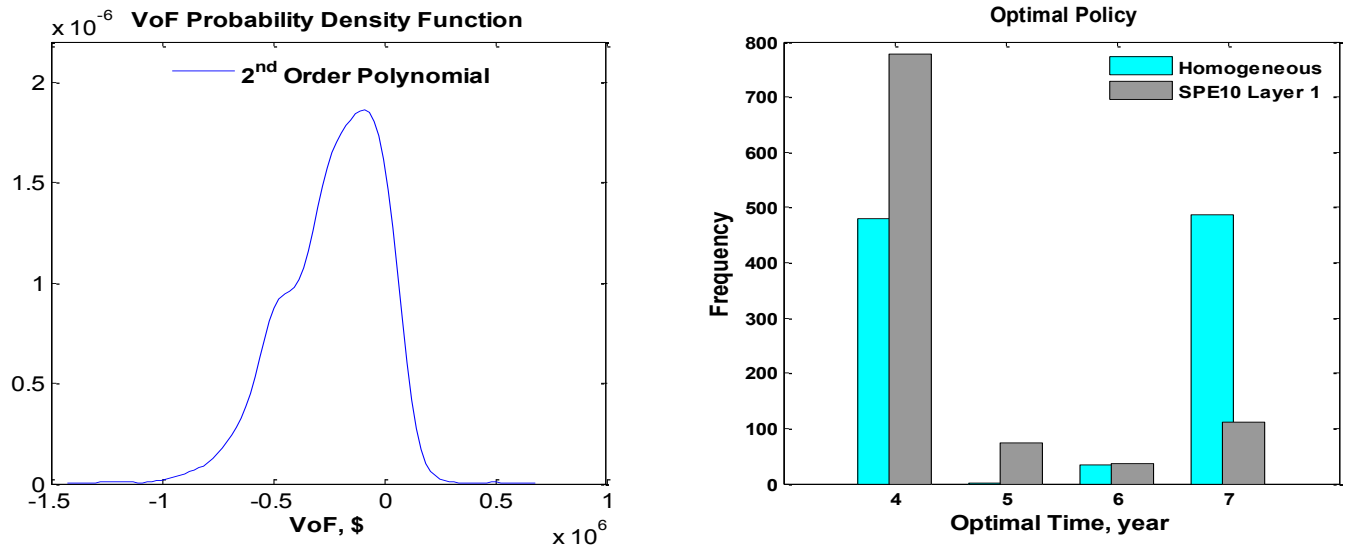


Fig 5.44– VoF PDF plot and optimal policy histogram for case study 2.

[24] Reproduced from **Alkhatib et al. (2013)**.

The effect of heterogeneity is clear in this case study. Furthermore for this specific permeability realization (layer 1), flexibility is not as beneficial as it was found in the previous case study. The following subsection discusses the factors that affect the performance of the LSM method with respect to heterogeneity.

By qualitatively comparing the results of the heterogeneous case with those obtained for the homogeneous case, it can be found that the conclusions regarding adding the mobility buffer, varying the static policy scenario and the discretization of the decision space might not remain valid for the heterogeneous case. It is anticipated that by adding mobility buffer, this will improve the performance of the surfactant flood and increase the VoF. This is discussed in the next section. As for the effect of varying the static policy scenario, this is thought to be reservoir unique so the findings for the homogeneous case will not be necessarily reproduced for the heterogeneous case.

The findings for the homogeneous case regarding the convergence of the VoF, basis function design and the use of clustering are thought to remain valid for the heterogeneous case because they are algorithm focused and will not be affected by changing the permeability field.

5.3.1 Mobility Control

To mitigate the effect of channeling on the propagation of the surfactant bank through the reservoir, a polymer mobility buffer is required. **Fig. 5.45** shows the results for using mobility control. **Table 5.8** shows the mean VoF (see **Appendix A** for polymer data). The improvement in VoF is clear. By mitigating the effect of channeling and maintaining the integrity of the surfactant bank, having flexibility in initiating the EOR process is beneficial for SP flooding. The policy histogram exhibits a similar trend to surfactant-only flooding.

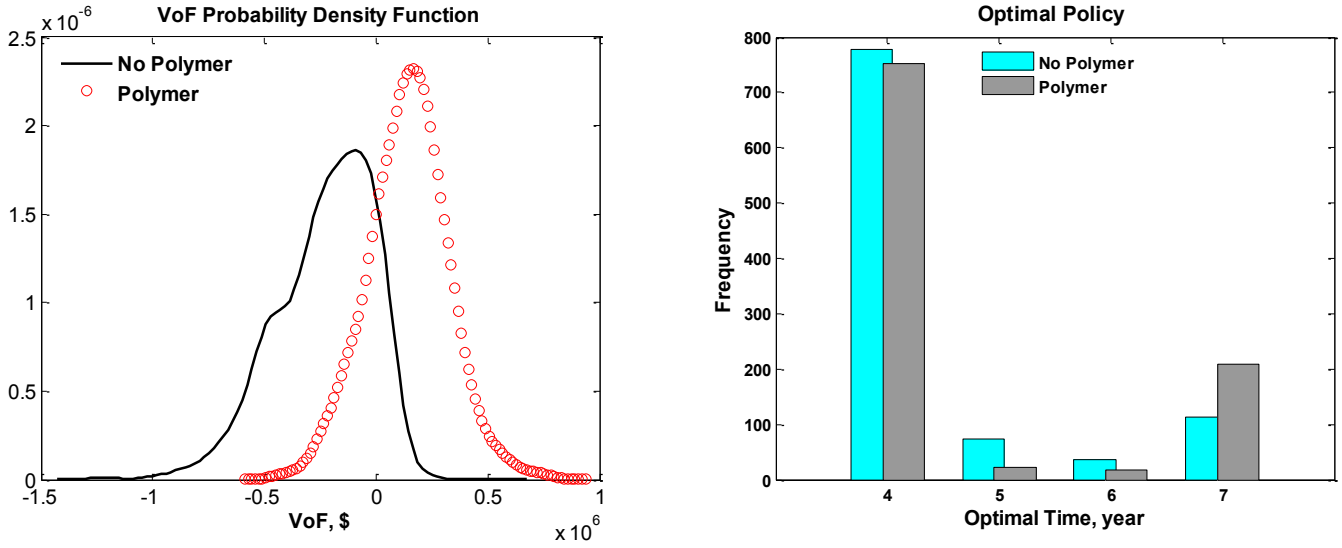


Fig 5.45– VoF PDF plot and optimal policy histogram for case study 2 with mobility control.

Table 5.8– VoF mean for case study 2 using mobility control.

Mobility Control	Value of Flexibility (mean, $)
No	-2.28e+05
Yes	1.42e+05

5.3.2 Well Placement

One of the factors that could influence the effect of channeling is well placement. **Fig. 5.46** shows the results obtained for using different well placements as illustrated in **Fig. 5.47**. A unique VoF PDF is obtained for each well placement. Although the policy histograms show the same trend, **Table 5.9** shows that VoF varies widely using different well placements. The results also show that the original well placement used produces the most optimal result.

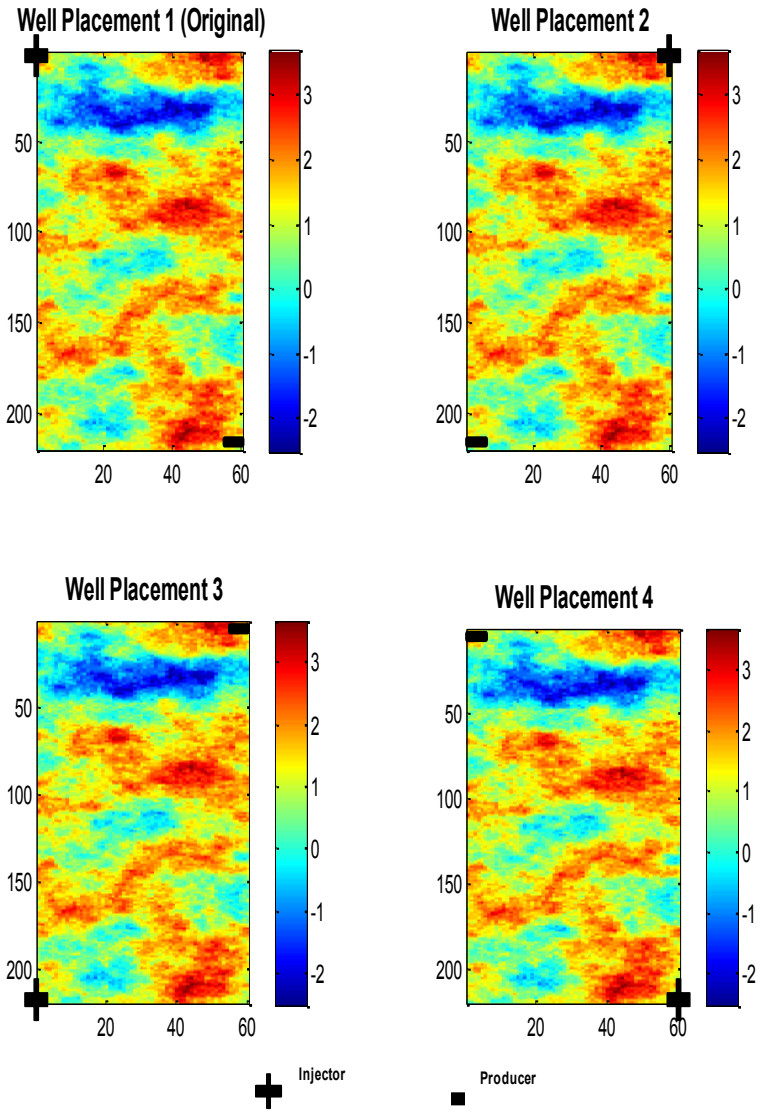


Fig 5.46– Well placements for case study 2.

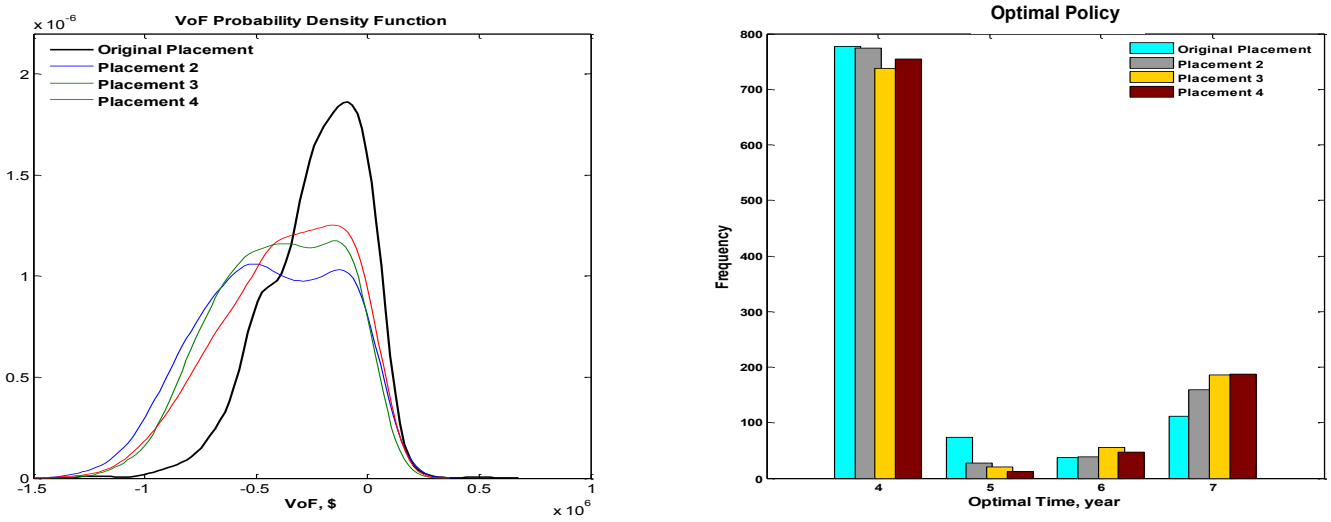


Fig 5.47— VoF PDF plot and optimal policy histogram for case study 2 using different well placements.

Table 5.9— VoF mean for case study 2 using different well placements.

Well Placement	Value of Flexibility (mean, $)
Original	-2.28e+05
Placement 2	-4.31e+05
Placement 3	-3.99e+05
Placement 4	-3.70e+05

5.3.3 Permeability Field

To accentuate the effect of heterogeneity on VoF, the LSM algorithm was applied to other layers of the SPE10 model using the same assumptions used for layer 1. The different layers are illustrated in **Fig. 5.48**. The results are shown in **Fig. 5.49**. The permeability field of layer 10 was found to produce the highest VoF compared to the other layers. The VoF PDF and policy histograms show a unique response for each reservoir model.

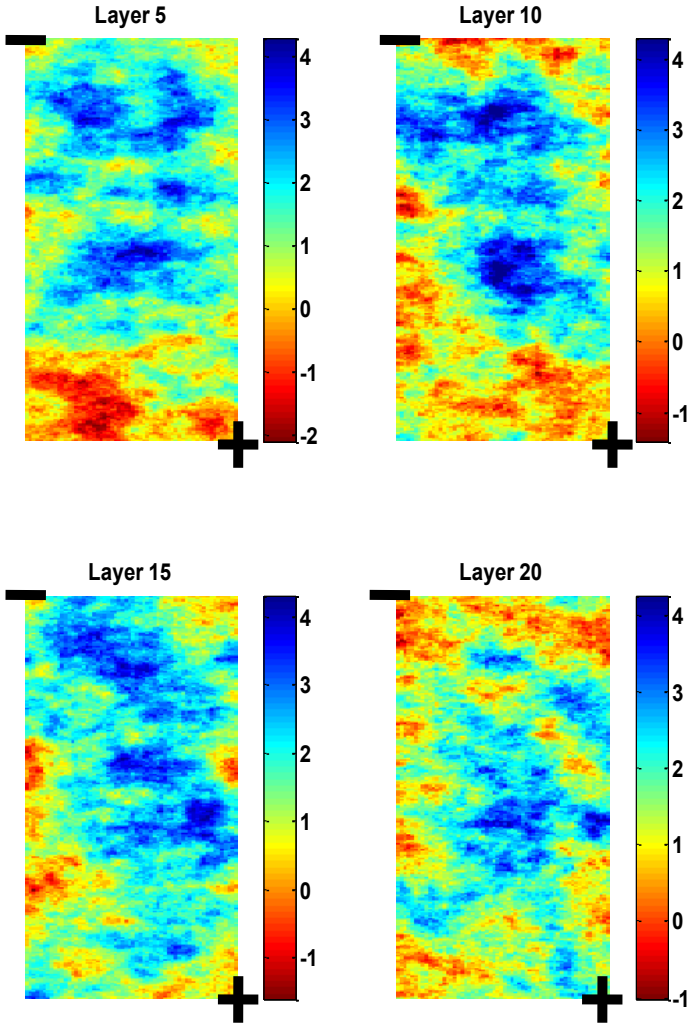


Fig 5.48– Permeability fields for layers 5,10, 15 and 20 of SPE10 model. The well placement is also shown. Logarithmic scale is used for permeability values.

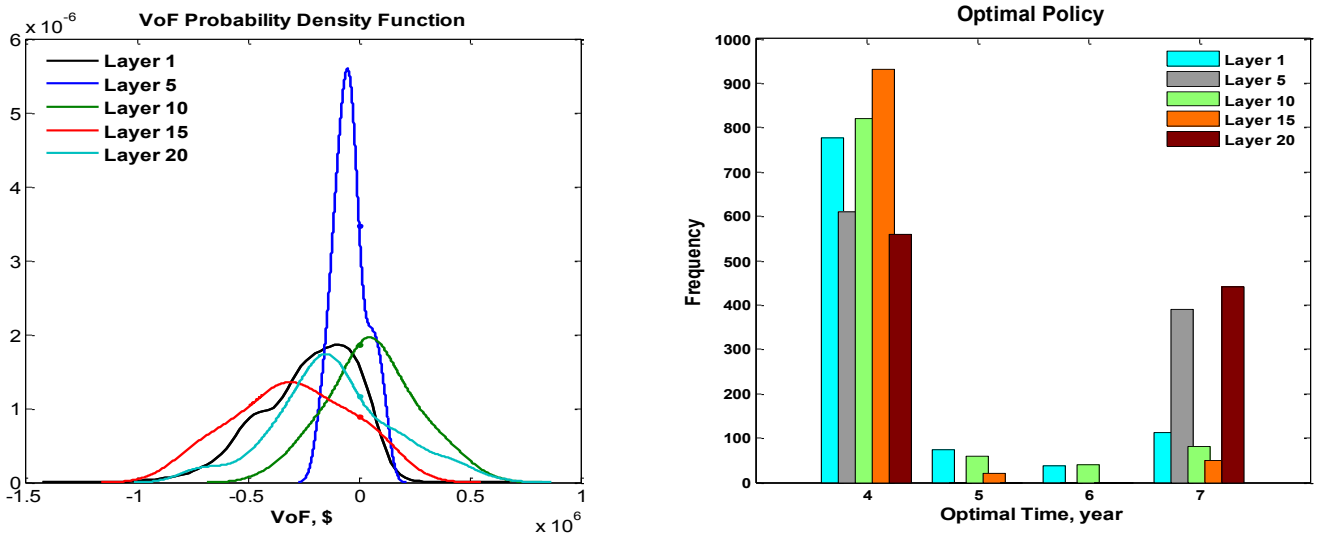


Fig 5.49– VoF PDF plot and optimal policy histogram for case study 2 using different permeability fields.

Table 5.10– VoF mean for case study 2 using different permeability fields.

Layer	Value of Flexibility (mean, $)
1	-2.28e+05
5	-3.93e+04
10	6.11e+04
15	-2.98e+05
20	-1.10e+05

The general relationship between well placement and the heterogeneity structure on the results is illustrated. Because this relationship affects the channeling in the reservoir, other heterogeneous reservoir models produce different results compared with those produced by the layer 1. Furthermore, using other well placement patterns such as line drive or using horizontal wells could also produce different results. Because the control variables (e.g. surfactant concentration, surfactant slug size… etc) were fixed these case studies, it is possible that if these variables were to vary we would obtain different results for the heterogeneous model. However, by adding different control strategies this would increase the computational requirements of applying the algorithm as more reservoir simulations would be required.

5.3.4 Summary

After applying the LSM method to a two-dimensional heterogeneous reservoir model, it is necessary to review the significance of the different results obtained. First, the importance of a mobility buffer to support the propagation of the surfactant slug was demonstrated. The VoF was enhanced for SP flooding compared with surfactant flooding. It is also clear that the LSM method would produce reservoir model unique results. This was shown by comparing results from different two-dimensional heterogeneous models. In this section, we considered only uncertainty in the time series of the permeability field by implementing a sequential upscaling of the reservoir model and assuming that the fine (original) model is realized at the latter decision nodes. It is important to consider the stochasticity of heterogeneity. This is discussed in the next section using two approaches: Gaussian and multiple-point statistics generated permeability fields.

5.4 Uncertainty in Heterogeneity

In this section, the LSM method is applied to SP flooding where a surfactant slug is injected and is followed by a mobility buffer. Two additional technical uncertainties are also incorporated: the viscosity multiplier effect (V_p) and polymer adsorption (D_p). The V_p in ECLIPSE controls the viscosity increase that is achieved by the addition of polymer. This is based on a Newtonian approach to polymer viscosity (**Schlumberger 2011**). V_p is assumed to follow a uniform distribution, $U\sim(1,10)$, where 1 is equivalent to no viscosity enhancement (i.e. viscosity will equal water viscosity) and the upper bound is equivalent to an enhancement of viscosity by 10 times that of water viscosity. D_p and D_s are assumed to follow a log-normal distribution, $\text{Ln } N\sim(-8,1)$. S_{orc} is assumed to follow the same distribution as in the previous case studies. Both parameters were assumed to vary with time similar to S_{orc} and D_s. D_p uses the same range adjustment parameters for D_s while V_p uses the same parameters as S_{orc}. Inverted five-spot pattern was used for both approaches. The reservoir and fluid data used was that of the SPE10 model (**Christie and Blunt 2001**). See **Appendix C** for the reservoir and constraint data used. The surfactant slug was assumed to have a concentration of 3% wt. and size 0.1 PV. The mobility buffer assumes a polymer concentration of 3% wt. and size 1 PV. The injection and production constraints are shown in **Appendix C**. The decision evaluated is also a timing decision similar to that analyzed in the previous case studies. However, the field life is extended to 15 years and the decision set is altered to $y_n = [5,7,9,11]$.

5.4.1 Moving Average Method

The moving average method is used to generate stochastic Gaussian two-dimensional permeability field realizations. First, a random two-dimensional field is generated using a normal distribution realization for each cell of a Cartesian grid. This is an uncorrelated field. Then these cells are averages using a moving circle technique (**Wallstrom et al. 1999**). Thus a new grid is then generated where each cell value is an average of the permeability values from the uncorrelated grid within a specific radius around the cell in the original grid. The radius of the circle used in the averaging approach defines the correlation length. Using a correlation length of 40 and starting with an initial random grid of 240x240, a correlated permeability grid of size 120x120 is obtained. See **Fig. 5.50**.

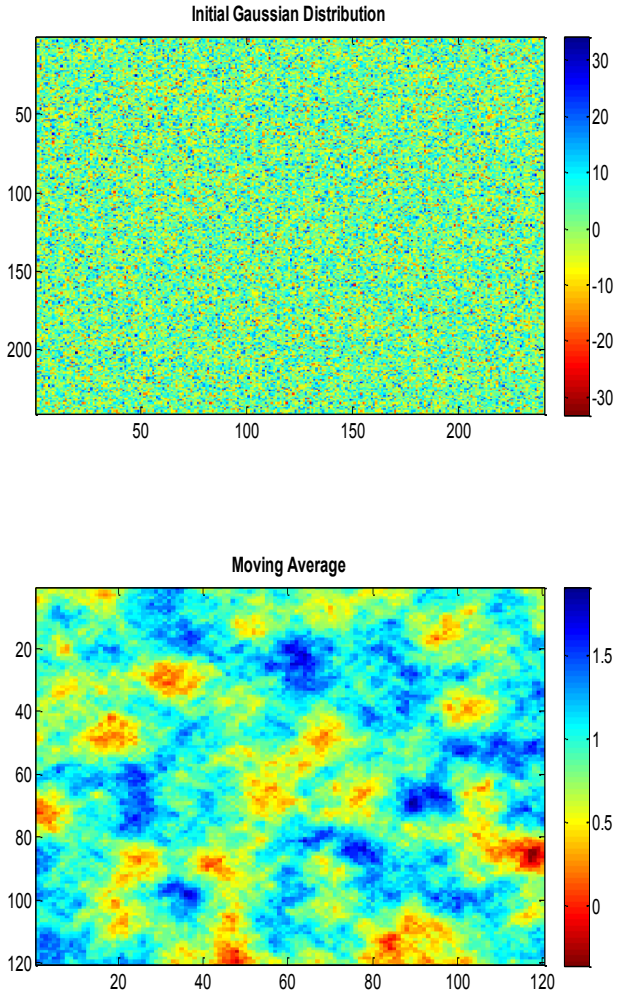


Fig 5.50— Uncorrelated and correlated permeability grid obtained using the moving average method. The scale for the correlated grid is logarithmic.

Heterogeneity was also assumed to vary with time. This was modeled by using a similar approach to pressure solver method used for case study 2. Here the renormalization method (**King 1989**) was applied to produce sequential upscaled models. **Fig. 5.51** shows the evolution of heterogeneity with time in terms of natural logarithm of permeability in millidarcy and **Fig. 5.52** shows the well placement. The permeability fields evolve and become finer in detail moving from left to right. The original geologically detailed model represents the most evolved state of permeability (at rightmost panel of **Fig. 5.51**). Then, an absolute upscaling permeability is performed on the 120×120 grid layout to coarsen the model to 60×60 grid. Then the new layout is mapped back to a 120×120 grid. This stage is performed by substituting each cell with four cells of similar values for permeability. This procedure was used to produce the 30×30 and 15×15 grids.

The renormalization approach is a well-known permeability upscaling method that uses an explicit formula to substitute for a 2×2 grid cells with permeabilities $\{k_1, k_2, k_3, k_4\}$ by an equivalent permeability $\mathbf{k}*$:

$$k^* = \frac{2(k_1+k_2)(k_3+k_4)(k_{12}+k_{34})}{3(k_1+k_3)(k_2+k_4)+\frac{1}{2}(k_1+k_2+k_3+k_4)(k_{12}+k_{34})} \quad \text{Eq. 5.8}$$

, where $k_{12} = \frac{2k_1k_2}{(k_1+k_2)}$ and $k_{34} = \frac{2k_3k_4}{(k_3+k_4)}$ .Both the moving average and renormalization methods were coded using MATLAB.

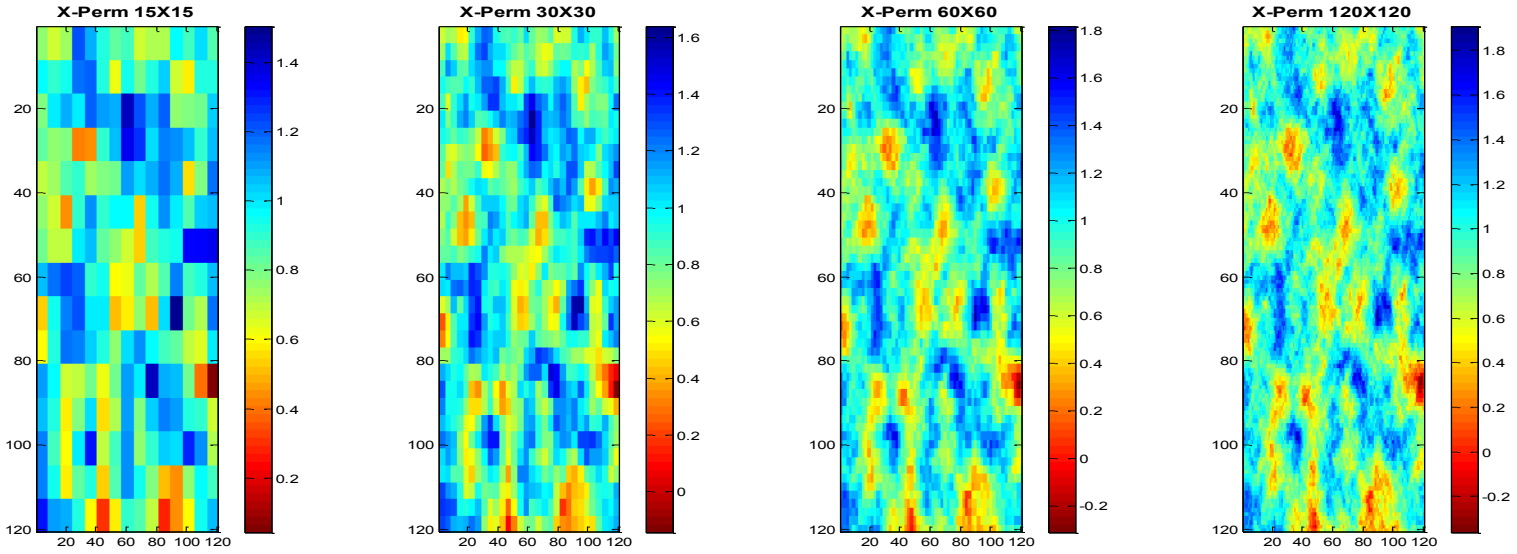


Fig. 5.51— Heterogeneity variation with time, with the far left showing the coarsest realization and the far right showing the finest realization of the permeability field. The scale is logarithmic.

When applying the LSM method, a unique permeability field sample is realized for each path. For a run of 10^3 paths, 10^3 permeability field realizations are obtained. The results are shown in **Fig. 5.53**. Flexibility is valuable for most realizations (VoF is positive) and the optimal policies show that most realizations favour SP flooding at y=6. In addition, **Fig. 5.53** and **Table 5.11** shows the results of assuming that heterogeneity does not vary with time where the fine scale realizations (120x120) is used for the duration of the simulation run. The results show that the VoF is shifted to the left indicating that the mean VoF is less than the mean VoF of varying heterogeneity with time. If it assumed that the fine scale model is the near "true" realization of the permeability field for each path (i.e. for each LSM realization), then the results illustrate how the initial assumptions of reservoir characterization could affect decision making. In this case, it was found that VoF was over optimistic in comparison with the "true" realization. Furthermore, there is also a clear discrepancy in the optimal policy histogram.

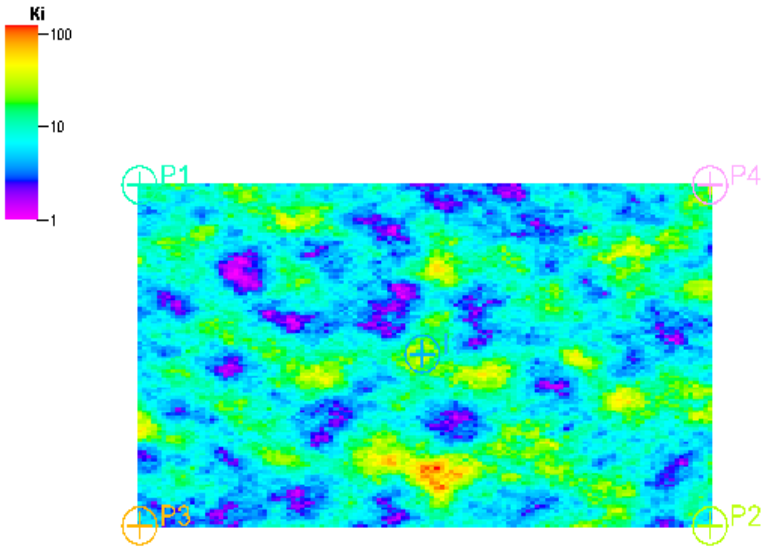


Fig. 5.52— Inverted five-spot pattern that is used for reservoir models obtained via the moving average method.

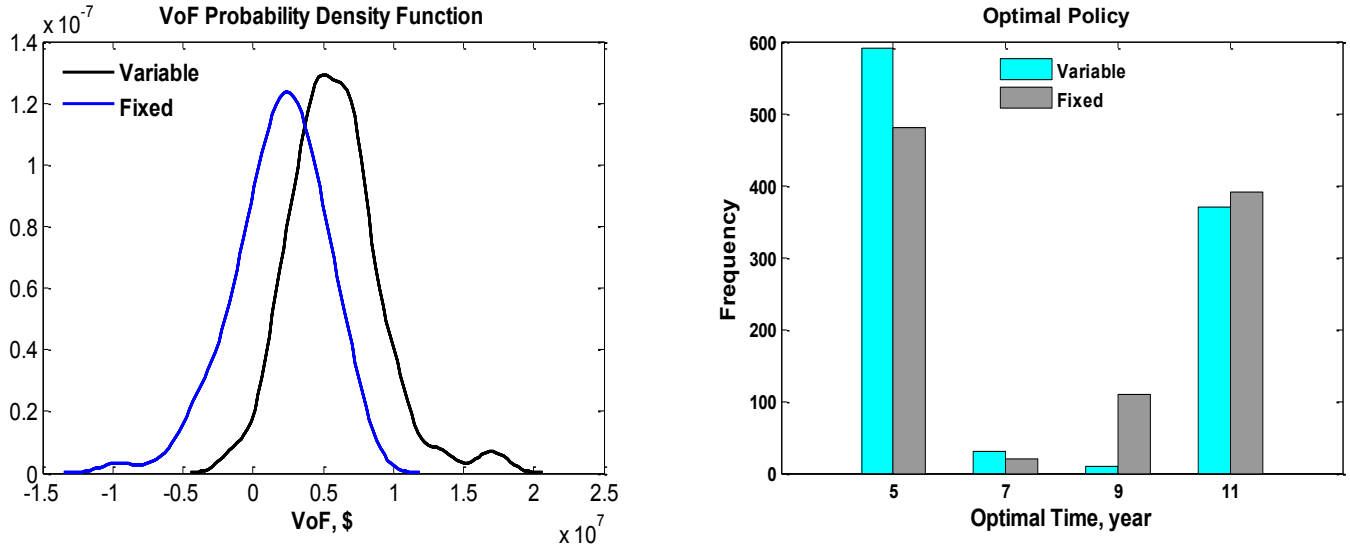


Fig. 5.53— VoF PDF and policy histogram for the moving average permeability realizations with renormalization with time. The results for fixed heterogeneity with time (fine scale constant through time) were also added for comparison.

Table 5.11— VoF mean for moving average generated permeability.

Heterogeneity with Time	Value of Flexibility (mean, $)
Variable	5.80e+06
Fixed	1.90e+06

5.4.2 Multiple-Point Statistics

In the previous subsection, a Gaussian stochastic approach was used to generate the two-dimensional permeability fields. This approach is sufficient for generating random permeability fields although it does not reproduce the main patterns of a

reservoir. For this purpose, multiple-point geostatistical methods can be used. The Stanford Geostatistical Modeling Software (SGeMS) was used to generate these realizations. This is an open source library (**SGeMS 2012**). SGeMS was incorporated with the LSM code by using the MATLAB routines developed by **Hansen (2011)** that allow for SGeMS to be called from MATLAB. There are two main multiple-point methods: single normal equation simulation (SNESIM) (**Guardiano and Srivastava 1993; Strebelle 2002**) and filter-based algorithm (FILTERSIM). The SNESIM approach reads the conditional distributions from a training image. The main disadvantage of this method is that it requires a richly detailed training image (**Remy et al. 2011**). The FILTERSIM algorithm mitigates this requirement by accepting approximate replicates of the conditioned data event (**Remy et al. 2011**). This algorithm classifies local patterns present in the training image into a reasonable number of similar looking patterned bins. FILTERSIM performs this classification using linear filters that are applied to the pixel data set that defines the pattern (**Schneiderman and Kanade 2004**). FILTERSIM is useful when a large number of categorical variables (>4) are desired to be simulated jointly, whereas SNESIM is best used for a reasonable (small) number of categories are present given the availability of a large and varied training image (**Remy et al. 2011**).

It was desired to generate realizations for a channelized reservoir model. See **Fig. 5.54**. A unique realization is achieved per each path as illustrated in the flowchart in **Fig. 4.4**. A set of sample realizations is shown in **Fig. 5.55**. The sequential increase in detail of the realization with time is achieved using the renormalization method discussed in the previous subsection. See **Fig. 5.56** for a set of sample upscaled realizations.

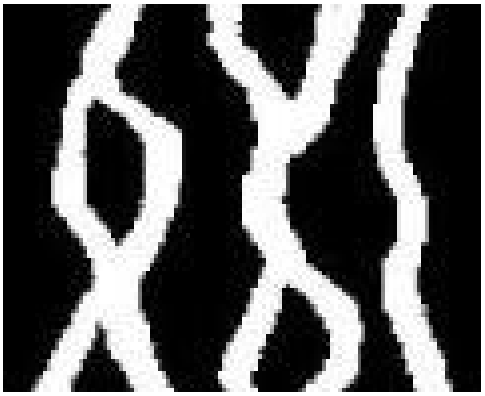


Fig. 5.54– Original channelized training image.

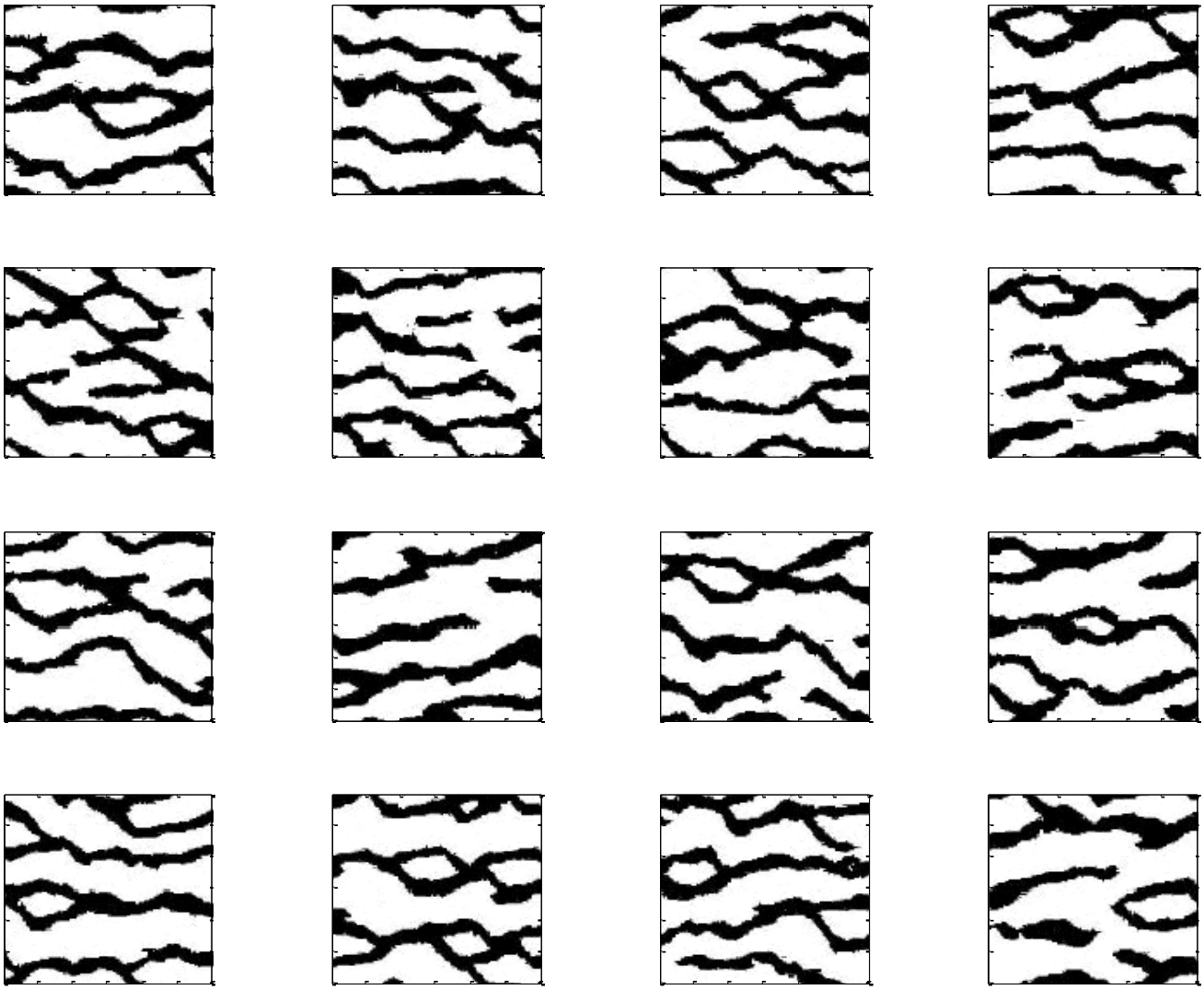


Fig. 5.55– Sample realizations generated from the training image using FILTERSIM algorithm.

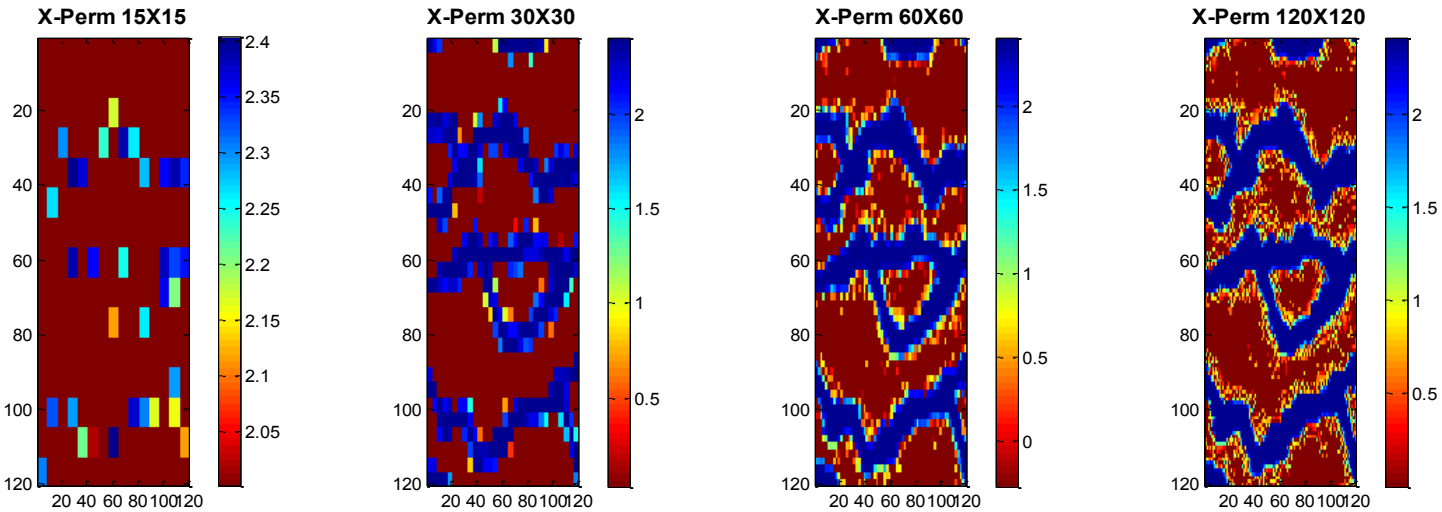


Fig. 5.56– Sample upscaled realizations generated from the training image using FILTERSIM algorithm.

The results of the applying the LSM method to the FILTERSIM generated realizations are shown in **Fig. 5.57** and **Table 5.12**. For this example, the discrepancy in the mean VoF and policy histogram are more pronounced when comparing the varying heterogeneity with the fixed heterogeneity run. The discrepancy illustrates a significant shift in both policy outcome and the VoF. This again highlights the effect of early assumptions of reservoir heterogeneity on decision making. It is important to note that sequentially upscaling the reservoir models generated by FILTERSIM can result in ambiguity of the channels in the most upscaled model. See the left most side of **Fig. 5.56**. However, these were used to demonstrate the method.

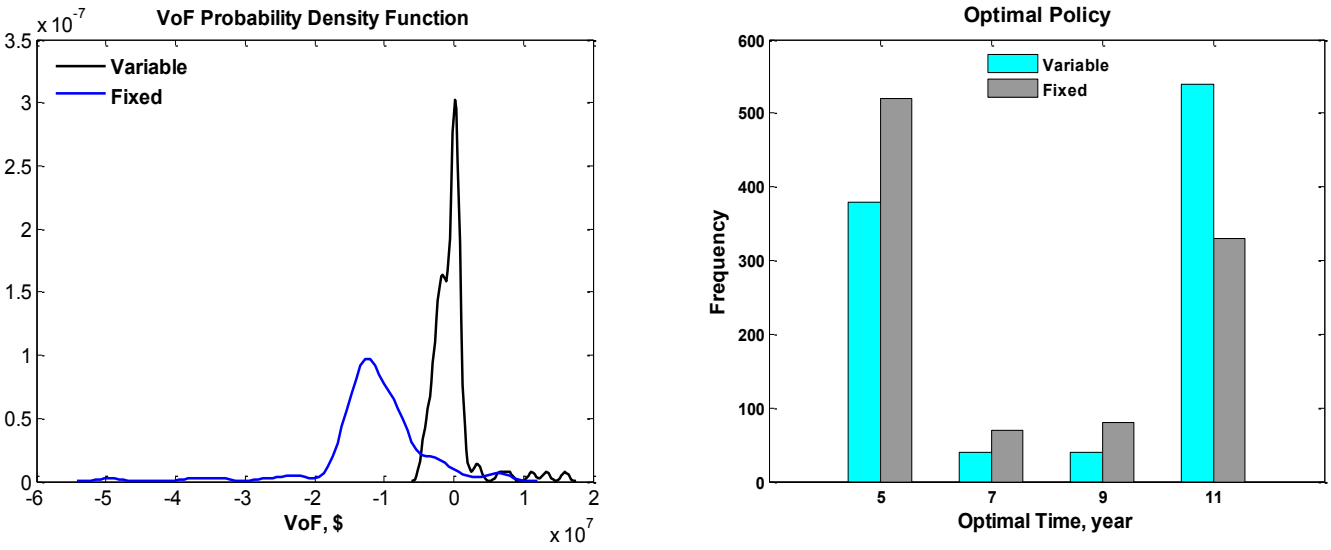


Fig. 5.57– VoF PDF and policy histogram for the FILTERSIM generated permeability realizations with renormalization with time. The results for fixed heterogeneity with time (fine scale constant through time) were also added for comparison.

Table 5.12– VoF mean for FILTERSIM generated permeability.

Heterogeneity with Time	Value of Flexibility (mean, $)
Variable	-2.25e+05
Fixed	-1.13e+07

5.4.3 Summary

This section demonstrates that the LSM method can be extended to incorporate stochastic modelling of permeability and this was illustrated by using Gaussian and multiple-point geostatistical generated permeability realizations. The effect of uncertainty in the time series of heterogeneity was modeled using the renormalization approach. The results show that as expected, reservoir models generated from different methods produce different outcomes. The effect of varying heterogeneity with time was found to produce over-optimistic VoF compared with using the fine-scale reservoir model throughout the duration of the field life. This gives some insight on how the reservoir model is updated can effect decision making. These applications were performed for two-dimensional reservoir models and can be extended to three-dimensional reservoir models. It is possible to use more sophisticated approaches to update the reservoir model with time such as history matching methods.

5.5 Concluding Remarks

This chapter attempted to apply the LSM algorithm to evaluate VoF for a surfactant-polymer flooding process. The LSM method was introduced and discussed in greater detail in the context of its application to stylized case studies.

The LSM algorithm was capable of incorporating economic and technical uncertainties and also take into consideration how the realization of these variables evolves with time. Its application depends on the design of the option or decision that is desired to be optimized. The initial results for case study one show that flexibility is beneficial in the implementation of the surfactant-polymer flooding process when compared to a static policy scenario. From this perspective, VoF evaluation approach is useful in creating value from uncertainty for surfactant-polymer flooding processes.

Basis function design was found to be another important component in this algorithm because it could potentially have a significant influence on the results, especially when a finer decision space discretization is used. In these cases an increasing the number of time steps the algorithm produced similar results to the coarser decision space case. This raised suspicion on whether the algorithm was performing correctly. Further investigation found that for results to converge as the number of time steps increased, an increasing number of basis functions is necessary which results in an exponential increase in the number of samples. This introduces a significant limitation on the applicability of the algorithm for higher dimensional problems (i.e. finer time discretization). This aspect would require further research and investigation when considering VoF evaluation using finer time steps.

For the original decision space discretization (yearly decisions) it was found that the algorithm did produce sufficiently converged results and thus application of the algorithm was limited to this case. It was also found that a simple basis function design was deemed sufficient after performing a sensitivity analysis towards using different polynomial orders and orthogonal polynomials in the design of the basis functions.

The regression method used was that of the ordinary least squares regression. Other advanced regression methods are also applicable with this algorithm such as weighted least squares or generalized moment methods (**Longstaff and Schwartz 2001**). Since the objective function (NPV) is a conditional on both economic and technical state variables, it is important to

incorporate both in the regression. Clustering linear regression (i.e. local regression) was used for this purpose. The clustering was based on the surfactant adsorption as it was found to have a strongly non-linear effect on the NPV. This approach produces a more accurate estimate of the continuation function which resulted in higher VoF which is desirable. Sampling methods could also influence performance. Because the algorithm uses an approximation in estimating the continuation value, the policy obtained using is considered to be a near-optimum rather than the global optimal policy; however as the accuracy in estimating the continuation value increases the results tend to converge to the global optimum **(Longstaff and Schwartz 2001; Gamba 2003; Glasserman and Yu 2004; Bender and Steiner 2010**). For the case studies presented above, standard uncertainty distributions were used for the technical state variable and a standard mean-reverting stochastic price model was used for the main economic state variable (the oil price). Different distributions and models can easily be used with this algorithm without any major adjustments. The initial sampling method for this algorithm is Monte Carlo sampling. This requires many realizations to achieve convergence which necessitates significant computational effort. For the simple examples in this study it was possible to run the algorithm to the order of 10^3 realizations; however using three dimensional complex reservoir models could be problematic.

The effect of heterogeneity was also shown on the results of the LSM method. It was found that the policy and VoF is reservoir model unique, which is expected. This can be explained by the effect of channeling on the sweep efficiency of SP flooding. In the examples presented above, injecting a mobility buffer did mitigate this effect and improve the VoF. Different approaches to uncertainty in heterogeneity were considered. Gaussian and multiple-point geostatistical methods were used to generate stochastic realizations of the permeability field. Uncertainty in the time series was also considered which is akin to the time evolution of the permeability field assumed for Ensemble Kalman filter methods. This was performed either using the pressure solver method or the renormalization approach. This was intended to mimic the increasing detail in the reservoir model that occurs with time due to new information. The LSM algorithm was shown to be applicable to reservoir model updating scenario. Other more complex approaches could be used such as history matching.

By valuing flexibility, the LSM algorithm gives a new outlook in implementing surfactant-polymer flooding processes in the field while also producing quantitative results. The method can incorporate different types of uncertainty. Another advantage of the LSM method is it easy scalability to include an increasing number of uncertain parameters compared with other methods. Different flexibilities could be valued to determine which flexibilities can provide the greatest value by mitigating adverse circumstance or capitalizing on better than expected circumstance depending on how uncertainty resolves with time. A major obstacle in extending the applicability of the LSM method to finer decision space discretization was encountered. This was found to require an increase in the number of basis functions required in the regression process in order to produce accurate results. This in turn would require a significant increase in the number of realizations which is computationally prohibitive due to the computational intensity of reservoir simulation. Applying the LSM algorithm to such cases would require further investigation of enhanced basis function design and its effect on the accuracy of the results.

6 The Probabilistic Collocation Method: Case Studies

The application of the LSM method was introduced in the previous chapter. The stochastic component of this method is based on MCS. MCS is a traditional uncertainty quantification approach that is usually used. The advantage of MCS is that it is independent of the number of random input variables. Convergence of solution statistics is relatively low for MCS however, thus requiring a large number of realizations (**Xiu 2007**). Other approaches such as non-sampling methods do not depend on repetitive use of deterministic solvers. These include perturbation methods and second-moment analysis. Their application is restricted to systems with relatively small random inputs and outputs, a difficult condition to satisfy for nonlinear problems where small random inputs may result in large random outputs (**Xiu and Hesthaven 2005**).

Experimental Design methods are also widely used in the petroleum industry in quantifying uncertainty. Although considered to be more efficient than MCS, it however does not incorporate the full probability distributions of the random input parameters in a consistent manner when creating the response surface. It also assumes inherently that the distributions of the parameters are uniform because all samples are equally weighted **(Li et al. 2011**). The probabilistic collocation method (PCM), which is also known as the deterministic-equivalent modelling method, was first introduced by **Tatang et al. (1997**). Probabilistic collocation methods have been widely used for computational fluid dynamics problems (**Mathelin and Hussaini 2003; Loeven et al. 2007; Loeven and Bijl 2008; Onorato et al. 2010**). They have also been applied to flow in porous media problems (**Li and Zhang 2007; Li and Zhang 2009; Li et al. 2011**). The main advantage of PCM is that it is non-intrusive and thus it can regard the reservoir simulator as a "black-box".

6.1 Case Studies

Initially, the PCM is applied to a few examples in order to demonstrate that it can quantify uncertainty efficiently for SP flooding. The output parameter was assumed to be the recovery factor. As mentioned earlier, there are numerous sources of uncertainty in surfactant-polymer flooding such as heterogeneity, surfactant and polymer adsorption, resident brine salinity and residual oil saturation to chemical flooding (**Kossack and Bilhartz 1976; Brown and Smith 1984, Hankins and Harwell 1996, Zheng et al. 2000; Anderson et al. 2006 and Cheng et al. 2012**). For the examples in this chapter, uncertainty in four variables was considered; the residual oil saturation to chemical flooding, the polymer viscosity multiplier and the surfactant and polymer adsorption rates.

The first example is of case study one in the previous chapter. This is a 10x10x10 three-dimensional homogeneous reservoir model with a quarter five-spot pattern. The second example is that of case study two in the previous chapter which is a two-dimensional heterogeneous model, specifically that of layer 1 of the SPE10 model (**Christie and Blunt 2001**) encompassing 220x60x1 grid cells. The well placement is also a quarter five-spot pattern. The third example is that of the three-dimensional PUNQ-S3 reservoir model (**PERM 2012**) having a total of 19x28x5 grid cells. The permeability field and the corner geometry data were maintained from the original model data while the reservoir data was modified. The well placement for this case study is illustrated in **Fig. 5.6**. One injector is located at the lower end of the reservoir with four producers placed in the high permeability channels at higher structural locations. The fluid data for the first three examples follow that of the reservoir models used in (**Alkhatib et al. 2013**) which resembles a slightly water wet black-oil system. The final example is that of an upscaled three dimensional portion of the SPE10 model having a total of 20x55x7 grid cells. The model incorporates the top lithology (top 35 layers) of the original SPE10 model which are then upscaled to 7 layers. The reservoir and fluid data are based on the SPE10 model data. This model assumes an inverted five-spot pattern. See **Fig. 6.1**.

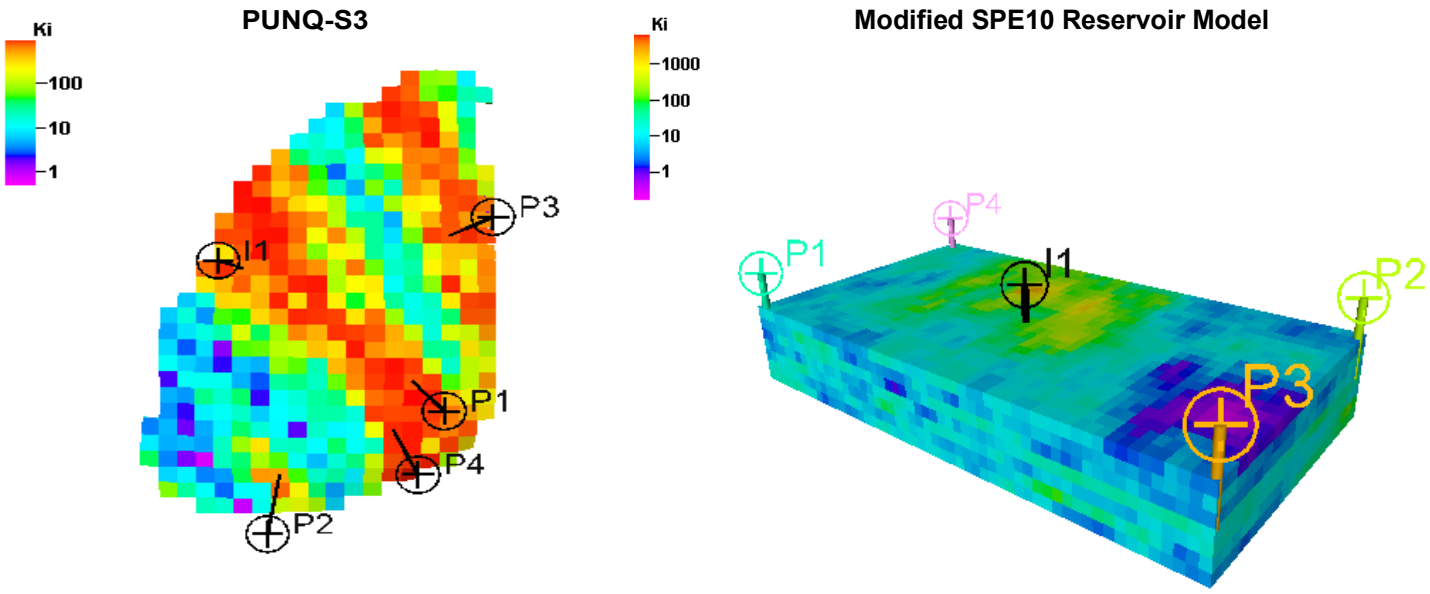


Fig. 6.1– Example reservoir models used showing well placement and permeability field. The legend for each model is shown in the upper left corner for the permeability values

For the first two examples, a gradual application of the probabilistic collocation method was performed. First a univariate random input was used (either residual oil saturation to chemical flooding or surfactant adsorption) assuming only surfactant flooding. Next the bivariate random inputs run was performed assuming both the residual saturation and the surfactant adsorption, again assuming only a surfactant flood. Then a multivariate random input run was performed assuming a surfactant-polymer flood where there are four state variables: residual oil saturation to chemical flooding (S_{orc}), surfactant adsorption (D_s), viscosity multiplier end point (P_{visc}) and polymer adsorption (D_p) which are assumed to obey the following distributions, respectively: uniform (0,0.2), normal (-8,1), uniform (1,10) and normal (-8,1). For the normally distributed parameters, a transformation of the following form is used:

$$D_i = e^q, \text{ where } i = s \text{ or } p \text{ and } q \sim N(-8,1) \qquad (6.1)$$

Table 6.1 Random input parameters and their distributions

Random Input	Distribution	Bounds
Residual oil saturation to surfactant flooding, fr	Uniform	[0,0.2]
Surfactant adsorption, g/g rock	Normal	(-8,1)
Polymer adsorption, g/g rock	Normal	(-8,1)
Polymer viscosity multiplier	Uniform	[1,10]

For the latter two examples, the results of the multivariate runs are presented. For all examples the injection policy is fixed at 3% wt. surfactant 0.10 PV slug, and for surfactant-polymer flooding this is followed by a 3% wt. Polymer 1 PV polymer mobility buffer. These were found to be the most efficient injection policies in terms of effectiveness and consumption of surfactant and polymer. The output parameter approximated by the method is the recovery factor. See **Appendix A** and **Appendix G** for surfactant/polymer properties and simulation constraints used. For all examples, two methods for solving for the coefficients of the output polynomial proxy are compared: Gaussian quadrature and linear regression.

6.1.1 Example 1: Homogeneous three-dimensional reservoir model

Fig. 6.2 to 6.5 shows the performance of different sampling methods used in the linear regression method and the Gaussian quadrature method. The output statistical results, the probability density functions, produced by the MCS and by the PCM are compared(where the statistics are generated via Monte Carlo simulation, albeit of the polynomial approximation model which requires significantly less computational effort than running the reservoir simulator).

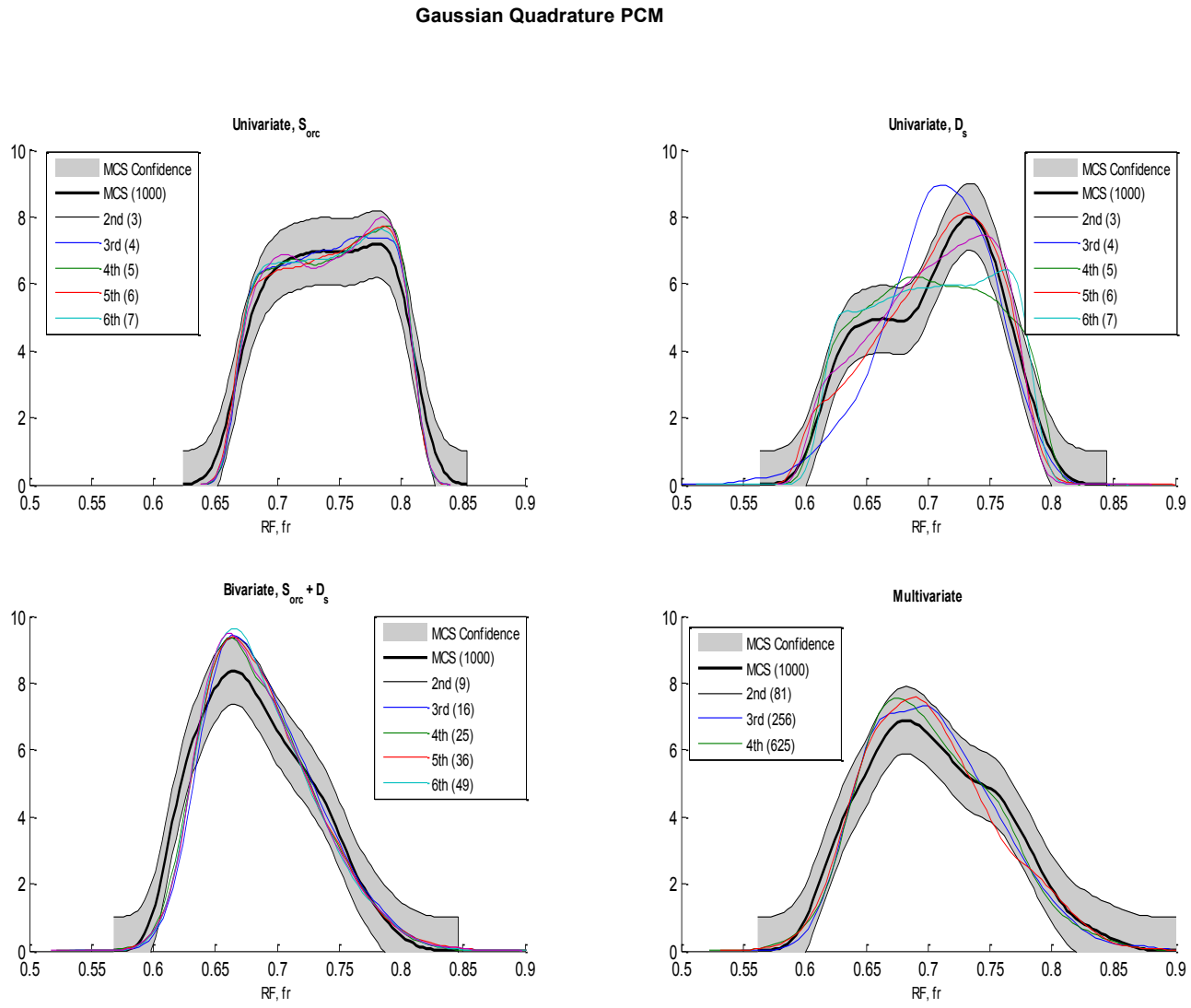


Fig. 6.2—Probability density function plots for example 1 for PCM by Gaussian quadrature. The number of collocation nodes used is shown in the legend in parenthesis for each approximation order

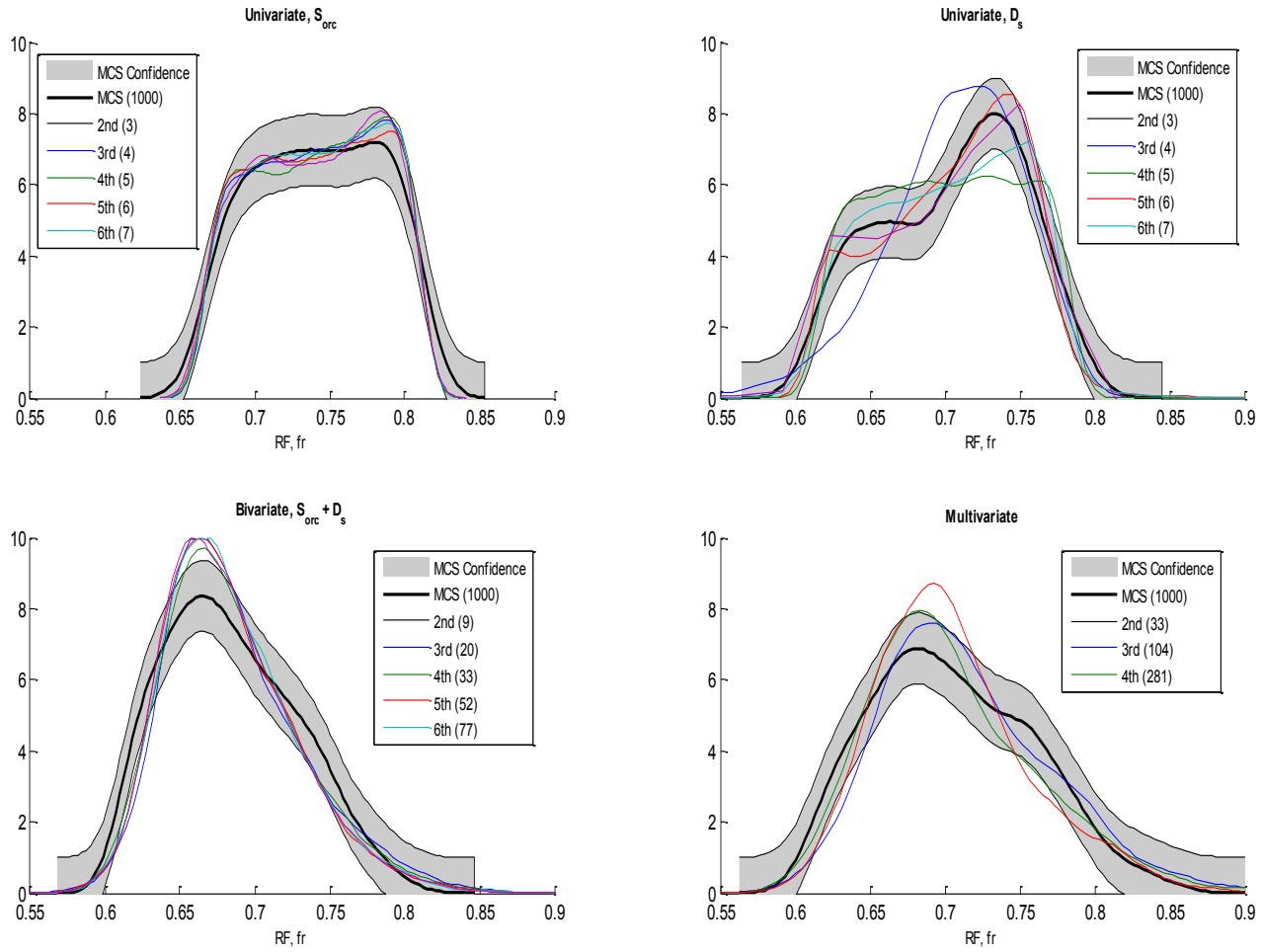


Fig. 6.3—Probability density function plots for example 1 for PCM by linear regression using boxed Fejer sampling. The number of collocation nodes used is shown in the legend in parenthesis for each approximation order.

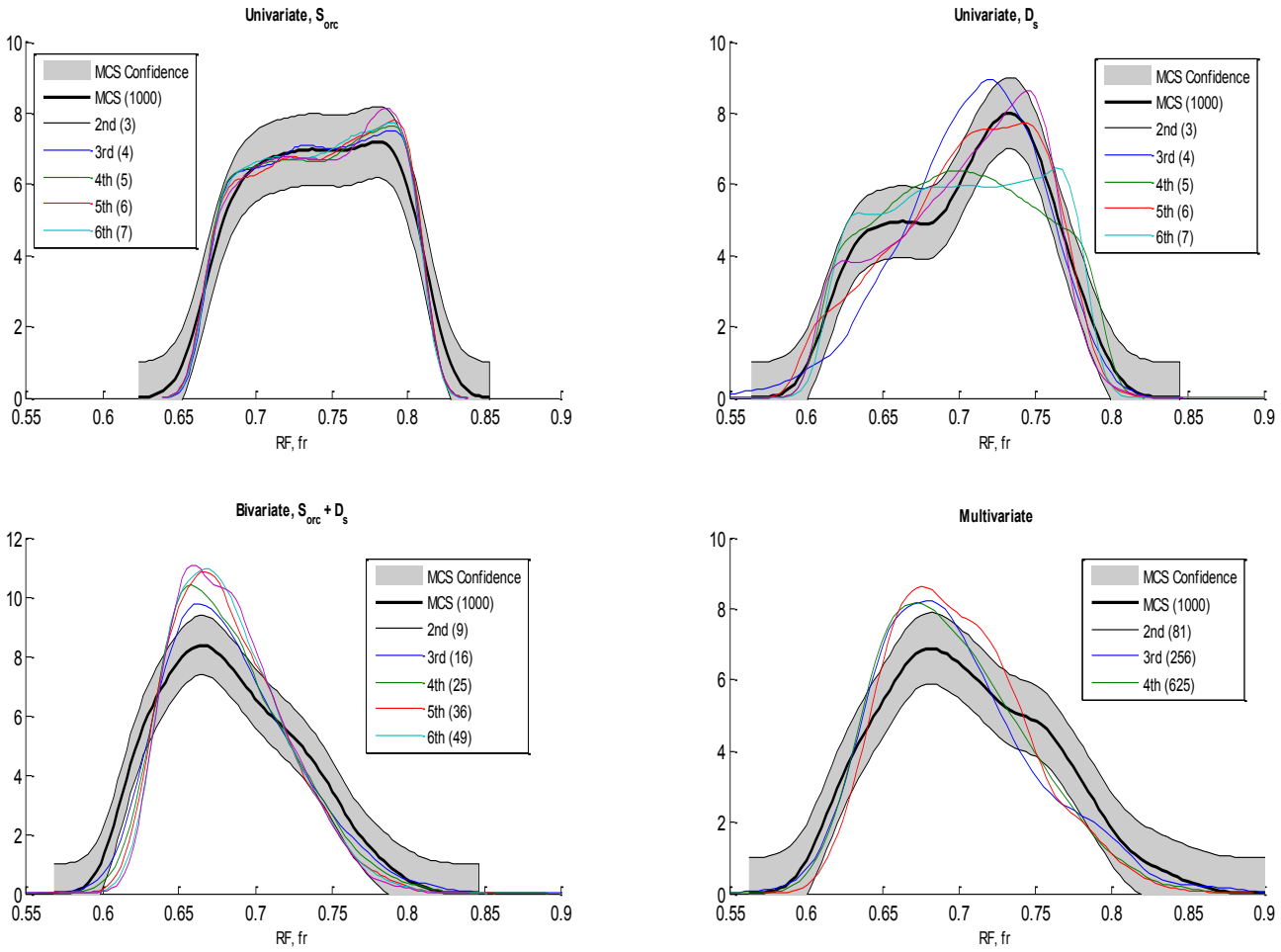


Fig. 6.4—Probability density function plots for example 1 for PCM by linear regression with quadrature sampling. The number of collocation nodes used is shown in the legend in parenthesis for each approximation order.

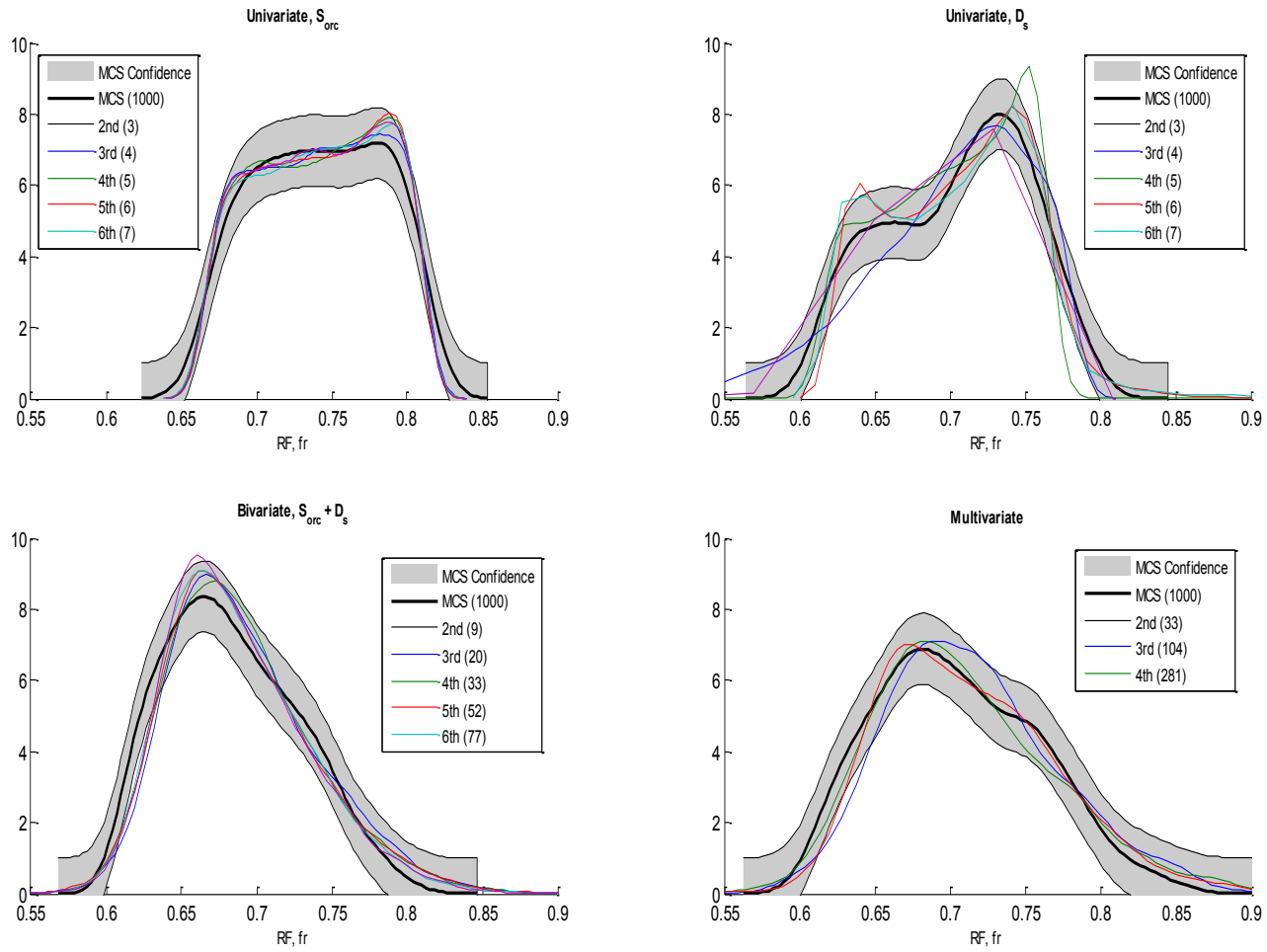


Fig. 6.5—Probability density function plots for example 1 for PCM by linear regression with mapped Fejer sampling. The number of collocation nodes used is shown in the legend in parenthesis for each approximation order.

For this example, when dealing with one random input, the probability distribution has a clear effect on the performance of the PCM. When assuming the random input is S_{orc} which is distributed uniformly, resulting PDF's are in good agreement with the MCS PDF. Both Gaussian quadrature and linear regression produced similar results. No significant difference between the different sampling methods was observed. More importantly, it was shown that an approximation requiring significantly fewer simulations can quantify uncertainty successfully. Increasing the order does not seem to improve the results significantly as well. If the single random input is distributed normally (as is the case for D_s), results showed more variety. In this case, the order of the approximation has a direct effect on the PDF. There is also an apparent difference between results obtained by Gaussian quadrature and linear regression. The Fejer sampling methods showed better matches compared with using quadrature nodes. For the bivariate and multivariate cases, Gaussian quadrature and linear regression using mapped Fejer nodes achieved the best visual agreement with the MCS PDF, while using linear regression with quadrature nodes did not produce results as good as Gaussian quadrature. It is also clear that most of the PDFs produced by the PCM are within the confidence intervals of the MCS PDF except for those obtained via linear regression with quadrature nodes indicating the relative agreement of the PCM PDFs with the MCS PDFs.

The accuracy of these different PCM methods is tested through the first two moments. **Fig. 6.6** shows the mean and standard variation plotted versus the polynomial approximation order for the multivariate case. Gaussian quadrature performs better than linear regression using quadrature nodes based on the first two moments; it is more stable as the approximation order varies. Although the Fejer mapped sampling seemed to achieve the best visual match with the MCS PDF, the Fejer boxed sampling outperforms it in terms of moments, and seems to approach the MCS moments with increasing approximation order. In general, the difference between the MCS and PCM moments were found to be within the uncertainty of the MCS produced values with the exception of the moments obtained via linear regression using quadrature sampling PCM.

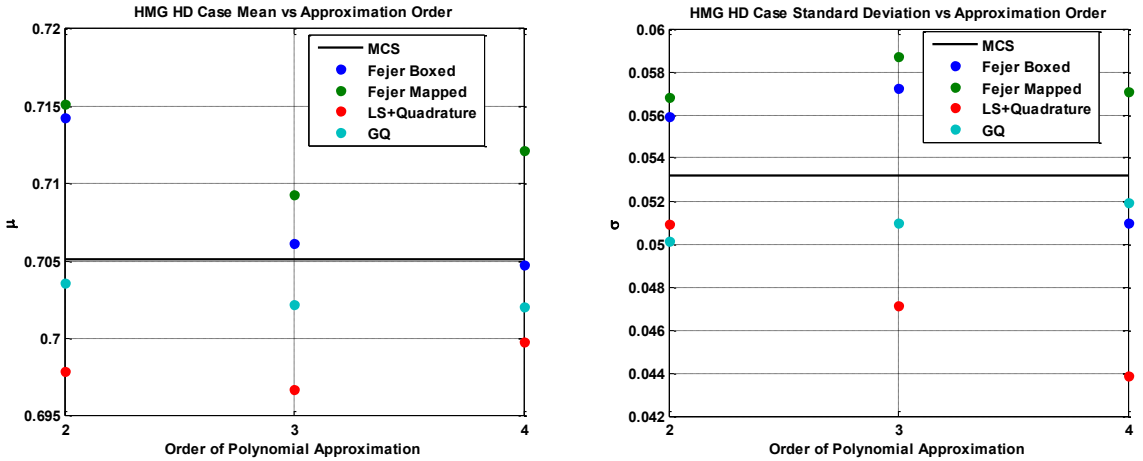


Fig. 6.6[25]– Plots of the first two moments as a function of approximation order for example 1 for multivariate PCM by Gaussian quadrature and linear regression using quadrature (LS+quadrature), Fejer mapped and boxed collocation nodes. (LS: linear regression, HD: high dimensional random input)

6.1.2 Example 2: Heterogeneous two-dimensional reservoir model

Example 2 illustrates the use of PCM on a highly heterogeneous two-dimensional reservoir model. Results are presented in **Fig. 6.7 to Fig. 6.10**. For the single random input cases, Gaussian quadrature produces more stable PDFs than linear regression using quadrature nodes. The mapped and boxed Fejer nodes produced relatively similar PDFs. For the bivariate case, the mapped Fejer nodes produce the better PDF match with MCS. As for the multivariate case, Gaussian quadrature and mapped Fejer nodes produce relatively good PDF agreement for a fourth order PCM. With regards to the confidence interval for this reservoir model, only the mapped Fejer PCM produced PDFs were found to be mostly within the MCS PDF bounds.

[25] Reproduced from **Alkhatib and King (2013a)**.

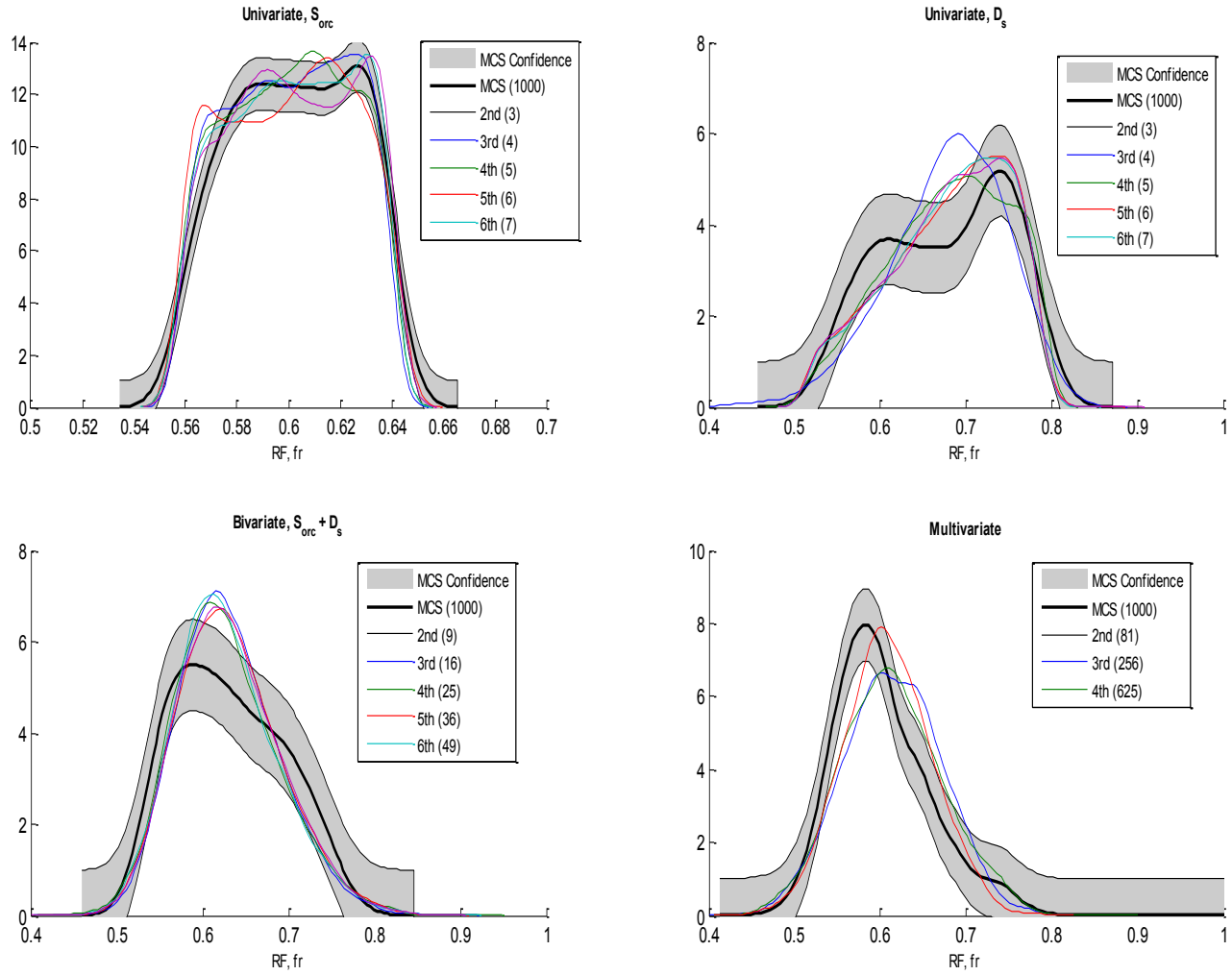


Fig. 6.7—Probability density function plots for example 1 for PCM by Gaussian quadrature. The number of collocation nodes used is shown in the legend in parenthesis for each approximation order.

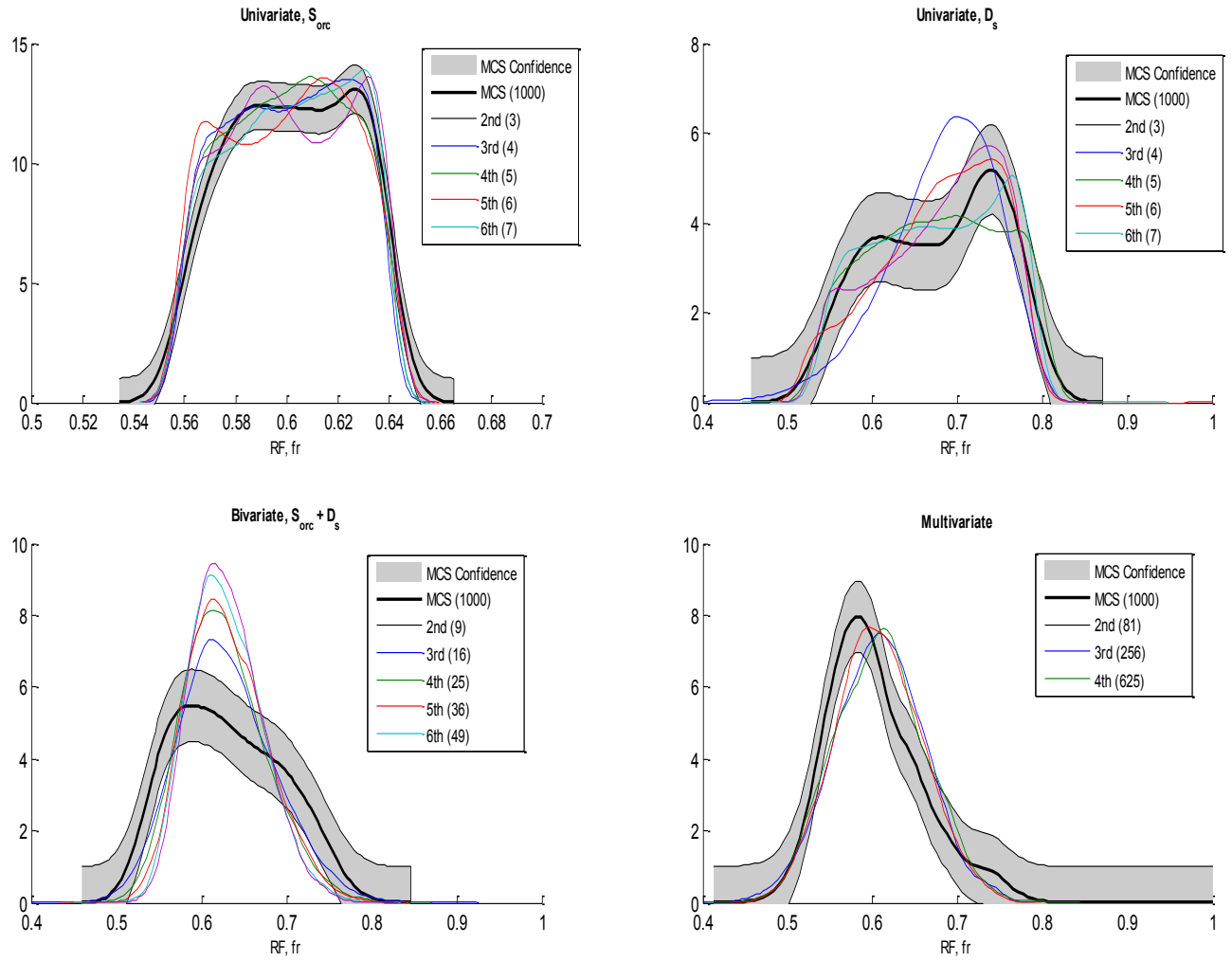


Fig. 6.8—Probability density function plots for example 1 for PCM by linear regression using quadrature. The number of collocation nodes used is shown in the legend in parenthesis for each approximation order.

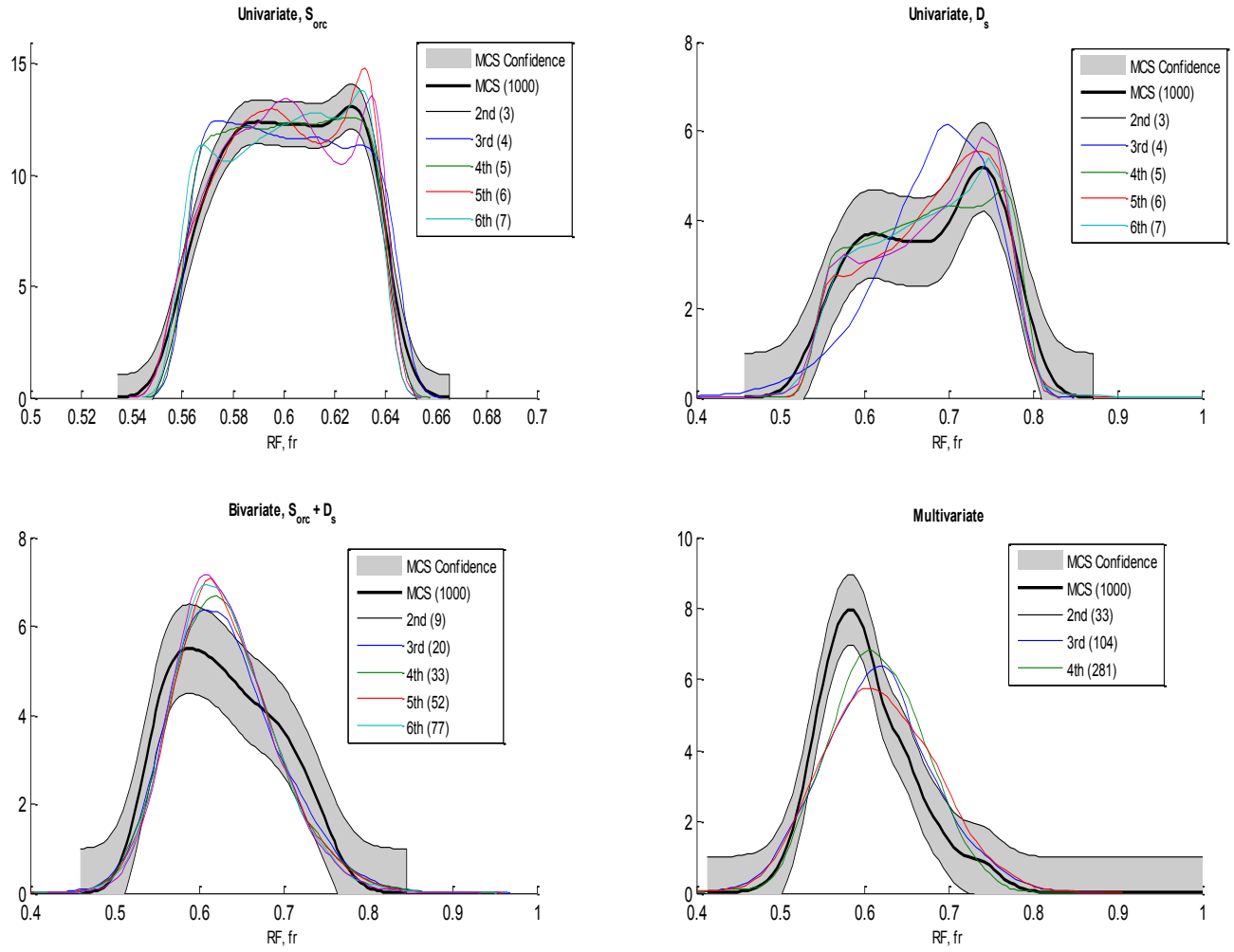


Fig. 6.9—Probability density function plots for example 1 for PCM by linear regression with boxed Fejer sampling. The number of collocation nodes used is shown in the legend in parenthesis for each approximation order.

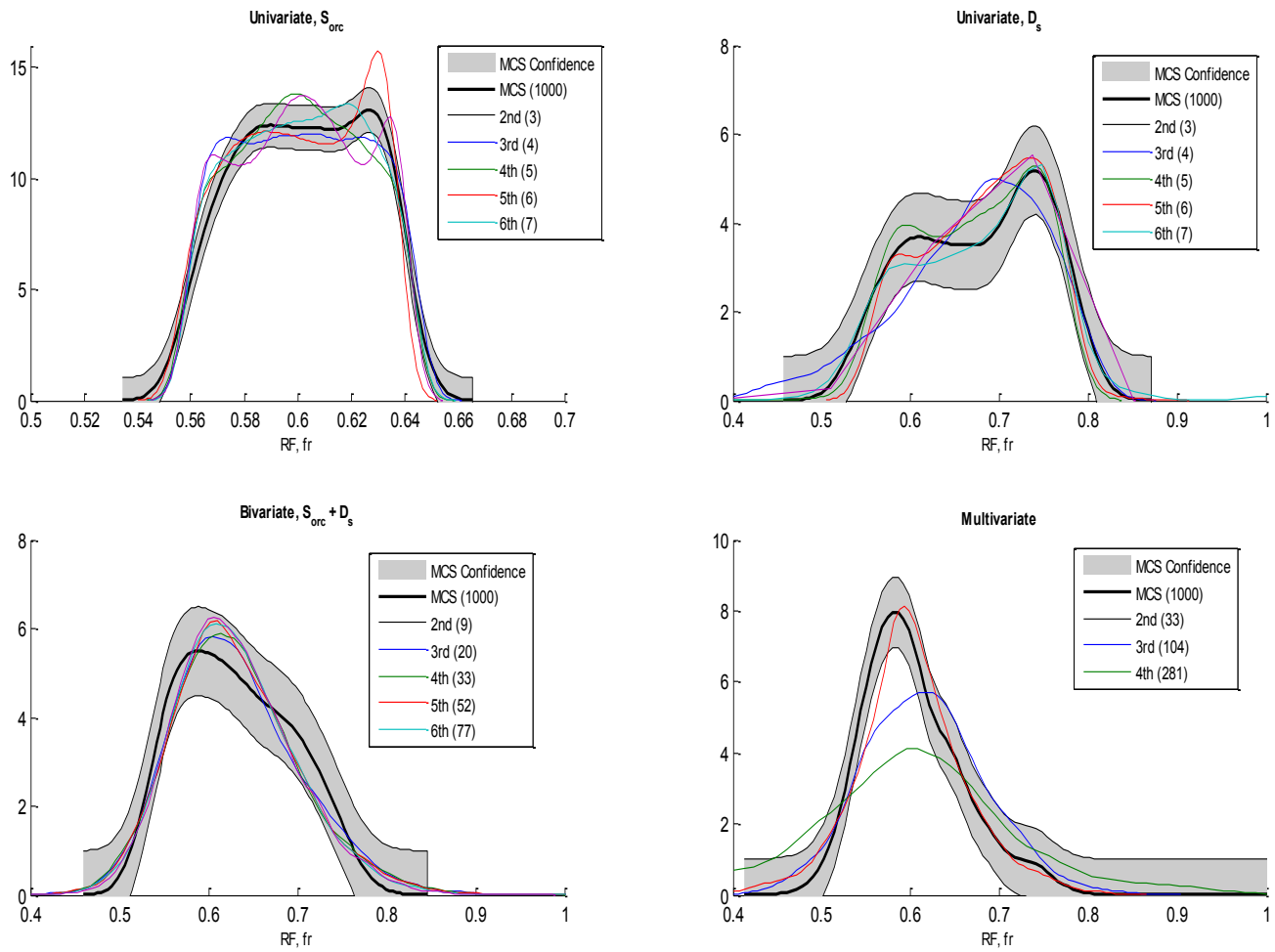


Fig. 6.10—Probability density function plots for example 1 for PCM by linear regression with mapped Fejer sampling. The number of collocation nodes used is shown in the legend in parenthesis for each approximation order.

The sensitivity of the mean and standard deviation to the PCM order for the multivariate case exhibits different behaviour compared to the other examples presented in this chapter, see **Fig. 6.11**. The variability of the mean with the order of the PCM shows that the mapped Fejer nodes achieve the best result compared with MCS, while the standard deviation shows that for all methods used the values are in the proximity of the MCS obtained value for a fourth order PCM. In general, the difference between the MCS and PCM moments were within the uncertainty of the MCS results indicating the relatively efficient performance of the PCM.

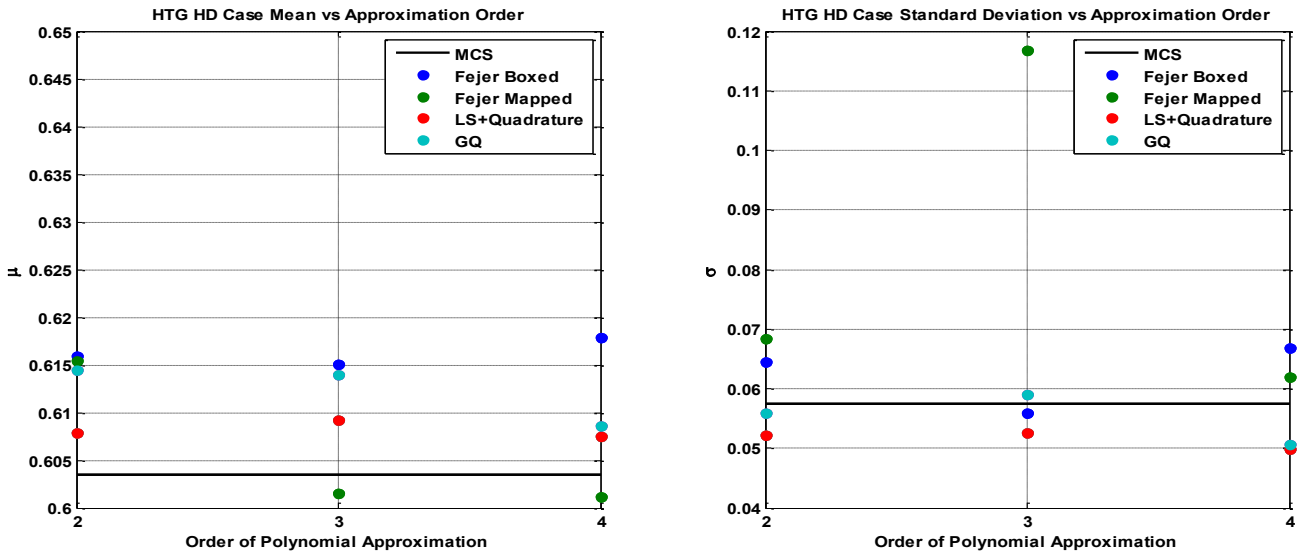


Fig. 6.11[26]— Plots of the first two moments as a function of approximation order for example 2 for PCM by Gaussian quadrature and linear regression, using quadrature (LS+quadrature), Fejer mapped and boxed collocation nodes.

6.1.3 Example 3: PUNQ-S3 three-dimensional reservoir model

For this example, a multivariate run was performed. From **Fig. 6.12** it is apparent that performing the PCM using linear regression with mapped Fejer sampling method achieves, visually, the best agreement with the MCS generated PDF requiring fewer collocation nodes than those required by Gaussian quadrature. When comparing Gaussian quadrature with linear regression with quadrature nodes, solving for the coefficients using Gaussian quadrature produce a better PDF match although not as good as that produced by mapped Fejer with linear regression. Furthermore, the boxed and mapped Fejer PDFs were within the confidence interval of the MCS PDF.

[26] Reproduced from **Alkhatib and King (2013a)**.

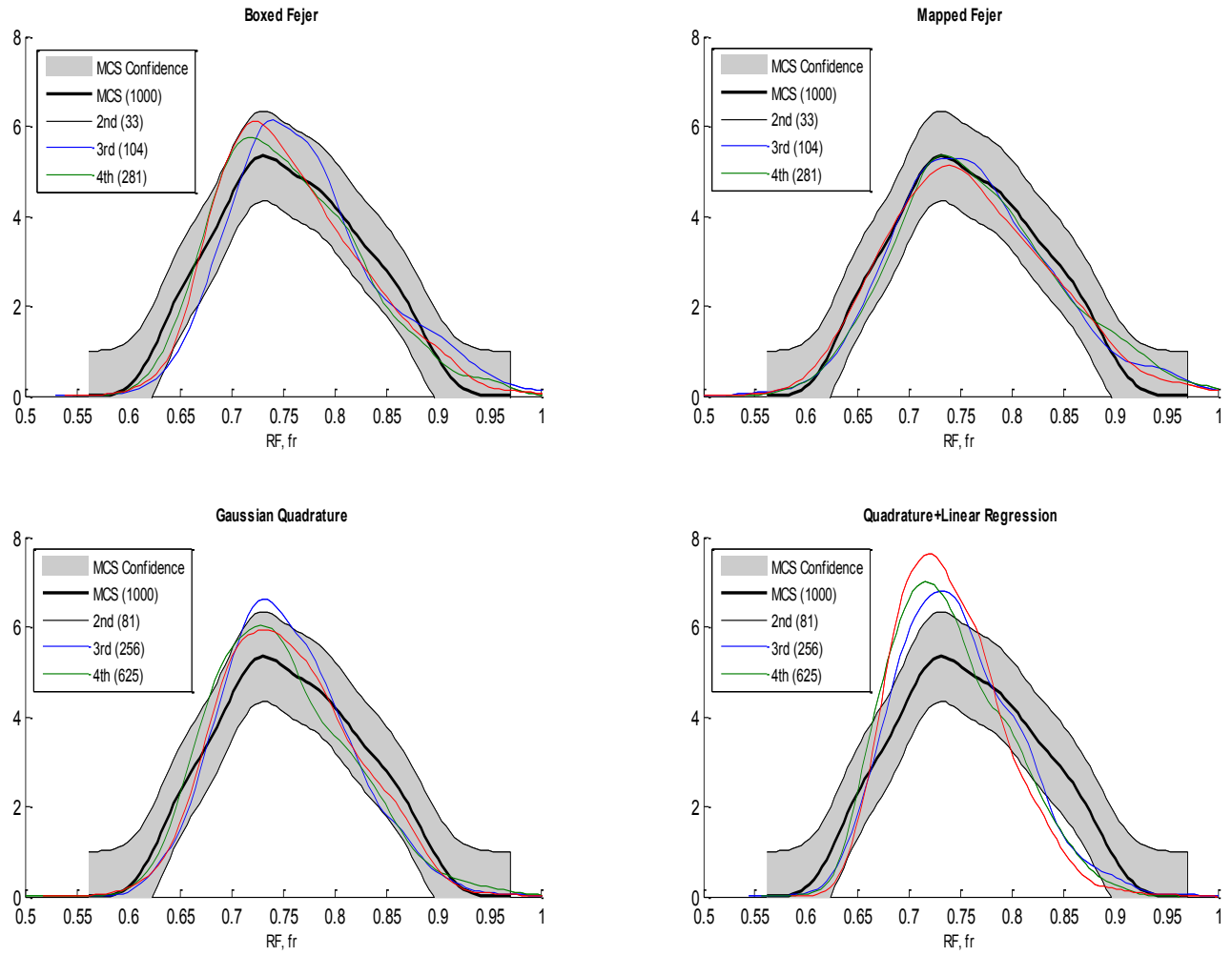


Fig. 6.12– Probability density function plots for example 3 for multivariate PCM by Gaussian quadrature and linear regression using quadrature, Fejer mapping and boxing collocation nodes. The number of collocation nodes used is shown in the legend in parenthesis for each approximation order.

In regards to the moment analysis, it was found that solving a fourth order PCM using Gaussian quadrature or Fejer mapped and boxed nodes with linear regression approached the MCS mean while boxed Fejer nodes achieved the nearest standard deviation value. The results were significantly better than those achieved using linear regression with quadrature nodes. See **Fig. 6.13**.

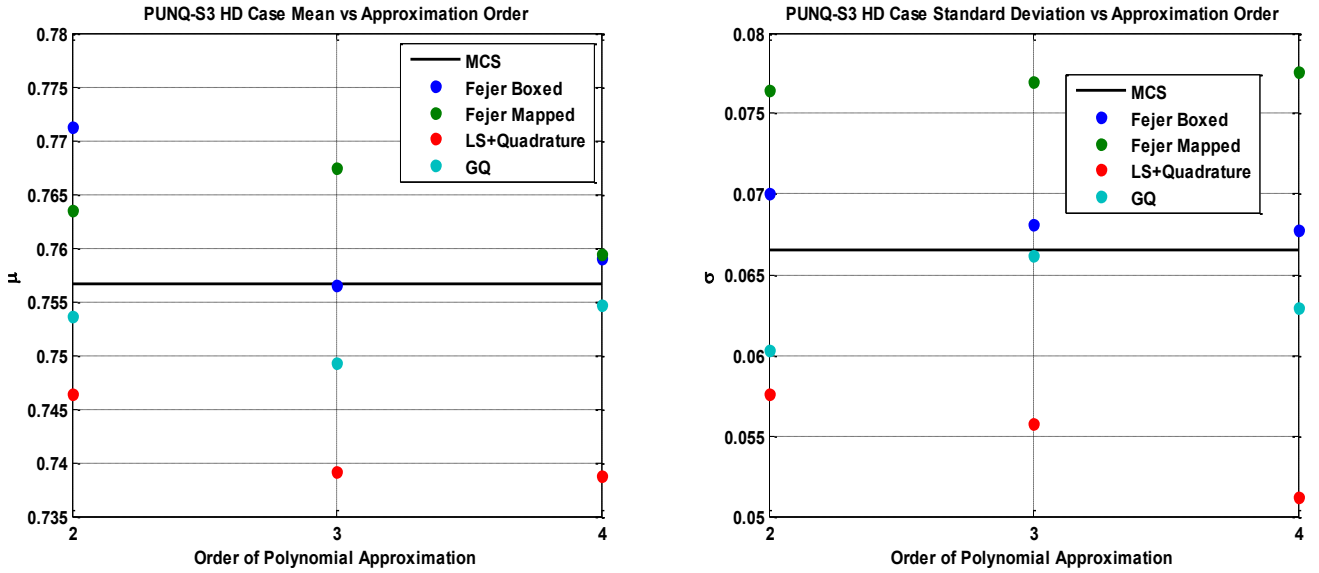


Fig. 6.13[27]— Plots of the first two moments as a function of approximation order for example 3 for PCM by Gaussian quadrature and linear regression using quadrature, Fejer mapped and boxed collocation nodes.

[27] Reproduced from **Alkhatib and King (2013a)**.

6.1.4 Example 4: Modified SPE10 three-dimensional reservoir model

The PDF obtained from the PCM using linear regression and Fejer mapped is in good visual agreement with that produced from the MCS. Once again, by using Gaussian quadrature better results are obtained compared with linear regression using the same quadrature nodes. See **Fig. 6.14**. The mapped Fejer produced PDF was found to be within the confidence region of the MCS PDF.

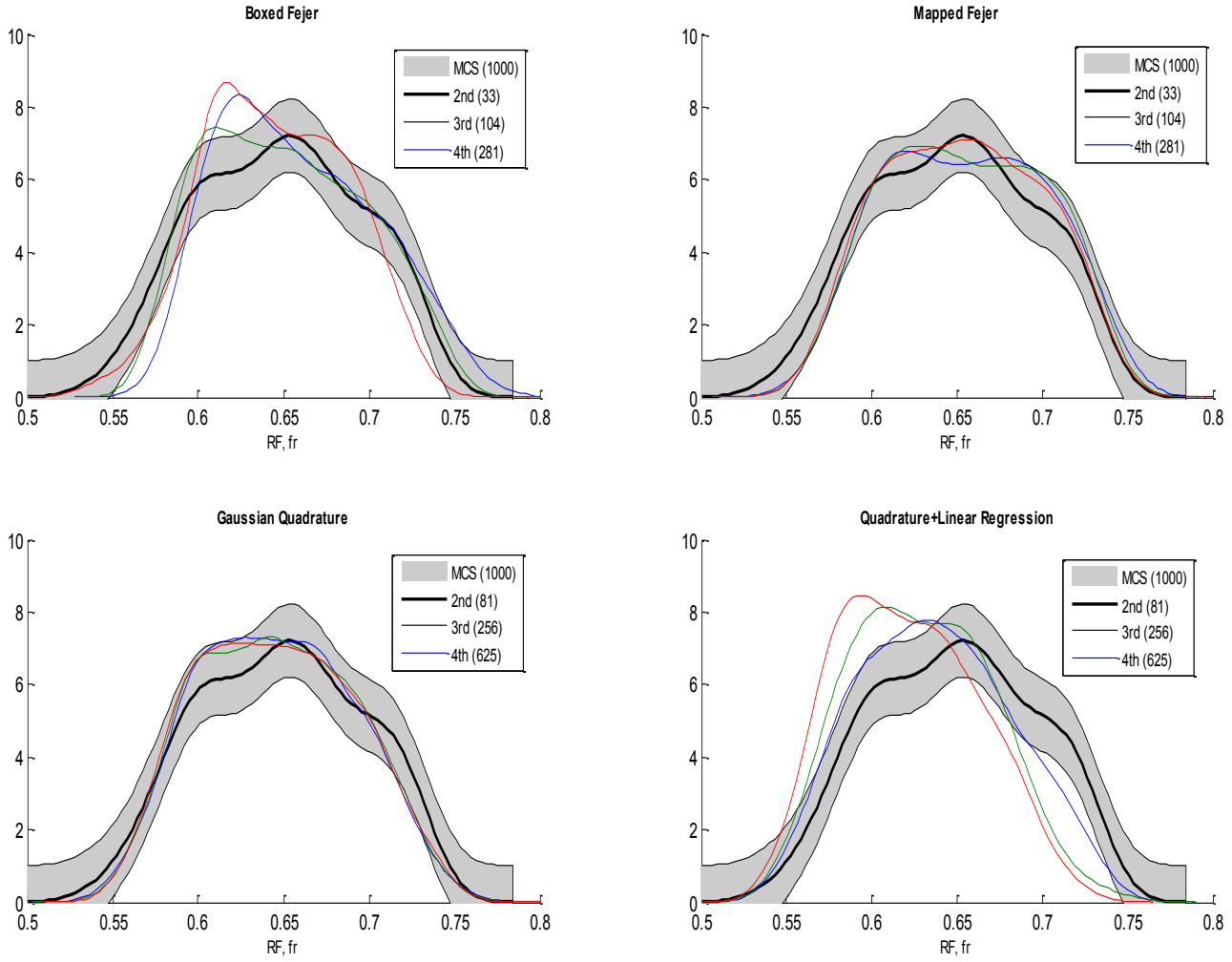


Fig. 6.14– PDF plots for the modified SPE10 reservoir model for multivariate PCM by Gaussian quadrature and linear regression using quadrature, Fejer Mapped and Boxed collocation nodes. The number of collocation nodes used is shown in the legend in parenthesis for each approximation order.

In terms of moments, Gaussian quadrature appears to be the least sensitive to the approximation order and performs significantly better than quadrature nodes with linear regression. The Fejer boxed nodes produced better results for the mean as a function of approximation order than the Fejer mapped nodes. See **Fig. 6.15**.

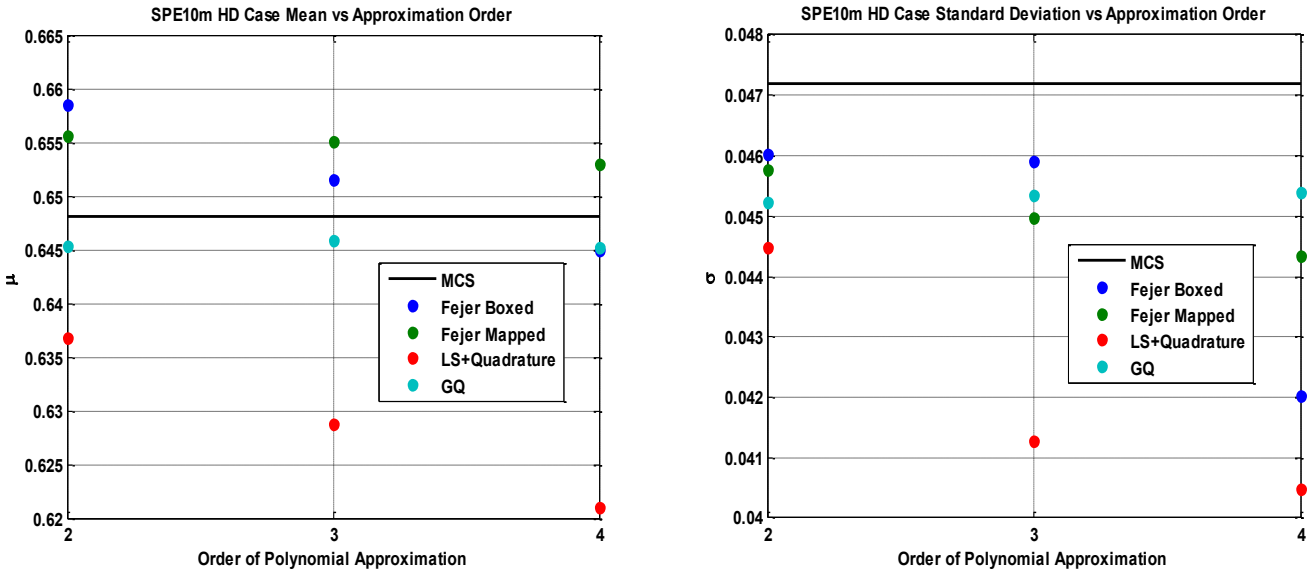


Fig. 6.15[28]**— Plots of the first two moments as a function of approximation order for example 4 for PCM by Gaussian quadrature and linear regression using quadrature, Fejer mapped and boxed collocation nodes.**

6.2 Discussion

The main objective of this chapter was to demonstrate that the PCM can be used to quantify parametric uncertainty for a chemical EOR process efficiently compared with traditional methods. The secondary objective was to compare Gaussian quadrature and linear regression in solving for the coefficients of the output polynomial chaos. To determine the accuracy of the PCM, usually the output proxy model is used to evaluate the response at the collocation nodes of the next-higher order and is then compared with the value of the response from the simulator to obtain an error estimate. This would require a significant computational effort, it was deemed sufficient to compare the first two moments with the MCS results coupled with the visual agreement between the PCM and MCS PDF's.

Results for the univariate and bivariate runs show that an effective approximation can be obtained while using a relatively small number of realizations to obtain the coefficients of the approximation model. For multivariate runs, however, the number of nodes increases more rapidly as the order of approximation increases. The curse of dimensionality is more manifest in these runs (**Alkhatib and King 2013a**). Yet, the results obtained for Fejer mapped nodes do show a relatively good visual match while using a reasonable number of realizations. When comparing the Gaussian quadrature approach and linear regression using quadrature nodes, for the higher dimensional problems Gaussian quadrature produces better

[28] Reproduced from **Alkhatib and King (2013a)**.

agreement with the MCS PDF and moments. Due to the use of Fejer nodes, in contrast to Clenshaw-Curtis nodes, it is possible to focus the sampling on the high probability regions and neglect the boundaries of the input distributions, making it more efficient when handling infinitely bound distributions such as normal distribution and reducing the number of collocation nodes needed.

For the high-dimensional (multivariate) runs, Fejer nodes produced mixed results. In terms of PDF, the mapped Fejer nodes achieved a better match than the boxed Fejer nodes; however, in terms of the first two moments it was found that boxed Fejer nodes produced a more stable output. A possible reason for this discrepancy (between visual and moment analysis) is that, in general, PCM does not approximate tail events very well as its main focus is to approximate the high probability region of the random inputs. Furthermore, the mapped Fejer nodes are relatively more compressed around the high probability region compared with the boxed Fejer nodes. In general, the PDFs produced by PCM using Fejer sampling were found to be mostly within the confidence region of the MCS PDF for all reservoir models.

A common theme that was encountered was that output PDF's usually have uniquely different shapes compared to the input PDF's. Because the numerical solver (ECLIPSE) is a non-linear model, output PDFs will not necessarily reproduce the input PDF. This could explain why even for the single random input parameter case where the variable is normally distributed the output PDF shape is quite distinct, transformations are therefore expected. When considering the effect of reservoir models on the performance of the PCM, it is apparent that different reservoir models would favour different PCM methods and produce different output distributions accordingly.

An attempt was made to see if using Richardson's extrapolation (**Richardson 1911**) can be used to extend the results obtained by PCM. This was done by applying the extrapolation to the estimated mean and standard deviation that were obtained using the PCM proxy polynomial (see **Figures 6.6, 6.11, 6.13 and 6.15**). The intention was to see if by using the extrapolation it would be possible to obtain estimates for the mean and the standard deviation for higher PCM orders using the low order estimates. A MATLAB routine (**Ulerich 2009**) was applied to these estimates. The results showed that applying the extrapolation produced values that did not vary significantly compared with the highest order PCM obtained values. At most, the estimated values would vary in the 4^{th} decimal place. The analysis was performed using a grid refinement factor of 3.

Fig. 6.16 illustrates the reduction in computational time that can be achieved using PCM. It shows that PCM can be faster than MCS upto 2 orders of magnitude for univariate and bivariate cases, and 1 order of magnitude for high-dimensional cases depending on the order of the proxy polynomial model. This shows a significant enhancement in quantifying uncertainty in contrast to MCS. For real reservoir models that consist of significantly larger number of grid cells, MCS will not be applicable because it is computationally prohibitive given the amount of time to complete one simulation run. Thus PCM can mitigate this problem to a certain extent and make it possible to quantify uncertainty for these reservoir models.

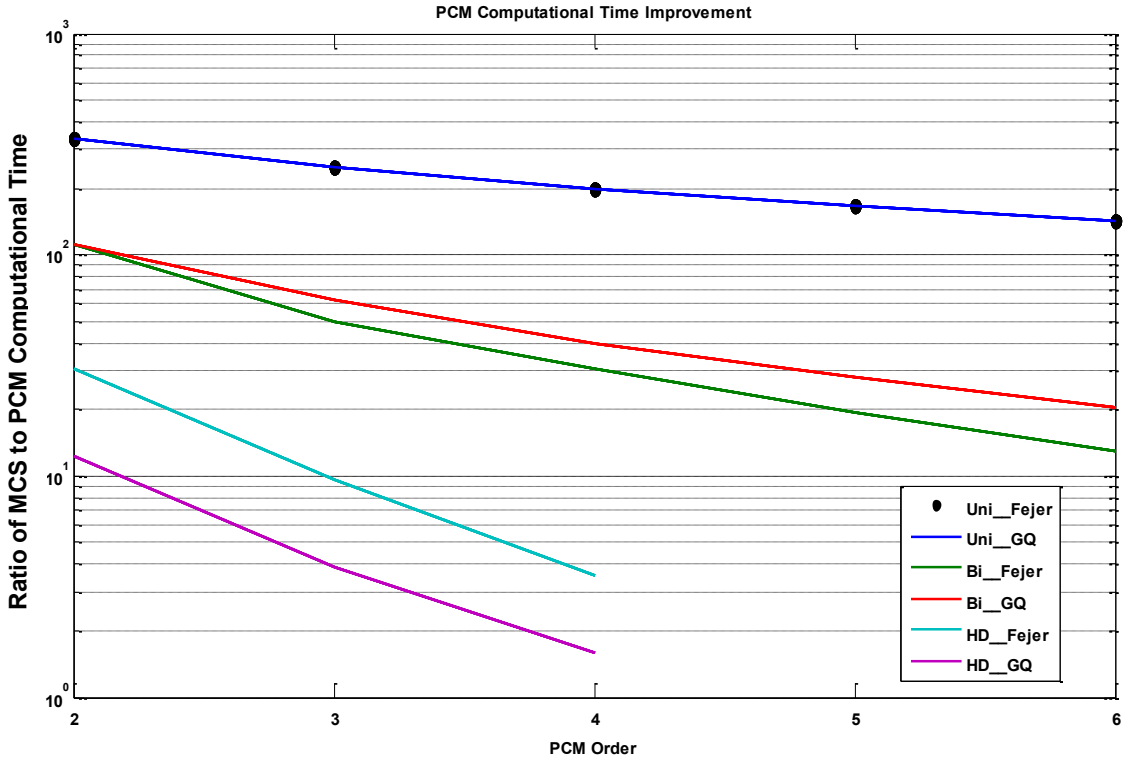


Fig. 6.16– Plot of computational time reduction achieved by PCM as a function of PCM order. The Y-axis shows the ratio of the computational time required to run MCS for 1000 realizations as the benchmark to the computational time required to run PCM. [Uni: Univariate, Bi: Bivariate and HD: High Dimensional]

Although using the PCM to quantify parametric uncertainty is more efficient than MCS, it still requires numerous realizations for high-dimensional random input runs. Simplified reservoir models were used in this chapter which made it possible to perform the PCM in a manageable time frame, however, improvements will be necessary to extend the PCM to high-dimensional cases for highly complex reservoir models which could require significant computational requirement to perform even one simulation run.

The sampling methods used to obtain the collocation nodes affect the efficiency of PCM. **Xiu and Hesthaven (2005)**, **Nobile et al. (2008)** and **Foo et al. (2008**) discuss the enhancement of PCM performance by using sparse sampling grids. Thus it could be beneficial to use sparse grid sampling methods to reduce the required computational effort. Another improvement would be to use sampling methods that are not directly dependent on the order of approximation, such as the method discussed in (**Sarma and Xie 2012**). This could enhance computational efficiency**.** In addition, it could be desired to use arbitrary distributions for the random input variables which could be more representative of reality (**Li et al. 2011**). This is possible by generating PCE's for arbitrary distributions numerically using, for example, the ORTHPOL (**Gautschi 1994**) suite of algorithms. In this chapter, the PCM was applied to quantify parametric uncertainty; it is also possible to apply the PCM for spatial uncertainty such as the permeability and porosity fields. This can be applied by approximating the permeability or porosity fields with the Karhunen-Loeve expansion (**Li and Zhang 2007; Li and Zhang 2009**).

6.3 Concluding Remarks

The PCM was applied to quantify parametric uncertainty for a surfactant-polymer flood. The output polynomial chaos coefficients were solved for using either Gaussian quadrature or linear regression. The different sampling methods used for the linear regression approach were: Gaussian quadrature, mapped and boxed Fejer sampling. The method was applied to four example models for random univariate, bivariate and multivariate runs. The recovery factor was chosen as the output parameter to be approximated. Results were compared with benchmark MCS runs. The metrics used for the efficiency of the method were the resulting PDFs and the first two moments.

In general, solving the output polynomial chaos coefficients with Gaussian quadrature was found to be more accurate than with linear regression using quadrature nodes. The boxed and mapped Fejer nodes did achieve good visual agreement in terms of the PDF with MCS, yet they produced mixed results in terms of the first two moments. When considering the number of nodes that Gaussian quadrature requires for a high-dimensional case, it is more efficient to use linear regression with Fejer sampling. PCM achieved a reduction in computational time of upto two orders of magnitude.

Sequence acceleration approaches such as the Richardson extrapolation were attempted using the PCM estimated statistical moments to see whether these lower order estimates could be used to obtain higher order estimates using the extrapolation. The results showed little variation on the PCM estimates. Other sequence acceleration techniques could be attempted. This would require further investigation.

The PCM can be enhanced to improve its performance. Some of these improvements include: approximation order independent sampling, improved sparse grid sampling, incorporating arbitrary random input distribution that can be more representative of reality and quantifying spatial uncertainty. The application of the method can be easily extended to other EOR processes for parametric uncertainty quantification. By quantifying uncertainty efficiently and robustly, it is possible to produce more accurate control policies and possibly realize the significant potential of chemical EOR processes. By coupling the PCM sampling techniques with the LSM method effectively replacing the Monte Carlo sampling element in the algorithm, it is desired that this would produce accurate VoF and optimal policies using significantly fewer samples. This is discussed in the next chapter.

7 The Least Squares Probabilistic Collocation Method: Case Studies

7.1 LSPCM Case Studies

After introducing the LSPCM, the approach is applied gradually to test whether it can approximate the performance of the LSM method in an efficient manner. First, the LSPCM is applied to different reservoir models assuming no uncertainty in the time series of the technical random parameters, $\mathbb{T}_i$. Then, the uncertainty in the time series is incorporated in the application of the LSPCM. Finally, the LSPCM applicability is extended to more complex decision scenarios.

7.1.1 Initial Application

The LSPCM algorithm was applied to three examples to evaluate the timing decision of SP flood. Each reservoir model will produce its unique response to the decision because of the different heterogeneity and reservoir fluid data sets for each model. The aim was to use the homogenous model as an initial attempt and then apply the method to heterogeneous permeability fields and well known benchmark reservoir models. In these applications, uncertainty in the time series of the technical state variables was not considered.

By substituting the Monte Carlo sampling with PCM sampling the aim is to achieve similar results to the LSM with significantly fewer simulation runs. **Fig. 7.1** shows the results of performing the LSPCM assuming a four dimensional random input case for a second, third and fourth order approximations using the following sampling methods: the Fejer and quadrature nodes. The PDFs of the VoF show that for the homogeneous model, using boxed Fejer nodes achieves relatively a good visual match with the MCS produced result. The PDF's for the PUNQ-S3 model show good visual agreement with the LSM PDF. Using the third order mapped Fejer nodes, relatively the same PDF as that of MCS can be obtained while using only 120 nodes. This is an improvement of a factor of 8.3 compared with MCS. As for the SPE10M model, the most visually efficient result was obtained using second order Gaussian quadrature nodes requiring 81 realizations resulting in an improvement of a factor of 12.3.

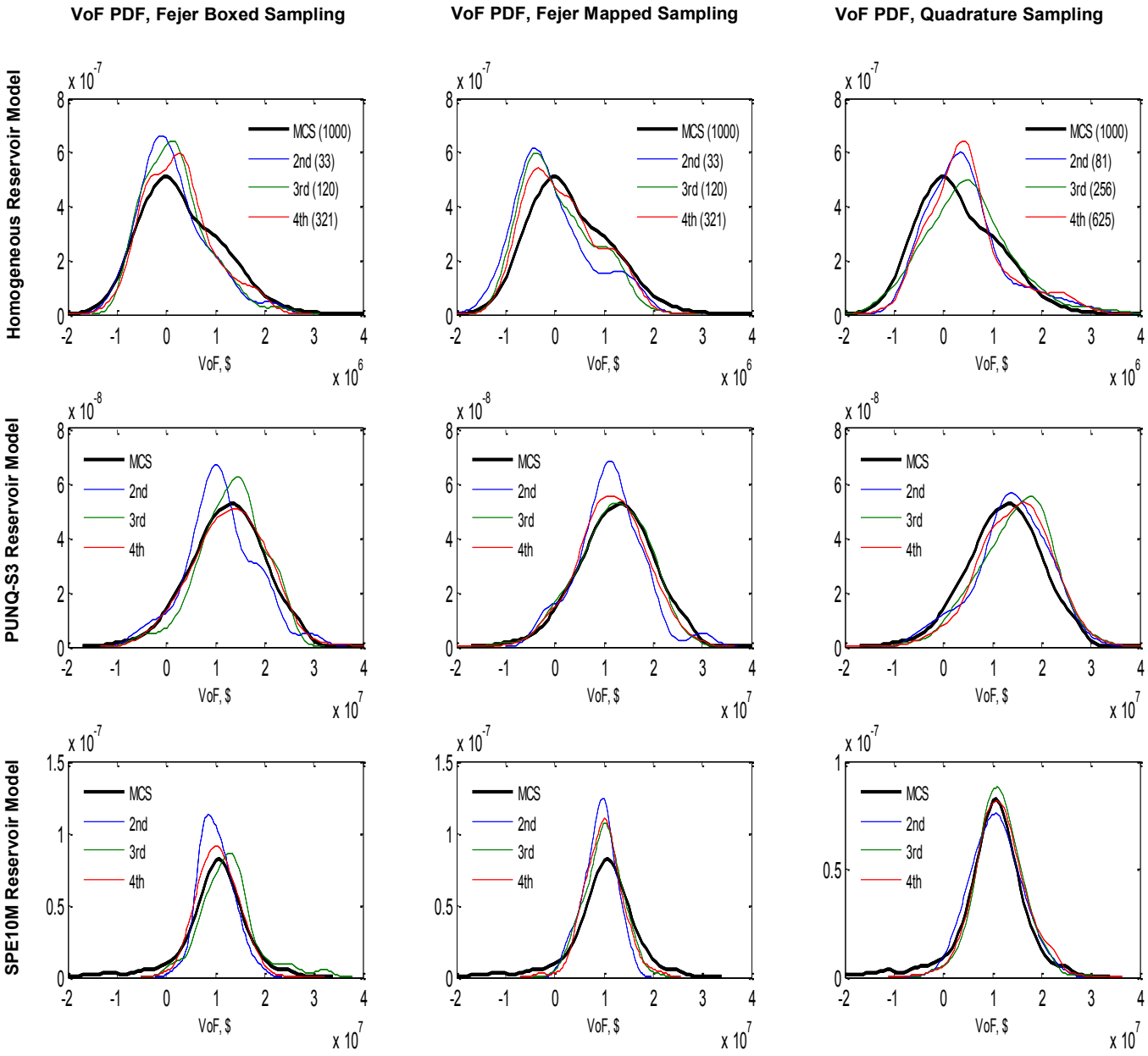


Fig. 7.1[29]– PDF for the option value (i.e. VoF) determined by the LSPCM method using second, third and fourth order collocation nodes compared with that determined by MCS (the original LSM). The number of realizations used is shown in parentheses for each sampling method in the first row. Each row is specific to a reservoir model while each column is specific to the sampling method mentioned at the top of the column.

Fig. 7.2 shows the optimal policy histograms for all the reservoir models. The histograms obtained using the LSPCM are scaled to the histogram produced by the LSM. For the homogeneous model, the scaled LSPCM histograms for all orders and sampling methods used exhibit similar trends to the LSM histogram. For the PUNQ-S3 model, the optimal policy histograms obtained by the LSPCM show good agreement with the LSM produced policy, the only exception were the results obtained by second order boxed Fejer samples, which show a clear discrepancy. The policy histograms obtained for the SPE10M model show a generally good agreement with the LSM produced policy histogram. To test the accuracy of the LSPCM, the Root Mean Square Relative Error (RMSRE) of the mean VoF is used. This based on assuming a benchmark of the LSM mean VoF. The RMRSE is defined as follows:

[29] This figure is reproduced from **Alkhatib and King (2013b)**.

$$\text{RMSRE} = \sqrt{\frac{1}{M}\sum_{i=1}^{M}\frac{\hat{F}_i - F}{F}} \qquad \text{Eq. 7.1}$$

, where M is the total number of realizations, $\hat{F}_i$ is the VoF determined from the LSPCM for realization i and F is the benchmark VoF (from the LSM). **Fig. 7.3** shows the plots of the RMSRE as a function of PCM order. For the homogeneous model, fourth order PCM sampling achieves relatively the best approximation. Third order PCM sampling using mapped Fejer nodes achieves the best performance relative the number of samples used; 120 as opposed to 321 for fourth order PCM. As for the modified SPE10 model, third order PCM sampling using mapped Fejer nodes achieve the most efficient approximation. In general, the RMSRE was found to decrease as the PCM order increased. The only exception was for the third order boxed Fejer nodes for the modified SPE10 model. Based on this metric, the LSPCM can produce relatively accurate results using significantly fewer samples.

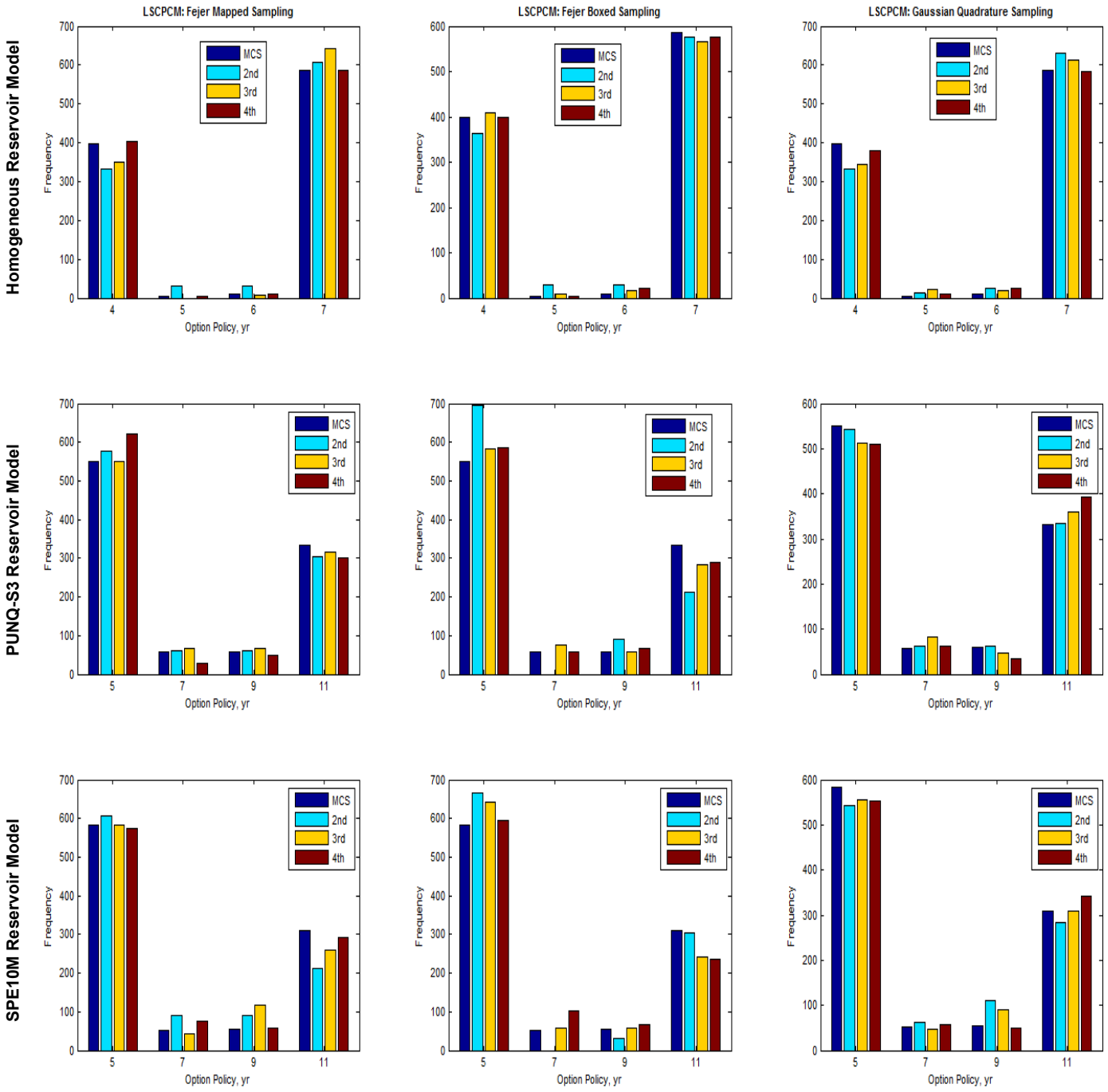


Fig. 7.2[30]– Histograms of the optimal policy produced by the LSPCM method using second, third and fourth order collocation nodes and compared with that produced by the LSM method. Each row is specific to a reservoir model while each column is specific to the sampling method mentioned at the top of the column. The frequency obtained for the LSPCM generated policy is scaled to the frequency of the LSM (using MCS) generated policy.

[30] This figure is reproduced from **Alkhatib and King (2013b)**.

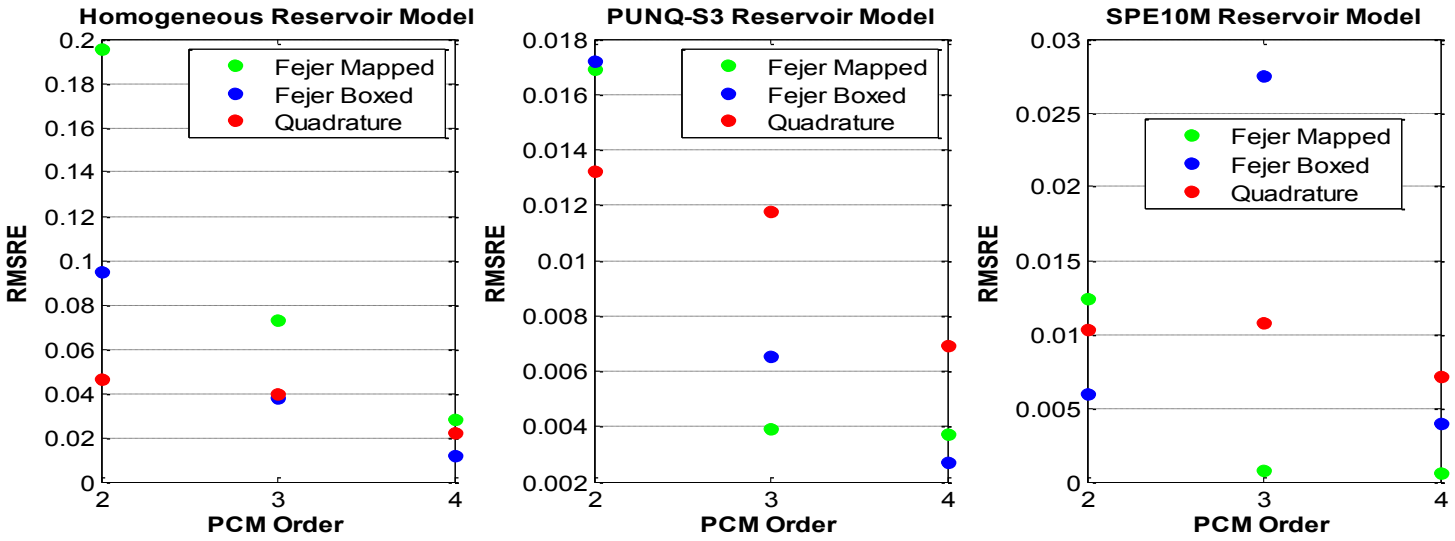


Fig. 7.3– RMSE plots as a function of PCM order for the different reservoir models.

Using both the VoF PDF and RMSRE results, the performance of the LSPCM was further analysed with respect to the LSM results. The following LSPCM runs were chosen for this comparison: Fourth order mapped Fejer sampling for the homogenous model, third order mapped Fejer sampling for the PUNQ-S3 model and second order Gaussian quadrature sampling for the SPE10M model. **Fig. 7.4** shows the results of this comparison. The first column shows the maximum (optimal) NPV values per realization plotted in ascending order. The corresponding static (no flexibility) policy NPV is plotted as well. For all reservoir models, most realizations achieve a higher NPV when flexibility is incorporated into the decision rather than the static policy. The second column shows the same plot in the first column, but for the results of the LSPCM algorithm chosen for comparison for each model. The general trends exhibited from the LSM results are maintained. The third column shows a plot of optimal NPVs for the LSM and the LSPCM algorithms per realization sorted in ascending order where the number of realizations for the LSPCM is scaled to the number of realization (10^3) used for the LSM algorithm. Once again, general agreement with the trends of the LSM algorithm is observed, although there are slight discrepancies in the extreme lower and higher optimal NPVs for the homogeneous and PUNQ-S3 models.

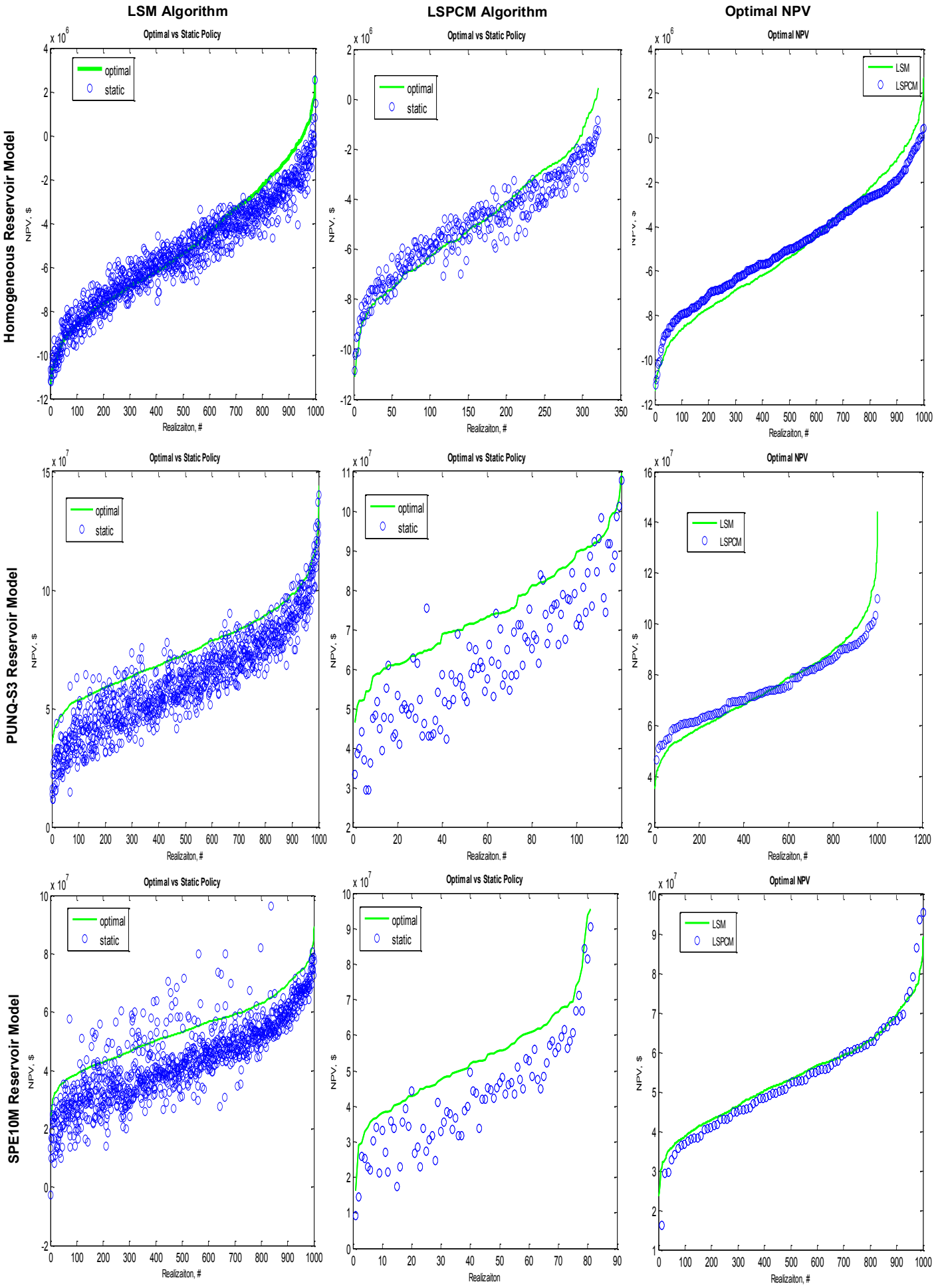


Fig. 7.4– Results comparing the performance of the LSPCM algorithm with the LSM algorithm for the homogeneous, PUNQ-S3 and SPE10M reservoir models without incorporating uncertainty in the time series.

In summary, the PCM can enhance the performance of the LSM method by using efficient sampling methods conditional on the random input probability distributions. By improving performance of up to an order of magnitude with respect to simulation time (refer to **Fig. 6.16**), the LSPCM significantly reduces the computational requirement by requiring fewer reservoir simulations. Given that the same decision problem was evaluated or the different reservoir models, the output was shown to be reservoir unique, which agrees with the results obtained by the original LSM method. The optimal policy histograms also show that the LSPCM was able to preserve the general trends that were generated by the LSM. Accuracy was measured by the RMSRE and found that the LSPCM can produce an efficient approximation of the LSM.

The technical random inputs were assumed to be constant throughout time for the applications in this subsection for simplicity. After demonstrating that the LSPCM can produce efficient approximations to the LSM method, the next task was to apply this method to capture the uncertainty in the time series for the technical random inputs similar to the approach followed in chapter 4 and in **Alkhatib et al. 2013**.

7.1.2 Incorporating Uncertainty in the Time Series

In the previous subsection, uncertainty in the time series of the technical random parameters, $\mathbb{T}_i$, was not considered. This is the objective of this subsection, where uncertainty in the time series will be incorporated with the LSPCM for the PUNQ-S3 reservoir model to test whether the LSPCM can produce an efficient approximation of the LSM method. **Fig. 7.5** shows the results obtained using the LSPCM. 2nd and 3rd order mapped Fejer nodes produce a good visual match with the MCS PDF. The policy histograms show that the general trends are maintained by the LSPCM.

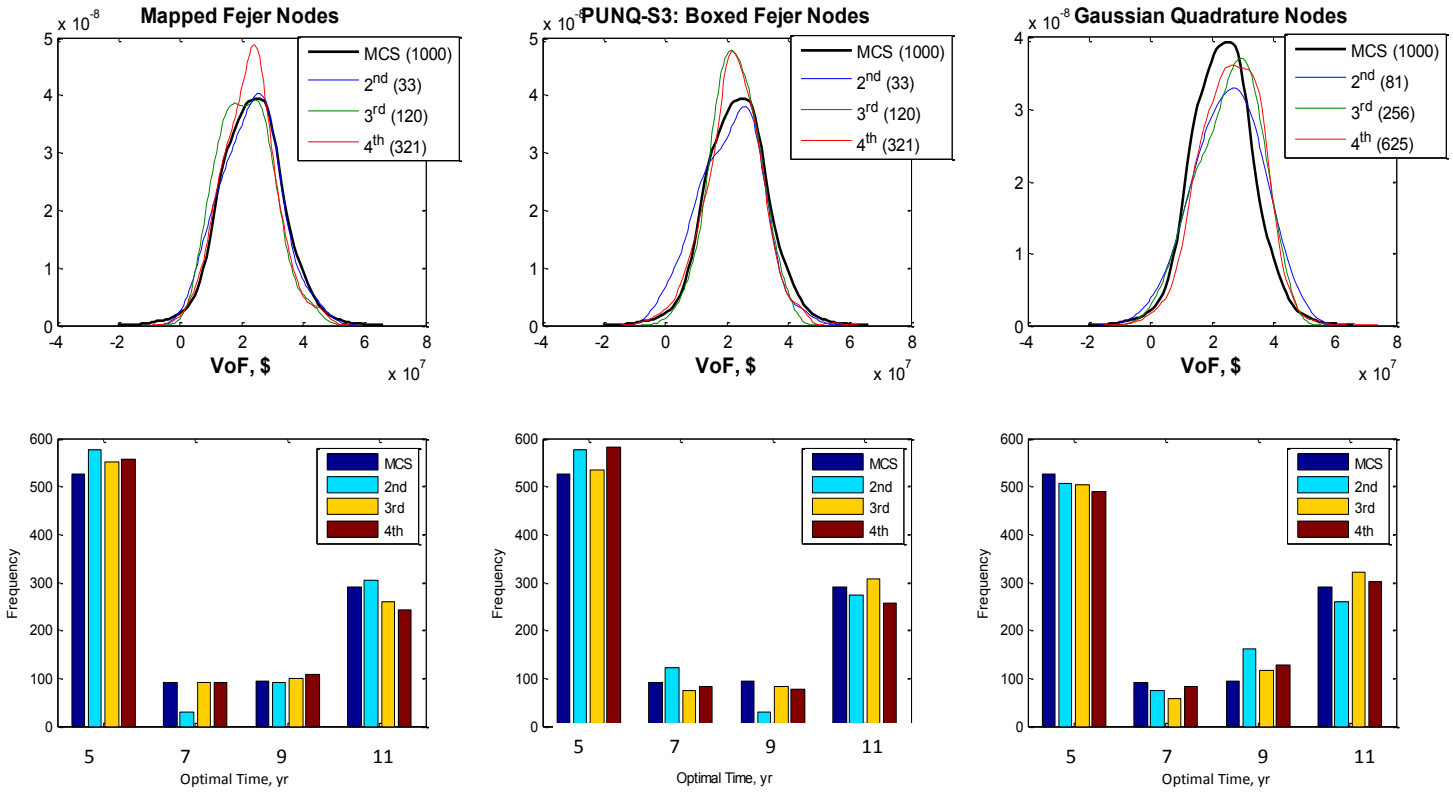


Fig. 7.5– VoF PDF plots and optimal policy histograms for the LSPCM generated results for the PUNQ-S3 reservoir model incorporating uncertainty in the time series. Histogram frequency values are scaled to 10^3 realizations.

The RMSRE are plotted in **Fig. 7.6**. A general decreasing trend with increasing order is observed. The RMSRES values are in the same order of magnitude as those obtained for the PUNQ-S3 model without considering uncertainty in the time series (see **Fig. 7.3**).

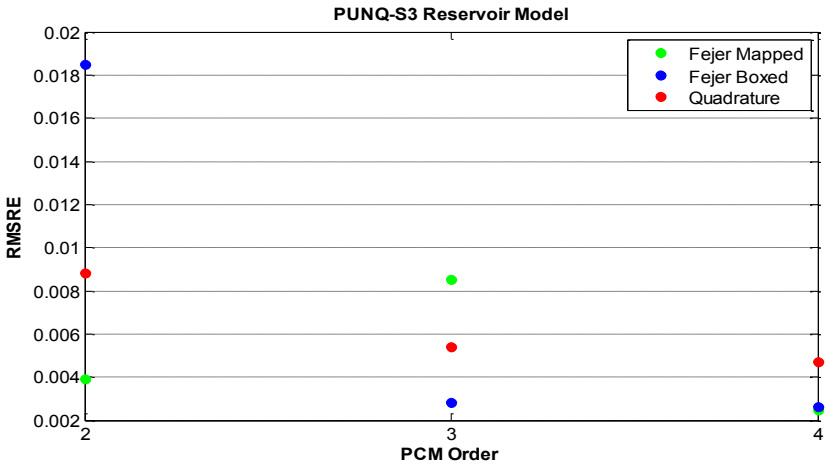


Fig. 7.6– RMSRE plots as a function of PCM order for the PUNQ-S3 reservoir model incorporating uncertainty in the time series.

Based on the results shown in **Fig. 7.5** and **7.6**, the LSPCM results obtained using 2nd order mapped Fejer nodes were chosen for further analysis. **Fig. 7.7** show that the optimal policy trend was maintained and that the optimal NPV comparison plot shows good agreement with the LSM obtained results. Thus it is sufficient to use the 33 nodes of the 2nd order mapped Fejer sampling to approximate the LSM Based on the results for the PUNQ-S3 reservoir model, extending the LSPCM to incorporate uncertainty in the time series of the technical parameters is possible. Application for other reservoir models might vary as response is reservoir-unique.

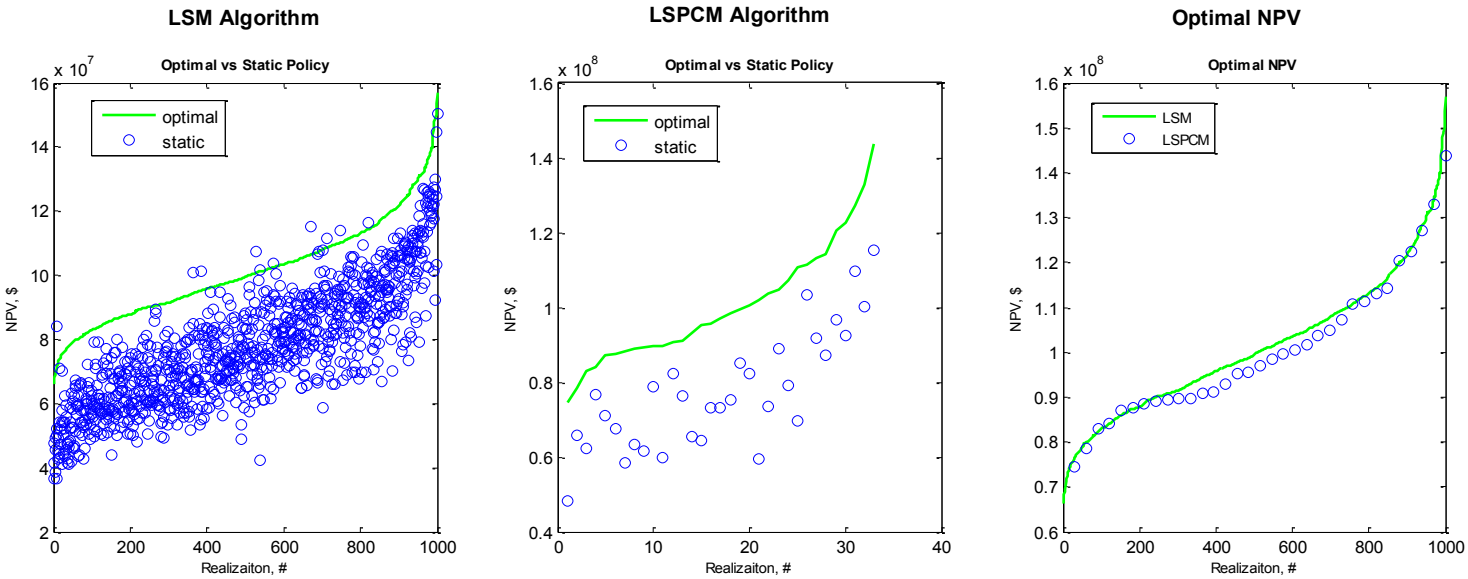


Fig. 7.7– Results comparing the performance of the LSPCM algorithm with the LSM algorithm for the PUNQ-S3 reservoir model incorporating uncertainty in the time series. The LSPCM results were obtained using 2nd order mapped Fejer nodes. Realizations are scaled to 10^3 realizations.

7.2 Possible Extensions

This section introduces some possible extensions the use of the LSM and LSPCM approaches. Initially, the LSM method was demonstrated using a simple decision scenario; timing the SP flooding process. There are possible extensions to the algorithm that can be applied to value more complex decisions involving multiple embedded decisions, where one decision gives the possibility to execute another decision or when there are mutually exclusive decisions to be undertaken at discrete decision times.

The scalability of the LSM method is also demonstrated with respect to other EOR processes. Alkaline-Surfactant-Polymer (ASP) flooding is considered where the additional decision of injecting alkaline prior to the SP slug is considered along with the timing of the process.

7.2.1 Mutually Exclusive Decisions

Previously a simple decision of when to start implementing the Surfactant-Polymer flood was considered. In reality, decisions are high-dimensional. In this section, an extension to the decision valuing framework demonstrated above is introduced. This extension will value the flexibility of having an additional decision embedded within the timing decision. This is defined as having mutually exclusive alternatives available where one alternative excludes the other alternatives once chosen. There are many control variables that need to be considered to implement the SP flood efficiently such as changing production constraints or chemical slug size. The existing timing decision is extended to incorporate flexibility in the surfactant slug size and concentration. Here two sets of controls are assumed for the injected surfactant slug: a high concentration small PV slug and a low concentration large PV slug. This corresponds to a 3% wt. 0.10 PV slug and a 0.6% wt. 0.50 PV surfactant slug. The mobility buffer properties were left unchanged; 3% wt. and 1PV polymer slug.

If there are U available mutually exclusive embedded decisions (alternatives) at any decision time, y, the optimal control can be defined as a couple (τ, u), where τ is the optimal initiation time and $u \in U$. The Bellman dynamic programming equation becomes:

$$\mathrm{OV}(y, \mathbb{P}_{i,y}, \mathbb{T}_{i,y}) = \max_{(\tau,u)}\left\{ e^{-r(\tau - y_n)}\, E_y^*\left[V_u(\tau, \mathbb{P}_{i,\tau}, \mathbb{T}_{i,\tau})\right]\right\} \quad \text{Eq. 7.2}$$

, which expands to:

$$\mathrm{OV}(y, \mathbb{P}_{i,y}, \mathbb{T}_{i,y}) = \max\left\{V_{u_1}(y_n, \mathbb{P}_{i,y_n}, \mathbb{T}_{i,y_n}), \dots, V_U(y_n, \mathbb{P}_{i,y_n}, \mathbb{T}_{i,y_n})\, e^{-r(y_{n+1} - y_n)}\, E_{y_n}^*\left[\mathrm{OV}(y_{n+1}, \mathbb{P}_{i,y_{n+1}}, \mathbb{T}_{i,y_{n+1}})\right]\right\}$$
Eq. 7.3

The decision rule along the path, x, then becomes:

If $\Phi\left(y_n, \mathbb{P}_{i,y_n}(x), \mathbb{T}_{i,y_n}(x)\right) \leq \max_h\{V_u\left(y_n, \mathbb{P}_{i,y_n}(x), \mathbb{T}_{i,y_n}(x)\right)\}$ then $(\tau, u)(x) = (y_n, \bar{u})$ Eq. 7.4

where $\bar{u} = \arg\max_h\{V_u\left(y_n, \mathbb{P}_{i,y_n}(x), \mathbb{T}_{i,y_n}(x)\right)\}$ Eq. 7.5

and $(\tau, u)(x) = (\tau(x), u(x))$. Eq. 7.6

The continuation value is then defined as:

$$\Phi\left(y_n, \mathbb{P}_{i,y_n}(x), \mathbb{T}_{i,y_n}(x)\right) = E^*_{y_n}\left[\sum_{i=n+1}^{N} e^{-r(y_i - y_n)} V\left(y_n, \mathbb{P}_{i,y_n}(x), \mathbb{T}_{i,y_n}(x), (\tau, u)(x)\right)\right] \quad \text{Eq. 7.7}$$

, which is approximated by Φ^J. In order to apply the decision rule OV needs to be estimated. Since $V_u\left(y_n, \mathbb{P}_{i,y_n}(x), \mathbb{T}_i(x)\right)$ is known for $u = 1, \ldots, U$, then we have:

$$OV_u(y_n, \mathbb{P}_{i,y_n}(x), \mathbb{T}_{i,y_n}(x)) = \max\{V_u\left(y_n, \mathbb{P}_{i,y_n}(x), \mathbb{T}_{i,y_n}(x)\right), \Phi_u\left(y_n, \mathbb{P}_{i,y_n}(x), \mathbb{T}_{i,y_n}(x)\right)\} \quad \text{Eq. 7.8}$$

Because this is a direct extension of the LSM algorithm, the convergence of the results are maintained (**Gamba 2003**).

For embedded decision regarding the surfactant slug properties, there are two elements in the control space,$U = [u_1, u_2]$. The control decision is embedded with the original timing decision, $Y = [y_1, y_2, y_3, y_4]$. This decision is valued for the three reservoir models used in **7.1.1**. Based on the findings of applying the LSPCM in **7.1.1**, the fourth order mapped Fejer sampling was used to approximate the technical uncertainties for the homogeneous reservoir model and the third order mapped Fejer sampling used for the PUNQ-S3 reservoir models. As for the modified SPE10 model, the second order Gaussian quadrature sampling was used. The results are shown in **Fig. 7.8**.

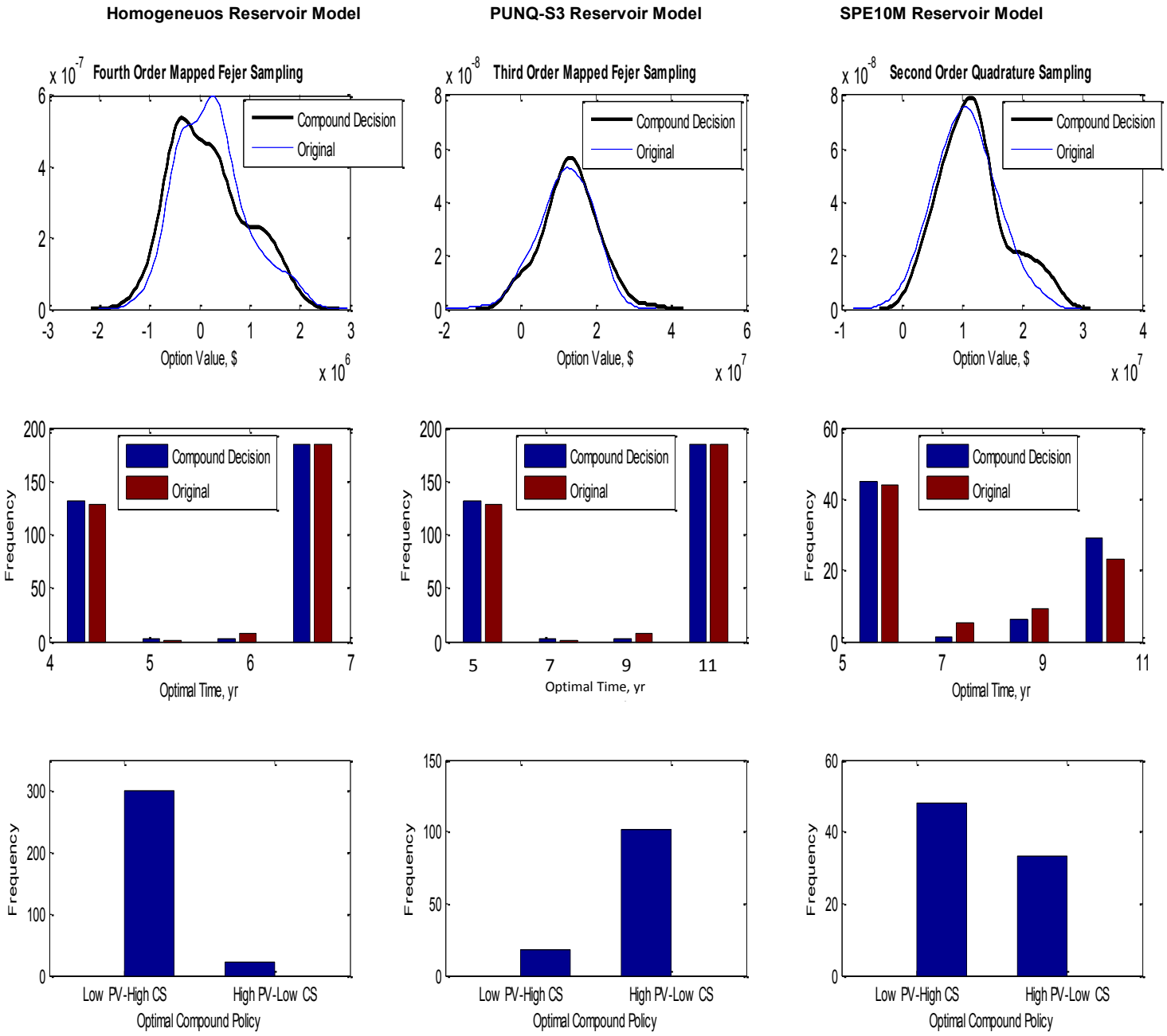


Fig. 7.8– Results for embedded decision scenario. The first row shows the PDFs of the option values. The second row shows the optimal policy histograms of the initiation decision and the third row shows the histograms of the optimal embedded policy which is the surfactant slug properties (CS: surfactant concentration).

The option value PDFs and the optimal policy histograms are compared with those of the same approximations for the initial timing decision. The option value PDFs show some discrepancy when compared to the initial decision for the PUNQ-S3 and SPE10M models. The homogeneous model PDFs show a larger discrepancy. As for the optimal policy histograms, more realizations would support later initiation given the ability to vary the control strategy for the SPE10M model. The PUNQ-S3 model exhibits a reverse tendency favoring earlier initiation. The homogeneous model produces little or no discrepancy where most realizations favored the original surfactant slug properties. The PUNQ-S3 model favored the high PV and low concentration slug properties for most realizations, whereas some realizations favored flexibility in surfactant slug control for the SPE10M model.

In general, flexibility in surfactant slug properties seems to be useful for the heterogeneous reservoir models and not useful for the homogeneous model. Varying the surfactant control parameters for the homogeneous reservoir model is of little value due to its simple permeability structure which ensures a smooth propagation of the surfactant bank, the original surfactant slug properties were sufficient enough to produce the incremental oil. Because the two other models are heterogeneous and relatively more realistic, the propagation of the surfactant bank will not be as smooth and varying the surfactant slug properties could be an important contingency conditional on the realization of the technical uncertainties. However, in general, acquiring flexibility in the surfactant slug properties does not alter the distribution of the option value significantly compared with the original decision. The method can be extended to other control decisions in a similar manner.

7.2.2 Application to Alkaline-Surfactant-Polymer Flooding

Applying the LSM method and the LSPCM to another chemical EOR process is demonstrated in this subsection. Here, the decision whether to inject alkaline along with the SP flood is coupled with the timing decision in order to reduce surfactant and polymer adsorption and thus improve oil recovery (**Lake 1989; Green and Willie 1998;Sheng 2011**). This is also applied to the PUNQ-S3 reservoir model. An additional technical uncertainty is included in this analysis: alkaline adsorption. It is assumed to follow the same distribution as that of surfactant and polymer adsorption, see **Table 7.1**. This results in five technical uncertainties which increase the dimensionality of the LSCPM so it will limit the maximum PCM order that can be used. Thus, 2nd and 3rd order Fejer nodes and 2nd order Gaussian quadrature nodes were used as the samples increase rapidly beyond that and the PCM becomes redundant when compared with MCS. The simulation of alkaline for ASP flooding is discussed in **Appendix H**. The alkaline is injected with the surfactant slug with a fixed concentration of 1 % wt**.** and 0.10 pore volume. The economic model incorporates the alkaline price [31]as a uniformly distributed parameter~ U[1,2] **$**/kg. See **Appendix I** for alkaline related properties used in ECLIPSE. The VoF is obtained based on a static scenario of ASP flooding. For this example, uncertainty in the time series of the technical parameters was not considered.

Table 7.1 Random input parameters and their distributions

Random Input	Distribution	Bounds
Residual oil saturation to surfactant flooding, fr	Uniform	[0,0.2]
Surfactant adsorption, g/g rock	Normal	(-8,1)
Polymer adsorption, g/g rock	Normal	(-8,1)
Polymer viscosity multiplier	Uniform	[1,10]
Alkaline adsorption, g/g rock	Normal	(-8,1)

Where the normally distributed parameters undergo a transformation of the following form:

$$D_i = e^q, \text{ where } i = \text{surfactant, polymer or alkaline and } q \sim N(-8,1) \qquad \text{Eq. 7.9}$$

[31] Alkaline price bounds are obtained from **Thomas (2006)**.

The results (see **Fig. 7.9**) show that the boxed and mapped Fejer nodes give reasonable VoF PDF matches with the MCS PDF. All sampling methods generally maintained the same trends as those observed for the LSM method. The results indicate that for most realizations, SP flooding was favored as opposed to ASP flooding. Since the VoF is based on an ASP flooding static scenario, this might indicate that the improvement in oil recovery due to reduced surfactant/polymer adsorption does not justify the added cost of the alkaline chemical. Other factors contribute to this such as the alkaline dependent surfactant/polymer adsorption multipliers, see **Appendix I**.

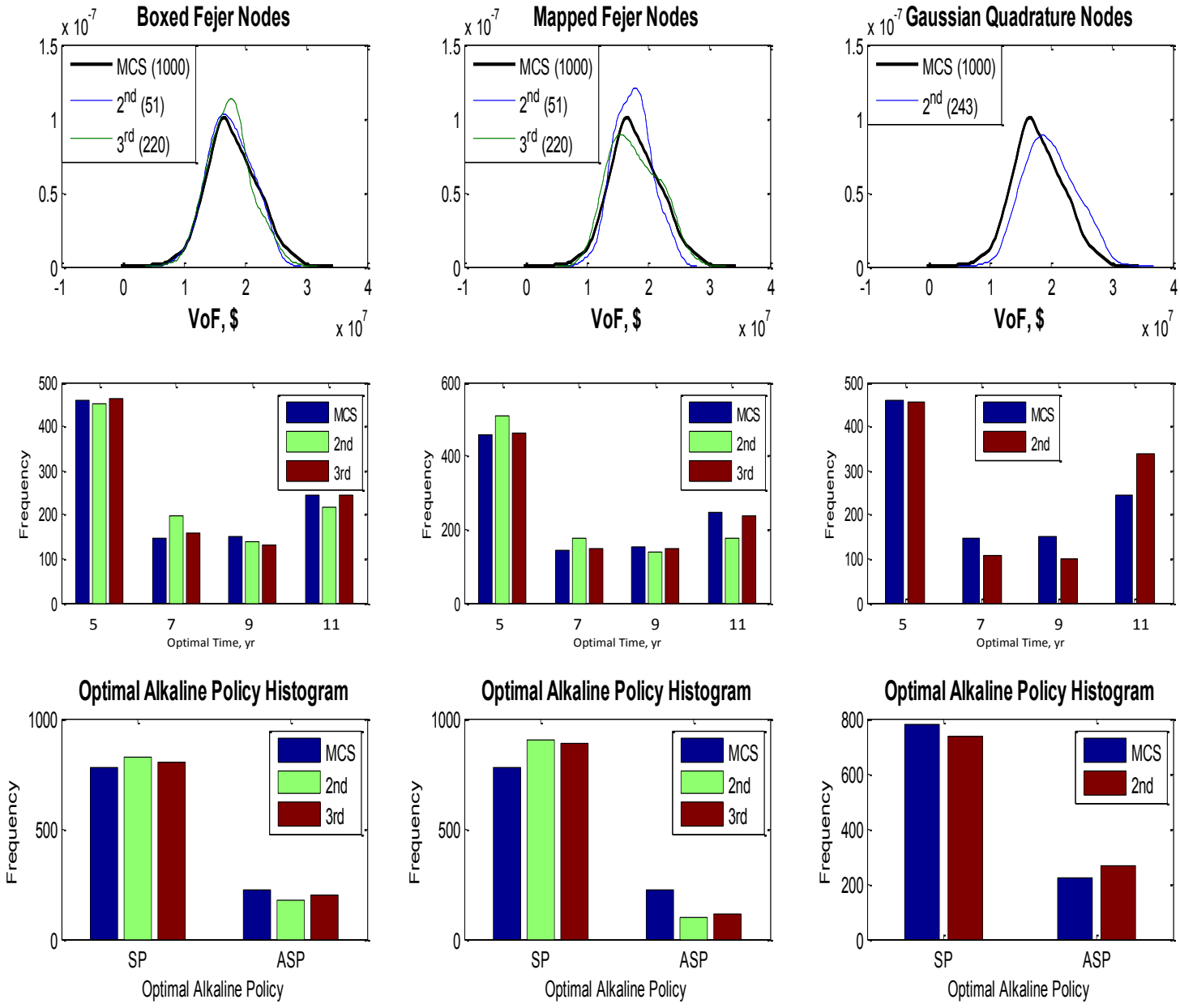


Fig. 7.9— VoF PDF and policy histograms for the ASP flooding decision evaluation for the PUNQ-S3 reservoir model. The first row shows the PDFs of the VoF. The second row shows the optimal policy histograms of the initiation decision and the third row shows the histograms of the optimal alkaline policy, the frequency is scaled to 10^3 realizations in order to be compared with the LSM generated results.

The RMSRE plot (see **Fig. 7.10**) shows that all sampling methods achieve a relatively accurate approximation of the LSM method. The third order Mapped Fejer nodes produce the most accurate approximation, although the second order boxed and mapped Fejer nodes achieve decent approximations. Using the most accurate results based on RMSRE, **Fig. 7.11** show the comparison plots between the LSM and LSPCM approaches. The plots show that the optimal policy obtained by these approaches always maximizes the objective function when compared to the static policy. Also, the comparison between the optimal policy plots obtained by the LSM method and the LSPCM shows very good agreement. Thus for a relatively more complex decision which incorporates another EOR process, the LSM and LSPCM produce meaningful policies while taking into consideration technical and economic uncertainties. Future application for this example would include uncertainty in heterogeneity and uncertainty in the time series of the technical parameters.

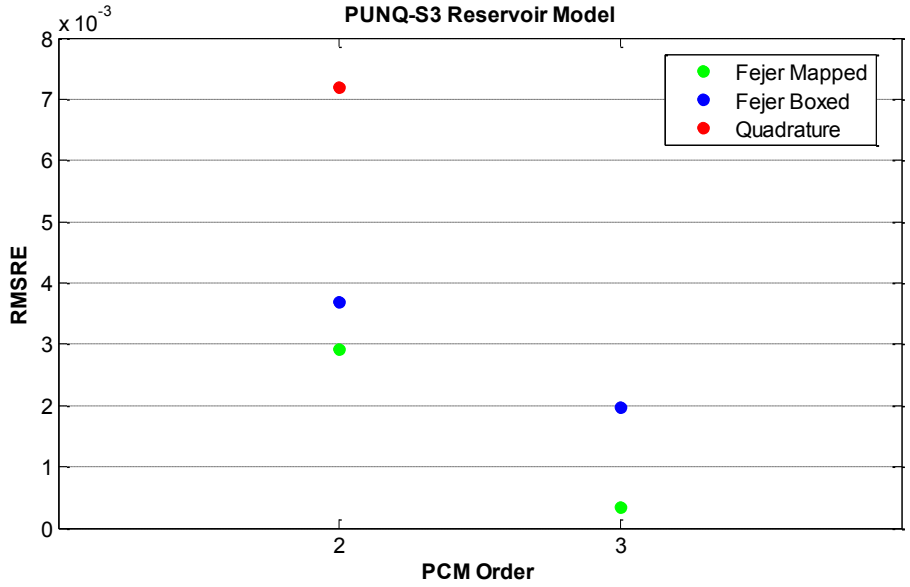


Fig. 7.10– RMSRE plots as a function of PCM order for the PUNQ-S3 reservoir model for the ASP flooding decision.

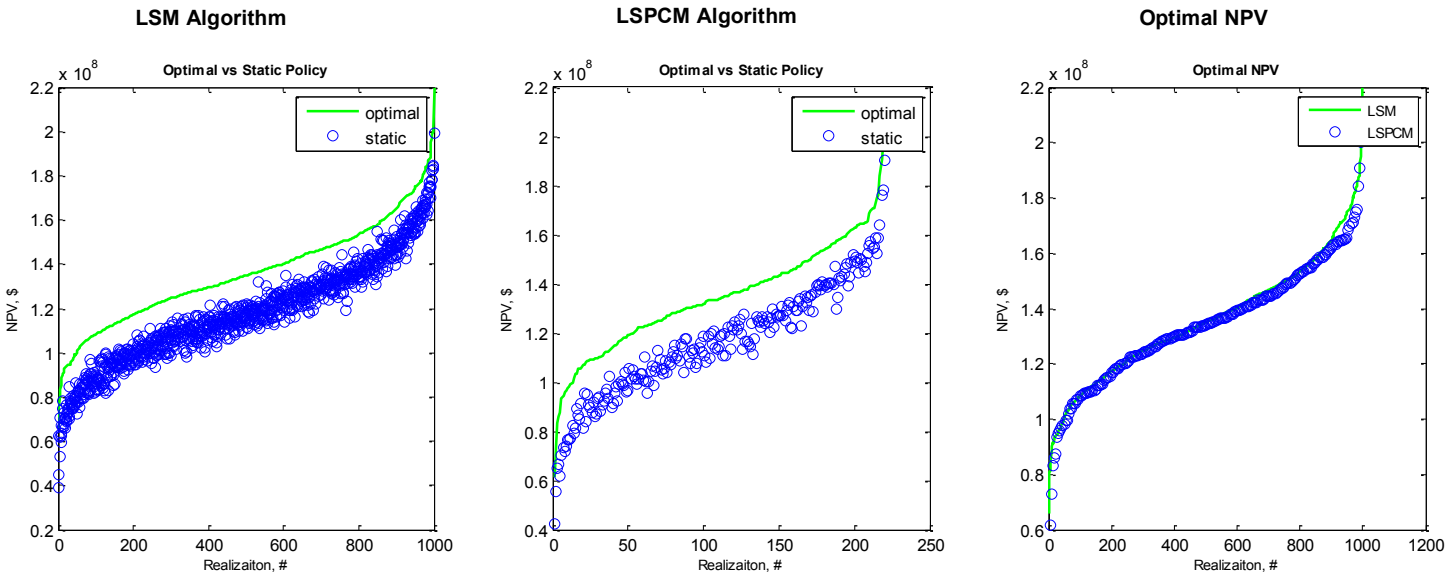


Fig. 7.11 –Results comparing the performance of the LSPCM algorithm with the LSM algorithm for the PUNQ-S3 reservoir model for the ASP flooding decision. The LSPCM results were obtained using 3rd order mapped Fejer nodes.

7.3 **Concluding Remarks**

This chapter discussed the application of the LSPCM approach as an efficient optimization of the LSM method with respect to computational requirement. The LSPCM was first demonstrated on three reservoir models which were used to demonstrate the PCM in Chapter 5. This initial application assumed no uncertainty in the time series of the technical random parameters. The purpose of this initial application was to demonstrate whether the LSPCM would produce accurate results efficiently with respect to the LSM method. Once this was established, uncertainty in the time series was then considered.

The results showed that LSPCM did produce relatively accurate results based on the VoF PDFs, policy histograms and on the RMSRE which used the LSM result as the benchmark for comparison. Thus, by approximating the technical state space using PCM sampling techniques, it is possible to enhance the performance of the LSM approach. Uncertainty in the time series was also captured by the LSPCM as shown in **7.1.2**. In general, results were also reservoir unique.

The other objective of this chapter was to apply the LSPCM to more sophisticated decision scenarios in order to demonstrate the scalability of the LSM approach in general. This was done by designing a complex decision scenario where the flexibility in surfactant slug properties was incorporated with the timing decision. The other scalability example relates to complex decisions and applicability to other chemical EOR processes; ASP flooding. In this example, the injection of alkaline was incorporated as an additional flexibility along with the timing decision. The benefit of adding alkaline would be to reduce surfactant adsorption. In this case, alkaline adsorption was added as an additional random technical parameter which does increase the dimensionality of the problem. The results showed that the LSPCM produces an accurate approximation of the LSM method and that using third order mapped Fejer nodes achieved the highest accuracy.

The efficiency of the sampling method could be improved further by using sparse grids for the Gaussian grids (**Xiu and Hesthaven 2005; Foo et al. 2008**), and to use sampling methods that have a weak dependency on the order of the approximation (**Sarma and Xie 2011**) as mentioned in Chapter 5.

The algorithm was extended to incorporate mutually exclusive decisions which can be used to model realistic decision scenarios. The example presented was based on varying the surfactant slug properties with respect to concentration and volume. Each reservoir model produces its unique response where the PUNQ-S3 and the SPE10M reservoir models did favor the flexibility in surfactant slug properties while the homogeneous model favored the original surfactant properties. This example shows that the approach can be scalable to more complex decision scenarios. A possible extension with respect to decision complexity would to be to incorporate compound decisions which are defined as decisions on decisions. For instance, after deciding to implement SP flooding at a specific decision node, a new decision is available to continue or stop the SP flooding process discretized over a certain range of time. This provides the opportunity to have flexibility in the duration of the SP flooding process conditional on how the technical and economic uncertainties evolve or resolve over time. The algorithm can be extended to incorporate such decision scenarios and convergence of the method is maintained because it is a direct extension of the LSM approach (**Gamba 2003**).

Uncertainty in heterogeneity is another important factor that could be incorporated into the method. For instance, it could be possible to use the PCM to approximate Gaussian or non-Gaussian generated permeability fields (**Li and Zhang 2009**) rather than using MCS in generating the moving average produced realizations. The LSPCM (and the LSM method) can be easily adaptable to other chemical EOR processes as shown. This only requires a well-defined decision scenario and the designation of the relevant uncertain parameters.

8 Conclusions and Recommendations

8.1 Conclusions

A decision making method was developed that can quantify the value of specifically designed decisions in the presence of uncertainty for surfactant-polymer flooding processes. This was based on the concept of the Value of Flexibility (VoF) where a decision is divided into a number of sub-decisions in order to allow for policy modification as new information is obtained. This approach differed from other surfactant-polymer flooding focused decision making methods in that: SP flooding was predicted using simple analytical models, uncertainty in the time series was not considered, some methods only considered technical uncertainty and neglected economic uncertainty, and none considered the upside potential that this uncertainty could create if it resolved favourably.

The Least-Squares MonteCarlo (LSM) method was applied to value flexibility for SP flooding. The application of the LSM method is straight-forward, easily scalable to handle multiple sources of uncertainty and the method is well suited for combining technical and economic parameters in addition to the uncertainty in the time series of these variables. Its application is based on the design of the option or decision that is desired to be optimized. By considering the uncertainty in the time series, this method provides an efficient means to capitalize on the upside opportunities that these uncertainties present or help mitigate worsening circumstances. A MATAB code was written to implement the LSM method.

Based on the case studies presented, the LSM was successful in producing the VoF for a specific decision and it showed that for many applications incorporating flexibility did create value.

Different sensitivities were tested. These include basis function design for determining the continuation value, varying the static policy base case, and using cluster based regression. The effect of finer discretization of the decision space was also investigated and the results exhibited a limitation of the algorithms applicability to higher dimensional problems. Further investigation found that a finer decision space discretization requires a significant increase in the number of stochastic realizations to converge because it requires higher order basis functions. This leads to prohibitive computational cost.

The effect of heterogeneity was also shown on the results of the LSM method. It was found that the policy and VoF is reservoir model unique, which is expected. Different approaches to uncertainty in heterogeneity were considered. Two-point and multiple-point geostatistical methods were used to generate stochastic realizations of the permeability field. This illustrates the scalability of the LSM algorithm by incorporating uncertainty in heterogeneity.

Applying the LSM method to more sophisticated decision scenarios requires significantly higher computational effort compared to the cases presented. The main focus in increasing the efficiency of the LSM method is to reduce the computational requirement of reservoir performance simulation by reducing the number of reservoir simulations needed. Enhancing the sampling efficiency of the technical variables was deemed to be a priority. This was performed using the probabilistic collocation method (PCM).

The applicability of the PCM was first demonstrated by quantify parametric uncertainty for SP flooding processes using a number of stylized reservoir models. In general, the results were reservoir unique where for some models the convergence of the PCM to the MCS benchmark was better than other models. Results also showed that reduction in computational time of more than 2 orders of magnitude can be achieved.

The PCM was coupled with the LSM method in order to enhance the performance of the LSM method. This was attempted by substituting the MCS component of the LSM method with the PCM sampling techniques introducing the LSPCM.. The LSPCM was then applied to a number of case studies. The initial application assumed no uncertainty in the time series of the technical random parameters. The purpose of the initial application was to demonstrate whether the LSPCM would produce accurate results efficiently with respect to the LSM method. Once this was established, uncertainty in the time series was then considered. The results showed that LSPCM produced relatively accurate results based on the VoF PDFs, policy histograms and on the RMSRE which used the LSM results as the benchmark for comparison. In general, results were found to be reservoir unique. By approximating the technical state space using PCM sampling techniques, it was possible to enhance the performance of the LSM approach. Incorporating uncertainty in the time series was then attempted and LSPCM was able to capture its effect.

The LSPCM was then applied to more sophisticated decision scenarios in order to demonstrate the scalability of the LSM approach in general. A complex decision scenario was designed where the flexibility in surfactant slug properties was incorporated with the timing decision. The other complex decision scenario modeled also demonstrated the LSPCM (and the LSM method) applicability to other chemical EOR processes; ASP flooding. In this example, the injection of alkaline was incorporated as an additional flexibility along with the timing decision. By injecting alkaline it is desired to reduce surfactant adsorption and enhance oil recovery. In this case, alkaline adsorption was included as an additional random technical parameter which increased the dimensionality of the problem.

In summary, the LSM method gives a new outlook on implementing SP flooding. By incorporating flexibility, it can show which flexibilities are worth considering and can possibly support successful field implementation. Since it is impossible to resolve uncertainty completely, methods such as the LSM method will be required especially when uncertainty is detrimental to successful field implementation.

The contributions of this thesis can be summarized into the following: an attempt to use real options theory to value flexibility in SP flooding processes, the development of an approximate dynamic programming approach to produce optimal policies, the robust quantification of parametric uncertainty for SP flooding using PCM and an attempt to improve the efficiency of the LSM method by coupling it with the PCM code in order to extend its applicability to more complex problems.

The algorithm still requires further testing and refinement to be applicable to real complex problems and complex reservoir models. The next section presents a summary of possible future directions of this research.

8.2 Recommendations for Future Work

More technical uncertainties are desired to be incorporated in the method such as the effect of salinity on the surfactant performance which could introduce a correlation with surfactant adsorption and consequently influence the recovery efficiency of the process.

For more realistic applications, incorporating dynamic control variables (such as varying the size and concentration of the injected chemical slug or varying the production constraints) in the evaluation method coupled with a higher discretized decision space (monthly or quarterly decisions rather than yearly decisions) is required. This can be applicable; however it will necessitate a significant computational effort and will require enhanced basis function design to produced convergent results.

Further investigation in the effect of decision space discretization on the accuracy of the results is required. As shown in the thesis, this aspect presented a significant disadvantage to the extension of LSM to problems with finer time-step discretization and was only applicable to coarse decision space representation.

For the examples presented above, the optimal policy determined was based on maximising one objective function. It is desired to investigate whether it is possible to extend the LSM method and the LSPCM to produce a multi-objective optimal policy. For instance, this could be first tested by incorporating the recovery factor with the NPV as the dual objective function.

The regression approach used was ordinary least squares and clustering (local regression). Other approaches could be used such as weighted least squares. An interesting possibility would be to use an approach based on Dirichlet process mixtures where the membership of a sample in a cluster is probabilistic (**Powell 2011)**.

The PCM component of the LSCPM can be enhanced by using: approximation-order independent sampling, improved sparse grid sampling or arbitrary random input distribution that can be more representative of reality. It is also possible to quantifying spatial uncertainty using PCM but this would require using the Karhunen-Leove expansion to approximate the spatial uncertainties (e.g. permeability or porosity) (**Li and Zhang 2009)**.

How heterogeneity evolves with time could be enhanced by using for instance Kalman-filter based approaches (**Burgers et al. 1998; Evensen 2003**) or history matching techniques (**Oliver and Chen 2011**).

The implementation of the algorithms in MATLAB could be enhanced by using parallelization. This could significantly increase the efficiency of the code on multiple core processors.

With respect to numerical simulation of SP flooding, extending the LSM method and the LSPCM to be coupled with other reservoir simulators such as UTCHEM in order to simulate the detailed chemical interactions and phase behavior. This could enhance the accuracy of simulating SP flooding in porous media.

Improvements could be applied to the economic modeling of the objective function as well. In this thesis, a standard mean reverting process was used to simulate the oil price over time. There are other advanced price models that could be used and the method can be extended to include these models directly such as 2-factor and 3-factor oil price models (**Cortazar and Schwartz 2003; Begg and Smit 2007**).

For the examples presented above, the optimal policy determined was based on maximising one objective function. It is desired to investigate whether it is possible to extend the LSM method and the LSPCM to produce a multi-objective optimal policy. For instance, this could be first tested by incorporating the recovery factor with the NPV as the dual objective function.

The approach can be scalable to more complex decision scenarios. A possible extension with respect to decision complexity would to be to incorporate compound decisions which are defined as decisions on decisions. For instance, after deciding to implement SP flooding at a specific decision node, a new decision is available to continue or stop the SP flooding process discretized over a certain range of time. This provides the opportunity to have flexibility in the duration of the SP flooding process conditional on how the technical and economic uncertainties evolve or resolve over time.

The LSM method or the LSPCM can also be applied for other EOR processes such as polymer, CO2 and thermal flooding. This would only require the definition of the relevant state variables, technical or economic, and to design the decision that is desired to be optimized while considering the constraint of computational requirement. For instance, the methods could be extended to evaluate decision in CO_2 storage by using the carbon credits as the objective function to be optimized.

References

Aanonsen, S., Naevdal, G., Oliver, D., Reynolds, A. and Valles, B. 2009. The Ensebmle Kalman Filter In Reservoir Engineering—a Review. *SPE J.* **14**(3):393-412. SPE-117274-PA. doi:10.2118/117274-PA.

Adams, W. and Schievelbein, V. 1987. Surfactant Flooding Carbonate Reservoirs. *SPE Reservoir Engineering* 2(4):619-626. (SPE12686-PA).

Alkhatib, A. and King, P. 2011. Applying Real Options Theory in |Determining Optimal Policies for a Surfactant Flood. Paper SPE 144869 presented at the SPE Enhanced Oil Recovery Conference, Kuala Lumpur, Malaysia, 19-21 July.

Alkhatib, A, Babaei, M. and King, P. 2013. Decision Making under Uncertainty: Applying the Least Squares Monte Carlo Method in Surfactant Flooding Implementation. *SPE J.* SPE-154467-PA (in press).

Alkhatib, A. and King, P. 2013a. Uncertainty Quantification of a Chemically Enhanced Oil Recovery Process: Applying the Probabilistic Collocation Method to a Surfactant-Polymer Flood. Paper SPE 164244 presented at the 18th Middle East Oil and Gas Show and Conference, Manama, Bahrain, 10-13 March. http://dx.doi.org/10.2118/164244-MS.

Alkhatib, A. and King, P. 2013b. The Use of the Least Squares Probabilistic Collocation Method in Decision Making in the Presence of Uncertainty for Surfactant-Polymer Flooding. Paper SPE 164860 presented at the 75th EAGE Conference & Exhibition incorporating SPE EUROPEC 2013, London, UK, 10-13 June.

Alsofi, A. and Blunt, M. 2011. The Design and Optimization of Polymer Flooding under Uncertainty. Paper SPE 145110 presented at the SPE Enhanced Oil Recovery Conference, Kuala Lumpur, Malaysia, 19-21 July. .http://dx.doi.org/10.2118/145110-MS.

Al-Sulaimani, H., Al-Wahaibi, Y., Al-Bahry, S., Elshafie, A., Al-Bemani, A., Joshi, S. and Ayatollahi, S. 2012. Residual-Oil Recovery Through Injection of Biosurfactant, Chemical Surfactant, and Mixtures of Both Under Reservoir Temperatures: Induced-Wettability and Interfacial-Tension Effects. *SPE Reservoir Evaluation & Engineering* **15**(2): 210-217. (SPE 158022-PA).

Amemiya, T., 1985, *Advanced Econometrics*. London: Basil Blackwell.

Anderson, G., Delshad, M., King, C., Mohammadi, H. and Pope, G. 2006. Optimization of Chemical Flooding in a Mixed-Wet Dolomite Reservoir. Paper SPE 100082 presented at the 2006 SPE/DOE Symposium on Improved Oil Recovery, Tulsa, Oklahoma, USA, 22-26 April. http://dx.doi.org/10.2118/100082-MS.

Anderson, M. 1979. Application of Risk Analysis to Enhanced Recovery Pilot Testing Decisions. *Journal of Petroleum Technology* **31**(12): 1525-1530.

Armstrong, M., Galli, A., Bailey, W. and Couet, B. 2004. Incorporating technical uncertainty in real option valuation of oil projects. *Journal of Petroleum Science & Engineering* **44**(1-2): 67-82.

Aven, T. and Korte, J. 2002. On the use of risk and decision analysis to support decision-making. *Reliability Engineering and System Safety* **79**(3):289-299.

Azzarone, D. and Bruni, T. 2008. Real Option Theory Complements the Stage and Gate Process: the Value of Information. Paper SPE 113634 presented at the 2008 SPE Europec/EAGE Annual Conference and Exhibition, Rome, Italy, 9-12 June.

Babaei, M., and King, P., 2012, A Modified Nested-Gridding for Upscaling Downscaling in Reservoir Simulation. *Transport in Porous Media* **93**(3):753-775. http://dx.doi.org/10.1007/s11242-012-9981-4

Bailey, W., Couet, B., Bhandari, A., Faiz, S., Srinivasan, S. and Weeds, H. 2004. Unlocking the Value of Real Options. Schlumberger. https://www.slb.com/~/media/Files/resources/oilfield_review/ors03/win03/p4_19.pdf. (Accessed on 20/05/2012).

Bailey, W., Mun, J. and Couet,B. 2002. A Stepwise Example of Real Options Analysis of a Production Enhancement Project. Paper SPE 78329-MS presented at the European Petroleum Conference, Aberdeen, United Kingdom, 29-31 October. doi: 10.2118/78329-MS.

Barua, J., Prescott, T. and Haldorsen, H. 1986. Financial and Technical Decision Making for Surfactant Flooding. Paper SPE15074 presented at the 56th SPE California Regional Meeting. Oakland, California, USA, 2-4 April. http://dx.doi.org/10.2118/15074-MS.

Begg, S. and Smit, N. 2007. Sensitivity of Project Economics to Uncertainty in Type and Parameters of Price Models. Paper SPE 110812 presented at the SPE Annual Technical Conference and Exhibition, Anahiem, California, USA, 11-14 November 2007.

Begg, S., Bratvold, R. and Campbell, J. 2002. The Value in Managing Uncertainty in Oil and Gas Investments. Paper SPE 77586 presented at the SPE Annual Technical Conference and Exhibition, San Antonio, TA, USA, 29 Septmeber-2 October .

Begg, S., Bratvold, R. and Campbell, J. 2004. Abandonment Decisions and the Value of Flexibility. Paper SPE 91131 presented at the SPE Annual Technical Conference and Exhibition, Houston, TA, USA, 26-29 September.

Begg, S.H. and Carter, R.R. and Dranfield, P. 1989. Assigning Effective Values to Simulator Gridblock Parameters for Heterogeneous Reservoirs. *SPE Reservoir Engineering* **4**(4):455-463. SPE 16754-PA. http://dx.doi.org/10.2118/16754-PA.

Bellman, R. 1957. *Dynamic Programming*. Princeton, New Jersey: Princeton University Press.

Bender, C. and Steiner, J. 2010. Least-squares Monte Carlo for backward SDEs. *Numerical Methods in Finance*. **12**:257-289.

Bensoussan. A., 1984. On the Theory of Option Pricing. *Acta Applicandae Mathematicae* **2**(2): 139-158. http://dx.doi.org/10.1007/BF00046576.

Black, F. and Scholes, M. 1973. The Pricing of Options and Corporate Liabilities. *The Journal of Political Economy* **81**(3): 637-654.

Boogert, A. and De Jong, C. 2008. Gas Storage Valuation Using a Monte Carlo Method. *The Journal of Derivatives* **15**(3): 81-98.

Bragg, J., Gale, W. and McElhannon, W. 1982. Loudon Surfactant Flood Pilot Test. Paper SPE 10862 preseneted at the 1982 SPE/DOE Third Joint Symposium on Enhanced Oil Recovery, Tulsa, Oklahoma, USA, 4-7 April.

Bratvold, R. and Begg, S. 2010. *Making Good Decisions*. Richardson, Texas: Society of Petroleum Engineers.

Bratvold, R. B., Laughton, D., Enloe,T., Borison,A. and Begg,S. 2005. A Critical Comparison of Real Option Valuation Methods: Assumptions, Applicability, Mechanics, and Recommendations. Paper SPE 97011 presented at the SPE Annual Technical Conference and Exhibition, Dallas, Texas, USA, 9-12 October. doi: 10.2118/97011.

Bratvold, R., Bickel, J. and Lohne, H. 2009. Value of Information in the Oil and Gas Industry: Past, Present, and Future. *SPE Reservoir Evaluation & Engineering* 12(4):630-638. SPE 110378-PA. http://dx.doi.org/10.2118/110378-PA.

Brown, C. and Smith, P. 1984. The Evaluation of Uncertainty in Surfactant EOR Performance Prediction. Paper SPE 13237 presented at the 59th SPE Annual Technical Conference and Exhibition, Houston, Texas, USA, 16-19 September. http://dx.doi.org/10.2118/13237-MS.

Burgers, G., Van Leeuwen, P. and Evensen, G. 1998. Analysis scheme in the ensemble Kalman filter. *Monthly Weather Review* **126**(6):1719-1724.

Camilleri, D., Fil, A., Pope, G., Rouse, B. and Sepehmoori, K. 1987. Comparison of an Improved Compositional Micellar/Polymer Simulator with Laboratory Corefloods. *SPE Reservoir Engineering* **2**(4):441-451. (SPE12083-PA).

Carcona, A. 1992. *Applied enhanced Oil Recovery*. Englewood Cliffs, New Jersey: Prentice Hall.

Cardoso, M. and Durlofsky, L. 2009. Linearized reduced-order models for subsurface flow simulation. *Journal of Computational Physics* **229**(3): 681-700.

Chen, T. and Pu, C. 2006. Study on Ultralow Interfacial Tension Chemical Flooding in Low permeability Reservoirs. *Journal of Xi'an Shiyou University* **21**(3):30-33.

Chen, Y., Oliver, D. and Zhang, D. 2009. Efficient Ensemble-Based Closed-Loop Production Optimization. *SPE J.* **14**(4):634-645. SPE 112873-PA.

Cheng, H., Shook, G., Taimur, M, Dwarakanath, V. and Smith, B. 2012. Interwell Tracer Tests to Optimize Operating Conditions for a Surfactant Field Trial: Design, Evaluation and Implications. *SPE Reservoir Evaluation & Engineering* **15**(2):229-242. http://dx.doi.org/10.2118/144899-PA.

Cheng, H., Shook, G., Taimur, M, Dwarakanath, V. and Smith, B. 2012. Interwell Tracer Tests to Optimize Operating Conditions for a Surfactant Field Trial: Design, Evaluation and Implications. *SPE Reservoir Evaluation & Engineering* **15**(2):229-242. http://dx.doi.org/10.2118/144899-PA.

Cheong, Y. and Gupta, R. 2005. Experimental Design and Analysis Methods for Assessing Volumetric Uncertainties. *SPE J.* **10**(3): 324-335. SPE 144899-PA. http://dx.doi.org/10.2118/80537-PA.

Chiara, N., Garvin, M. and Vecer, J. 2007. Valuing Simple Multiple-Exercise Real Options in Infrastructure Projects. *Journal of Infrastructure Systems* **13**(2): 97-104.

Chorn, L. G. and Croft, M. 2000. Resolving Reservoir Uncertainty to Create Value. *Journal of Petroleum Technology* **52**(8): 52-59.

Choudhury, A., King, A., Kumar, S. and Sabharwal, Y. 2008. Optimizations in Financial Engineering: The Least-Squares Monte Carlo method of Longstaff and Schwartz. Paper IEEE 4536290 presented at the IEEE International Symposium on Parallel and Distributed Processing, Miami, USA, 14-18 April.

Christie, M. and Blunt, M. 2001. Tenth SPE Comparative Solution Project: A Comparison of Upscaling Techniques. *SPE Reservoir Engineering and Evaluation* **4**(4):308-317. SPE 72469-PA. http://dx.doi.org/10.2118/72469-PA.

Chung, T. and Carroll, H. 1995. Application of Fuzzy Expert Systems for EOR Project Risk Analysis. Paper SPE presented at the 1995 SPE Annual Technical Conference & Exhibition, Dallas, TA, USA, 22-25 October.

Ciaurri, D., Conn, A., Mello, U. and Onwunalu, J. 2012. Integrating Mathematical Optimization and Decision Making in Intelligent Fields. Paper SPE 149780 presented at the SPE Intelligent Energy International, Utrecht, The Netherlands, 27-29 March.

Coats, K. 2003. IMPES Stability: The CFL Limit. *SPE J.* **8**(3):291-297. http:// dx.doi.org/10.2118/85956-PA.

Computer Modelling Group. 2012. STARS Advanced Processes and Thermal Reservoir Simulaotr. http://www.cmgl.ca/software/soft-stars.

Cooper, N., Southworth, R. and Walsh, D. 1985. Field Experience in the Bothamsall Surfactant Flood Project. Paper SPE 13990 presented at the SPE Offshore Europe Conference, Aberdeen, UK, 10-13 September. http://dx.doi.org/10.2118/13990-MS.

Copeland, T. and Antikarov, V. 2003. *Real Options: a practitioner's guide*. UK: Penguin Group.

Copeland, T. and Antikarov, V. 2005. Real Options: Meeting the Georgetown Challenge. *The Journal of Applied Corporate Finance* **17**(2): 17-31.

Cortazar, G. and Schwartz, E. 2003. Implementing a stochastic model for oil futures prices. *Energy Economics* **25**(3):215-238.

Cortazar, G., Gravet, M. and Urzula, J. 2008. The valuation of multidimensional American real options using the LSM simulation method. *Computers & Operations Research* **35**(1): 113-129.

Costa Lima, G. A., Suslick, S. B. and Avansi, G. D. 2008. The Impact of Some Real Options on the Efficient Frontier of Portfolios of Oil Production Projects. Paper SPE 116440 presented at the 2008 SPE Annual Technical Conference and Exhibition, Denver, Colorado, 21-24 September. doi: 10.2118/116440.

Costa, A., Schiozer, D., Moczydlower, P. and Bedrikovetsky, P. 2008. Use of Representative Models to Improve the Decision Making Process of Chemical Flooding in a Mature Field. Paper SPE 115442 presented at the 2008 SPE Russian Oil & Gas Technical Conference and Exhibition. Moscow, Russia. 28-30 October 2008. http://dx.doi.org/10.2118/115442-MS.

Cox, J., Ross, S. and Rubenstein, M. 1979. Option Pricing: A Simplified Approach. *Journal of Financial Economics* **7**:229-263.

Cox, J., Ross, S. and Rubinstein, M. 1979. Option Pricing: A Simplified Approach. *Journal of Financial Economics* **7**: 229-263.

Cunha, J. 2007. Recent Developments on Application of Decision Analysis for the Oil Industry. Paper SPE 108703 presented at the 2007 International Oil Conference and Exhibition, Veracruz, Mexico, 27-30 June.

Damodaran, A. 2005. The Promise and Peril of Real Options. Stern School of business. http://papers.ssrn.com/sol3/papers.cfm?abstract_id=1295849. (Accessed on 09/02/2010)

Dang, C., Chen, Z., Nguyen, N., Bae, W. and Phung, T. 2011.Develpment of Isotherm Polymer/Surfactant Adsorption Models in Chemical Flooding. Paper SPE 147872 presented at the SPE Asia Pacific Oil and Gas Conference and Exhibition, Jakarta, Indonesia, 20-22 September. http://dx.doi.org/10.2118/147872-MS.

Davidson, L. 2001. Practical Issues in Using Risk-Based Decision Analysis. Paper SPE 71417 presented at the 2001 SPE Annual Technical Conference and Exhibition, New Orleans, LA, USA, 30 September-3 October.

De Abreu, C. C. and Cavalcante. J. A. 2009. Economic Analysis Using a Real Option Model in an Exploratory Project. Paper SPE 122895 presented at the 2009 SPE Latin American And Caribbean Petroleum Engineering Conference, Cartagena, Colombia, 31 May - 3 June. doi: 10.2118/122895.

Dean, O. 1995. Moving Avergaes for Gaussian Simulation in Two and Three Dimensions. *Mathematical Geology* **27**(8): 939-960.

Delshad, M., Najafabadi, N., Anderson, G., Pope, G. and Sepehrnoori, K. 2009. Modeling Wettability Alteration by Surfactants in Naturally Fractured Reservoirs. *SPE Reservoir Engineering & Evaluation* **12**(3): 361-370. http:// dx.doi.org/10.2118/100081-PA.

Denault, M., Simonato, J. and Stentoft, L. 2011. A simulation-and-regression approach for stochastic dynamic programs with endogenous state variables. *Groupe d'études et de recherche en analyse des decisions*.

Deore, P. 2012. Decision Making in Upstream Oil and Gas Industry – An integrated Approach. Paper SPE 154999 presented at the SPE Oil and Gas India Conference and Exhibition, Mumbai, India, 28-30 March.

Department of Energy (DOE). 1986. Scientific Software-Intercomp: "Supporting Technology for Enhanced Oil Recovery- Chmeical Predictive Model". Venezuela-MEM/USA-DOE Fossil Energy Report III-5. p360.

Dezen, F. and Morooka, C. 2002. Alternatives for Deepwater Field Developments: A Real Option Approach. Paper SPE 14205-MS presented at the Offshore Technology Conference, Houston, Texas, USA, May 6-9. doi: 10.4043/14205-MS.

Dias, M. 2004, Monte Carlo Simulation of Stochastic Processes, http://www.puc-rio.br/marco.ind/sim_stoc_proc.html (accessed 17 July 2012).

Dias, M. 2004. Valuation of exploration and production assets: an overview of real options models. *Journal of Petroleum Science and Engineering* **44**( ): 93-114.

Dinnie, N., Fletcher, A. and Finch, J. 2002. Strategic Decision Making in the Upstream Oil and Gas Industry: Exploring Intuition and Analysis. Paper SPE 77910 presented at the SPE Asia Pacific Oil and Gas Conference and Exhibition, Melbourne, Australia, 8-10 October.

Dixit, A. and Pindyck, R. 1994. Investment under Uncertainty. Princeton, New Jersey: Princeton University Press.

DOE. 1986. Scientific Software-Intercomp: "Supporting Technology for Enhanced Oil Recovery – Chemical Predictive Model" Venezuela-MEM/USA-DOE Fossil Energy Report **3**(5):360.

DOE. 2008. DOE's Enhanced Oil Recovery Program: An Archive of Important Results. Nationa Energy Technology Laboratory. http://www.netl.doe.gov (Accessed 17/02/2012).

Donaldson, E., Chilingarian, G. and Yen, T. (eds). 1989. *Enhanced Oil Recovery, II: Processes and Operations, Volume 2*. : Amsterdam, The Netherlands: Elsevier.

ECLIPSE Blackoil Reservoir Simulation Training and Exercise Guide, Version 2.0. 2008. Schlumberger.

Eldred, M. 2009. Recent Advances in Non-Intrusive Polynomial Chaos and Stochastic Collocation Methods for Uncertainty Analysis and Design. Paper AIAA 2009-2274 presented at the 50th AIAA/ASME/ASCE/AHS/ASC Structures, Structural Dynamics, and Materials Conference, Palm Springs, CO, 4-7 May.

Energy Information Agency (EIA). 2012. NYMEX Futures Price Data. http://www.eia.gov/dnav/pet/pet_pri_fut_s1_d.htm (accessed 10 July 2012).

Evans, R. 2000. Decision Analysis for Integrated Reservoir Management. Paper SPE 65148 presented at the SPE European Petroleum Conference, Paris, France, 24-25 October.

Evensen, G. 2003. The ensemble Kalman filter: Theoretical formulation and practical implementation. *Ocean Dynamics* **53**(4):343-367.

Evensen, G. 2007. Data Assimilation: The Ensemble Kalman Filter. Berlin: Springer Verlag.

Farajzadeh, R., Matsuura, T., Van Batenburg, D. and Dijk, H. 2012. Detailed Modeling of the Alkali/Surfactant/Polymer (ASP) Process by Coupling a Multipurpose Reservoir Simulator to the Chemistry Package PHREEQC. *SPE Reservoir Evaluation & Engineering* **15**(4):423-435. (SPE143671-PA).

Feinberg, J. 2012. Probabilistic Collocation Method Module (polychaos), https://bitbucket.org/jonathf/polychaos (accessed 7 July 2012).

Fejer, L. 1933. Mechanische Quadraturen mit positiven Cotesschen Zahlen. *Mathematische Zeitschrift* **37**(1): 287-309.

Feres, R. 2012. A few useful MATLAB functions. Washington University in St. Louis, Department of Mathematics.

Fernandez, D., Vidal, M. and Festini, D. 2012. Decision-Making Breakthrough Technology. Paper SPE 152524 presented at the SPE Latin American and Caribbean Petroleum Engineering Conference, Mexico City, Mexico, 16-18 April.

Ferrell, H., King, D. and Sheely, C. 1988. Analysis of the Low-Tension Pilot at Big Muddy Field, Wyoming. *SPE Formation Evaluation* **3**(2):315-321. (SPE12683-PA).

Field, R. and Mircea, D. 2007. Convergence Properties of Polynomial Chaos Approximations for L_2 Random Variables, public report, Sandia National Laboratories.

Foo, J., Xiaoliang, W. and Karniadakis, G. 2008. The Multi-Element Probabilistic Collocation Method: Error Analysis and Applications. *Journal of Computational Physics* **227**(22): 9572-9595.

Foss, B and Jensen, J. 2011. Performance Analysis for Closed-Loop Reservoir Management. *SPE J.* **16**(1): 183-190. SPE 138891-PA.

Franchl, J. and Carroll, H. 1988. Evaluation of the Wilmington Field Micellar/Polymer Project. *SPE Reservoir Engineering* **3**(2): 609-616. http://dx.doi.org/10.2118/12681-PA.

Friedmann, F. 1986. Surfactant and Polymer Losses During Flow Through Porous Media. *SPE Reservoir Engineering* **1**(3):261-271. (SPE11779-PA).

Galli, A., Armstrong, M. and Jehl,B.. 1999. Comparing Three Methods for Evaluating Oil Projects: Option Pricing, Decision Trees, and Monte Carlo Simulations. Paper SPE 52949 presented at the SPE Hydrocarbon Economics and Evaluation Symposium, Dallas, Texas, USA 21-23 March. doi: 10.2118/52949.

Galvis, C. F. and Villarreal, J. 2008. Extended Binomial Trees for Real Options Valuation in E&P Projects. Paper SPE 118251 presented at the 2008 Abu Dhabi International Exhibition and Conference, Abu Dhabi, UAE,3-6 November. doi: 10.2118/118251.

Gamba, Andrea. 2002. An Extension of Least Squares Monte Carlo Simulation for Multi-options Problems. Paper. Presented at the 6th Annual Real Options Conference, Paphos, Cyprus. July 4-6, 2002.

Gao, P., Towler, B., Li, Y. and Zhang, X. 2010. Integrated Evaluation of Surfactant-Polymer Floods. Paper SPE 129590 presented at the SPE EOR Conference at Oil & Gas West Asia, Muscat, Oman, 11-13 April. http://dx.doi.org/10.2118.129590-MS.

Gautschi, W. 1994. Algorithm 726: ORTHPOL–a package of routines for generating orthogonal polynomials and Gauss-type quadrature rules. *ACM Transactions on Mathematical Software* **20(1):** 21-62.

Gerbacia, W. 1978. The Evaluation of Surfactant Systems for Oil Recovery Using Statistical Design Principles and Analysis. Paper SPE 7070 presented at the SPE Symposium on Improved Methods of Oil Recovery, Tulsa, Oklahoma, USA, 16-17 April. http://dx.doi.org/10.2118/7070-MS.

Ghanem, R. and Spanos, P. 1991. Stochastic Finite Elements: A Spectral Approach. New York: Springer-Verlag.

Gharbi, R. 2005. Application of an expert system to optimize reservoir performance. *Journal of Petroleum Science & Engineering* **49**(3-4):261-273.

Glittier, W. and Krumrine, P. 1985. A Novel Approach for Risk Assessment in Chemical EOR Projects. Paper SPE 13767 presented at the SPE 1985 Hydrocarbon Economics and Evaluation Symposium, Dallas, Texas, USA, 14-15 March. http://dx.doi.org/10.2118/13767-MS.

Glover, C., Puerto, M., Maerker, J. and Sandvik, E. 1979. Surfactant Phase Behaviour and Retention in Porous Media. *SPE J.* **19**(3):183-193. http://dx.doi.org/10.2118/7053-PA.

Gogarty, W. 1976. Status of Surfactant or Micellar Methods. *Journal of Petroleum Technology* **28**(1):93-102. SPE5559-PA.

Gogarty, W. 1983a. Enhanced Oil Recovery Through the use of Chemicals-part 1. *Journal of Petroleum Technology* **35**(9):1581-1590.

Gogarty, W. 1983b. Enhanced Oil Recovery Through the use of Chemicals-part 2. *Journal of Petroleum Technology* **35**(10):1767-1775.

Gogarty, W., Meabon, H. and Milton, H. 1970. Mobility Control Design for Miscible-Type Waterfloods Using Micellar Solutions. *Journal of Petroleum Technology* **22**(2):141-147.

Golub, G. and Welsch, J. 1969. Calculation of Gauss Quadrature Rules. *Mathematics of Computation* **23**(106): 221-230.

Graciaa, A., Fortney, L., Lester, N., Schechter, R., Wade, W. and Yiv, S. 1982. Criteria for Structuring Surfactants to Maximize Solubilization of Oil and Water: Part 1-Commercial Nonionics. *SPE J.* **22**(5):743-749.

Grayson, C. 1960. The Calculus of Common Sense. Paper SPE 309 presented at the 1962 AIME Annual Meeting, New York, New York, USA, 18-22 February. http://dx.doi.org/10.2118/309-MS.

Grayson, C. 1962. Bayesian Analysis A New Approach to Statistical Decision-Making. *Journal of Petroleum Technology* **14**(6):603-607.

Green, D. and Willhite, G. 1998. *Enhanced Oil Recovery*. Richardson, Texas: Society of Petroleum Engineers.

Guardiano, F. and Srivastava, R. 1993. Multivariate geostatistics: beyond bivariate moments. *Geostatistics-Troia* **1**: 133-144.

Hahn, W. J., Pepperdine, U., Dyer, J. and Brandao, L. E. 2007. Using Decision Analysis to Solve Real Option Valuation Problems: Building a Generalized Approach. Paper SPE 108066 presented at the 2007 SPE Hydrocarbon Economics and Evaluation Symposium, Dallas, Texas, USA, 1-3 April. doi: 10.2118/108066.

Hale, N. 2011. Gauss Quadrature Nodes and Weights. Mathematical Institute, Oxford University. http:// http://www2.maths.ox.ac.uk/chebfun/examples/quad/html/GaussQuad.shtml. (accessed 05/04/2013).

Hammershaimb, E., Kuuskraa, V. and Stosur, G. 1983. Recovery Efficiency of Enhanced Oil Recovery Methods: A Review of Significant Field Tests. Paper SPE 12114 presented at the 58th Annual Technical Conference and Exhibition, San Francisco, CA, USA, 5-8 October. http://dx.doi.org/10.2118/12114-MS.

Han, C., Delshad, M., Sepehrnoori, K. and Pope, G. 2005. A Fully Implicit, Parallel, Compositional Chemical Flooding Simulator. Paper SPE 97217 presented at the 2005 SPE Annual Technical Conference and Exhibition, Dallas, TA, USA, 9-12 October. . http://dx.doi.org/10.2118/97217-MS.

Hankins, N. and Harwell, J. 1996. Case Studies for the Feasibility of Sweep Improvement in Surfactant-Assisted Waterflooding. *Journal of Petroleum Science and Engineering* **17**(1):41-62. http://dx.doi.org/10.1016/S0920-4105(96)00055-1

Hansen, T. 2011. Mgstat. http://mgstat.sourceforge.net/ (accessed on 08/10/2012).

Harwell, J., Schechter, R. and Wade, W. 1984. Optimal Injection Strategies for the Propagation of Surfactant Mixtures through Porous Media. *SPE J.* **24**(5):545-554.

Healy, R. and Reed, R. 1977. Immiscible Microemulsion Flooding. *SPE J.* **17**(2):129-139.

Healy, R., Reed, R. and Stenmark, D. 1976. Multiphase Microemulsion Systems. *SPE J.* **16**(3):147-160.

Herschel, W. and Bulkley, R. 1926. Konsistenzmessungen von Gummi-Benzollösungen. *Kolloid Zeitschrift* **39**(4): 291-300.

Hirasaki, G. 1981. Application of the Theory of Multicomponent, Multiphase Displacement to the Three-Component, Two-Phase Surfactant Flooding. *SPE J.* **21**(2):191-204.

Hirasaki, G. 1982. Ion Exchange with Clays in the Presence of Surfactant. *SPE J.* **22**(2):181-192.

Hirasaki, G. Van Domselaar, H. and Nelson, R. 1983. Evaluation of the Salinity Gradient Concept in Surfactant Flooding. *SPE J.* **23**(3):486-500.

Hirasaki, G., Miller, C. and Puerto, M. 2011. Recent Advances in Surfactant EOR. *SPE J.* **16**(4):889-907. SPE 115386-PA. http://dx.doi.org/10.2118/115386-PA.

Holland, K. and Porter, L. 1983. Single-Well Evaluation Program for Micellar/Polymer Recovery, Main and 99 West Pools, West Coyote Field, California. Paper SPE 11990 presented at the 58th Annual Technical Conference and Exhibiton, San Francisco, CA, USA, 5-8 October. http://dx.doi.org/10.2118/11990-MS.

Holm, L. 1982. Design, Performance, and Evaluation of the Uniflood Micellar Polymer Process-Bell Creek Field. Paper SPE 11196 presented at the 57th SPE Annual Fall Technical Conference and Exhibition, New Orleans, Louisiana, USA, 26-29 September.

Howard, R. 1966. Decision Analysis: Applied Decision Theory. *Proceedings of the Fourth International Conference on Operational Research*, 55-71.

Howard, R. 1988. Decision Analysis: Practice and Promise. *Management Science* **34**(6):679-695.

Howard, R. 1996. Options. In Zeckhayser, R., Keeney, R. and Sibenius, J. (Eds). *Utility Theories: Measuremetns and Applications.* Bostong, MA: Kluwer Academic Publisheers, pp. 27-55.

Howard, R. 2007. The Foundations of Decision Analysis Revisited. In Edwards, W., Miles, R. and von Winterfeldt, D. (Eds). *Advances in Decision Analysis: From Foundations to Applications*. New York, NY: Cambridge University Press, pp. 32-56.

Howard, R. and Matheson, J. 1968. An Introduction to Decision Analysis. In *The Principles and Applications of Decision Analysis*, ed. Howard, R. and Matheson, J. Menlo Park, California: Strategic Decisions Group.http://dx.doi.org/10.2118/1579-G. http://www.slb.com/services/software/reseng/eclipse.aspx.

Howell, J. and Thomas, B. 1980. Evaluation of Injection Well Stimulation as Applied to a Large Micellar/Polymer Project. *Journal of Petroleum Technology* **32**(5): 777-784.

http://www.slb.com/services/software/reseng/eclipse.aspx.

Huh, C. 1979. Interfacial Tension and Solubilization Ability of a Microemulsion Phase that Coexists with Oil and Brine. *Journal ofColloid Interfacial Science* **71**(2):408-426.

Hultzsch, P., Lake, L. and Gilbert, R. 2007. Decision and Risk Analysis Through the Life of the Field. Paper SPE 107704 presented at the 2007 SPE Hydrocarbon Economics and Evaluation Symposium, Dallas, TA, USA, 1-3 April.

Iglauer, S., Wu, Y., Shuler, P., Blanco, M., Tang, Y. and Goddard, W. 2004. Alkyl Polyglycoside Surfactants for Improved Oil Recovery. SPE/DOE 89472 presented at the 2004 SPE/DOE Fourteenth Symposium on Improved Oil Recovery, Tulsa, Oklahoma, 17-21 April.

Jafarizadeh, B. and Bratvold, R. B. 2009. Taking Real Options into the Real World: Asset Valuation through Option Simulation. Paper SPE 124488 presented at the 2009 SPE Annual Technical Conference and Exhibition, New Orleans, Louisiana, USA, 4-7 October. http://dx.doi.org/10.2118/124488.

Jakobsen, S. and Hovland, F. 1994. Surfactant Flooding: Technical and Economical Conditions To Succeed. SPE Paper 27824 presented at the SPE/DOE Improved Oil Recovery Symposium, 17-20 April, Tulsa, Oklahoma.

Karakaya, E. 2012. Perceived Value and Popularity of Decision Analysis Tools in Upstream Asset Valuations. Paper SPE 162675 presented at the SPE Hydrocarbon, Economics and Evaluation Symposium, Calgary, Alberta, Canada, 24-25 September.

Karambeigi, M., Zabihi, R. and Hekmat, Z. 2011. Neuro-simulation modelling of chemical flooding. *Journal of Petroleum Science and Engineering* **78**(2):208-219. http://dx.doi.org/10.1016/j.petrol.2011.07.012.

Karatras, I., 1988, On the Pricing of American Options. *Applied Mathematics and Optimization* **17**(1): 37-60. http://dx.doi.org/10.1007/BF01448358.

Keeney, R. and Raiffa, H. 1976. *Decisions with Multiple Objectives: Preferences and Value Tradeoffs.* New York: Wiley.

King, P.R.,1989, The use of renormalization for calculating effective permeability, Transport in Porous Media, 4(1), 37–58. http://dx.doi.org/10.1007/BF00134741

Knickerbocker, B., Pesheck, C., Davis, H. and Scriven, L. 1982. Patterns of Three-Liquid Phase Behavior Illustrated by Alcohol-Hydrocarbon-Water-Salt Mixtures. *Journal of Physical Chemistry* **86**(3):393-400.

Knickerbocker, B., Pesheck, C., Davis, H. and Scriven, L. 1982. Patterns of Three-Liquid Phase Behavior Illustrated by Alcohol-Hydrocarbon-Water-Salt Mixtures. *Journal of Physical Chemistry* **86**(3):393-400.

Kossack, C. and Bilhartz, H. 1976. The Sensitivity of Micellar Flooding to Reservoir Heterogeneities. Paper SPE 5808 presented at the SPE Improved Oil Recovery Symposium, Tulsa, Oklahoma, USA. 22-24 March. http://dx.doi.org/10.2118/5808-MS.

Krumrine, P., Falcone, J. and Campbell, T. 1982. Surfactant Flooding 1: The Effect of Alkaline Additives on IFT, Surfactant Adsorption, and Recovery Efficency. *SPE J.* **22**(4):503-513.

Lake, L. W. 1989. *Enhanced Oil Recovery*. Englewood Cliffs, New Jersey: Prentice Hall.

Li, H. and Zhang, D. 2007. Probabilistic Collocation Method for Flow in Porous Media: Comparisons with other Stochastic Methods. *Water Resources Research* **43**(9). W09409, http://dx.doi.org/doi:10.1029/2006WR005673.

Li, H. and Zhang, D. 2009. Efficient and Accurate Quantification of Uncertainty for Multiphase Flow with the Probabilistic Collocation Method. *SPE J.* **14**(4): 665-679. http://dx.doi.org/doi:10.2118/114802-PA

Li, H., Sarma, P. and Zhang, D. 2011. A Comparative Study of the Probabilistic-Collocation and Experimental-Design Methods for Petroleum-Reservoir Uncertainty Quantification. *SPE J.* **16**(2):429-439. doi: 10.2118/140738-PA

Li, Z., Zheng, H., He, Z. and Cheng, Y. 2002. Compatibility of Oil-Displacing agents. In: Yu, J., Song, W., Li, Z. et al. (Eds.), Fundamentals and Advances in combined Chemical Flooding, Chapter 13, China Petrochemical Press.

Lima, G. and Suslick, S. 2005. An Integration of Real Options and Utility Theory for Evaluation and Strategic Decision-Making in Oil Development and Production Projects. Paper SPE 94665-MS presented at the SPE Hydrocarbon Economics and Evaluation Symposium, Dallas, Texas, USA, 03-05 April. doi: 10.2118/94665-MS.

Lin, G. and Tartakovsky, A. 2009. An Efficient, High-Order Probabilistic Collocation Method on Sparse Grids for Three-Dimensional Flow and Solute Transport in Randomly Heterogeneous Porous Media. *Advances in Water Resources* **32**(5): 712-722.

Liu, S., Li, R.m Miller, C. and Hirasaki, G. 2010. Alkaline/Surfactant/Polymer Processes: Wide Range of Conditions for Good Recovery. *SPE J.* **15**(2):282-293.

Loeven, G. and Bijl, H.2008. Probabilistic Collocation Used in a Two-Step Approach for Efficient Uncertainty Quantification in Computational Fluid Dynamics. *Computer Modelling in Engineering and Science* **36**(3): 193-212.

Loeven, G., Witteveen, J. and Bijl, H.2007. Probabilistic collocation: an efficient non-intrusive approach for arbitrarily distributed parametric uncertainties. Paper AIAA 2007-317 presented at the 45th AIAA Aerospace Sciences Meeting and Exhibit, Reno, NA, 8-11 January.

Lohne, A. and Fjelde, I. 2012.Surfactant Flooding in Heterogeneous Formations. Paper SPE 154178 presented at the Eighteenth SPE Improved Oil Recovery Symposium, Tulsa, Oklahoma, USA, 14-18 April. http://dx.doi.org/10.2118/154178-MS.

Lohrenz, J., Bray, B. and Clark, C. 1964. Calculating Viscosities of Reservoir Fluids from Their Compositions. *Journal of Petroleum Technology* **16**(10):1171-1176.

Longstaff, F. A. and Schwartz, E. S. 2001. Valuing American Options by Simulation: A Simple Least-Squares Approach. *The Review of Financial Studies* **14**(1): 113-147. http://dx.doi.org/10.1093/rfs/14.1.113.

Lorenz, P., Trantham, J., Zornes, D. and Dodd, C. 1986. A Postflood Evaluation Test of the North Burbank Surfactant/Polymer Pilot. *SPE Reservoir Engineering* **1**(4):341-353. http://dx.doi.org/10.2118/12695-PA.

Lowry, P., Ferrell, H. and Dauben, D. 1986. A Review and Statistical Analysis of Micellar-Polymer Field Test Data. National Petroleum Technology Office, US DOE.

Luehrman, T. 1997. What's It Worth? A General Manager's Guide to Valuation. *Harvard Business Review* **75**(3): 132-142.

Luehrman, T. 1998a. Investment Opportunities as Real Options: Getting Started on the Numbers. *Harvard Business Review* **76**(4): 3-15.

Luehrman, T. 1998b. Strategy as a Portfolio of Real Options. *Harvard Business Review* **76**(5): 89-99.

Luenberger, D. 1998. Investment Science. In pp 291-292, 340, 371-373 and 458-470. New York, New York: Oxford University Press.

Mackie, S., Welsh, M. and Lee, M. 2006. An Oil and Gas Decision-Making Taxonomy. Paper SPE 100699 presented at the 2006 SPE Asia Pacific Oil & Gas Conference and Exhibition, Adelaide, Australia, 11-13 September.

Maerker, J. and Gale, W. 1992. Surfactant Flood Process Design for Loudon. *SPE Reservoir Engineering* **7**(1):36-44. SPE 20218-PA. http://dx.doi.org/10.2118/20218-PA.

Manrique, E., Izadi, M., Kitchen, C. and Alvarado, V. 2009. Effective EOR Decision Strategies With Limited Data: Field Cases Demonstration. *SPE Reservoir Evaluation and Engineering* **12**(4):551-561. SPE-113269-PA. http://dx.doi.org/10.2118/113269-PA.

Markland, J. T. 1992. Options Theory: A New Way Forward for Exploration and Engineering Economics? Paper SPE 24232 presented at the SPE Oil & Gas Economics, Finance and Management Conference, London, UK, 28-29 April. doi: 10.2118/24232.

Mathelin, L. and Hussaini, M. 2003. A stochastic collocation algorithm for uncertainty analysis. National Aeronautics and Space Agency, http://ntrs.nasa.gov/archive/nasa/casi.ntrs.nasa.gov/20030016674_2003020380.pdf (accessed 29 June 2012).

Matlab®, version 7.14. 2012. Natick, Massachusetts: The Mathworks, Inc.

McKay, M.D., Beckman, R.J. and Conover, W.J. 1979, A Comparison of Three Methods for Selecting Values of Input Variables in the Analysis of Output from a Computer Code. *Technometrics (American Statistical Association)* **21** (2): 239–245. doi:10.2307/1268522

McNamee, P. and Celona, J. 1990. *Decision Analysis with Supertree*. South San Franscisco, California: The Scientific Press.

Moreno, M. and Navas, J. 2003. On the Robustness of Least-Squares Monte Carlo (LSM) for Pricing American Derivatives. *Review of Derivatives Research* **6**(2):107-128.

Murtada, H. and Marx, C. 1982. Evaluation of the Low Tension Flood Process for High-Salinity Reservoirs-Laboratory Investigation under Reservoir Conditions. *SPE J.* **22**(6):831-846. (SPE 8999-PA).

Najafabadi, N., Delshad, M., Han, C. and Sepehrnoori, K. 2012. Formulaiton for a Three-Phase, Fully Implicit, Parallel, EOS Compositional Surfactant-Polymer Flooding Simulator. *Journal of Petroleum Engineering and Science* **86-87**:257-271.

Nelson, R. 1981. Further studies on phase relationships in chemical flooding. In: Shah, D. (Ed.), Surface Phenomena in Enhanced Oil Recovery. Plenum Press, pp. 73-104.

Nelson, R. 1982. The Salinity-Requirement Diagram- A Useful Tool in Chemical Flooding Research and Development. *SPE J.* **22**(2): 259-270.

Nelson, R. and Pope, G. 1978. Phase Relationships in Chemical Flooding. *SPE J.* **18**(5):325-338.

Newendorp, P. and Schuyler, J. 2000. *Decision Analysis for Petroleum Exploration*, 2nd Edition. Aurora, Colorado: Planning Press.

Nobile, F., Tempone, R. and Webster, C. 2008. A Sparse Grid Stochastic Collocation Method for Partial Differential Equations with Random Input Data. *SIAM J. NUMER. ANAL* **46**(5): 2309-2345.

Ogunyomi, B., Jablonowski, C. and Lake, L. 2011. Field Development Optimization Under Uncertainty: Screening-Models for Decision Making. Paper SPE 146788-MS presented at the SPE Annual Technical Conference and Exhibition, Denver, CO, USA, 30 October – 2 November.

Oliver, D. and Chen, Y. 2011. Recent progress on reservoir history matching: a review. *Computational Geosciences* **15**(1): 185-221.

Omran, M. and Duggan, T. 1999. Applying Modern Portfolio Theory to Upstream Investment Decision Making. *Journal of Petroleum Technology* **51**(3):50-53. SPE 54774.

Onorato, G., Loeven, G., Ghornaiasl, G., Bijl, H. and Lacor, C. 2010. Comparison of intrusive and non-intrusive polynomial chaos methods for CFD applications in aeronautics. Paper 1809 presented at the European Conference on Computational Fluid Dynamics, ECCOMAS CFD, Lisbon, Portugal, 14-17 June.

P. Glasserman, B. Yu, Number of paths versus number of basis functions in American option pricing, Ann. Appl. Probab. 14 (2004) 2090–2119.

Paddock, J., Siegel, D. and Smith, J. 1998. Option valuation of claims on real assets: the case of offshore petroleum leases. *Quarterly Journal of Economics* **103**(3):479-508.

Patacchini, L., De Loubens, R. and Moncorge, A. 2012. Four-Fluid-Phase, Fully Implicit Simulation of Surfactant Flooding. Paper SPE 161630 presented at the Abu Dhabi International Petroleum Exhibition & Conference, Abu Dhabi, UAE, 11-14 November. http://dx.doi.org/10.2118/161630-MS.

Paul, G., Lake, L, Pope, G. and Young, G. 1982. A Simplified Predictive Model for Micellar-Polymer Flooding. Paper SPE 10733 presented at the SPE California Regional Meeting, San Francisco, CA, USA, 24-26 March.

PERM PUNQ-S3 Test Case. Petroleum Engineering and Rock Mechanics Group (PERM). http://www3.imperial.ac.uk/earthscienceandengineering/research/perm/punq-s3model/onlinedataset (accessed 5 May 2012).

Petroleum Experts Ltd. 2012. Reveal Software. http://www.petex.com/products/?ssi=8

Pope, G. 1980. The Application of Fractional Flow Theory to Enhanced Oil Recovery. *SPE J.* **20**(3): 191-205.

Pope, G., Tsaur, K., Schechter, R. and Wang, B. 1982. The Effect of Several Polymers on the Phase Behaviour of MIcellar Fluids. *SPE J.* **22**(6): 816-830.

Pope, G., Wang, B. and Tsaur, K. 1979. A Sensitivity Study of Micellar/Polymer Flooding. *SPE J.* **19**(6):357-368. SPE 7079-PA. http://dx.doi.org/10.2118/7079-PA.

Powell, W. B. 2011. Approximating Value Functions. In *Approximate Dynamic Programming: Solving the Curses of Dimensionality*. Chap 8. Princeton, New Jersey: John Wiley and Sons.

Private communication from journal review comments. 2012. Decision Making Under Uncertainty: Applying the Least Squares Monte Carlo Method in Surfactant Flooding Implementation. *SPE J.* (in press).

Prouvost, L., Pope, G. and Rouse, B. 1985. Microemulsion Phase Behavior: A Thermodynamic Modeling of the Phase Partitioning of Amphiphilic Species. *SPE J.* **25**(5):693-703.

Puerto, M. and Reed, R. 1983. A Three-Paramter Representation of Surfactant/Oil/Brine Interaction. *SPE J.* **23**(4): 669-682.

Puerto, M., Hirasaki, G., Miller, C. and Barnes, J. 2012. Surfactant Systems for EOR in High-Temperature, High-Salinity Environments. *SPE J.* **17**(1): 11-19.

PYTHON, version 2.7.3. 2012. Python Software Foundation, http://www.python.org/download/releases/2.7.3/.

Rasmussen, M. L. and Civan, F. 2005. Value Assessment Using the Modified Black-Scholes Equation. Paper SPE 94520-MS presented at the 2005 Hydrocarbon Economics and Evaluation Symposium, Dallas, Texas, USA, 03-05 April. doi: 10.2118/94520-MS.

Raterman, K., Kremesec, V. and Suffridge, F. 1988. Evaluation of Low-Concentration Surfactant Flooding in the Absence of Mobility Control Agents. Paper SPE 17394 presented at the SPE Enhanced Oil Recovery Symposium, Tulsa, Oklahoma, USA, 16-21 April. http://dx.doi.org/10.2118/17394-MS.

Red-Horse, J. and Paez, T. 1998. Uncertainty evaluation in dynamic system response. *Proceedings-SPIE the International Society for Optical Engineering* **2**:1206-1212.

Reed, R. and Healy, R. 1977. Some Physico-Chemical Aspects of Microemulsion Flooding: A Review. Improved Oil Recovery by Surfactant and Polymer Flooding, Shah, D. and Schechter, R. (eds),. New York, USA: Academic Press.

Regtien, J. 2010. Extending the Smart Fields Concept To Enhanced Oil Recovery. Paper SPE 136034 presented at the 2010 SPE Russian Oil & Gas Technical Conference and Exhibition, Moscow, Russia, 26-28 October.

Remy, N., Boucher, A. and Wu, J. 2011. Applied Geostatistics with SGeMS: A User's Guide. New York, USA: Cambridge University Press.

Reppert, T., Bragg, J. Wilkinson, J., Snow, T., Maer, N. and Gale, W.1990. Second Ripley Surfactant Flood Pilot Test. Paper SPE 20219 presented at the SPE/DOE Enhanced Oil Recovery Symposium, Tulsa, Oklahoma, USA, 22-25 April. http://dx.doi.org/10.2118/20219-MS.

Richardson, L. 1911. The approximate arithmetical solution by finite differences of physical problems including differential equations, with an application to the stresses in a masonry dam. *Philosophical Transactions of the Royal Society A* **210**(459-470): 307-357.

Rosenblatt, M. 1952. Remarks on a Multivariate Transformation. *The Annals of Mathematical Statistics* **23**(3): 470-472.

Roshanfekr, M., Johns, R., Pope, G., Britton, L., Linnemeyer, H., Britton, C. and Vyssotski, A. 2012. Simulation of the Effect of Pressure and Solution Gas on Oil Recovery from Surfactant/Polymer Floods. *SPE J.* **17**(3):705-716.

Saito, R., De Castro, G., Mezzomo, C. and Schiozer, D. 2001. Value assessment for reservoir recovery optimization. *Journal of Petroleum Science & Engineering* **32**(2-4):151-158.

Sanz, C. and Miller, M. 1994. A Decision Analysis Approach to the Design of a Chemical Flooding Process. Paper SPE 27036 presented at the SPE Latin American/Caribbean Petroleum Engineering Conference. Buenos Aires, Argentina. 27-29 April. http://dx.doi.org/10.2118/27036-MS.

Saputelli, L., Ramirez, K., Chegin, J. and Cullick, S. 2009. Waterflood Recovery Optimization Using Intelligent Wells and Decision Analysis. Paper SPE 120509 presented at the 2009 SPE Latin American and Caribbean Petroleum Engineering Conference, Cartagena, Colombia, 31 May-3 June.

Sarma, P. and Xie, J. 2011. Efficient and robust uncertainty quantification in reservoir simulation with polynomial chaos expansions and non-intrusive spectral projection. Paper SPE 141963 presented at the SPE Reservoir Simulation Symposium, The Woodlands, TX, 21-23 February.

Schlumberger. ECLIPSE Reservoir Simulation Software Technical Description. 2011. London, UK: Schlumberger.

Schlumberger. ECLIPSE Reservoir Simulation Software. 2010. http://www.slb.com/services/software/reseng.aspx.

Schneiderman, H. and Kanade, T. 2004. Object detection using the statistics of parts. *International Journal of Computer Vision* **56**(3): 151-177.

Shen, P., Wang, J., Yuan, S., Zhong, T. and Jia, X. 2009. Study of Enhanced-Oil-Recovery Mechanism of Alkali/Surfactant/Polymer Flooding in Porous Media from Experiments. *SPE J.* **14**(2):237-244. http:// dx.doi.org/10.2118/126128-PA.

Shupe, R. 1981. Chemical Stability of Polyacrylamide Polymers. *Journal of Petroleum Technology* **33**(8):1513-1529. (SPE9299-PA).

Sick, G. and Gamba, A. 2010. Some Important Issues Involving Real Options: An Overview. *Multinational Finance Journal* **14**(1/2): 73-123.

Smith, J. and McCardle, K. 1999. Options in the Real World: Lessons Learned in Evaluating Oil and Gas Investments. *Operations Research*: **47**(1):1-15.

Smith, W. 2010. On the Simulation and Estimation of the Mean-Reverting Ornstein-Uhlenbeck Process. http://commoditymodels.files.wordpress.com/2010/02/estimating-the-parameters-of-a-mean-reverting-ornstein-uhlenbeck-process1.pdf (downloaded 9 January 2012).

Solairaj, S., Britton, C., Kim, D., Weerasooriya, U. and Pope, G. 2012.Measurement and Analysis of Surfactant Retention. Paper SPE 154247 presented at the Eighteenth SPE Improved Oil Recovery Symposium, Tulsa, Oklahoma, USA, 14-18 April. http://dx.doi.org/10.2118/154247-MS.

Stanford Geostatistical Modeling Software (SGeMS). 2012. Remy, N., Boucher, A. and Wu, J. http://sgems.sourceforge.net/.

STARS Reservoir Simulator. 2012. Computer Modelling Group LTD. http://www.cmgl.ca/software/soft-stars.

Stentoft, L. 2004. Assessing the Least Squares Monte-Carlo Approach to American Option Valuation. *Review of Derivatives Research* **7**(2):129-168.

Stoll, W., AlShureqi, H., Finol, J. Al-Harthy, A., Oyemade, S., De Kruijf, A., Van Wunnik, J., Arkesteijn, F. Bouwmeester, R. and Faber, M. 2011. Alkaline/Surfactant/Polymer Flood: From the Laboratory to the Field. *SPE J.* **14**(6):702-712.

Strebelle, S. 2002. Conditional Simulation of Complex Geological Structures Using Multiple-Point Statistics. *Mathematical Geology* **34**(1): 1-21.

Stripe, J., Arisaka, K. and Durandeau, M. 1993. Integrated Field Development Planning Using Risk and Decision Analysis To Minimise the Impact of Reservoir and Other Uncertainties: A Case Study. Paper SPE 25529 presented at the SPE Middle East Oil Technical Conference & Exhibition, 3-6 April.

Suslick, S. and Schiozer, D. 2004. Risk analysis applied to petroleum exploration and production: an overview. *Journal of Petroleum Science and Engineering* **44**(1-2):1-9. http://dx.doi.org/10.1016/j.petrol.2004.02.001

Suslick, S., Furtado, R. and Nepomuceno, F. 2001. Integrating Technological and Financial Uncertainty for Offshore Oil Exploration: An Application of Multiobjective Decision Analysis. Paper SPE 68579 presented at the SPE Hydrocarbon Economics and Evaluation Symposium, Dallas, TA, USA, 2-3 April.

Szabo, M. 1979. An evaluation of water-soluble polymers for secondary oil recovery, parts I and II. *Journal of Petroleum Technology* **31**(5):553-570. (SPE6601-PA).

Tabary, R., Douarche, F., Bazin, B., Lemouzy, P., Moreau, P. and Morvan, M. 2012. Design of a Surfactant/Polymer Process in a Hard Brine Context: A Case Study Applied to Bramberge Reservoir. Paper SPE presented at the SPE EOR Conference at Oil and Gas West Asia, Muscat, Oman, 16-18 April. http://dx.doi.org/10.2118/155106-MS.

Taggart, D. and Russell, G. 1981. Sloss Micellar/Polymer Flood Post Test Evaluation Well. Paper SPE 9781 presented at the 1981 SPE/DOE Second Joint Symposium on enhanced Oil Recovery, Tulsa, OK, USA, 5-8 April. http://dx.doi.org/10.2118/9781-MS.

Tatang, M., Pan, W., Prinn, R. and McRae, G., 1997. An Efficient Method for Parametric Uncertainty Analysis of Numerical Geophysical Models. *Journal of Geophysical Research* **102**(18): 21925-21932. http://dx.doi.org/10.1029/97JD01654

Taugbol, K., Ly, T. and Austad, T. 1995. Chemical flooding of oil reservoirs 3. Dissociative surfactant-polymer interaction with a positive effect on oil recovery. *Colloids and Surfaces A: Physicochemical and Engineering Aspects* **103**(1-2):83-90.

Thakur, G. 1995. The Role of Technology and Decision Analysis in Reservoir Management. Paper SPE 29775 presented at the SPE Middle East Oil Show, Bahrain, 11-14 March.

Thomas, S. 2006. Chemical EOR: The Past – Does It Have a Future? Paper SPE 108828 based on a speech presented as an SPE Distinguished Lecture during the 2005-2006 season.

Todd, M. and Longstaff, W. 1972. The Development, Testing, and Application for a Numerical Simulator for Predicting Miscible Performance. *Journal of Petroleum Technology* **24**(7): 874-882.

Todd, M., Dietrich, J., Goldburg, A. and Larson, R. 1978. Numerical Simulation of Competing Chemical Flood Designs. Paper SPE 7077 presented at the SPE Symposium on Improved Methods of Oil Recovery, Tulsa, OK, USA, 16-17 April.

Tomich, J., Laplante, L. and Snow, T. 1987. Technical and Economic Complexities Associated with Surfactant Flooding. Paper WPC 22236 presented at 12th World Petroleum Congress, Houston, Texas, USA. April 26-May l.

Trantham, J. 1983. Prospects of Commercialization Surfactant/Polymer Flooding North Burbank Unit. *Journal of Petroleum Technology* **35**(5):872-880. SPE 9816-PA. http://dx.doi.org/10.2118/9816-PA.

Trushenski, S. 1977. Micellar flooding: sulfonate-polymer interaction. In: Shah, D. and Schechter, R. (Eds), Improved Oil Recovery by Surfactant and Polymer Flooding. Academic Press, pp. 555-575.

Trushenski, S., Dauben, D. and Parrish, D. 1974. Micellar flooding, fluid propagation, interaction, and mobility. *SPE J.* **14**(4): 633-645.

Uhlenbeck, G. and Ornstein, L., 1930. On the Theory of the Brownian motion. *Physical Review* **36**(5): 823-841. http://link.aps.org/doi/10.1103/PhysRev.36.823

Ulerich, R. 2009. Richardson Extrapolation Module, http://www.mathworks.com/matlabcentral/fileexchange/24388-richardson-extrapolation (accessed 9 November 2009).

UTCHEM Technical Documentation. 2000. Austin, Texas: University of Texas at Austin.

Von Neumann, J. and Morgenstern, O. 1947. *Theory of Games and Economic Behaviour*, 2nd Edition. Princeton, New Jersey: Princeton University Press.

Walls, M. 2004. Combining decision analysis and portfolio management to improve project selection in the exploration and production firm. *Journal of Petroleum Science & Engineering* **44**(1-2):55-65.

Wallstrom, T., Hou. S., Christie, M., Durlofsky, L. and Sharp, D. 1999. Accurate scle up of two phase flow using renormaliation and nonuniform coarsening. *Computational Geoscience* **3**: 69-87.

Wang, C., Li, G. and Reynolds, A. 2009. Production Optimization in Closed-Loop Reservoir Management. *SPE J.* **14**(3):506-523. SPE109805-PA.

Wang, W. and Gu, Y. 2005. Experimental Studies of the Detection and Reuse of Produced Chemicals in Alkaline/Surfactant/Polymer Floods. *SPE Reservoir Evaluation & Engineering* **8**(5):362-371.

Wang, Y., Zhao, F., Bai, B. Zhang, J., Xiang, W., Li, X. and Zhou, W. 2010. Optimized Surfactant IFT and Polymer Viscosity for Surfactant-Polymer Flooding in Hetergeneous Formations. Paper SPE 127391 presented at the 2010 SPE Improved Oil Recovery Symposium, Tulsa, OK, USA, 24-28 April. http://dx.doi.org/10.2118/127391-MS.

Warren, J. and Price, H. 1961. Flow in Heterogeneous Porous Media. *SPE J.* **1**(3):153-169. SPE 1579-G.

Weiss, W. and Baldwin, R. 1985. Planning and Implementing a Large-Scale Polymer Flood. *Journal of Petroleum Technology* **37**(4): 720-730. http://dx.doi.org/10.2118/12637-PA.

White, H. 1984. *Asymptotic Theory for Econometricians.* New York: Academic Press.

Widmyer, R., Williams, D. and Ware, J. 1988. Performance Evaluation of the Salem Unit Surfactant/Polymer Pilot. *Journal of Petroleum Technology* **40**(9): 1217-1226.

Wiener, N. 1938. The homogeneous Chaos. *American Journal of Mathematics* **60**(4): 897-936.

Wilkinson, D., Bailey, W. and Couet, B. 2005. Alternative Approaches to Real Option Valuation: A Critical Appraisal. Paper SPE 97065-MS presented at the 2005 SPE Annual Technical Conference and Exhibition, Dallas, Texas, USA, 9-12 October. doi: 10.2118/97065-MS.

Willigers, B. and Hansen, T. 2008. Project valuation in the pharmaceutical industry: a comparison of least-squares Monte Carlo real option valuation and conventional approaches. *R&D Management* **38**(5): 520-537.

Willigers, B. J. A. and Bratvold, R. B. 2009. Valuing Oil and Gas Options by Least-Squares Monte Carlo Simulation. *SPE Projects, Facilities & Construction* **4**(4): 146-155. http://dx.doi.org/10.2118/116026-PA.

Willigers, B., Begg, S. and Bratvold, R. Valuation of Swing Contracts by Least-Squares Monte Carlo Simulation. Paper SPE 133044 presented at the SPE Asia Pacific Oil & Gas Conference and Exhibition, Brisbane, Australia, 18-20 October.

Winsor, P. 1954. *Solvent Properties of Amphiphilic Compounds*. London, UK: Butterworths.

Wyatt, K., Pitts, M. and Surkalo, H. 2008. Economics of Field Proven Chemical Flooding Technologies. Paper SPE 113126 presented at the SPE/DOE Symposium on Improved Oil Recovery, Tulsa, Oklahoma, USA, 20-23 April. http://dx.doi.org/10.2118/113126-MS.

Xiu, D. 2007. Efficient Collocational Approach for Parametric Uncertainty Analysis. *Communications in Computational Physics* **2**(2): 293-309.

Xiu, D. and Hesthaven, J.2005. High-order collocation methods for differential equations with random inputs. *SIAM Journal on Scientific Computing* **27**(3): 1118-1139.

Xiu, D. and Karniadakis, G. 2002. The Wiener-Askey polynomial chaos for stochastic differential equations. *SIAM Journal on Scientific Computing* **24**(2): 619-644.

Xu, L., Sepehrnoori, K., Dyer, J. and van Rensburg, W. 2012. Application of Real Options to Valuation and Decision-making in the Petroleum E&P Industry. Paper SPE 162929 presented at the SPE Hydrocarbon, Economics, and Evaluation Symposium, Calgary, Alberta, Canada, 24-25 September.

Xu, W., Ayirala, S. and Rao, D. 2008. Measurement of Surfactant-Induced Interfacial Interactions at Reservoir Conditions. *SPE Reservoir Evaluation & Engineering* **11**(1):83-94.

Yao, Y. H., Begg, S., Van Der Hoeak, J., Behrenbruch, P. And Bratvold, R. B. 2006. A Case Study for Comparison of Different Real Option Approaches in Petroleum Investments. Paper SPE 101031 presented at the 2006 SPE Asia Pacific Oil & Gas Conference and Exhibition, Adelaide, Australia, 11-13 September. doi: 10.2118/101031.

Yeten, B., Brouwer, D., Durlofsky, L. and Aziz, K. 2004. Decision analysis under uncertainty for smart well development. *Journal of Petroleum Science & Engineering* **4**(3-4):183-199.

Zettl, M. 2000. Extending the Option Pricing Theory for the Valuation of E&P Projects. Paper SPE 62968-MS presented at the SPE Annual Technical Conference and Exhibition, Dallas, Texas, USA, 1-4 October. doi: 10.2118/62968-MS.

Zhang, J., Delshad, M., Sepehnoori, K. and Pope, G. 2005. An Efficient Reservoir-Simulation Approach To Design and Optimize Improved Oil-Recovery-Processes With Distributed Computing. Paper SPE 94733 presented at the SPE Latin American and Caribbean Petroleum Engineering Conference, Rio de Janeiro, Brazil, 20-23 June. http://dx.doi.org/10.2118/94733-MS.

Zheng, C., Gall, B., Gao, H. and Bryant, R. 2000. Effects of Polymer Adsorption and Flow Behavior on Two-Phase Flow in Porous Media. *SPE Reservoir Evaluation and Engineering* **3**(3): 216-223. http://dx.doi.org/10.2118/64270-PA.

Zolotukhin, A. 1992. A New Decision Making in Reservoir Engineering. Paper SPE 22356 presented at the SPE International Meeting on Petroleum Engineering, Beijing, China, 24-27 March.

Appendices

5.1 A: Reservoir and Surfactant Properties for Homogeneous and SPE10 Layers 1, 5, 10, 15 and 20 Reservoir Models

Table A1: Homogeneous and SPE Layers (1,5,10,15 and 20[32]) Reservoir Simulation Model Properties

Grid	10x10x10 Cells
Dimensions	142x142x8.2 m
K_h	100 mD
K_v	10 mD
Porosity, %	20%
Top of Reservoir	1500 m

Table A2: Immiscible Relative Permeability Data[33]

S_w	k_{rw}	k_{row}	p_{cwo}
0.2	0	0.9	50
0.22	0	0.803	45
0.3	0.001	0.487	25
0.4	0.009	0.221	12.5
0.5	0.045	0.078	6.3
0.6	0.154	0.014	2.5
0.7	0.387	0.001	1.3
0.73	0.48	0	1.1
0.8	0.8	0	0.8

[32] SPE10 layer models use the same reservoir and fluid properties as the homogeneous model with the exception of the permeability field and being two-dimensional rather than three-dimensional.
[33] Data source is ECLIPSE Technical Description 2010.1.

Table A3 Surfactant Viscosity and Surfactant/Oil Surface Tension

Surfactant Concentration (% wt.)	Surfactant Water Viscosity (cp)	Surfactant Water/Oil Surface Tension (dynes/cm)
0	1.0	0.05
0.028	1.1	10^{-6}
0.057	1.2	10^{-6}
0.23	1.3	10^{-6}

Table A4: Capillary De-Saturation Curve[34]

Log_{10} (Capillary Number)	Miscibility Function
-9	0
2	0
5	1
10	1

Table A5: Reservoir Simulation Constraints

Constraint	Limit Value
BHP Min, N/m^2	1.72E+06
Oil Rate, m^3/d	3.18 (Max)
Water Cut, %	None
W_{inj} Max Pressure, N/m^2	3.17E+06

Table A6 Polymer Properties

Property	Value
Dead Pore Space Factor	0.16
Residual Resistance Factor	1.5
Adsorption	Irreversible

[34] Data source is ECLIPSE Technical Description 2010.1.

Appendix B: Basis Function Orthogonal Polynomials

The first four polynomials are given below for the different orthogonal types used in chapter 4.

A. Probabilists' Hermite Polynomials:

$H_e(x) = 1$

$H_e(x) = x$

$H_e(x) = x^2 - 1$

$H_e(x) = x^3 - 3x$

B. Legendre Polynomial:

$P_0(x) = 1$

$P_1(x) = x$

$P_2(x) = (\frac{1}{2})(3x^2 - 1)$

$P_3(x) = (\frac{1}{2})(5x^3 - 3x)$

C. Chebyshev Polynomial:

First type	Second type
$T_0(x) = 1$	$U_0(x) = 1$
$T_1(x) = x$	$U_1(x) = 2x$
$T_2(x) = 2x^2 - 1$	$U_2(x) = 4x^2 - 1$
$T_3(x) = 4x^3 - 3x$	$U_3(x) = 8x^3 - 4x$

Appendix C: Reservoir and Fluid Data for Moving Average and FILTERSIM Reservoir Models

Table C1: Reservoir Simulation Model Properties

Grid	120x120 Cells
Dimensions	366x670x10 m
Porosity, %	20%
Top of Reservoir	3660 m

Table C2: Immiscible Relative Permeability Data[35]

S_w	k_{rw}	k_{row}	p_{cwo}
0.20	0	1	50
0.25	0.0069	0.840	45
0.30	0.027	0.694	25
0.35	0.062	0.562	12.5
0.40	0.111	0.444	6.3
0.45	0.173	0.340	2.5
0.50	0.250	0.250	1.3
0.55	0.340	0.173	1.1
0.60	0.444	0.111	0.8

Table C2 Simulation Constraints the Case Studies

Constraint	Moving Average/FILTERSIM
Producer Oil Rate, m^3/d	24
Injector Water Rate, m^3/d	400
Water Cut, %	None
BHP min, bar	17
Max Injection Pressure, bar	550

[35] Data source is **Christie and Blunt (2001)**.

Appendix D: Orthogonal Polynomials Used for PCM

Since the case studies in this thesis used normal and uniform random variables, the generation of polynomials for these random variable types is described further. For Gaussian random variables, the PCE is based on Hermite polynomials, where as an example the multivariate Hermite polynomial $\Gamma(x)$ of the nth order is defined as:

$$\Gamma_n\left(x_{i_1},\dots,x_{i_n}\right) = e^{\frac{1}{2}x^T x}(-1)^n \frac{\partial^n}{\partial x_{i_1}\dots\partial x_{i_n}} e^{\frac{1}{2}x^T x} \quad \text{Eq. D.1}$$

For uniform random variables, the PCE is based on Legendre polynomials and can be defined for a multivariate Legendre polynomial $\Gamma(x)$ of the nth order as:

$$\Gamma_n\left(x_{i_1},\dots,x_{i_n}\right) = \frac{1}{2^n n!}\frac{\partial^n}{\partial x_{i_1}\dots\partial x_{i_n}}(x^2-1)^n \quad \text{Eq. D.2}$$

The orthogonal polynomials obey the three-term recurrence relationship:

$$\pi_{i+1}(x) = (x-\alpha_i)\pi_i(x) - \beta_i\pi_{i-1}(x) \quad \text{Eq. D.3}$$

$$\pi_0(x) = 0 \quad \text{Eq. D.4}$$

$$\pi_1(x) = 1 \quad \text{Eq. D.5}$$

, for $i = 2,3,\dots,N$. Where α_i and β_i are the recurrence coefficients determined by the weighting function (which is the PDF of the variable being approximated) $\omega(x)$ and $\{\pi_i(x)\}_{i=1}^{N}$ is a set of monic orthogonal polynomials with

$$\pi_i(x) = x^i + \mathcal{O}\left(x^{i-1}\right),\ i = 1,2,\dots,N \quad \text{Eq. D.6}$$

Appendix E: Golub-Welsch Algorithm for Gaussian Quadrature

Gaussian quadrature approximates a definite integral of a function as a weighted sum of the function values at certain points within the integration domain:

$$\int_{-1}^{1} f(x)dx \approx \sum_{i=1}^{n} w_i f(x_i) \quad \text{Eq. E.7}$$

For arbitrary bounds, this expression becomes:

$$\int_{a}^{b} f(x)dx = \int_{a}^{b} w(x)g(x)dx \approx \sum_{i=1}^{n} w_i f(x_i) \quad \text{Eq. E.8}$$

, where $w(x)$ is the weight function

The Golub-Welsch algorithm (**Golub and Welsch 1969**) is a classical approach used to compute the Gaussian nodes and weights by reducing the problem to a symmetric tridiagonal eigenvalue problem (**Hale 2011**). Using the three-term recurrence relation in the matrix form,

$$J\widetilde{P} = x\widetilde{P} \quad \text{Eq. E.9}$$

, where $\widetilde{P} = [p_0(x), p_1(x), \dots, p_{n-1}(x)]^T$ Eq. E.10

, and $p_n(x)$ are the three-term recurrence relation generated orthogonal polynomials that are associated with the corresponding weight function

J is the Jacobi matrix:

$$J = \begin{pmatrix} a_0 & 1 & 0 & \dots & \cdots & \cdots \\ b_1 & a_1 & 1 & 0 & \cdots & \cdots \\ 0 & b_2 & a_2 & 1 & 0 & \dots \\ 0 & \vdots & \dots & \dots & \dots & 0 \\ \cdots & \vdots & 0 & b_{n-2} & a_{n-2} & 1 \\ \cdots & \cdots & \dots & 0 & b_{n-1} & a_{n-1} \end{pmatrix} \quad \text{Eq. E.11}$$

The nodes of the Gaussian quadrature (i.e. the zeros of the polynomials, x) are obtained by determining the eignevalues of the Jacobi matrix.

This algorithm was implemented by the polychaos PYTHON module developed by **Feinberg (2012)**.

Appendix F: Inverse Cumulative Distribution Function and Inverse Rosenblatt Transform

The inverse cumulative distribution function is defined as:

$F^{-1}(t)$ such that $t \in [0,1]$ and $F(x) = t$ Eq. F.12

$X = (X_1, \dots, X_k)$ is a random vector with the distribution function $F(x_1, \dots, x_2)$. The conditional cumulative distribution functions are defined as:

$F_1(x_1) = P(X_1 \leq x_1)$, Eq. F.13

$F_2(x_2|x_1) = P(X_2 \leq x_2|X_1 = x_1)$, Eq. F.14

…

$F_k(x_k|x_1, \dots, x_{k-1}) = P(X_k \leq x_k|X_1 = x_1, \dots, X_{k-1} = x_{k-1})$, Eq. F.15

Rosenblatt's transformation is defined as $z = (z_1, \dots, z_k) = Tx = T(x_1, \dots, x_k)$, where:

$z_1 = P\{X_1 \leq x_1\} = F_1(x_1)$, Eq. F.16

$z_2 = P\{X_2 \leq x_2|X_1 = x_1\} = F_2(x_2|x_1)$, Eq. F.17

…

$z_k = P\{X_k \leq x_k|X_{k-1} = x_{k-1}, \dots, X_1 = x_1\} = F_k(x_k|x_1, \dots, x_{k-1})$, Eq. F.18

The inverse Rosenblatt transform is defined as: $x = T^{-1}(z)$ Eq. F.19

Forward transform maps the realizations of the random vector X into the space of realizations of uncorrelated, standard normal random variables, Z. The inverse transform produces the inverse mapping (**Red-Horse and Paez 1998**).

These are implemented by the polychaos PYTHON module developed by **Feinberg (2012)**.

Appendix G: Surfactant-Polymer Properties and Simulation Constraints

Simulation constraints used for the PUNQ-S3 and the modified SPE10 reservoir models are shown in Table 2. The producer oil rate and bottom hole pressure (BHP) constraints are applied to each of the four producers in these two models.

Table G1 Simulation Constraints the Case Studies

Constraint	Homogeneous/SPE10 Layer 1	PUNQ-S3	SPE10M
Producer Oil Rate, m^3/d	3.17	32	24
Injector Water Rate, m^3/d	80	280	400
Water Cut, %	None	None	None
BHP min, bar	17	17	17
Max Injection Pressure, bar	310	310	550

Appendix H: Alkaline Model in ECLIPSE

The alkaline-surfactant-polymer flooding process simulation in section **6.3.2** was based on ECLIPSE. The alkaline model is a simplified model which does not consider the in-situ surfactant creation nor phase behaviour. The model does take into account some effects of the alkaline in ASP flooding. This focuses on alkaline effect on water-oil surface tension and adsorption of polymer and surfactant.

The alkaline is assumed to exist in the aqueous phase and the conservation equation that describes the distribution of the injected alkaline is defined as follows (**ECLIPSE Technical Description 2010**):

$$\frac{d}{dt}\left(\frac{VS_wC_a}{B_rB_w}\right)+\frac{d}{dt}\left(V\rho_rC_a^a\frac{1-\varphi}{\varphi}\right)=\sum\left[\frac{Tk_{rw}}{B_w\mu_{s\,eff}}(\delta P_w-\rho_wgD_z)\right]C_a+Q_wC_a \qquad \text{Eq. H.1}$$

, where ρ_r and ρ_w are the rock and water density respectively

C_a is the alkaline concentration

C_a^a is the adsorbed alkaline concentration

$\mu_{s\,eff}$ is the effective viscosity of the salt

D_z is the cell depth

B_w and B_r are the water and rock formation volume respectively

T is the transmissibility

k_{rw} is the water relative permeability

S_w is the water saturation

V is the block pore volume

Q_w is the water production rate

P_w is the water pressure

g is the gravity acceleration

The default setting is to update the alkaline concentration at the end of a time step once the inter-block phase flows are determined. Alkaline adsorption is assumed to be instantaneous and is modelled using an adsorption isotherm. The effect of alkaline on water-oil surface tension is considered in this model and is defined as a combined effect with surfactant. The water-oil surface tension is modified in the following manner:

$$\sigma_{wo}=\sigma_{wo}(C_s)A_{st}(C_a) \qquad \text{Eq. H.2}$$

, where $\sigma_{wo}(C_s)$ is defined as the surface tension at a specific surfactant concentration and at zero alkaline concentration. $A_{st}(C_a)$ is defined as the surface tensions multiplier at a specific alkaline concentration.

The effect of alkaline on surfactant and polymer adsorption is modelled by modifying the adsorbed mass of surfactant or polymer:

$$V\rho_r C_{s,p}^a \frac{1-\varphi}{\varphi} A_d(C_a) \qquad \text{Eq. H.3}$$

, where V is the cell pore volume

$C_{s,p}^a$ is the surfactant or polymer adsorbed concentration

$A_d(C_a)$ is the adsorption multiplier at a specific alkaline concentration.

Appendix I: Alkaline Properties

Table I1 Surfactant/Polymer Adsorption Multipliers as a function of Alkaline Concentration

Alkaline Concentration (% wt.)	Alkaline-Surfactant Adsorption Multiplier	Alkaline-Polymer Adsorption Multiplier
0	1.0	1.0
0.028	0.99995	0.99995
0.057	0.99500	0.99500
0.28	0.50	0.50

Table I2 Water/Oil Surface Tension Multipliers as a Function of Alkaline Concentration

Alkaline Concentration (% wt.)	Alkaline-Surfactant Adsorption Multiplier
0	1.0
0.028	0.90
0.057	0.90
0.14	0.90